DYNAMICS OF PROMOTED GAS-SOLID FLUIDIZED BED USING SECONDARY FLUIDIZING MEDIUM

Thesis submitted in partial fulfilment of the requirements for the degree of

DOCTOR OF PHILOSOPHY

by

YASHOBANTA KUMAR MOHANTY

Under the Supervision of

Prof. (Dr.) Kartick Chandra Biswal

And Co-Supervision

of

Prof. (Dr.) Bibhupada Mohanty

September 2007

DEPARTMENT OF CHEMICAL ENGINEERING
National Institute of Technology, Rourkela
Orissa -769 008, India

DEDICATION

—In loving memory of my late beloved mother and sister-in-law

Preface

Fluidization—a fluid-solid contacting technique extensively used by industries over the last six decades— transforms fine solids into a fluid-like state through contact with gas or liquid. This method of contacting has a number of unusual characteristics, and fluidization engineering is concerned with its efforts to take advantage of this behaviour and put it to industrial uses.

Most of the chemical and mineral processing industries use equipment to carry out gas-solid contacting operations involving flow through fixed or fluidized beds. The operations involved in the gas-solid contacting are fluid bed catalytic cracking, drying, transportation, combustion, reduction, etc.

Research work undertaken hitherto mainly focuses on the effect of individual parameters like pressure drop, fluctuation ratio, expansion ratio, mixing characteristic, etc on fluidization quality, particularly in the lower velocity range. But the present work makes an endeavour to study both the individual as well as the combined effect of these parameters on fluidization quality in the entire velocity range. Besides, the novelty of present work lies in the fact that this work has studied the hydrodynamics involved during secondary air supply due to its versatile effects on residence time, mixing, combustion, gasification, reduction of SOx and NOx, etc.

ACKNOWLEDGEMENT

Words are never a true vehicle to express our feelings. Nevertheless, I have made a vain attempt to do it in the following paragraphs.

At the outset, I would like to thank my Supervisor, **Professor (Dr) Karttik Chandra Biswal**, Chemical Engineering Department, National Institute Technology (NIT), Rourkela for his invaluable and patient guidance as well as continual support and encouragement throughout this work.

I am especially indebted to **Professor (Dr) Gopendra Kishore Roy**, Chemical Engineering Department, NIT, Rourkela for his invaluable suggestion and encouragement, without which this thesis would have not seen the light of day. I also thank all other members of the staff in the Department of Chemical Engineering, NIT, Rourkela.

I owe Professor **(Dr) Bibhupada Mohanty** a deep sense of gratitude for his kind supervision throughout this doctoral work.

I take this opportunity to thank the management of Gandhi Institute of Engineering and Technology (GIET), Gunupur for their moral encouragement and support. My thanks are also due to Mr Subash Chandra Pattnaik and other members of the faculty at GIET, Gunupur for their invaluable assistance all through this work.

Most important of all, I would like to express my gratitude to my parents, my brother and wife for their constant love, undying inspiration and selfless dedication to my education. I am also equally indebted to all those who have contributed, directly or indirectly, to this present work.

Last but not the least, I am sure this section would not come to an end without remaining indebted to God Almighty— the Guide of all guides—who has dispelled the envelope of my ignorance with His radiance of knowledge.

Yashobanta Kumar Mohanty
Ph D Scholar
Roll No 50400001

C E R T I F I C A T E

This is to certify that the thesis entitled "**Dynamics of Promoted Gas-Solid Fluidized Bed Using Secondary Fluidizing Medium**", being submitted by Mr. Yashobanta Kumar Mohanty (bearing Roll No. 50400001) of Chemical Engineering Department, National Institute of Technology, Rourkela in partial fulfillment of the requirements for award of the degree of "**Doctor of Philosophy**", is a bona fide record of research done by him under our supervision and guidance.

The work incorporated in this thesis has not been submitted earlier, in part or in full, for the award of any other degree or diploma of this or in any other University or Institution.

Prof. (Dr.) K. C. Biswal
Supervisor
Department of Chemical Engineering
National Institute of Technology
Rourkela - 769008
INDIA

Prof. (Dr.) B. P. Mohanty
Co-supervisor
Department of Chemical Engineering
GIET, Gunupur - 765022
Orissa
INDIA

TABLE OF CONTENTS

PREFACE ……. i

ACKNOWLEDGEMENT ……. ii

CERTIFICATE …….. iii

TABLE OF CONTENTS ……... iv - vii

LIST OF TABLES …….. viii - x

LIST OF FIGURES …… xi – xv

LIST OF PUBLICATIONS ……. xvi-xvii

ABSTRACT …… xviii - xix

INTRODUCTION ……. 01-02

CHAPTER 1 …….. 03-64

Literature Survey

1.1 History of fluidization and its application…… 03

1.2 Particle characteristics…… 05

1.2.1 Particle size……. 05

1.2.2 Particle density……. 05

1.2.3 Particle shape factor……. 06

1.2.4 Particle regime……. 06

1.2.5 Terminal settling velocity and drag coefficient…… 08

1.3 Regimes of fluidization and their characteristics….. 10

1.3.1 Minimum fluidization velocity…… 12

1.3.2 Minimum bubbling velocity…….. 15

1.3.3 Slugging……. 18

1.3.4 Turbulent bed……. 18

1.3.5 Transport Velocity…….. 21

1.3.6 Pneumatic transport……. 22

1.3.7 Phase diagram ……. 24

1.4 Pressure fluctuations …….. 27

1.5 Quality of fluidization …… 32

1.5.1 Uniformity index method……. 32

1.5.2 Fluctuation ratio…… 32

1.5.3 Expansion ratio……. 34

1.6 Baffles/promoters…….. 34

1.7 Distributor…… 37

1.8 Solids segregation and mixing……. 38

1.9 Artificial neural network…….. 45

1.10 Statistical approach…… 46

Scope of the present work…….. 49

Notations

References

Chapter 2 …… 65-74

Experimental aspects

2.1 Air compressor……..... 65

2.2 Air accumulator……65

2.3 Silica gel column……. 65

2.4 Rotameters…….. 65

2.5 Air distributor……. 66

2.6 Fluidizer…….. 66

2.7 Manometer…….. 67

2.8 Supporting structure…… 67

2.9 Experimental Procedure…….. 67

2.10 Baffles/Promoters……. 67

2.11 Secondary air…… 68

2.12 Segregation and mixing…… 68

Chapter 3 …… 75-99

Effect of distributor plate on bed dynamics

3.1 Introduction…… 75

3.2 Development of models …… 78

3.3 Results and discussion……... 80

3.4 Conclusions…… ... 83

Notations

References

Chapter 4 ……100-120

Effect of column internal diameter on bed dynamics

4.1 Introduction……. 100

4.2 Development of models ……. 101

4.3 Results and discussion……. 103

4.4 Conclusions……. 105

Notations

References

Chapter 5 …….. 121-147

Effect of promoters on bed dynamics

5.1 Introduction……. 121

5.2 Development of models …….. 123

5.3 Results and discussion……. 125

5.4 Conclusions……... 127

Notations

References

Chapter 6 ……148-183

Effect of secondary fluidizing medium on bed dynamics

6.1 Introduction……148

6.2 Development of models…….153

6.3 Results and discussion……... 156

6.4 Conclusions……... 159

Notations

References

Chapter 7 …… 184-214

Mixing characteristics of binary mixtures

7.1 Introduction……184

7.2 Development of models…….. ……189

7.3 Results and discussion…… ……191

7.4 Conclusions……. 194

Notations

References

Chapter 8 …….215-217

Conclusions and Scope of Future Work

8.1 Conclusions…….. 215

8.2 Scope of future work……. …...217

Appendix 1 …….. 218-223

Appendix 2 ……. 234-235

List of Tables

1.1 Development of Fluidized Bed Technology……..4

1.2 Values of C_1 and C_2 Obtained by Various Authors…….17

1.3 Reported Experimental Data on U_k 20

1.4 A Summary on Regime Diagram as Proposed by Various Authors……26

1.5 Sign for Calculating the Effects……...47

3.1 Scope of the Experiment……..94

3.2 Factorial Design and Analysis…….95

3.3 Analysis of Fluctuation Ratio, Expansion Ratio and Pressure Drop Data…..96

3.4 Comparison of Fluctuation Ratio Data…….. 97

3.5 Comparison of Expansion Ratio ……... 98

3.6 Comparison of Pressure Drop Data……... 99

4.1 Scope of the Experiment……112

4.2 Factorial Design Analysis …….113

4.3 Analysis of Fluctuation and Expansion Ratios Data, (r) and (R)……..114

4.4 Comparison of Fluctuation Ratio (Factorial Design Method) …….115

4.5 Comparison of Expansion Ratio Data (Factorial Design Method)……116

4.6 Comparison of Fluctuation Ratio Data ……117

4.7 Comparison of Expansion Ratio Data …….118

4.8 Comparison of Fluctuation Ratio Data ……119

4.9 Comparison of Fluctuation Ratio……...120

5.1 Scope of the Experiment……137

5.2 Factorial Design and Analysis ……...138

5.3 Analysis of Fluctuation Ratio Data (r)……...139
5.4 Analysis of Expansion Ratio Data (R)……...140
5.5 Selected Structures of Neural Network Models…….141
5.6 Comparisons of Fluctuation Ratio Data in the Case of Un-promoted Bed…142
5.7 Comparisons of Fluctuation Ratio Data in the Case of Rod Promoted Bed..143
5.8 Comparisons of Fluctuation Ratio Data in the Case of Disc Promoted Bed.144
5.9 Comparisons of Expansion Ratio Data in the Case of Un-Promoted Bed…145
5.10 Comparisons of Expansion Ratio Data in the Case of Rod Promoted Bed.146
5.11 Comparisons of Expansion Ratio Data in the Case of Disc Promoted Bed.147
6.1 Scope of the Experiment……171
6.2 Factorial Design and Analysis……. 172
6.3 Analysis of Fluctuation Ratio (r) and Expansion Ratio (R) Data……..173
6.4 Selected Structures of Neural Network Models……174
6.5 Comparison of Fluctuation Ratio and Expansion Ratio Calculated through Factorial Design Approach ……175
6.6 Comparison of Fluctuation Ratio Data for Primary Air Supply (Factorial Design Approach)……..176
6.7 Comparison of Fluctuation Ratio Data for Primary and Secondary (Simultaneous) Air Supplies (Factorial Design Approach)……177
6.8 Comparison of Expansion Ratio Data for Primary Air Supply (Factorial Design Approach)……178
6.9 Comparison of Expansion Ratio Data for Primary and Secondary (Simultaneous) Air Supplies (Factorial Design Approach)…….179
6.10 Comparison of Fluctuation Ratio Data in Case of Primary Air……...180
6.11 Comparison of Fluctuation Ratio Data in Case of Secondary Air……...181
6.12 Comparison of Expansion Ratio Data in Case of Primary Air……182
6.13 Comparison of Expansion Ratio Data in Case of Secondary Air……183
7.1 Scope of the Experiment……205
7.2 Factorial Design Analysis ……..206
7.3 Analysis of Mixing Index Data……..207
7.4 Selected Structures of Neural Network Models…….208

7.5 Comparison of (Factorial Design Data with Experimental Data) Mixing Index Data……209
7.6 Comparison of Mixing Index Data in the Case of Primary Air Supply…….210
7.7 Comparison of Mixing Index Data in the Case of Rod Promoter……..211
7.8 Comparison of Mixing Index Data in the Case of Disc Promoter…….212
7.9 Comparison of Mixing Index Data in the Case of Simultaneous Primary and Secondary air Supply ……..213
7.10 Comparison of (Output of ANN Approach with Experimental Data) Mixing Index Data……214

List of Figures

1.1 Changes in fluidization regimes with increasing gas velocity …… 11
2.1 Experimental set-up…….. 69
2.2 Taking observations for static bed height……. 69
2.3 Compressor……... 70
2.4 Compressor connected to the air accumulator……. .70
2.5 Silica gel column…….. 71
2.6 Rotameters and manometers connected with the set-up…….. 71
2.7 Distributor plates (6, 8 and 10% open area of cross-section of the column cross section)…… 72
2. 8 Distributor plate (12% open area of cross-section)……. 72
2.9 Fluidizer…… 73
2.10 Perspex flange and conical section of the column……. .74
2.11 Disc and rod types of promoters…… .74
3.1 Effect of distributor plate on Pressure drop for d_p = 0.000725m and h_s = 0.10 m …… 86
3.2 Effect of distributor plate on Pressure drop for d_p = 0.000725m and h_s = 0.08 m…… 86
3.3 Effect of bed height on fluctuation ratio for 8% distributor plate and d_p = 0.00055m…… 87
3.4 Effect of bed height on fluctuation ratio for 12% distributor plate and d_p = 0.000725m……. 87
3.5 Effect of particle size on fluctuation ratio for 10% distributor plate…… 88
3.6 Effect of distributor plate on fluctuation ratio for d_p = 0.013m and h_s = 0.01m ……. 88
3.7 Effect of distributor plate on fluctuation ratio for d_p = 0.00055m and h_s = 0.12m……..89
3.8 Effect of distributor area on fluctuation ratio for d_p = 0.00055m and h_s =0.12m……..89

3.9 Effect of distributor plate on expansion ratio for d_p = 0.00055m and h_s = 0.10m…… 90

3.10 Effect of particle size on expansion ratio for 12% distributor plate and h_s = 0.08m …… 90

3.11 Effect of bed height on expansion ratio for 12% distributor plate and d_p = 0.0013m……... 91

3.12 Effect of bed height on expansion ratio for 12% distributor plate and d_p = 0.000725m…….. 91

3.13 Comparison of pressure drop data…… 92

3.14 Comparison of fluctuation ratio data…… 92

3.15 Comparison of expansion ratio data……. .93

4.1 Effect of column diameter on fluctuation ratio for d_p = 0.00055m and h_s = 0.08m…….107

4.2 Effect of column diameter on fluctuation ratio for d_p = 0.00055m and h_s = 0.10m……107

4.3 Effect of column diameter on fluctuation ratio for d_p = 0.00055m and h_s = 0.12m…… 108

4.4 Effect of bed height on fluctuation ratio for d_p = 0.00055m and D_c = 0.127m……..108

4.5 Effect of bed height on fluctuation ratio for d_p = 0.00055m and D_c = 0.1524m……109

4.6 Effect of column diameter on expansion ratio for d_p = 0.00055m and h_s = 0.08m……109

4.7 Effect of column diameter on expansion ratio for d_p = 0.00055m and h_s = 0.10m…….110

4.8 Effect of column diameter on expansion ratio for d_p = 0.00055m and h_s = 0.12m…….110

4.9 Effect of bed height on expansion ratio for d_p = 0.00055m and D_c = 0.127m…….111

5.1 A typical three layer Neural Network……..131

5.2 Schematic representation of distributor plate and promoters……..131

5.3 Effect of bed height on fluctuation ratio for dolomite
(particle size = 0.000725m)…… 132
5.4 Effect of bed height on fluctuation ratio for dolomite
(particle size = 0.0013m in the case of rod promoter)…….132
5.5 Effect of bed height on expansion ratio for sand
(particle size = 0.00055m in the case of disc promoter)……..133
5.6 Effect of promoters on fluctuation ratio for sand
(particle size = 0.00055m and static bed height = 0.14m)…….133
5.7 Effect of promoters on fluctuation ratio for refractory brick
(particle size = 0.0013m and static bed height = 0.10m)……...134
5.8 Effect of promoters on expansion ratio for refractory brick
(particle size = 0.0017m and static bed height = 0.10m)……134
5.9 Effect of promoters on expansion ratio for refractory brick
(particle size = 0.0013m and static bed height = 0.14m)……135
5.10 Comparison of fluctuation ratio for un-promoted bed……. 135
5.11 Comparison of fluctuation ratio for rod promoter…….136
5.12 Comparison of expansion ratio for disc promoter…….136
6. 1 Schematic representation of the experimental set-up…….163
6. 1A Schematic representation of the experimental set-up……..163
6.2 Schematic representations of the air distributors…….164
6.3 Comparison of pressure drop……...164
6.4 Comparison of pressure drop for dolomite
(particle size = 0.00055m and static bed height = 0.14m)…….**165**
6.5 Comparison of pressure drop for dolomite
(particle size = 0.00055m and static bed height = 0.14m)…….. 165
6.6 Effect of bed height on fluctuation ratio for dolomite
(particle size = 0.000725m in the case of primary air)……...166
6.7 Effect of primary, and primary and secondary (simultaneous)
air on fluctuation ratio for dolomite of particle size = 0.0013 m ……166
6.8 Effect of primary, and simultaneous primary and secondary air
on fluctuation ratio for dolomite of particle size = 0.0013 m ……167

6.9 Effect of primary, and primary and secondary air (simultaneous) on expansion ratio for refractory brick of particle size = 0.0013 m……167
6.10 Comparison of fluctuation ratio for primary air supply……168
6.11 Comparison of fluctuation ratio for secondary air supply ……168
6.12 Comparison of expansion ratio for primary air supply……..169
6.13 Comparison of expansion ratio for secondary air supply……..169
6.15 Comparison of fluctuation ratio for primary air supply through statistical analysis approach……...170
6.16 Comparison of fluctuation ratio for secondary air supply through statistical analysis approach……...170
7.1 Effect of experimental conditions on jetsam concentration at different sample heights for laterite and iron particles at h_s = 0.08m and G_f=1.275 kg/m^2s……..198
7.2 Effect of experimental conditions on jetsam concentration at different sample heights for laterite and iron particles at h_s = 0.14m and G_f = 2.55 kg/m^2s …….199
7.3 Effect of experimental conditions on jetsam concentration at different sample heights for coal and iron particles at h_s = 0.08m and G_f = 1.275 kg/m^2s……199
7.4 Effect of experimental conditions on jetsam concentration at different sample heights for coal and iron particles at h_s = 0.14m and G_f = 2.55 kg/m^2s……..200
7.5 Effect of particle density on jetsam concentration at different sample heights for h_s = 0.14m and G_f=2.55 kg/m^2s in the case of disc promoter ……200
7.6 Effect of particle density on jetsam concentration at different sample heights for h_s = 0.14m and G_f=2.55 kg/m^2s in the case of rod promoter……..201
7.7 Effect of particle density on jetsam concentration at different sample heights for h_s = 0.14m and G_f=2.55 kg/m^2s in the case of primary air……..201
7.8 Effect of particle density on jetsam concentration at different sample heights for h_s = 0.14m and G_f=2.55 kg/m^2s in the case of simultaneous primary and secondary air supply……...202
7.9 Effect of mass velocity on jetsam concentration for coal and iron particles at h_s = 0.08m and particle size of 0.00055m in the case of disc promoter…….202

7.10 Effect of mass velocity on jetsam concentration for coal and iron particles at h_s = 0.08m and particle size of 0.00055m in the case of simultaneous primary and secondary air supply……203

7.11 Comparison of mixing index calculated from the same input data in the case of primary air supply……203

7.12 Effect of experimental conditions on jetsam concentration at different sample heights for dolomites of different sizes; 0.00055m and 0.0013m at h_s = 0.10m and G_f=1.445 kg/m^2s……..204

7.13 Effect of mass velocity on jetsam concentration at different sample heights for dolomites of different sizes; 0.00055m and 0.0013m at h_s = 0.08m in the case of simultaneous primary and secondary air supply……..204

List of Publications

Sl No	Title	Name of the Journal	Vol/Year
1	Dynamics of Gas-Solid Fluidized Bed of Irregular Particles through Secondary Fluidizing Medium	Indian Chemical Engineer	Vol. 49, 2 (2007) 134-142
2	Effect of Distributor Area on the Dynamics of Gas – Solid Fluidized Beds - A Statistical Approach	Indian Chemical Engineer	Vol. 49, 1 (2007) 01 - 10
3	Effect of Promoters on the Dynamics of Gas-Solid Fluidized Bed—Statistical and ANN Approaches	The journal of China Particuology	Vol. 5 (2007) 401-407
4	Effect of Column Diameter on Dynamics of Gas-Solid Fluidized Bed- A Statistical Approach	Indian Journal of Chemical Technology	2007 (Under review)
5	Mixing Characteristics of Binary Mixtures Using Promoters and Secondary Fluidizing Medium	Powder Technology	**2008 (In press)**
6	Effect of Secondary Fluidizing Medium on the Bed Fluctuation and Expansion in the Case of Gas-Solid Fluidization – Statistical and ANN Approaches	Chemical Engineering Journal	2007 (Under review)
7	Effect of Promoters and Secondary Fluidizing Medium on Mixing– Statistical and ANN Approaches	Asia Pacific Journal of Chemical Engineers	**2008 (In Press)**
8	Prediction of Bed Fluctuation and Expansion Ratios for Gas-Solid Fluidization in Cylindrical Beds	Indian Chemical Engineer	2007 (Under review)
9	A Mathematical Model for the Effect of Promoters on the Dynamics of Gas – Solid Fluidized Bed	Indian Journal of Chemical Technology	2006 (Under review)
10	Utilization of Mill Rejects of Power Plants through Circulating Fluidized Bed	International Conference on Impact of Industrialization on Environmental Pollution—Its	13-15 October (2006) 49 -51.

	Combustion—A Green Power Technology	Control and Abatement, at GIET, Gunupur, Rayagada, Orissa- 765 022.	
11	Effect of Baffles on Dynamics of Gas-Solid Fluidized Bed	Journal of Institution of Engineers (India)	Vol 81, March (2001) 32-34.

ABSTRACT

Many thermal power generating units are, of late, increasingly following the concept of circulating fluidized bed, and using secondary air in the fluidizer for the improvement of quality of fluidization and combustion, of course without understanding the real hydro-dynamics involved. Owing to the scarcity of good quality of coal and an ever-increasing demand for electricity for the complete combustion of low grade coal, the introduction of secondary air is one of the best solutions. Several sponge iron production units have been entangled with the problem of converting carbon into carbon dioxide.

Extensive experimental work and industrial applications provide unambiguous evidence that it is precisely these fluctuations that are responsible for extremely high values of effective coefficients of heat and mass transport to determine the dynamic properties of disperse mixtures. In general, large scale fluctuations strongly depend on various external conditions such as geometric properties of the disperse flow and quality of the gas distribution in fluidized beds. Whereas the small scale fluctuations depend merely on the local hydrodynamic situations and more inherent to macroscopically uniform states with no inner circulation and bubbles.

The objective of the present work is to improve the quality of fluidization through the design of the distributor plate, finding the effects of column internal diameter, using bed internals (promoters of rod and disc types), and gas distribution from the bottom of the column (called primary) and the side ports (called secondary air). The quality of fluidization has been expressed in terms of:

(i) pressure drop
(ii) fluctuation ratio
(iii) expansion ratio
(iv) mixing index.

Four distributors of varying open areas of cross-section, i.e., 6, 8, 10 and 12 % of column cross-sectional area, three cylindrical columns of different sizes, i.e. 0.099m, 0.127m and 0.1524 m, two different promoters, i.e. rod and disc types, air flow rate, i.e. primary and simultaneous primary and secondary have been used in the experimentation. During fluidization, the bed pressure drop, fluctuation and expansion data have been noted.

The use of secondary air in fluidized bed offers several advantages, viz., creation of oxidation and reduction zones in the fluidized bed combustor control over particle residence time, reduction of toxic gases like SO_X and NO_X in the flue gas, control over reaction rates, pneumatic transport, etc. Experiments have been carried out by supplying primary air from below (through the distributor plate) and secondary air (a fraction of air supplied through the side ports of column in the middle of each static bed) through a pipe having fine holes directed only towards the top of the column like a sparger pipe. In order to fluidize the entire bed material, the secondary air flow begins some time after the minimum fluidization condition is reached with the primary air only. A 50:50 mixture (by weight) has also been taken for the experimentation. Samples have been collected through the side ports and then separated through a magnetic separator. After knowing the jetsam and flotsam percentage, the mixing index values have been calculated.

The variables affecting pressure drop, fluctuation ratio, expansion ratio and mixing index are static bed height, particle density, particle size and mass velocity of air. Statistical, dimensional analysis and artificial neural network approaches have been adopted for the development of model equations for pressure drop, fluctuation ratio, expansion ratio and mixing index. The developed equations can be successfully utilized for different applications of the fluidized bed.

Introduction

Fluidization is an operation by which fine solids are transformed into a fluid-like state through contact with gas or liquid. It is a fluid-solid contacting technique, which has found extensive industrial applications over the last six decades. This method of contacting has a number of unusual characteristics, and fluidization engineering is concerned with its efforts to take advantage of this behaviour and put it to industrial uses.

Fluidization can be broadly of two types, viz, aggregative or bubbling and particulate. Particulate fluidization is mostly encountered in a liquid-solid system, while aggregative fluidization is a characteristic of the gas- solid type. In the case of liquid-solid contact, the action in the bed is strongly influenced by the particle size. The efficiency of aggregative fluidization depends upon the uniformity of fluidization, which is a result of good gas-solid contact. However, aggregative fluidization often results in inherent drawbacks like bubbling, channelling and slugging. This results in a poor gas-solid contact thereby affecting the quality of fluidization.

Fluidized beds have found extensive industrial applications as compared to fixed beds, and have become a versatile fluid-solid contacting device in chemical, biochemical and metallurgical industries. Extensive use of fluidization began in the petroleum industry with the development of fluid bed catalytic cracking. Presently, fluidization technique has found extensive applications in various fields like:

i. Physical operations
   a. Coating of metal with plastic
   b. Drying of solids
   c. Transportation
   d. Heating
   e. Adsorption, etc
ii. Chemical operations
   a. Coal gasification

b. Synthesis reactions
c. Cracking of hydrocarbons
d. Combustion and incineration
e. Carbonization and gasification
f. Roasting of sulphide ores
g. Reduction of iron oxide, etc

In order to improve the quality of fluidization and increase the range of applicability of gas-solid fluidized beds, different methods have been suggested. These methods include using bed internals like fixed packings, nozzles, probes, structural members, horizontal and vertical tubes for heat exchange, and different types of distributors and baffles/promoters of various geometries to break up the bubbles. The chief advantage of fluidization lies in the fact that solid particles are vigorously agitated by the fluid passing through the bed, thus resulting in little or no temperature gradient with highly exothermic or endothermic reactions. Fluidized beds are among the most important reactor systems in the chemical industry because of its excellent mixing ability and high heat and mass transfer rates, in situations of relatively low pressure drops.

In this present work, an attempt has been made to study the bed dynamics with a view to improving the quality of fluidization in gas-solid fluidized beds by providing different distributors, promoters, columns and types of airflow such as primary and simultaneous primary and secondary. It may be noted that earlier investigators have mainly stressed on the usefulness of primary air supply. Though some metallurgical industries, thermal power stations, etc. are using secondary air supply, they do so without having a considerable knowledge about its real bed dynamic aspects. It is these bed dynamic aspects that the present work aims at highlighting apart from other aspects of the primary air supply. The effect of all the above parameters has been studied for different bed heights, particle sizes, particle densities and mass velocities of air. Quantitative measurements of fluidization quality have been represented through pressure drops, fluctuation ratio, expansion ratio, and mixing index.

Literature Survey *Chapter - 1*

Plenty of literature exists on pressure drop, drag on fixed beds, hydrodynamics, baffle effects, distributor effects, and mixing and segregation. There are a good number of approaches and correlations/models describing the hydrodynamic behaviour of fixed and fluidized beds separately, but all of them have limitations of voidages and ranges of particle Reynolds numbers. There have also been a few attempts to generalize the equations describing the flow through fixed and fluidized beds. Almost all of these equations are based on the vast experimental data existing in the literature on fixed and particulate fluidized beds comprising spherical particles, viz., glass beads, aluminium, ceramics, urea, sago and non-spherical particles, viz., dolomite, refractory brick, sand, coal, iron, laterite, etc. The extensive literature survey reveals that more realistic generalizations based on experiments on commercial solids in particular are necessary in view of the importance of a wide range of porosities (voidages) and particle Reynold's numbers dealt with for the design of such gas-solid systems of commercial importance.

1.1 History of Fluidization and Its Applications

Winkler is credited with describing the first fluidized bed in 1921 and industrial fluidized bed applications began with a large-scale Winkler gasifier in 1926. This was the first application of coarse-powder fluidization. Table-1 lists the development highlights of fluidization science and technology since the first use of fluidized beds. Fluidized bed catalytic cracking of crude oil to gasoline (FCC) was commercialized in 1942, and is still the major application of fine-powder fluidization. Several catalytic applications such as acrylonitrile synthesis, phthalic anhydride and Fischer-Tropsch synthesis of fuels from coal-based gas extended the range following FCC.

In the 1970's, Lurgi commercialized the circulating fluidized bed (CFB) for coarse powders, which operates above the terminal velocity of all the bed particles. The bed inventory in a CFB is continually entrained out of the vessel, recovered and re-

circulated. Polyethylene began to be produced in fluidized beds, and is now a major application.

The 1980's saw commercialization of circulating fluidized bed combustion and production of polypropylene in fluidized beds. New areas of application were production of semiconductors and ceramic materials by chemical vapour deposition in fluidized bed and the use of liquid fluidized beds for biological applications.

Table 1.1 Development of Fluidized Bed Technology

Year	Applications
1920's	Winkler Gasifier-Coarse Powder Fluidization
1940's	Fluid Catalytic Cracking (FCC)-Fine Powder Fluidization Phthalic Anhydride Ore Roasting Drying
1950's	Fluid Hydroforming Fischer-Tropsch Acrylonitrile Spouted Bed
1960's	Three – Phase Biochemical Processes Bubbling Bed Combustors
1970's	Circulating Fluidized Beds (CFB's Lurgi & Battelle) FCC Risers High Density Polyethylene
1980's	Polypropylene CFB Combustors Semiconductors by Chemical Vapour Deposition. Fluidization of Group C Powders Immobilization of Enzymes/Mammalian cell Fermentation Waste Incineration.

1.2 Particle Characteristics

The most important properties for fluidization are particle size, particle density and sphericity. Fluidized bed design procedures require an understanding of particle properties.

1.2.1 Particle Size

The solid particles used in a fluidized bed are not identical in size and hence follow a particle size distribution. An average particle diameter, $d_{p,}$ is generally used for the design. It has been found that it is necessary to give relatively more emphasis to the lower end of the particle size distribution (fines), which can be done by using the surface mean diameter (average particle size) as given below:

$$d_{sv} = \frac{1}{\sum\left(\frac{X_i}{dp_i}\right)} \qquad \text{... (1.1)}$$

The surface mean diameter is the diameter of a sphere of the same surface area to volume ratio as the actual particle, which is usually not a perfect sphere. The surface mean diameter, (which is sometimes referred to as 'sauter mean diameter') is the most useful particle size correlation because hydrodynamic forces act at the outside surface of the particle.

1.2.2 Particle Density

Density is a characterization factor of a mass of solids. Bulk density is a measure of the weight of assemblage of particles divided by the volume they occupy. This measurement includes the voids between the particles and the voids within the porous particles. The term solid density is the density of the solid material if it has zero porosity. Fluid bed calculations generally used the particle density, ρ_p, which is the weight of a single particle divided by its volume (including the pores).

Mastellone and Arena (1999) studied the effect of particle size and density on solid distribution along the riser of a circulating fluidized bed and concluded that an increase in particle density from 1800 to 2600 kg/m^3 led to a higher solid concentration at the riser bottom.

1.2.3 Particle Shape Factor

The shape of an individual particle is expressed in terms of the sphericity, which is independent of particle size. The sphericity, ϕ, of a particle is the ratio of the surface area of a sphere, whose volume is equal to that of the particle, divided by the actual surface area of the particle. For a non-spherical particle, the sphericity is defined as:

$$\phi = \frac{6V_P}{d_P S_P} \qquad \ldots (1.2)$$

For a spherical particle of diameter, d_p, ϕ= 1.0.

1.2.4 Particle Regime

In 1973, Geldart classified powders depending on their fluidizability using air at the ambient temperature.

Group B particles are those, which have an average particle size exceeding about 100μm. Dense particles (e.g., glass, sand, ore, etc) are likely to be in group B. Many of the gas-solid reactions are operated industrially with this size group of particles. Group A particles are smaller and / or lighter than group B particles. Most manufactured catalysts are in this category, with particle sizes ranging from about 10 to 130 μm. These particles are cohesive due to inter-particle forces and when gas velocity is increased beyond U_{mf}, the bed continues to expand smoothly without the formation of bubbles.

Group C particles are smaller and lighter than Group A particles and are cohesive. They are usually less than 30μm in average particle diameter. The large external surface area and low mass of these particles produce large attractive forces. The particles do not flow well in pipes and are difficult to fluidize. Thus, gas flows through the bed in

channels are called “rat holes”. When fluid bed measurements are performed on group C systems at low gas velocities, a low pressure drop is observed since the gas is flowing in a channel without encountering most of the particles. Often group C particles can be fluidized by using a high gas velocity to overcome the cohesive forces between the particles or with the use of ‘fluidization aids’ such as large particles, fibrous carbon particles, etc.

Group D particles are large, of the order of 1.0 or more millimeters (1000μm) in average particle size. In a fluidized bed, they behave like the group B particles. High gas velocities are required to fluidize group D particles. It is often more economical to process them in spouted beds, where lower gas flow rates are required. Dried grains and peas, roasted coffee beans and metal ores, are these types of solids and are normally processed in shallow beds or in spouted beds. Further studies have led to a number of modifications and refinements of Geladarts Chart. For example, an A/C classification for particles was proposed in the uncertain transition zone between group A and group C particles. These solids flow well when fluidized (i.e. group A influence), but they permanently de-fluidize on any horizontal surface, thereby blocking and plugging the horizontal pipe (i.e. group C influence).

Though Geldart’s classification of solids is used most widely, different approaches have also been presented to define boundaries between groups of particles such as A/B boundary, A/C boundary, B/D boundary etc. Monceaux et al. (1986) have attempted to distinguish between groups A and C by considering the balance between hydrodynamic and cohesive forces. It gives the criterion that a powder belongs to group C if

$$\frac{10\left(\rho_P - \rho_g\right)d_p^3 g}{F_H} < 10^{-2} \qquad \ldots (1.3)$$

where F_H is the adhesive force transmitted on a single contact between two adjacent particles.

Jovanovic and Catipovic (1983) proposed a classification of particles according to the predominant mechanism of gas bypassing and wall-to-bed heat transfer.

1.2.5 Terminal Settling Velocity and Drag Coefficient

From the hydrodynamic force balance (considering gravity, buoyancy and drag but neglecting inter-particle forces), the single particle terminal settling velocity, U_t, can be written as:

$$U_t = \left[\frac{4gd_p(\rho_P - \rho_g)}{3\rho_g C_{ds}} \right]^{\frac{1}{2}} \quad \ldots (1.4)$$

Assuming spherical particles, the drag coefficient in the laminar, stokes low regime is

$$C_{ds} = \frac{24}{R_{eP}} \quad \ldots (1.5)$$

where the particle Reynolds number is defined as: $R_{ep} = (\rho_g U_g d_p / \mu_g)$.

The single (spherical) particle terminal velocity is then:

$$U_t = \frac{g(\rho_P - \rho_g) d_P^{\,2}}{18\mu_g} \qquad \text{for } R_{ep} < 0.4. \quad \ldots (1.6)$$

For large particles, C_{ds} is 0.43 and

$$U_t = \left[\frac{3.1(\rho_p - \rho_g) g d_p}{\rho_p} \right]^{\frac{1}{2}} \quad \text{for } R_{eP} > 500 \quad \ldots (1.7)$$

This equation indicates that for small particles, viscosity is the dominant gas property and for large particles, density is more important. Both equations neglected inter-particle forces.

The single particle terminal settling velocity is only a mathematical limit concept, since most gas-solid operations operate with high concentration of solids. Particles

interact strongly with each other thermodynamically such as by drag reduction due to shielding, and via inter-particle forces. The actual slip velocity between particle and gas becomes much higher than the single particle terminal settling velocity; in many cases, tens or even hundreds times higher.

In general, the slip velocity, or the 'effective terminal' velocity for a particle in suspension, U_t is:

$$U_{slip} = U_t^* = U_t . F(\varepsilon) \quad \text{... (1.8)}$$

where F (ε) is the drag coefficient, being a function of the voidage. For a batch fluidized bed, without any solid transport ($U_s = 0$, $U_{slip} = - U_g$), F (ε) can be written as:

$$F(\varepsilon) = \frac{(\rho_P - \rho_g)(1-\varepsilon)g}{U_{slip}} \quad \text{... (1.9)}$$

Equation 1.9 can be reduced to one variable (ε) equation, if U_{slip} is a unique function of ε. For a batch fluidized bed, U_{slip}, is related to voidage (ε) in various forms as given below:

(i) Richardson – Zaki type, represented by the work of Avidan and Yerushalmi: (1982) $U_{slip} = U_t * \varepsilon^{n-1}$ ...(1.10)

(ii) Matsen's equation (1982) for bubbling bed as:

$$U_{slip} = \frac{U_B(\varepsilon - \varepsilon_{mf}) + U_{mf}(1-\varepsilon)}{\varepsilon(1-\varepsilon)} \quad \text{... (1.11)}$$

(iii) Quadratic empirical equation by Leung and Jones (1976):

$$U_{slip} = a\varepsilon^2 + b\varepsilon + C \quad \text{... (1.12)}$$

The above bed expansion equations (U_{slip} versus ε relationships) are valid for dense phase gas-solid systems (up to a bed voidage of approximately 0.85). For lean phase fluidization, with higher bed voidage, the bed materials at higher gas velocity are expected to go out of the bed and so, would be required to be returned to the bed continuously. For such high voidage experiments, with solids circulating into and out of a circulatory fluidized bed, Avidan and Yerushalmi (1982) had shown that the ($U_{slip} - \varepsilon$) relationship was dependent on the solids circulation rate. Such dependence was explained by Matsen (1982), who noticed significant effects of acceleration and friction.

From the above discussion, it is apparent that the choice of the drag coefficient F (ε) is simple for the well–developed dense flow but for lean phase flow, no such relationship exists except the empirical equations presented by Avidan and Yerushalmi (which are solid velocity dependent). Nestor et al. (2002) developed a mathematical model for the description of the packed bed structure in the region close to the vessel wall for the case of uniform spherical packing. The model represented a better alternative to the traditional empirical relation for estimating radial voidage variations in the region close to the vessel wall.

1.3 Regimes of Fluidization and Their Characteristics

Various regimes of fluidization as defined by Yerushalmi and Cankurt (1979), and Grace (1982) are shown in Fig. 1.1. When a bed of solid materials resting on a distributor plate is contacted with an upward flow of gas in a fluidizer, the bed gradually transforms from packed to fluidized (bubbling) bed, then to slugging bed (if fluidizer diameter is small and L/D_C is high), followed by turbulent and fast fluidized bed (FFB) and finally to pneumatic conveying. As the gas flow rate is increased, the pressure drop across the bed increases and a point is reached when the pressure drop across the bed is just sufficient to support the weight of the particles in that section. This point is termed as incipient fluidization and the corresponding velocity is known as incipient or minimum fluidization velocity, (U_{mf}).

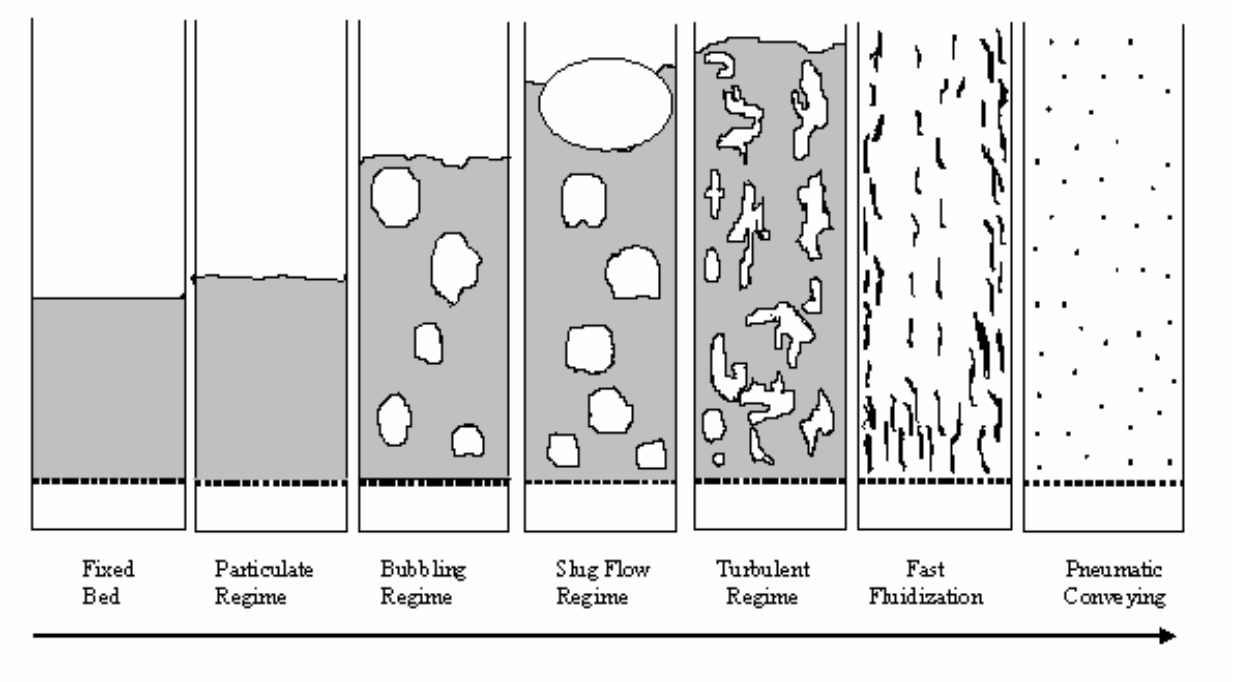

Fig 1.1 Changes in Fluidization Regimes with Increasing Gas Velocity

With further rise in gas velocity, the bubbling fluidization regime appears. The bubbles originate near the distributor, coalesce and rise to the surface and burst periodically with irregular pressure fluctuation of appreciable amplitude.

Various characteristic velocities such as minimum fluidization velocity (U_{mf}), minimum bubbling velocity (U_{mb}), minimum slugging velocity (U_{ms}), onset of turbulent fluidization (U_k), etc. are important in defining different regimes of fluidization.

The first regime map of a spout fluid bed has been reported by Nagarkati and Chatterjee (1974). Their regime map was based on visual observation, like most regime maps that have been published since then (He et al.; 1992, Sutanto et al.; 1985 and Vakovic et al.; 1984). But visual observation has two drawbacks— (i) non- intrusive visual access to the spout channel is usually difficult and sometimes, impossible and (ii) visual observations are difficult to capture in a quantitative measure.

Zhang and Tang (2004) based their regime mapping on spectral analysis of pressure drop fluctuations. This method only requires access to the bed with a pressure sensor, which is usually much less difficult than the visual access and produces quantitative results.

Littman et al. (1985) studied the overall behaviour of the bed but neglected the details of particle motion. Kawaguchi et al. (2000) and Link et al. (2004) used a discrete particle model to carry out a detailed study of the particle behaviour in a spouted bed and a spout fluid bed. They solved the volume averaged Navier–stokes equations for the gas phase, taking two-way coupling into account. Newton's second law was used to compute the motion of each individual particle.

Tsuji et al. (1993) modelled encounters between particles with a soft sphere approach; Hoomans et al. (1996) used a hard sphere approach. The soft sphere approach was most suited to model systems in which de-fluidized zones can prevail, whereas the hard sphere approach was more suited in vigorously fluidized systems, viz, spout-fluid beds because a steep velocity gradient in the gas phase is present near the spout region and the particle Reynolds numbers, especially near the spout mouth, were much higher than those encountered in regular (bubbling) fluidized beds.

Link et al. (2005) reported results of a combined experimental and simulation study on the various regimes, which could be encountered during spout-fluid bed operation. For most regimes, the developed model was able to predict the appropriate regime.

1.3.1 Minimum Fluidization Velocity, U_{mf}

The minimum fluidization velocity, U_{mf}, is a measure of superficial gas velocity at which there is a transition from fixed bed to fluidized bed. When a gas is passed upward through a packed bed of fine particles, the pressure drop increases with gas velocity according to Ergun's equation (Eq 1.13), until, on the microscopic scale, the

drag on an individual particle exceeds the force exerted by gravity, or, on the macroscopic scale, the pressure drop across the bed equals the weight of the bed per unit area.

$$\frac{\Delta P}{Z} = \frac{150(1-\varepsilon)^2 \mu_g U_g}{\phi^2 \varepsilon^3 d_p{}^2} + \frac{1.75(1-\varepsilon) U_g{}^2 \rho_p}{\varepsilon^3 \phi d_p} \quad \text{... (1.13)}$$

$$\varepsilon = \frac{\text{volume of bed - volume of solids}}{\text{volume of bed}}$$

$$= 1 - \frac{m_s \rho_b}{m_b \rho_s}$$

Since voids are empty spaces, $m_b = m_s$

$$\varepsilon = 1 - \frac{\rho_b}{\rho_s}$$

where ρ_b is the bulk density of the bed (= m_s/bed volume).

Numerous equations are available for calculating U_{mf} from the solid and gas properties: densities of solid and gas (ρ_p, ρ_f), particle diameter (d_p), sphericity (ϕ), and voidage at minimum fluidization condition (ε_{mf}). Those equations are usually modifications or transformations of the Ergun's equation, Eq 1.13, for flow in packed bed. Solving simultaneously the Ergun's equation and the theoretical maximum pressure drop across the bed (W/A_C) and through the observation that $\frac{(1-\varepsilon_{mf})}{\phi^2 \varepsilon^3{}_{mf}} \approx 11$ and $\frac{1}{\phi \varepsilon_{mf}^3} \approx 14$, Wen and Yu (1966) obtained the following equation, which is most widely used:

$$\text{Re}_{mf} = \sqrt{C_1^2 + C_2 Ar} - C_1 \quad \text{… (1.14)}$$

where Re_{mf} = Reynolds number at minimum fluidization,

Ar = Archimedes number $= \frac{\rho_g (\rho_s - \rho_g) g d_p^3}{\mu_g^2}$, and

C_1, C_2 are constants.

A large number of pairs of values for C_1 and C_2 have been proposed by various authors (Table 1.2) either to achieve greater generality or to fit specific experimental data. Coudere (1985) has published a very comprehensive review of the equation proposed for calculating U_{mf} along with the experimental conditions used to determine them.

Recently, there have been several studies on the independent effects of temperature and pressure on U_{mf}. In fine powders, U_{mf} decreases with an increase in temperature and is hardly affected by pressure. While in coarse powders, increased temperature causes an increase in U_{mf} and a decrease in pressure (King and Harrison, 1982). Svoboda and Hartman (1981) have also reported extensive data on U_{mf} at high temperature for limestone, lime, coal ash, etc. Rowe et al. (1982) found that the minimum fluidization velocity, $U_{mf,}$ was independent of gas density, but varied inversely as viscosity (approximately as $\mu^{-0.87}$) and increased with average particle size ($d_p^{1.8}$). Rincon et al. (1994) suggested a correlation for the prediction of minimum fluidization velocity of a multi-component system:

$\frac{1}{U_M} = \frac{1}{U_{12...n}} = \sum_{i=1}^{n} \frac{x_i}{U_i}$, where x_i and U_i (i = 1, 2, 3…) are the weight fractions and minimum fluidization velocities of individual component.

Murthy et al. (2003) studied the hydrodynamics of a stirred gas-solid fluidized bed and found that the minimum fluidization velocity increases with an increase in stirred speed, particle size and static bed height. Murthy and Chandrasekhar (2004) used statistical approach method to study the hydrodynamics of stirred fluidized beds and proposed the following equation for minimum fluidization velocity (U_{mf}):

U_{mf} =306.34+18.065A+8.5B+165.62D+…… +5.56BD … (1.15)

Felipe and Rocha (2007) analyzed an experimental method for the evaluation of minimum fluidization velocity in gas-solid fluidized bed based on pressure fluctuation measurements, in which U_{mf} is determined by the relationship between the standard deviation of pressure measurements and fluid velocity.

Liu et al. (2007) studied the minimum fluidization and minimum bubbling velocities of silica sand particles in air-blown micro-beds and found that an optimal combination of bed diameter and particle size in the range of static bed heights from 20 to 50 mm in micro-fluidized bed reactor devised to perform reactions with minimal suffering from external gas mixing and diffusion.

1.3.2 Minimum Bubbling Velocity

A special characteristic of gas-solid fluidized bed is the formation of gas bubbles, which are responsible for particle circulation and consequent high thermal conductivity of the bed but are detrimental both from chemical and mechanical points of view. For any fluidization unit, the velocity at which fluidization starts and slugging or enhanced rate of entrainment occurs are the two limits of the operating range.

An increase in gas flow beyond the minimum fluidization velocity can cause the extra gas to flow in the form of bubbles. The section of the bed outside the bubbles is called the emulsion phase ($U > U_{mf}$); here the fixed bed transforms into a bubbling bed with the fluid drag being given as:

$$F_D = \Delta P.A = A.L(1-\varepsilon)(\rho_s - \rho_g)g$$

$$\therefore \frac{\Delta P}{L} = (1-\varepsilon_{mf})(\rho_s - \rho_g)g \qquad \ldots (1.16)$$

Due to buoyancy force, a bubble rises through the emulsion phase and its size increases.

A bubble carrying some particles in its wake erupts at the bed surface throwing particles into the space above the bed, called the freeboard, beyond a certain height called the transport disengaging height (TDH). Particle disengagement is negligible and the flux rate of particles carried away is also known as the elutriation rate. The bubble rise velocity is given by:

$$U_b = K(U - U_{mf}) + 0.71(gD_b) \qquad \ldots (1.17)$$

where D_b is the bubble diameter.

Fine powders like cracking catalyst exhibit behaviour not found in coarse solids, viz., the ability to be fluidized at velocity beyond U_{mf} without the formation of bubbles. The bed expands, apparently smoothly and homogeneously, until a velocity is reached at which small bubbles appear at the surface, which resembles miniature volcanoes and disappears when the side of the column is gently taped. Further increase in gas velocity produces, at first, a slight increase in bed height followed by a reduction. Relatively large bubbles burst through the bed surface periodically, causing the bed to collapse rapidly. It then re-inflates slowly to collapse again as another swarm of bubbles burst through. The average of the velocities at which the bubbles appear and disappear, is called minimum bubbling velocity (or bubble point) and generally coincides with the minimum bed height for deep beds.

Geldart and Abrahamsen (1978) measured U_{mb} for 23 different particles (d_p = 20 – 72 μm, ρ_p = 1.1 – 4.6 g/cm^3), using ambient air, helium argon, Co_2 and Freon–12. They found that U_{mb}/U_{mf} was strongly dependent on the weight fraction of particles smaller than 45 μm (thus P_{45} μm) and for these systems, they proposed the following in SI units:

$$\frac{U_{mb}}{U_{mf}} = \frac{2300\rho_g^{0.13}\mu_g^{0.52}e^{(0.72P_{45})}}{d_P^{0.8}\left(\rho_P - \rho_g\right)^{0.93}} \qquad \ldots (1.18)$$

where P_{45} μm ≈ 0.1, and the powder is fluidized by air in ambient conditions, U_{mb} ≈100 d_P.

Simone and Harriott (1980) observed that U_{mb} was independent of particle density. King and Harrison's (1982) data showed agreement with the power on gas density of 0.06. Godard and Richardson (1966) indicated 0.1, when Guedes and Carvalho (1981) found an even higher dependency.

Piepers et al. (1984) presented data, which showed that power was dependent on the type of gas. Up to pressure equal to 15 bars, U_{mb} for a catalyst in hydrogen was affected very little, in nitrogen as $\rho_g^{0.13}$, and in argon as $\rho_g^{0.18}$.

Table 1.2 values of C_1 and C_2 obtained by various Authors

Authors	C_1	C_2
Wen and Yu (1966) (284 data points from the literature)	33.7	0.0408
Richardson (1971)	25.7	0.0365
Saxena and Vogel (1977) (Dolomite at high temperature and pressure)	25.3	0.0571
Babu et al. (1978) (correlation of reported data until 1977)	25.2	0.0651
Grace (1982)	27.2	0.0408
Chitester (1984) (Coal, char, Ballotini up to 64 bar)	28.7	0.0494
Thonglimp et al. (1984)	31.6	0.0425
Lucas et al. (1986)	29.5	0.0357
Lucas et al. (1986)	32.1	0.0571
Lucas et al. (1986)	25.2	0.0672

Rowe (1984) studied the effect of pressure on minimum fluidization and bubbling velocities in a bed of alumina powder, 175 × 125 × 500 mm^3 deep, which was fluidized with nitrogen. They found that for the alumina powder, U_{mb}/U_{mf} increased to about 1.25 to 30 bar, and thereafter did not increase so rapidly with pressure, while at atmospheric pressure, the 450 μm alumina behaved as Geldart group B particles, which started bubbling as soon as they were fluidized (e.g. $U_{mb}/U_{mf} = 1.0$).

For a given bed, the size of the bubble increases as the fluidizing velocity or the bed height is increased. If the bed is small in cross-section and deep, the bubble may

increase to a size comparable to the diameter or width of the bed. In this case, the bubble passes through the bed as a slug; this phenomenon is known as slugging. The criterion for slug formation (Yang, 1976), maximum stable bubble size (Geldart, 1986), etc are available in literature. Singh and Roy (2005) studied that under similar operating conditions minimum bubbling velocity and the fluidization index (the ratio of minimum bubbling velocity to minimum fluidization velocity, $\frac{u_{mb}}{u_{mf}} = \frac{2300\,\rho_g^{0.126}\,g^{0.934}\,\exp^{(0.176F)}}{dp^{0.8}\,g^{0.934}\,(\rho_p - \rho_g)^{0.934}}$;

F = fraction of powder less than 45 μm) are maximum in case of either semi-cylindrical conduit or hexagonal conduit for most of the operating conditions and minimum in case of square one.

1.3.3 Slugging

If the bed is small in cross-section and deep, the bubble may increase to a size of about the diameter of the bed. The bubble passes through the bed as slug. This is known as slugging and there is a large fluctuation of pressure drop across the bed.

1.3.4 Turbulent Bed.

A continuous increase in velocity may increase the bubble fraction and cause an expansion of the emulsion phase and thinning of the emulsion walls separating the bubbles. The bubble phase loses its identity due to rapid coalescence and break-up. These result in a violently turbulent bed with particles thrown into the free board above the highly diffused bed surface; such beds are called turbulent beds. The pressure drop across the bed fluctuates rapidly. The amplitude of fluctuation after reaching the peak value at the velocity Uc and then reduces to a steady value as the fluidizing velocity is increased further to the velocity U_K.

The transition from the bubbling to the turbulent bed does not take place suddenly. The onset of this transition starts at the velocity U_c and is completed at U_k. This approach about turbulent flow region has been reported in numerous studies (for

example, Lanneau; 1960, Kehoe and Davidson; 1971, Massimilla; 1973, Thiel and Potter; 1977, Canada et al.; 1978, Yerushalmi and Cankurt; 1979). Table 1.3 summarises available experimental data reported in this connection. In addition to the pressure fluctuation method, U_k was determined by methods like capacitance probe, X-ray photography and visual observation.

It has been reported by various investigators that besides the particle properties, the column size affects the value of U_k. This can be explained by the fact that the bubbling behaviour depends on the stable bubble size (and hence the pressure fluctuation and extent of turbulence), which again is inherently affected by the column size. By taking this effect into account, Bi and Fan (1992) proposed the following correlation:

$$\mathrm{Re}_k = 16.31 Ar^{0.136} \left(\frac{U_t}{\sqrt{gD_t}} \right)^{0.941} \quad \text{for Ar} \le 125 \qquad \text{... (1.19)}$$

For B and D groups of particle, U_k and U_{tr} do not appreciably vary since the group $\left(\frac{U_t}{\sqrt{gD_t}} \right)$ has an exponent of only 0.0015 and so, its contribution becomes insignificant. The equation in this case is:

$$\mathrm{Re}_k = 2.274 Ar^{0.419} \left(\frac{U_t}{\sqrt{gD_t}} \right)^{0.0015} \cong 2.274\ \mathrm{Ar}^{0.419} \qquad \text{... (1.20)}$$

which is the same as for Re_{tr}.

Considering the data of Kehoe and Davidson, Yang and Chitester (1988) suggested an equation for U_k, whose correlation coefficient is 0.9017. Thus,

$$U_k = 11.43 + 15.90 \ln \left(\frac{U_t}{\sqrt{gD_t}} \right) + 10.29 \ln \left(\frac{\rho_p}{\rho_g} \right) \qquad \text{... (1.21)}$$

where U_k is given in cm/s.

Table 1.3 Reported Experimental Data on U_k

Reference	Solids	d_p (μm)	D_t, (mm)	ρ_s (kg/m^3)	U_k, (m/s)	Re_k	Exptl. Methods
Kehoe & Davidson (1971)	Catalyst A	22	100	1100	0.11	0.16	XP
	Ballotini	22	100	2200	0.35	0.51	XP
	Ballotini	22	50	2200	0.40	0.59	CP
	Ballotini	22	620×6	2200	0.35	0.51	CP
	Catalyst B	26	100	1100	0.18	0.31	CP, XP
	Catalyst B	26	100	1100	0.32	0.30	CP
	Catalyst B	26	520×6	1100	0.17	0.56	CP
	Catalyst C	55	100	1100	0.44	1.61	XP
	Catalyst C	55	50	1100	0.50	1.83	CP
	Catalyst C	55	100	1100	0.50	1.83	CP
Massimilla (1973)	Catalyst	50	156	1000	0.35	1.18	CP
Carotenuto et al. (1974)	Catalyst	60	152	940	0.20	0.80	PF, CP
	Alumina	95	152	1550	1.00	6.33	PF, CP
Thiel & Potter (1977)	FCC	60	51	930	0.41	1.64	V
	FCC	60	102	930	0.22	0.88	V
	FCC	60	218	930	0.0225	0.09	V
Crescitelly et al. (1978)	Ludox	60	152	1400	0.33	1.32	PF, CP
Canada et al. (1978)	GB	650	300×300	2480	2.56	112.0	PF, CP
	GB	2600	300×300	2920	4.19	733.6	PF, CP
Yerushalmi & Cankurt (1979)	Dicalite	33	152	1670	1.07	2.35	PDF
	FCC	49	152	1070	0.61	1.99	PDF
	HFZ – 20	49	152	1450	1.37	4.48	PDF
	HFZ – 20	49	510×50	1450	1.07	3.50	PF
	Alumina	103	152	2460	2.74	18.81	PDF
	Alumina	103	510×50	2460	2.55	17.51	PF
	Sand	268	152	2650	5.50	98.27	PDF
Satija & Fan (1985)	GB	1000	102	2767	3.87	260.6	PF
	Alumina	2320	102	3537	5.34	834.6	PF
	Alumina	5500	102	3537	7.66	2840.0	PF
	Alumina	6960	102	3537	8.49	3984.1	PF
Rhodes & Geldart (1986)	Vermiculite	223	152	327	1.98	30.70	PDF
	Alumina	42	152	1015	1.38	4.03	PDF
	CBZ – 1	38	152	1308	1.44	3.80	PDF
	E – catalyst	40	152	1618	1.45	4.03	PDF
	FRF – 5	66	152	2335	2.52	11.55	PDF
	Sand	69	152	2665	2.80	13.42	PDF
Mori et al.	FCC	56	50	729	1.26	4.7	PF

(1988)	Catalyst Catalyst	78 134	50 50	2400 2400	2.10 2.30	10.9 20.6	PF PF
Leu et al. (1990)	Sand	90	108	2600	1.67	10.1	PF
Perales et al. (1990)	Sand FCC	120 – 1200 80	92 92	2650 1715	- 2.10	20-270 12.0	PDF PDF
Jiang & Fan (1991)	PE PE GB GB	3400 4500 2000 5000	102 102 102 102	1010 920 2500 2500	4.60 5.02 6.99 8.65	1037 1498 1001 2890	V V V V
Singh & Roy (2006)	Dolomite Coal	725 1290	101.6 101.6	2817 1600	1.16 1.14	- -	V V
Mohanty et al. (2007)	Dolomite Dolomite Dolomite	550 725 1290	99 99 99	2817 2817 2817	1.6 1.7 1.8	- - -	V V V

CP = Capacitance Probe PF = Pressure Fluctuation
XP = X – Ray Photography PDF = Pressure drop fluctuation
V = Visual GB = Glass beads FCC = Fluid cracking catalyst

1.3.5 Transport Velocity, U_{tr}

The transport velocity may be regarded as the boundary, which divides vertical gas-solid flow regimes into two stages. Below it, lies the bubbling (or turbulent) bed and above, the transport regime. Neglecting some carryover, the bubbling bed experiences no net flow of solids to use Lanneau's words: "The solids are in captive state". As against this, the transport regime encompasses states ranging from dilute phase flow to fast bed conditions. The transport velocity of FCC catalyst, for example, lies between 1.2 to 1.5 m/s.

To determine U_{tr}, several methods have been used, the most common being ($\Delta P/L$) plot against solids feed rate, G_s with fluid velocity as the parameter. Other methods include saturation carrying capacity (Chen et al., 1980; Li and Kwauk, 1980), bed expansion (Avidan and Yerushalmi, 1982), elutriability of particles from a fluidized bed (Le Palud and Zenz, 1989), the emptying time decay of bed particles (Han et al., 1985; Perales et al., 1990) and the pressure fluctuation (Leu et al., 1990; Yang et al., 1990).

1.3.6 Pneumatic Transport

Considering the up-flow of air plus a continuous feed of fine solids to a vertical tube, if the air velocity is high enough and the feed rate of solids is low enough, then all the solids will be carried up the tube as separate particles widely dispersed in the gas. Up to a point one may change the flow rates of gas or solid and still maintain a lean dispersed up-flowing gas-solid mixture. This regime is called pneumatic transport regime.

Conventional pneumatic conveying operates in this regime using high velocities (roughly 20 U_t for small particles) in order to prevent the setting of particles, particularly on horizontal surfaces of the flow system. The mass flow ratio of a solid to a gas is usually 1:20, which represents high voidage. Normally, for an air-sand system, this corresponds to a voidage of 0.98 to 0.99. There is no interaction between particles, hence, for enough downstream from the particle feed port, it can be assumed that $U_s = U_t$.

When gas velocity is reduced or solid flow rate is increased, a condition is reached where the character of the mixture changes drastically, with clumping, slugging and solid falling below the solids feed port. This transition is called the choking condition and it represents the limit of the pneumatic transport regime. Choking can lead to immediate shut down in conventional pneumatic conveying systems whose blowers are not designed to deliver a high enough pressure to handle fluidized transport of solids.

Pneumatic transport of solids can be classified into four different regimes: horizontal dilute phase flow, vertical dilute phase flow, horizontal dense phase flow and vertical dense phase flow. The parameter of solids / gas loading (kg of solid/ kg of gas) in the conveying line has often been used to distinguish between dilute and dense phase flow. Solids / gas loading of roughly 0.01 to 15 kg of solid/ kg of gas were used to denote dilute phase flow, while dense phase flow was characterized by solids / gas loadings of roughly 15 to over 200kg of solids per kg of gas.

In the design of industrial dilute phase pneumatic conveying systems, the main consideration is generally that of choosing the correct velocity at which to transport the solids. Too low a velocity will result in unacceptable unstable slugging flow; too high a velocity will result in excessive gas requirement and high pressure drops. The operation near choking will result in the minimum gas requirement for pneumatic solids transfer. It may be noted that the choking region is a very unstable one. A small decrease in the gas velocity near choking causes the average pressure drop in the lift line to rise rapidly. This is accompanied by large fluctuations in the pressure drop, as the line starts to choke.

The particle velocity in vertical dilute phase conveying line is an important parameter, because it determines the residence time of the solids in the line. The solids velocity in the conveying line is generally defined as $U_s = |U_g - U_t|$, where slip velocity, $U_{slip,}$ is often approximated by the terminal velocity of particles, U_t.

Hinkle (1953) used high speed photography to measure particle velocity and proposed a correlation:

$$U_s = U_g\left[1 - 0.1233 d_p^{0.3} \rho_p^{0.5}\right] \quad \text{... (1.22)}$$

It was shown that this relationship applied within ± 20%.

Nakamura and Capes (1973) carried out experiments in a 7.6 cm diameter riser using a wide variety of solids and concluded that slip velocity was often greater than the terminal velocity and the deviation between U_{slip} and U_t was greater for particle recirculation in the lift line.

Matsen (1981) proposed that the slip velocity is basically a function of the voidage of dilute flowing suspension. He had argued that as the voidage decreased (due to increased solids loading, for example), the slip velocity increased. He attributed this to cluster formation.

Many correlations were presented to determine the pressure drop in vertical pneumatic conveying lines such as Hinkle, 1953; Curran and Gorin, 1968; Konno and

Saito, 1969; Rose and Duckworth, 1969; Richard and Wiersma, 1973; Knowlton and Bachovchin, 1976; Leung and Jones, 1976; Yang, 1976 etc. The modified Konno and Saito (1969) correlation, given below, has been found to predict the pressure drop better than the other correlations.

$$\Delta P_T = \frac{U_g^{\,2}\rho_g}{2} + G_s U_s + \frac{2 f_g \rho_g U_g^{\,2} L}{D_t} + \frac{0.057 U_g \rho_g \theta L g}{\sqrt{g D_t}} + \frac{G_s L g}{U_s} + \rho_g L g \qquad \ldots (1.23)$$

Where, $U_s = U_g - U_t$, $\theta = G_s / U_g \rho_g g$

If the gas and solids are already accelerated in the lift line, then the first two terms of right hand side of Eq. 1.23 should be omitted from the calculation of pressure drop.

1.3.7 Phase Diagram

Various attempts have been made to plot the flow regimes of gas-solid suspensions on a single diagram in order to show how the regimes are related to each other. In practice, different workers had developed phase diagrams with widely differing viewpoints of the same phenomena by plotting constant value lines of a parameter of interest as a function of two of the independent flow variables. Properties treated included gas flow rate, solids flux, voidage, pressure gradient, loading ratio, etc for specific piping systems; aeration rate, slide valve opening and overall system pressure drop are also of importance.

The first so-called “fluid-solids phase diagram” was due to Zenz (1953). He plotted lines of constant particle mass flux on coordinates of gas velocity and pressure gradient, showing there in the moving bed, dense bubbling bed and dilute phase flow. His approach was rather qualitative, with practically no discussion on the theory or calculation procedure. But this phase diagram was considered as a good representation of gas particle flow.

Yerushalmi et al. (1978) presented a qualitative fluidization map for fine solids in a sufficiently large bed, where instability was absent. They plotted the slip velocity versus solids volumetric concentration, depicting different fluidization regimes, viz., bubbling, slugging, turbulent and fast fluidization. The figure showed that a narrow turbulent regime exists, which was distinct from the fast bed regime. According to them, in the bubbling and turbulent regimes, the fluidized bed density depended only slightly on the solid rate and the relationship between slip velocity and solid concentration was fairly unique.

Stromberg (1983) illustrated the regime of fast fluidization for silica and by plotting the particle concentration versus superficial gas velocity for different solids circulation rate. Matsen (1983) produced a flow regime diagram based on slip velocity. Squires et al. (1985) extended the work of Yerushalmi et al. (1978) and expanded their phase diagram by including the dilute phase pneumatic transport and choking. Kwauk et al. (1986) developed a phase diagram by presenting lines of constant mass flux on coordinates of gas velocity and voidage. They included dilute phase pneumatic transport in their diagram.

The phase diagram of Takeuchi et al. (1986) defined the fast fluidization region as one bounded by two gas velocities, which they termed U_{FF} and U_{DT}. The phase diagram was plotted for FCC particles with the coordinates of solids circulation rate and superficial gas velocity. U_{FF} was defined as the gas velocity below which solid circulation flux can not be maintained constant while decreasing the riser gas velocity. They defined this as the onset of fast fluidization regime. U_{DT} was characterized as the gas velocity at which pressure gradients measured at different heights in the riser, approach a constant value for a given solids mass flux.

Drahos et al. (1988) presented similar phase diagrams showing the fast fluidization. They defined U_{FF} as the locus of choking velocity, while U_{DT} as the locus of gas velocity at constant pressure drop. The locus meets at the point termed as transport velocity.

The phase diagram proposed by Rhodes (1989) is of the same form as that of Squires et al. (1985). The diagram clearly illustrates the relationship between bubbling / slugging fluidization, entrainment, dilute and dense phase pneumatic transport and the so-called fast fluidization regime. Using the existing correlations available in the literature, Rhodes flow regime diagram may be made quantitative, thereby enabling a flow regime to be identified with a first approximation from knowledge of powder properties, gas velocity, imposed solids flux, etc. Table 1.4 presents a summary on regime diagrams proposed by various authors.

Table 1.4 A Summary on Regime Diagram as Proposed by Various Authors

Authors	Plots	Remarks
Zenz (1953) (for general system)	Plots of pressure gradient vs velocity with constant lines mass flux	Qualitative approach, delineate co-current upward moving gas solid into moving bed, dense bubbling bed and dilute phase flow
Yerushalmi et al. (1978) (Based on experimental data on high velocity fluidization)	Plots of slip velocity vs solids concentration at constant solids mass flux	Packed bed, bubbling bed turbulent and fast fluidization on the same diagram
Kwauk et al. (1986) (Based on extensive experimental data on FFB using iron ore, Al_2O_3)	Phase diagram presenting lines of constant mass flux on co-ordinates of gas velocity and voidage	Bubbling, turbulent and fast fluidization regimes were shown in the map
Stromberg (1983) (for silica sand system)	Illustrated regions of fast fluidization by plotting the particle concentration Vs superficial gas velocity for different solids circulation rate	Identification of regimes of fast fluidization
Matsen (1983)	Slip velocity vs solids circulation rate with lines of constant voidage	Representation of bubbling, turbulent and fast fluidization regimes
Squires, Kwauk and Avidan (1985)	Extension of the earlier phase diagram developed by Yerushalmi et al. (1978)	The plot includes in addition to regimes depicted earlier, dilute phase pneumatic transport and choking
Takeuchi et al. (1986)	Proposed a flow regime diagram which defines limiting gas and solid velocity for fast fluidization	The phase diagram was plotted for FCC particles with the coordinates of solids circulation rate and superficial gas velocity
Rhodes (1989)	Both quantitative and qualitative diagram based on experimental data	Flow regime diagram for Gp A particles was drawn. It can be extended to Gp B particles as well. (Gp- Geldart particle Size)
Link et al. (2005)	Proposed flow regimes in a spout- fluid bed	A regime map for a 3D spout – fluid bed was composed employing spectral analysis of pressure drop fluctuations and fast video recordings.

1.4 Pressure Fluctuations

Pressure fluctuations have been observed in most fluidized beds and so, the need for evaluation of an index to judge the quality of fluidization was strongly felt. The extent of pressure fluctuations in a fluidized bed is a complex function of particle properties, bed geometry, pressure in the bed, and flow conditions of the fluid.

Many investigators (Leva, 1959; Kang et al., 1967; Lirag and Littman, 1971; Verloop and Heertjes, 1974 and Fan et al., 1981) have studied pressure fluctuations of fluidized beds. Leva (1959) measured the pressure drop and power requirements in a stirred fluidized bed and found that the pressure drop and power consumption at the minimum fluidization velocity decreases and increases respectively with increase in stirrer speed.

Hiby (1967), and Lirag and Littman (1971) measured pressure fluctuations and concluded that a change in bed height, resulting from bubble eruption at the bed surface, causes pressure fluctuations. However, Kang et al. (1967) concluded that changes in gas flow and porosity of dense phase (owing to the action of bubbles) are the principal sources of pressure fluctuations.

Moritomi et al. (1980) measured pressure fluctuations in the plenum chamber as well as in the bed, and derived an equation for predicting the angular frequency of natural oscillations of the fluidized bed.

Rowe (1984) conducted an experiment with a typical powder fluidized by nitrogen at room temperature and found that with increase in particle size the pressure drop also increases but, U_{mf}, is virtually independent of pressure.

Chitester et al. (1984) studied the characteristics of fluidization at high pressure and suggested a modification of the Ergun equation, i.e.

$$(R_e)_{mf} = \sqrt{\left((28.7)^2 + 0.0494\,Ar\right)} - 28.7 \qquad \text{... (1.24)}$$

Also for different solid materials, the expanded bed height does not always increase with increased pressure at a given gas velocity. At the highest pressure, the bed appears to be homogeneous, and excellent mixing at high pressure is confirmed.

Recently an analysis of pressure fluctuations in the plenum chamber and the free board has been made for the diagnosis of the fluidized state (Kage et al., 1991; Kaneko et al., 1988). Lee and Kim (1988) studied pressure fluctuations in turbulent beds. Leu and Lan (1990) studied pressure fluctuations in two-dimensional beds at an elevated temperature. Hong et al. (1990) used statistical properties to interpret the data on pressure fluctuations.

Schnitzlein and Weinstein (1988) have used instantaneous pressure signals along the bed height as the basis of their study in order to determine the characteristics of the flow within these regions and the dependence of these characteristics on the axial position in each region and on the flow parameters, i.e. superficial gas velocity and solid rate.

Satija et al. (1985) have studied pressure fluctuations and the choking criterion for vertical pneumatic conveying of fine particles. Perales et al. (1990) have determined transition velocities from bubbling to fast fluidization, and proposed correlations to predict those.

Bai et al. (1996) studied flow structure in the FFB based on fluctuation behaviour of solid momentum. Measurements of time series of local solids momentum were carried out along the radial direction at both upper and lower parts of the bed for different operation conditions. By examining the probability distribution, standard deviation and power spectral density function, flow behaviour in the upper dilute region was found to be much different from that in the bottom dense region. By changing the experimental conditions (gas velocity, solids circulation rate, etc), detailed micro-scale structures (flow

patterns) were identified by Bai et al. (1996) based on measured pressure signals from different radial positions.

Yerushalmi and Cankurt (1979) were the first to make a detailed study on fluidization at a high velocity. The bed used by them comprised a 15.2 cm × 8.5 m height FFB connected to a 34.3 cm slow bed through a transfer line. The pressure drop was shown as a function of gas velocity, U_g and solid circulation rate, G_s. From the $(\Delta P/L) - U_g - G_s$ plots, they determined the velocity of transition from turbulent to fast fluidization. Different materials like dicalite 4200 (2 - 16μm), FCC catalyst (0 - 300μm), and hydrated alumina (40 – 200 μm) were used for their investigation.

Li et al. (1981) obtained extensive data on pressure drop and voidage in a FFB, while using a wide range of materials such as alumina powder (54μm), iron pyrites (56μm), FCC catalyst (56μm), and iron powder (105 μm). A series of plots of voidage versus height of the riser was presented from the axial voidage distribution and they demonstrated the coexistence of the dense and dilute phases.

Li et al. (1988) also investigated the effects of operating pressure on axial voidage profile in FFB, on the basis of the solid rate and saturation carrying capacity of flowing gas, K*, free operating zones had been identified, viz,

$G_s = K^*$, $G_s < K^*$ and $G_s > K^*$.

For $G_s = K^*$, they found an s-shaped voidage profile.

Zhang et al. (1985) obtained pressure drop across a bed of 0.11m, 0.10m, 0.8m height, where FCC catalyst and two kinds of silica gel particles were fluidized. Arena et al. (1986) had compared the hydrodynamic behaviour of two CFB fast columns of 0.041m and 0.012m ID. FCC catalyst and glass beads of 70μm and 90μm average sizes were used as the bed solids. Axial profiles of solid volume fraction (1- ε) were directly measured by means of quick closing values and then compared with those estimated from experimental pressure drop data. They proposed a diffusion / segregation mechanism for

the gas-solid interaction phenomena in the bed so as to predict the derivatives of S-shaped axial voidage profile at the inflection point.

Brereton and Stromberg (1986) found that the pressure profiles could be approximately described with the help of the following equation i.e.

$$P = a\, Z^{b} \qquad \ldots (1.25)$$

where a and b are constants.

Kato et al. (1989) measured the particle hold up and axial pressure drop in a FFB, they observed that particle hold up was affected by the superficial gas velocity, the circulation rate of particle, particle Reynold's number, tube diameter and axial distance from the distributor.

Kojima et al. (1989) measured the velocity and static pressure profile in a CFB and observed that the particle velocity at the axis of the bed increased with an increase in the gas velocity.

Choi et al. (1990) measured the axial voidage profile in a cold model CFB of sand particles. Correlations were presented to predict solids circulation rate and axial voidage profile in the bed.

Kato et al. (1991) investigated the local structure of gas particle flow in a CFB. Three typical fluidization modes namely, pneumatic transport, fast fluidization and turbulent fluidization were investigated from the pressure measurements. They further observed that the particle hold up distribution was affected by the superficial gas velocity and circulation rate.

Zaho et al. (2001) proposed a model for the determination and predictability of dynamics underlying pressure fluctuations by measuring and analyzing the time series of pressure signals at different locations in a bubble bed.

Murthy et al. (2003) found that the pressure drop at minimum fluidization velocity increases with particle size due to increase in weight of particles and decreases with stirring speed.

Murthy and Chandra Sekhar (2004) used statistical approach method to study the hydrodynamics of stirred fluidized beds and proposed the following equation for pressure drop at minimum fluidization velocity (ΔP_{mf}).

$$\Delta P_{mf} = 1823.75 - 53.75A + 716.25\ B + 93.75\ D - 33.75\ BD \quad \ldots (1.26)$$

Zhong et al. (2006) studied the hydrodynamic characteristics of a spout-fluid bed and found that the bed pressure drop appears as a spouted bed characteristic when increasing the spouting gas velocity and keeping the fluidizing gas velocity constant, while it appears a fluidized bed characteristic when increasing the fluidized gas velocity and keeping the spouting gas-velocity constant.

Cabral et al. (2006) studied the pressure drop in a vibrating and non-vibrating fluidized bed and found that the pressure drop across the fluidized bed with no vibration is more than that at vibrating condition.

Wu et al. (2007) studied the multi resolution analysis of pressure fluctuations in a gas solid fluidized bed and found that polyethylene particle systems have quite different bubble properties compared with glass beads under comparable operating conditions. The combination of statistical, chaos and wavelet analysis proved to be an effective method to characterize multi-scale flow behaviour in the gas-solids fluidized bed.

Felipe and Rocha (2007) studied the minimum fluidization velocity of gas-solid fluidized beds by pressure fluctuation measurements and found that both the methods of pressure measurements i.e., absolute and differential showed to be appropriate.

Sau et al. (2007) studied the minimum fluidization velocities and maximum bed pressure drops for gas-solid tapered fluidized beds and concluded that there is a porosity effect on minimum fluidization velocities where it is negligible on pressure drop.

1.5 Quality of Fluidization

Quality of fluidization can be measured in three different ways.

1.5.1 Uniformity Index Method

In this method, the fluidized bed density is expressed in terms of capacitometer voltage by means of dielectric properties of the elements in the bed. The condenser plates are placed inside the fluidized column and variations in the bulk densities are noted for a definite time interval. Uniformity index is defined as the ratio of the percentage of average deviation to the frequency. For perfect uniformity, the index has a value of zero.

1.5.2 Fluctuation Ratio

The fluctuation ratio (r) is defined as the ratio of the highest to the lowest bed heights occupied by particles of the fluidized bed for any particular gas flow rate over the minimum fluidization velocity. Fluctuation is a common phenomenon in aggregative fluidization. Different types of baffles/promoters are used to reduce the fluctuation ratio by which the quality of fluidization can be improved.

Leva (1959) correlated fluctuation ratio to bed characteristics by the following equations:

$r = e^{m} \frac{\left(G_f - G_{mf}\right)}{G_{mf}}$, where "m" is related to particle diameter.

Beyond a certain limiting value of $\frac{\left(G_f - G_{mf}\right)}{G_{mf}}$, the fluctuation ratio pertaining to the slugging zone follows smoothly from the non-slugging zone.

Singh (1995) studied the effect of various system parameters on fluctuation ratio in the case of non columnar beds, viz, square, hexagonal, cylindrical and semi-cylindrical ones. Correlations for fluctuation ratio are given below:

1. Cylindrical bed

$$r = 1.95\left(\frac{d_p}{D_c}\right)^{0.04}\left(\left(\frac{D_c}{h_s}\right)\times\left(\frac{\rho_f}{\rho_s}\right)\right)^{0.04}\left(\frac{G_f - G_{mf}}{G_{mf}}\right)^{0.05} \quad \text{... (1.27)}$$

2. Semi-cylindrical Bed

$$r = 2.323\left(\frac{dp}{dc}\right)^{0.08}\left(\left(\frac{Dc}{hs}\right)\times\left(\frac{\rho_f}{\rho_f}\right)\right)^{0.04}\left(\frac{G_f - G_{mf}}{G_{mf}}\right)^{0.07} \quad \text{… (1.28)}$$

3. Hexagonal Bed

$$r = 2.3\left(\frac{dp}{dc}\right)^{0.06}\left(\left(\frac{Dc}{hs}\right)\times\left(\frac{\rho_f}{\rho_f}\right)\right)^{0.05}\left(\frac{G_f - G_{mf}}{G_{mf}}\right)^{0.06} \quad \text{... (1.29)}$$

4. Square Bed

$$r = 2.55\left(\frac{dp}{dc}\right)^{0.09}\left(\left(\frac{Dc}{hs}\right)\times\left(\frac{\rho_f}{\rho_f}\right)\right)^{0.04}\left(\frac{G_f - G_{mf}}{G_{mf}}\right)^{0.05} \quad \text{... (1.30)}$$

Under similar operating conditions, fluctuation ratio has been observed to be maximum in the case of square bed and minimum in the case of semi-cylindrical bed. It has also been concluded that for a bed of a given configuration, the fluctuation ratio becomes maximum at a particular velocity ratio (G_f/G_{mf}) and thereafter it either decreases or remains constant with velocity ratio.

Singh and Roy (2006) predicted the fluctuation ratio in cylindrical and non-cylindrical beds and concluded that the fluctuation ratio is the maximum in the case of square bed and is the least in the case of semi- cylindrical bed. Fluctuation ratio becomes

maximum at a particular gas mass velocity ratio (G_f/G_{mf}), for a particular bed and then it decreases due to slug formation or remains constant at higher velocity ratio.

1.5.3 Expansion Ratio

A packed bed expands as the upward fluid velocity through it is increased beyond the point of minimum fluidization and further expansion depends on particle size, design of bed structure and particularly on the design of distributor. Higher bed expansion occurs in the case of lower particle sizes and densities.

Singh and Singh (2003) predicted the expanded bed height and suggested the two equations (1.31) and (1.32) for the lower and upper sections of the column i.e.

$$R_{lower} = 4.7\times10^{-2}\left[\left(R_{ep}\right)^{0.58}\left(\frac{dp}{Dt}\right)^{1.25}\left(\frac{\rho_P}{\rho_f}\right)^{-0.49}\right] \quad \text{... (1.31)}$$

$$R_{lower} = 5.166\times10^{-3}\left[\left(R_{ep}\right)^{0.782}\left(\frac{dp}{Dt}\right)^{-1.407}\left(\frac{\rho_P}{\rho_f}\right)^{0.39}\right] \quad \text{… (1.32)}$$

Kumar and Roy (2002) developed a correlation for bed expansion ratio (R) for a bed having distributor and promoter as:

$$\left(R-1\right) = G_R{}^{0.726}\left(\frac{\rho_s}{\rho_f}\right)^{0.533}\left(\frac{Ado}{Ac}\right)^{0.183}\left(\frac{dp}{do}\right)^{0.284}\left(\frac{hs}{Dc}\right)^{-0.396}\left(\frac{D_e}{D_c}\right)^{0.229} \quad \text{... (1.33)}$$

1.6 Baffles/Promoters

Different types of bed internals used for improving the quality of fluidization are nozzles, immersed objects, slotted baffles, horizontal baffles and vertical baffles. Baffles are used to ensure good contact between gas and solid with high rates of heat and mass transfer with a low pressure drop. The use of a suitable promoter and a proper gas distributor can improve fluidization quality by minimizing slugging and reducing the size

of bubbles and their growth. The gas-solid fluidization is characterised by the formation of gas bubbles, and the quality of fluidization can largely be improved by introducing different types of promoters and distributors of varying cross-sectional areas and configurations.

Balakrishnan and Rao (1975) studied the effect of horizontal screen disk baffled fluidized beds on pressure drop and minimum fluidization velocity.

Hoffmann (2000) studied the manipulating fluidized beds by using internals for fine powders and found that it is possible to manipulate the working of fluidized beds to some extent by introducing internals into the bed. Zin et al. (1980, 1982) observed an improvement in the breaking up of bubbles and the circulation of the solid particles in the fluidized bed with pagoda-shaped promoters.

Chandra et al. (1981) compared the effect of multi-baffled fluidized bed with the fluidized bed having concentric baffle with a spacing of 18.5mm and concluded that the fluidization in concentric baffled beds were non-uniform.

Krishnamurthy et al. (1981) studied the effect of horizontal baffles on the quality of fluidization. Stirrer type baffles were used by Agarwal and Roy (1987), co-axial rod and co-axial disk type promoters by Kar and Roy (2000) for their studies on fluidization quality. Mohanty and Singh (2001) predicted the fluctuation ratio of a baffled bed in a column 15 cm in internal diameter and found that the use of circular and rod types of promoters can reduce the fluctuation ratio

Kumar and Roy (2002) studied the effect of co-axial rod, disk and blade types of promoters on bed fluctuation in gas-solid fluidized bed with varying distributor open areas and found that bed fluctuation decreases significantly with an increase in the blockage area of a rod or disk promoter as compared to the un-prompted beds.

Kumar and Roy (2002) studied the effect of rod, disc and blade promotes on bed expansion in a gas-solid fluidized bed and found that the reduction in bed expansion in the case of the promoted bed over the un-promoted one can be attributed to the breaking up of bubbles and controlling their size and growth.

Kumar and Roy (2004) compared the minimum bubbling velocities in the case of promoted and un-promoted beds and found that bubble formation is delayed in the case of a bed having more peripheral contacts with the fluid flow.

Kumar and Roy (2004) further found that correlations using dimensional analysis approach and ANN-models can satisfactorily be used for prediction of the bed expansion ratio, and the ANN method represents the system behaviour more accurately than the dimensional analysis approach. Kumar and Roy (2005) also predicted a model equation by using the statistical approach method for the bed fluctuation ratio as under:

$$r = 1.668 + 0.309X_1 + 0.173X_2 - 0.114X_3 + 0.112X_4 + 0.079X_1X_2 \quad \ldots. (1.34)$$

Kumar and Roy (2007) studied the effect of distributor to bed pressure drop ratio in promoted gas-solid fluidized beds and found that the ratio increases with mass velocity, decrease in open area and promoters.

Patil et al. (2007) studied the influence of internal baffles in a fluidized sand bed and found that the bed without baffles exhibited distinctive segregation of chopped switchgrass particles and the annular plate baffles are provided with best mixing of biomass as compared to half-circle plate baffles.

Kato et al. (2007) studied the average mass transfer coefficient on the baffles increased with decreasing baffle diameter. The number of baffles, the clearance between the vessel wall, the position of the baffles and the position of the impeller did not affect the average mass transfer coefficient. The local mass transfer coefficient of the baffles near the impeller was larger than those in other positions.

1.7 Distributor

In order to improve the quality of fluidization, changing the distributor design is one of the important areas in fluidization. A number of investigations have stressed the use of distributors to improve fluidization quality and to increase the range of applicability of gas-solid fluidized beds.

Ghose and Saha (1987) showed that the quality of bubble formation is strongly influenced by the type of distributor. Saxena et al. (1979) studied the effect of distributors on a gas-solid fluidized bed. Swain et al. (1996) used distributors having three mm diameter orifices distributed in two zones, viz, the annular and central with equal open area, which varied from 2.28 to 6.36 percent of the column cross-section and proposed the following correlation for bed fluctuation ratio (r):

$$r = 3.316\left(\frac{G_f}{G_{mf}}\right)^{0.60}\left(\frac{\rho_s}{\rho_f}\right)^{-0.23}\left(\frac{Ado}{Ac}\right)^{0.24}\left(\frac{dp}{D_C}\right)^{-0.43}\left(\frac{hs}{Dc}\right)^{-0.35}\left(\frac{A_A}{A_c}\right)^{-0.11} \quad \text{... (1.35)}$$

Kumar et al. (2002) studied the effect of varying distributor areas on fluctuation ratio and proposed the following correlation:

$$(r-1) = 0.24G_R^{\,0.85}\left(\frac{\rho_s}{\rho_f}\right)^{0.63}\left(\frac{Ado}{Ac}\right)^{0.21}\left(\frac{dp}{d_C}\right)^{0.41}\left(\frac{hs}{Dc}\right)^{-0.36} \quad \text{… (1.36)}$$

Sathiyamoorthy and Horio (2003) studied the influence of aspect ratio and distributor plate in a gas fluidized bed and concluded that the distributor type, aspect ratio and operating velocity influence the quality of fluidization. The critical aspect ratio was found to fall linearly with the increasing operating velocity.

Luo et al. (2004) studied the effect of gas distributor on performance of dense phase high density fluidized bed for separation and found that the higher the pressure

drop of gas distributor is, the better the fluidizing performances of the fluidized bed is. The fluidized bed with uniform and stable density for mineral separation can be formed when pressure drop of the gas distributor is higher than its critical value.

Sasic et al. (2006) studied the effect of air distributor on pressure drop and found that there is a strong interaction between the fluidized bed and the air supply system in the form of pressure waves. For low air-distributor pressure-drop a clear interaction was found, whereas with a high air-distributor pressure-drop, pressure fluctuations in the plenum were not related to the fluctuations in the bed.

Zhong et al. (2006) have found that the total bed pressure drop appears a spouted bed characteristic when increasing the spouting gas velocity and keeping the fluidizing gas velocity constant, while it appears a fluidized bed characteristic when increasing the fluidizing gas velocity and keeping the spouting gas velocity constant.

Mohanty et al. (2007) have found that a distributor plate having 10% open area of cross-section of the column cross-section gives a better result in terms of bed pressure drop, fluctuation and expansion as compared to 6%, 8% and 12% open areas of cross-section.

1.8 Solid Segregation and Mixing

When dissimilar solids exhibiting a wide size distribution and /or different solid densities are fluidized, segregation of solids will always occur. The solid particles that are easier to fluidize usually tend to be elutriated by the fluidization gas, and others sink and remain at lower levels. As a result, a dynamic equilibrium is obtained between mixing and segregation tendencies.

Solid mixing studies combined with gas flow analysis are the basis for designing a commercial fluidized bed reactor. Bubbling gas fluidized beds containing mixtures of powders of different physical properties often exhibit a vertically non-uniform blend of

particles. Thus, although fluidized beds are known for their good mixing characteristics, the solid mixing is often incomplete, when particles of different properties are present in the bed. A knowledge of the degree and the rate of segregation are important for several reasons. In most industrial applications of fluidized beds, good mixing is required for uniform product quality or in order to avoid de-fluidization of parts of the bed. In some applications, on the other hand, the tendency for segregation is utilized, e.g. continuous removal of a product.

Heertjes et al. (1967) suggested that the wake material scattered into the freeboard by the bursting of the bubbles contribute significantly to the horizontal movement of solids.

Chen and Keairns (1975) presented a limited amount of data on the rate of separation in a char-dolomite system with an unmixed starting mixture. Kondukov and Sosna (1965) and Gelperin et al. (1967) suggested a phase equilibrium diagram for a segregating mixture. Using the analogy between a fluidized bed and a liquid, they suggested that a segregating mixture in a fluidized bed resembled a liquid-solid system. Yang and Keairns (1982) studied the rate of particle separation in a fluidized bed 7.0 cm in diameter, using crushed acrylic plastic particles as flotsam and dolomite particles as jetsam, and concluded that for mixtures of different jetsam concentrations, the rate and degree of particle separation were different but generally completed in less than 15 sec. in all cases.

A qualitative model for particle mixing in a gas-solid fluidized bed has been developed by Gibilaro and Rowe (1974) based on four physical mechanisms, viz, overall particle circulation, interchange between the wake and bulk phases, axial dispersion and segregation. Rowe et al. (1965) presumes that solid mixing will occur by inter-particle diffusion or eddy diffusion as in true fluids. Some solids are seen flowing up and others flowing down the bed due to the bubble rise. This up-low and down-flow of solids with an interchange between streams is the basis for various counter-flow models. Solid exchange between the bubble wake and the emulsion phase is one of the fundamental rate

processes that largely affect the direct mixing in fluidized beds (Chiba and Kabayashi, 1977; Kunii and Levenspiel, 1969).

Nienow et al. (1972) studied the role of particle size, density and air flow rate on the segregation or de-mixing behaviour in a gas-solid fluidized bed, and concluded that a fairly wide particle size difference can be tolerated, while small density difference leads to ready settling of denser particles.

Most gas fluidized beds, which are operated under bubbling or turbulent fluidization regime (e.g., Grace,1986), contain non-uniform mixtures of particles. For some applications, the solid materials (reactants or catalysts) are composed of different sizes and/or densities (e.g. Rowe and Nienow, 1975). For some other cases, the binary or multi-solids systems are formed by addition of other kinds of solids that differ from the original bed material (Aznar et al., 1992). To increase the fines holdup, and thus to improve the contacting between gas and fine solids in transport risers, addition of coarse particles may also be necessary (Bi et al., 1992). Research of the hydrodynamic behavior of fluidized beds containing non-uniform mixtures of particles has, so far, largely been confined to binary mixtures. Most of these research works have paid attention to solids mixing and segregation that are expected in relatively lower gas velocities (Rowe and Nienow, 1975, Nienow et al., 1987). Many authors also studied the minimum and completed fluidization velocities of such systems (Rowe and Nienow, 1975, Aznar et al., 1992). Note that most successful applications of binary solids fluidized beds, however, involved higher gas velocities in which well-defined bubbling or slugging has given way to a more turbulent hydrodynamic region. Research at higher gas velocities, however, is scarce.

Nicholson and Smith (1966) studied the axial mixing of particles differing in density in a fluidized bed and proposed a first order rate equation to describe the progress of mixing in short mixing time. Fan and Chang (1979) studied the fluidization and solid mixing characteristics of very large particles, where bubble or slug induced drift and gross solid circulation appeared to be the predominant solid mixing mechanism.

Hoffmann (2000) concluded that it is possible to manipulate the working of fluidized beds to some extent by introducing internals into the bed. The particle segregation can be enhanced by reducing axial mixing. Vibration can be brought into the heart of the bed by applying the vibration to internals spanning the bed vessel. Powders which are not fluidizable in a conventional bed can be fluidized in this way.

Gibilaro and Rowe (1974) derived a mathematical model, which correctly predicts the uniform composition of the upper part of the bed, the sharp discontinuity of a segregated bottom layer of pure jetsam and the way this layer is destroyed, as the segregating tendency is overcome by the mixing process.

Rowe and Nienow (1976) studied the mixing aspects by using two separate layers of flotsam and jetsam as a starting mixture.

Kroger et al. (1980) studied particle mixing in a centrifugal fluidized bed, and found that bubbles are the primary mechanism causing radial mixing for Geldart-B and Geldart-D particles.

Miyauchi (1981) studied the vertical mixing of solids in vigorously fluidized beds (u_o>10 cm/s) of fine Geldart A solids and found that the mixing data could reasonably be represented by the dispersion model.

$$D_{sv} = 12\, u_o^{1/2}\, d_t^{0.9} \qquad \text{... (1.37)}$$

Avidan and Yerushalmi (1985) found that the dispersion model better represented the mixing during turbulent fluidization, where the bed looked close to homogeneous, but fitted the data poorly when the bed was in the bubbling regime.

Buyevich and Kapbasov (1994) studied the momentum equations governing the vertical distribution of particles of different sizes and densities in a homogenous fluidized bed and concluded that the conventional kinetic theory of gaseous mixtures, in which

such force differences are usually not taken into account and the relative motion is conceived as a phenomenon of purely diffusional origin, is sufficient for expressing mean forces of the interaction between the particulate components in terms of observable variables.

Beeckmans and Agarwal (1994) developed a correlation for predicting segregation for both steady and unsteady state conditions.

Fan et al. (1986) studied the particle mixing in the radial direction of a gas-solid fluidized bed by using heated particles as the tracer particles. A stochastic model has been proposed mechanistically for the lateral mixing of particles in a shallow gas-solid fluidized bed, which results in the so-called Uhlenbeck – ornstien process.

Fan and Chen (1990) reviewed the major developments in solid mixing since 1976 (170 publications) and concluded that there are three major categories of characterization of states of solid mixtures, rates and mechanisms of solid mixing processes, and design and scaling up of mixers or blenders.

The homogeneity of a solid mixture or the distribution of its composition is often quantified by a mixing index. Most of the available mixing indexes are based on the variance of the concentration of a certain key component among spot samples. These mixing indexes can only depict the microscopic behaviour of a solid mixture. The definition of a geometric mixing index based on the number of contact points between different solid phases has lately received increased attention.

Three major mechanisms such as diffusion, convection and diffusion-convection have been proposed and numerous mathematical expressions for the rates of solid mixing based on these mechanisms have been developed. While many of the models and expressions are deterministic or macroscopic, some resort to stochastic approaches. The particle mixing system is neither macroscopic nor microscopic, but mesoscopic in nature.

Fan et al. (1990) proposed a mathematical equation for a size variant, equal-density system of particles for mixing Index (I_M):

$$I_M = k \times \left(\frac{\overline{dp}}{d_F} \right)^k \times \left(\frac{U}{U - U_F} \right)^n \quad \ldots (1.38)$$

where k = co-efficient of correlation, $\overline{dp}$ = average particle size of the mixture (m), d_F = diameter of the floatsam particle (m), U = superficial velocity of the fluidizing medium (m/s), U_F = minimum fluidization velocity of the floatsam particles(m/s) , 'k' and 'n' are the exponents of the variables.

Quin et al. (1999) studied particle mixing in rotating fluidized beds and concluded that for particles of the same material, the two layers of particles do not mix until bubbles appear. This result was similar to that of Menon and Durian (1997), who concluded that bubbles are responsible for the bulk motion of particles in a conventional fluidized bed. After the critical minimum fluidization velocity, particles inside the bed start to move radially, and mixing occurs rapidly. Bubbles are a strong source of particle motion, and the bed becomes totally fluid-like. It was also found by Quin et al. (1999) that the minimum bubbling velocity is dependent on the size and density of the particles. For Geldart-B particles, the minimum bubbling velocity is equal to the minimum fluidization velocity, whereas for Geldart-A particles, the minimum bubbling velocity is larger than the minimum fluidization velocity. Mixing occurs due to the difference in densities and fluidization properties of the two layers.

Gilbertson and Eames (2001) found that when horizontal bands are present, the thickness of the lower layer of coarse particles decreases with increasing gas flow rate depending on the proportion of fine particles in the bed. The efficiency of mixing by the bubbles in the fluidized bed is very much less then that expected from gas bubbles in liquid.

Gravina et al. (2004) compared the segregation porosity of the pumice fall and of the pyroclastic flow starting material and concluded that only the former exhibits significant segregation.

Lu and Hsiau (2005) studied discrete elementary method to simulate the behaviour of granular mixing in vibrated beds and concluded that the mixing rate constants, calculated from the time evolutions of mixing degree, increase with the increasing electrostatic number in power law relations.

Sahoo and Roy (2005) studied the mixing characteristics of homogeneous binary mixture of regular particles (Geldart BD type) in a cylindrical gas-solid fluidized bed and developed a mathematical model for calculation of mixing index (I_M):

$$I_M = C_j \times \left(\frac{W}{J} \right) \quad \text{... (1.39)}$$

where C_j = concentration of jetsam particles at any height in the bed (amount of jetsam particles in the sample drawn at a height in kg/amount of that in the original mixture in kg), W = weight of the total bed material (kg), and J= weight of the jetsam particles taken in the bed (kg).

Chaikittisilp et al. (2006) analysed solid particle mixing in inclined fluidized beds and found that an increase in the angle of inclination leads to a decrease in the fraction of the bed becoming fluidized due to the tendency of flowing air, which prefers to leave the bed through the region with the lower resistance. A 10° inclination could give rise to enhanced degree of mixedness of solid particles as compared to other inclination conditions.

Patil et al. (2007) studied the influence of internal baffles on mixing characteristics and found that the bed without baffles showed distinctive segregation nature. Internal baffles were effective in altering the fluidization of biomass-sand mixtures. Of the baffles tested, the annular plate showed the best performance as compared to coil and half-circle plate baffles.

Mujumdar et al. (2007) investigated the mixing and segregation behaviour of granular flow in a sectorial shaped container, subjected to sinusoidal oscillations and found that the mixing and segregation of particles takes place in a particular range of frequency zone.

1.9 Artificial Neural Network (ANN)

Computing through neural networks is one of the recently growing areas of artificial intelligence. Neural networks are promising due to their ability to learn highly non-linear relationship. Wasserman (1989) and Chitra (1993) define artificial neural network (ANN) model as a computing system made up of a number of simple, highly inter-connected nodes or processing elements, which process information by its dynamic system response to external impacts.

The back propagation algorithm for training has been used in the present study. Several applications of artificial neural networks for modelling of non-linear process system and subsequent control have been reported by Singh and Mohanty (2002).

Kumar and Roy (2004) found that correlations using dimensional analysis approach as well as ANN-models can satisfactorily be used for the predication of bed expansion ratio, and the ANN method represents the system behavior more accurately than the dimensional analysis approach.

In the present case, a software package for artificial neural network in Mat lab version, 6.5.0.180913 a release 13 has been used for back propagation algorithm. Three typical layers, viz, (i) input (I), (ii) hidden and (H) (iii) output (O) have been chosen. Four nodes in the input layer, three neurons in the hidden layer and one node in the output layer have been taken.

1.10 Statistical Approach

The method of experimentation is based on statistical design of experiments (Factorial Design Analysis) in order to bring out the interaction effect of variables, which could not be found otherwise by conventional experimentation, and to explicitly find out the effect of each of the variables quantitatively on the response. The number of experiments required for development of a model equation from factorial design is considerably less in comparison to conventional experimentation.

Davis (1978) found that factorial design analysis can be used for many experimental situations for the experimentation of the effect of varying two or more factors .The various variables of a factor examined in an experiment are known as levels. The set of levels of all factors employed in a given trial is called the treatment or treatment combination. The numerical result of a trial based on a given treatment is called the response corresponding to the treatment.

When there are no interactions, the factorial design gives the maximum efficiency in the estimation of the effects. When interaction exists, their nature being unknown, a factorial design is necessary to avoid misleading conclusions. In the factorial design, the effect of a factor is estimated at several levels of the other factors, and the conclusion holds over a wide range of conditions.

The effect of a factor is the change in response produced by a change in the level of a factor. When a factor is examined at two levels only, the effect is simply the difference between the average response of all trials carried out at the first level of the factor and that of all trials at the second level.

Table 1.5 Sign for Calculating the Effects (Yate's Technique)

Total	A	B	C	D	AB	AC	AD	BC	BD	CD	ABC	ABD	ACD	BCD	ABCD
+	-	-	-	-	+	+	+	+	+	+	-	-	-	-	+
+	+	-	-	-	-	-	-	+	+	+	+	+	+	-	-
+	-	+	-	-	-	+	+	-	-	+	+	+	-	+	-
+	+	+	-	-	+	-	-	-	-	+	-	-	+	+	+
+	-	-	+	-	+	-	+	-	+	-	+	-	+	+	-
+	+	-	+	-	-	+	-	-	+	-	-	+	-	+	+
+	-	+	+	-	-	-	+	+	-	-	-	+	+	-	+
+	+	+	+	-	+	+	-	+	-	-	+	-	-	-	-
+	-	-	-	+	+	+	-	+	-	-	-	+	+	+	-
+	+	-	-	+	-	-	+	+	-	-	+	-	-	+	+
+	-	+	-	+	-	+	-	-	+	-	+	-	+	-	+
+	+	+	-	+	+	-	+	-	+	-	-	+	-	-	-
+	-	-	+	+	+	-	-	-	-	+	+	+	-	-	+
+	+	-	+	+	-	+	+	-	-	+	-	-	+	-	-
+	-	+	+	+	-	-	-	+	+	+	-	-	-	+	-
+	+	+	+	+	+	+	+	+	+	+	+	+	+	+	+

The model equations are assumed to be linear and the equations take the general form.

$$Y = a_0 + a_1A + a_2B + a_3C + a_4D + a_5AB + \ldots + a_{14}BCD + a_{15}ABCD \quad \ldots (1.40)$$

The coefficients are calculated by the Yate's technique, i.e. $a_i = \sum \alpha_i y_i / N$ ... (1.41)

where A, B, C and D are factorial design symbols; a_i is the coefficient; y_i is the response; α_i is the level of variables and N is the total number of treatments which is equal to 2^n (n = number of variables or dimensionless groups which affect the response or output).

In order to find any coefficient i.e., a_0, a_1, $a_2 \ldots$ a_{15}, each column of Table 1.5 will be considered for the α value i.e., +ve or –ve. From the experimental findings the response values i.e., y_i will be taken (maximum and minimum level).

Kumar and Roy (2005) predicted a model equation by using the statistical approach method for the bed fluctuation ratio as under:

$$r = 1.668 + 0.309X_1 + 0.173X_2 - 0.114X_3 + 0.112X_4 + 0.079X_1X_2 \quad \ldots. (1.42)$$

Brunet and Merlen (2007) studied the statistical approach of sedimentation flows and concluded that this method can be successfully utilized for analyzing the hydrodynamic interaction effects.

Scope of the present work

From the foregoing analysis of the literature survey, it has been observed that quite a few correlations exist for predicting the behaviour of gas-solid fluidized beds. High velocity fluidization is a useful tool for efficient gas-solid contacting process, and can be used in chemical reactors, both for catalytic and non-catalytic reactions. During 1980s and early 1990s, considerable research efforts were made to understand the bed dynamic aspects of different fluidized beds, identifying the various regimes of fluidization and their characteristic velocities.

Earlier, investigations were mainly concerned with the study of the behaviour of overall hydrodynamics of fast fluidized bed, and the pressure profiles along the riser height were used to measure the cross-sectional average voidages. Localised variation in solid movement was interpreted in terms of fluctuation ratio, expansion ratio and instantaneous pressure fluctuation at the wall.

In view of the existing gap in the knowledge, an attempt has been made in the present thesis to obtain experimental data for pressure drop, fluctuation ratio, expansion ratio and mixing characteristics in a gas-solid fluidized bed. A detailed investigation of experimental conditions related to the improvement of quality of fluidization has been studied.

i) Experiments have been extensively carried out to study the effectiveness of distributors in order to improve the quality of fluidization. The flow rates, bed heights, particle sizes, densities and distributors of varying open areas, i.e. 6%, 8%, 10%and 12% of the column cross-sectional area have been used. Correlations for bed pressure drop at minimum fluidization velocity, fluctuation ratio and expansion ratio have been developed by using statistical approach.

ii) The effect of column diameter on fluctuation ratio and expansion ratio has been studied for different particle sizes, particle densities and bed heights.

iii) Studies have been made to investigate the effect of rod and disc types of promoters on fluctuation ratio and expansion ratio through statistical, dimensional analysis and ANN approaches.

iv) Extensive investigations have been made to study the effect of secondary fluidizing medium on fluctuation ratio, expansion ratio and pressure drop. Artificial Neural Network (ANN), dimensional analysis and statistical approach models have been developed for primary as well as simultaneous primary and secondary fluidizing mediums.

v) Detailed studies on mixing and segregation characteristics of gas-solid fluidized beds for promoted, primary and simultaneous primary and secondary have been made. Correlations for mixing index have also been developed for different conditions of the gas-solid fluidized bed, which are useful tools for scientific understanding as well as design of fluidized bed reactors, fluidized bed combustors, etc.

Notations

A	Cross-sectional area of the column, m^2
A_r	Archimedes number, dimensionless
D_c	Diameter of column, m
d_p	Particle diameter, m
d_{sv}	Average particle size, m
F_D	Drag force, N
G_f	Fluid mass velocity, kg/m^2s
G_{mf}	Minimum fluidization mass velocity, kg/m^2s
L	Length of column, m
R_e	Reynolds's number, dimensionless
u_{mf}	Minimum fluidization velocity, m/s
u_p	Particle velocity, m/s
u_s	Settling velocity, m/s
U_t	Terminal velocity, m/s
V_{Dt}	Velocity at onset of fast fluidization, m/s
V_{FF}	Velocity at fast fluidization, m/s
V_g	Gas velocity, m/s
V_s	Solid velocity, m/s
u_{mb}	Minimum bubbling velocity, m/s
u_c	Critical velocity, m/s
u_k	Fluidization velocity in turbulent bed, m/s

Greek Symbols

ρ_p	Particle density, kg/m^3
ρ_g	Density of gas , kg/m^3
μ_g	Gas viscosity, kg/m s
Δ_p	Pressure drop, N/m^2

References

1. Agarwal, S.K. and Roy, G.K., A Qualitative Study of Fluidization Quality in Baffled and Conical Gas-solid Fluidized Bed, Journal of Institution of Engineers India, 68 (1987) 35.

2. Arena, U., Cammarota, A. and Pistane, L., High Velocity Fluidization Behaviour of Solid in a Laboratory Scale Circulating Bed, Circulating Fluid Bed Technology, Vol. I, P. 119, P. Basu, ed., Pergamon Press, Toronto (1986).

3. Avidan, A. A. and Yerushalmi, J., Bed Expansion in High Velocity Fluidization, Powder Technology, 32 (1982) 223.

4. Avidan, A., Ph.D. Dissertation, City College of New York, 1980; Avidan, A. and Yerashalmi, J., AIChE J., 31(1985) 835.

5. Aznar, M.P., Gracia-Gorria, F.A. and Corella, J., Minimum and maximum Velocities for Fluidization for Mixtures of Agricultural and Forest Residues with a Second Fluidized solids, Int. Chem. Eng., 32 (1992) 95.

6. Bai, D., Shibuya, E**.,** Masuda, Y., Nakagawa, N. and Kato, K., Flow Structure in a Fast Fluidized Bed, Chem. Eng. Sci., 51(6) (1996) 957.

7. Balakrishnan, D and Raja Rao, M., Pressure Drop and Minimum Fluidization Velocity in Baffled Fluidized Beds, Indian Journal of Chemical Technology, 13 (1975) 199.

8. Beeckmans, J.M. and Agarwal, R., Studies on Transport Processes in a Segregating Fluidized Bed, Powder Technology, 80 (1994)17.

9. Bi, H. and Fan, L. S., Existence of Turbulent Regime in Gas-Solid Fluidization, AIChE J., 38(2) (1992) 297.

10. Bi, H.T., Jiang, P.J., Jean, R.H. and Fan, L.S., Coarse Particle Effects in a Multisolid Circulating Fluidized Bed for Catalytic Reactions, Chem. Eng. Sci., 47 (1992) 3113.

11. Brereton, C. and Stromberg, L., Some Aspects of the Fluid Dynamic Behaviour of Fast Fluid Beds, Circulating Fluidized Bed Technology, Vol. I, P. 133, P. Basu, ed., Pergamon Press, Toronto (1986).

12. Brunet, Y. and Merlen, A., Statistical Approach of Sedimentation Flows, Powder Tech., 175 (2007) 3.

13. Buyevich, A.Yu. and Kapbasov, SH. K., Random Fluctuations in a Fluidized Bed, Chemical Eng. Sci., 49 (1994) 1229**.**

14. Cabral, R.A.F., Telis-Romero, J., Telis, V.R.N. and Finzer, J. R. D, Journal of Food Engineering (online 24 October 2006).

15. Canada, G.S., McLaughlin, M.H. and Staub, F.W., Flow Regimes and Void Fraction Distribution in Gas Fluidization of Large Particles in Beds without Tube Banks, AIChE Symp. Ser., 74(176) (1978) 14.

16. Carotenuto, L., Crescitelli, S. and Donsi, G., High Velocity Behaviour of Fluidized Beds: Characterization of Flow Regimes, Ing. Chim. Ital., 10 (1974)185.

17. Chaikittisilp, W., Taenumtrakul, T., Boonsuwan, P., Tanthapanichakoon, W. and Charinpanitkul, T., Analysis of Solid Particle Mixing in Inclined Fluidized Beds Using DEM Simulation, Chem. Eng. J., 122 (2006) 21.

18. Chandra Y., Rao, N.J., Paneser, P.S. and Krishna, N. G., Gas-solid's Fluidization in Baffled Beds, Indian Chemical Engineer, XXIII, 48, (1981).

19. Chen, B. Y., Li, F. W., Wang, S. and Kwauk, M.,The Formation and Prediction of Fast Fluidized Beds, Chemical Metallurgy (in Chinese), 4 (1980) 20.

20. Chen, J.L.P., Keairns, D.L. and Can., J., Chem. Eng., 53 (1975) 395.

21. Chiba, T. and Kabayashi, H., J., Chem. Eng. of Japan, 10 (1977) 205.

22. Chitester, D.C, Kornosky, R.M., Fan, L. S. and Danko, J. P., Characteristics of Fluidization at High Pressure, Chem. Eng. Sci., 39 (1984) 253.

23. Chitra, S.P., Use Neural Network for Problem Solving, Chemical Engineering Progress, (April 1993) 44.

24. Choi, J.H., Yi, C.K. and Son, J.E. Axial Voidage Profile in a Cold Model Circulating Fluidised Bed, 3rd Int. Conf. on Circulating Fluidized Beds Proc., p. 4-9, Nagoya, Japan(October 15-18,(1990).

25. Coudere, J.F., Fluidization, J. F. Davidsons, R.Cliff, and D.Harrison, eds., Academic Press, 2nd edition (1985).

26. Crescitelly, S., Donsi, G., Russo, G. and Clift, R. High Velocity Behaviour of Fluidized Beds: Slugs and Turbulent Flow, Chisa Conference, Prague1 (1978).

27. Curran, G.P. and Gorin, E., Prepared for Office of Coal Research, Contract No.14-01-0001-415, Interim Report No. 3, Book 6, Washington, D.C. (1968).

28. Davis, O.L., Design and Analysis of Industrial Experiments, 2nd ed., Longman Publishers, (1978).

29. Drahos, J., Cermak, J., Guardani, R. and Schugerl, K., Characterization of Flow Regime Transition in a Circulating Fluidized Bed, Powder Technology, 56 (1988) 41.

30. Fan,L.T., Ho, T.C., Hiraoka, S. and Walawender, W.P., Pressure Fluctuation in a Fluidized Bed, AIChE J.,27(3) (1981)388.

31. Fan, L.T. and Chang, Y.,The Canadian Journal of Chem. Engg. (1979) Feb, 57.

32. Fan, L.T., Chen, YI – Ming and Lai, F.S., Recent Developments in Solids Mixing, powder Tech., 61 (1990) 255.

33. Fan, L.T., Song, J.C.and Yutani, N., Radial Particle Mixing in Gas-solids Fluidized Beds, Chem. Eng. Sci., 41 (1986) 117.

34. Felipe, C.A.S. and Rocha, S.C.S., Powder Tech., 174 (2007) 3.

35. Geldart, D., and Abrahamsen, A.R., Powder Technology,19 (1978) 133.

36. Geldart, D., Gas Fluidization Technology, 9. 88, John Wiley and S.Chitester, eds., (1986).

37. Gelperin, N.I., Einstein, V.G., Nosov, G.A., Mamoshkina, V.V.and Rebrova, S.K, Teor. Osn, Khim, Tekhnol. 01 (1967) 383.

38. Ghosh, A and Saha, R.K., Multiorific Distributor Plates in a Gas – solid fluidized bed, Indian chemical Engineers, 29 (1987) 50.

39. Gibilaro, L.G. and Rowe, P.N., A Model for a Segregating Gas-fluidized Bed, 29 (1974) 1403.

40. Gilbertson, M.A. and Eames, I. Segregation Patterns in Gas – fluidized Systems, Journal of Fluid Mechanics, 433 (2001) 347.

41. Godard, K., and Richardson, J.F., Fluidization, Instn.Chem.Engrs.Symp.Ser., 126(1996).

42. Grace, J.R., Fluidized Bed as Chemical Reactors, in Gas Fluidization Technology, D. Geldart, Ed., Wiley, New York (1986) 287.

43. Grace, J.R., Handbook of Multiphase System, P. 8-1, G. Hetsroni, ed., Hemisphere, Washington,D.C.(1982).

44. Gravina,T., Lirer, L., Marzocchella, A., Petrosino, P. and Salatino, P., Fluidization and Attrition of Pyroclastic Granular Solids, j. of volcanology and Geothermal Research,138 (2004).

45. Guedes de Carvalho, J.R.F., The Stability of slugs in Fluidized Beds of Fine Particles,Chem. Eng. Sci., 36 (1981) 1349.

46. Han,G.Y., G.S. Lee,and S.D.Klim, Hydrodynamic of a Circulating Fluidized Bed,Korean J.Chem. Eng., 2 (1985) 141.

47. He. Y.L., Lim, C.J. and Grace, J.R., Spout bed and spout – fluid bed behaviour in a column of diameter 0.91m, Canadian Journal of Chemical Engineering, 70 (1992) 848.

48. Heertjes, P.M., Nie, L.H. de and Verloop, J., in Proc., Int. Symp. on Fluidization, A.A.J. Drinkenburg, ed., P.47b, Netherlands Unv. Press, Amsterdam (1967).

49. Hiby, J.W., Peirodic Phenomena Connected with Gas-Solid Fluidization,Int. Symp. Of Fluidization Proc., P. 99, Eindhoven, Netherland Univ. Press, Amsterdam (1967).

50. Hinkle, B.L., Ph.D. Thesis. Georgia Institute of Technology (1953).

51. Hoffmann, A.C., Fanssen, L.P.B., and Prins, J., Particle Segregation in Fluidized Binary Mixtures, Chem. Eng. Sci., 48 (1993) 1583.

52. Hoffmann, Alex .C, Manipulating Fluidized Beds by Using Internals, Fluidization with Baffles, NPT process Technology, No – 7 (2000) 20.

53. Hong, S.C., Jo, B.R., Doh, D.S.and Choi, C.S.Determination of Minimum Fluidization Velocity by the Stastical Analysis of Pressure Fluctuations in a Gas-Solid Fluidized Bed, Powder Tech., 60 (1990) 215.

54. Hoomans B.P.B., Kuipers, J.A.M., Briels, W.J. and Swaaij, W.P.M.V., Discrete Particle Simulation of Bubble and Slug Formation in a Two–dimensional Gas – fluidized Bed a Hand Sphere Approach, Chemical Engineering Science, 51 (1996) 99.

55. Jovanovic, G., and Catipovic, N.,A New Approach in Classifying Solids in Building Gas-fluidized Beds,Fluidization, Vol. IV, P.69, D. Kunii and R. Toei., Engineering Foundation (1983).

56. Kage, H., Iwasaki, N., Yamaguchi, H. and Matsuno, Y. Frequency Analysis of Pressure Fluctuation in Fluidized Bed Plenum,J. Chem. Eng. Japan, 24(1), 76(1991).

57. Kaneko, Y., Yutani, N. and Horio, M., Asian Conf. On Fluidized-Bed and Three Phase Reactors proc., Tokyo, 14(1988).

58. Kang, W.K., Sutherland, J.P. and Osberg, G.L., Pressure Fluidizations in a Fluidized Bed with and Without Screen Cylindrical Packings,Ind. Eng. Chem.Fund.,6 (1967) 499.

59. Kar S. and Roy, G.K., Effect of co – axial rod promoters on the dynamics of a batch gas – solid fluidized bed, Indian chemical Engineer, section A, 42 (2000) 170.

60. Kato, K., Shibasaki, H., Tamura, K. Arita, S. Wang, C. and Takarada, T.,Particle Holdup in a Fast Fluidized Bed,J. Chem. Eng. Japan, 22(2), (1989) 130.

61. Kato, K., Takarada, T., Tamura, T. and Nishino, K. Particle Hold-up Distribution in a CFB, Circulating Fluidized Bed Technology,Vol. III, p.145,P.Basu,M.Horio,and M. Hasatani, eds., Pergamon Press, Toronto(1991).

62. Kato, Y., Kamei, N., Tada, Y., Iwasaki, Y., Nagatsu, Y., Iwata, S., Lee, Y. and Koh, S., Transport Phenomena Around Cylindrical Baffles in an Agitated Vessel Measured by an Electrochemical Method, J.of Chem. Engg. Japan, 40 (2007) 01.

63. Kawaguchi T.K., Sakamoto, M., Tanaka, T. and Tsuji, Y. Quasi – three dimensional numerical simulation of spouted beds in cylinder, Powder Technology, 109 (2000) 3.

64. Kehoe, P.W.K. and Davidsons, J.F., Continuously Slugging Fluidized Beds, Inst. Chem.Eng.(Lond.) Symp. Ser., 33 (1971) 97.

65. King D.F. and Harrison, D., The Dense Phase of a Fluidised Bed at Elevated Pressures, Trans. Instn. Chem. Engrs., 60 (1982) 26.

66. Knowlton, T.M. and Bachovchin, D.M., Fluidization Technology, D.L. Keairns, ed., Hemisphere Publication Crop., Washington, D.C. (1976).

67. Kojima, T., Ishihara, K.I., Guilin, Y. and Furusawa, T., Measurement of Solids behaviour in a fast fluidized bed, J. Chem. Eng. Japan, 22 (4), (1989) 341.

68. Kondukov, N.B.and Sosna, M.H., Khim. Prom., 6 (1965) 402.

69. Konno, H. and Saito, S.J., Pneumatic Converting of solids Through Straight Pipes,J.Chem. Eng.japan, 2 (1969) 211.

70. Krishnamurty S., Murthy, J.S.N., Roy, G.K. and Pakala, V.S., Gas – solid Fluidization in Baffled Bed, Journal of The Institution of Engineers India, 61 (1981) 38.

71. Kroger, D.G., Levy, E.K.G., Abdelnaurg, J.C. and Chen, Fluidization, Grace, J. and Matsen, J.M., ed., Plenum Press, New York, (1980) 453.

72. Kumar A. and Roy, G.K., Effect of Different Types of Promoters on Bed Expansion in a gas – solid Fluidized Bed with Varying Distributor Open Area, Journal of Chemical Engineering of Japan, 35, (2002) 681.

73. Kumar, A and Roy, G.K. Effect of a Co-axial Rod, Disk and Blade Type Promoters on Bed Fluctuation in a Gas-solid Fluidized Bed with Varying Distributor Open Area, Journal of The Institution of Engineers – India, 82 (2002) 61.

74. Kumar, A and Roy, G.K., J. of The Institution of Engs. India, 84 (2004) 55.

75. Kumar, A. and Roy, G.K., Artificial Neural Network-based Prediction of Bed Expansion Ratio in Gas-solid Fluidized Bed with Disc and Blade Promoters, Journal of Institution of Engs. India, 85 (2004) 12.

76. Kumar, A. and Roy, G.K., Bubble Behaviour in Gas-solid Fluidized Beds with Co-axial Rod, Disk and Blade Type Promoters, Journal of Institution of Engs. India, 84 (2004) 55.

77. Kumar, A. and Roy, G.K., Statistical Analysis of Bed Fluctuation Ratio in Gas-solid Fluidized Bed with Rod Promoter, Journal of Institution of Engs. India, 86 (2005) 119.

78. Kumar, A and Roy, G.K.,Distributor to Bed Pressure Drop Ratio in Promoted Gas-s solid Fluidized Beds, Journal of Institution of Engs. India, 87 (2007) 11.

79. Kunii, D. and Levenspiel, O., Fluidization Eng., Wiley New York, (1969).

80. Kwauk, M., Ningde, W., Youchu, L., Bingyu, C. and Zhiyuan, S., Fast Fluidization at ICM,Circulating Fluidized Bed Technology, Vol. p. 33, P. Basu, ed., Pergamon Press, Toronto(1986).

81. Lanneau, K.P., Gas-solid Connecting in Fluidized Beds, Trans. Inst. Chem. Engrs., 38 (1960) 125.

82. Le Palud, T., and Zenz, F.A., Supercritical Phase Behavior of Fluid-Particle Systems, Fluidization, Vol. VI, p.121, J.R. Grace, L.W. Shemilt, and M.A. Bergougnou,eds., Engineering Foundation, Newyork(1989).

83. Lee, J.S., and Kim, S.D. Pressure Fluctuations in Turbulent fluidized Beds,J.Chem. Eng. Japan, 21(5), 515(1988).

84. Leu, L.P., and Lan, C.W., Measurement of Pressure Fluctuations in Two-Dimensional Gas solid Fluidized Beds at Elevated Temperature,J.Chem. Eng. Japan, 23(5), (1990) 555.

85. Leu, L.P., Huang, J.W. and Gua, B.B., Asian Conf. on Fluidized Bed and Three-Phase Reactors Proc.,71(1990).

86. Leung, L.S. and Jones, P.J., Fluidization Technology, Vol.II, D.L. Keairns, Hemisphere Publishing Crop. Washington, D.C.(1976).

87. Leva M., Fluidization, McGraw Hill Book Co. Inc – London, (1959).

88. Li, J., Tung, Y., and Kwauk, M., Energy Transport and Regime Transition in Particle-Fluid Two-phase flow, Circulating Fluidized Bed Technology, Vol.II, p.75, P.Basu and J.F. Large,eds., Pergamon Press, Toronto(1988).

89. Li,Y., and Kwauk, M., The Dynamics of Fast Fluidization , Fluidization,p.537,J.R. Grace and J.M. Matsen, eds, Plenum Press, New York(1980).

90. Li,Y., Chen, B., Wang, F., Wang, Y.and Guo, M., Rapid Fluidization, Int. Chem. Eng., 21 (1981) 670.

91. Link J.M., Cuypers, A., Deen N.G., and Kuipers, J.A.M., Flow Regimes in a Spout – Fluidized Bed; A Combined Experimental and Simulation Study, Chemical Engineering Science, 60 (2005) 3425.

92. Link J.M., Zeilstra, C., Deen, N.G. and Kuipers, J.A.M., Validation of a Discrete Particle Model in a 2D Spout – Fluid Bed Using Non-intrusive Optical Measuring Techniques, Canadian Journal of Chemical Engineering, 82 (2004) 30.

93. Lirag, R.C. and Littman, H., Statistical Study of the Pressure Fluctuations in a Fluidized Bed, AIChE Symp.Ser., 67(116), (1971) 11.

94. Littman N., Morgan , M.H., Narayanan, P.V., Kim, S.J. and Day, J.Y. An Asymmetric Model of Flow in the Annulus of a Spouted Bed of Coarse Particles Model, Experimental Verification and Residence time distribution, Canadian Journal of Chemical Engineering, 63 (1985) 188.

95. Liu, X., Xu, G. and Gao, S., Chemical Engineering Journal (2007).

96. Lu, L.S. and Hsiau, S.S., Powder Tech., 160, 3 (2005) 170.

97. Luo, Z., Zhao, Y., Chen, Q., Tao, X. and Fan, M., Internal Journal of Mineral Processing, 74 (2004).

98. Massimilla, L., Behavior of catalytic Beds of Fine Particles at high Velocities,AIChE Symp.Ser., 69(128), (1973) 11.

99. Mastellone, M.L. and Arena, U., The Effect of Particle Size and Density on Solids Distribution along the Riser of a Circulating Fluidized Bed, Chemical Engineering science, 54 (1999) 5383.

100. Mat Lab Version, 6.5.0.18093a Release 13.

101. Matsen, J.M., 73rd Annual AIChE Meeting Proc.New Orleans (1981).

102. Matsen, J.M., A Phase Diagram for Gas-particle Flow,Fluidization, p.225, D.Kunil and R.Toei, eds., Engineering Foundation, New York (1983).

103. Matsen, J.M., Mechanism of Chocking and Entrainment, Powder Technology, 32 (1982) 21.

104. Menon, N. and Durian, D.J., Phys. Rev. Lett, 79 (1997) 3407.

105. Miyauchi, T., Adv. Chem. Eng., 11, (1981)275.

106. Mohanty Y.K. and Singh, R.K., Effect of Baffles on Dynamics of a Gas-solid Fluidized bed, Journal of The Institution of Engineers India, 81 (2001) 32.

107. Mohanty, Y.K., Biswal, K.C. and Roy, G.K., Effect of Distributor Area on theDynamics of Gas-Solid Fluidised Beds: A Statistical Approach, Ind. Chem. Eng., 49 (2007) 01.

108. Monceaux, L., Azzi, M., Molodstof, Y. and Large, J.F., Overall and Local Characterisation of Flow Regimes in a Circulating Fluidized Bed, Circulating Fluidized Bed Technology, Vol.I, p.185, P.Basu, ed., Pergamon Press, Toronto (1986).

109. Moritomi,H., Mori, S., Araki, K. and Moriyama, A., Periodic Pressure Fluctuations in a Gaseous Fluidized Bed, Kagaku Kogaku Ronbunshu,Tokyo,6(4), (1980) 392.

110. Murthy, J.S.N., and Chandra Sekhar, P., Studies on Hydrodynamics of Mechanically Stirred Fluidized Beds – A statistical Approach, Indian Chemical Engineer, 46, No – 2, (2004) 84.

111. Murthy, J.S.N., Chandra Sekhar, P., Haritha, K., Balram, P. and Anjani, S., Hydrodynamic Characteristics of Stirred Gas-solid Fluidized Beds, The Institution of Engineers – India, 83 (2003) 39.

112. Mujumdar, A., Horio, M., Robi, P.S., Swarnkar, R. and Malik, M., Experimental Investigation and Validation of Mixing and Segregation Behavior of Granular flow in a Sectorial Container, J. of Chem. Engg. Japan, 40 (2007) 01.

113. Nakamura, K., and Capes, C.E., Vertical Pneumatic Conveying: A Theoretical Study of Uniform and Annular Particle Flow Models, Canadian J. of Chem. Engg., 51 (1973) 39.

114. Necholson, W.J. and Smith, J.C., Chem. Eng. Progress, 66 (1966) 83.

115. Nestor J. M., Wilson I. Salvat, Osvaldo M. Martinez, and Guillerme F. Berreto, Packed bed structure: Evaluation of radial particle distribution, The Canadian Journal of Chemical Engineering, 80 (2002) 186.

116. Nienow, A.W., Naimer, N.S., and Chiba, T., Chem. Eng. Commun., 62 (1987) 53.

117. Nienow, A.W., Rowe, P.N. and Agbim, A.J., PACHEC Conference, Kyoto, Japan, (1972) Oct. 10.

118. Patil, K.N., Huhnke, R.L., and Bellmer, D.D., Agricultural Engineering International: the CIGR E-Journal, EE 06 016, IX (2007).

119. Perales, J.F., Coll, T., Llop, M.F., Puigjaner, L., Arnaldos, P.J., and Casal, J., On the Transition from Bubbling to Fast Fluidization Regimes,3rd Int. Conf. on Circulating Fluidized Beds proc., P 4-1,Nagoya,japan(October 15-18,1990).

120. Piepers, H.W., Cotaar, E.J.E., Verkooijen, A.H.M and Rietema, K., EFCE Conf. on Role of Particle Interaction in Powder Mechanics, Powder Technology, 37 (1984) 55.

121. Quin, G., Bagyi, I., Pfeffer, R. and Shaw, H., Particle Mixing in Rotating Fluidized Beds: Inferences about the Fluidized State, Particle Tech and Fluidization, 45 (1999) 1401.

122. Rhodes, M.J., The Upward Flow of Gas/Solid Suspension. Part 2: A Particle Quantitative Flow Regime Diagram for the Upward Flow of Gas/solid Suspension, Chem. Eng. Res. Design, 67 (1989) 30.

123. Richard, P.C. and Wiersma, S., Pneumo Transport 2 Conferences, Guildford, A1-1-15(1973).
124. Rincon, J.,Guardiola, J.,Romero,A. and Ramos,G., J.of Chem. Engg. of Japan, 27 (1994) 2.
125. Rose, H.E. and Duckworth, R.A., Transport of Solid Particle in Liquid and Gases,The Engineer, 227,392,430,478(1969).
126. Rowe, P.N., Partridge, B.A., Cheney, A.G., Henwood, G.A. and Lyali, A., Trans. Inst. Chem. Eng., 43 (1965) T 271.
127. Rowe, P.N. and Nienow, A.W., Chem Eng. Sci., 30 (1975) 1365.
128. Rowe, P.N., The Effect of Pressure on Minimum Fluidization Velocity, Chemical Engineering Science, 39, No – 1 (1984) 173.
129. Rowe, P.N., Nienow, A.W., Powder Tech., 15 (1976)141.
130. Rowe, P.N., Foscolo, P.U., Hoffmann, A.C. and Yates, J.G., Fine Powders Fluidized at Low Velocity at Pressures up to 20 bar with Gases of Different Viscosity, Chemical Engineering Science, 37, No – 7 (1982) 115.
131. Sahoo, A. and Roy, G.K., Prediction of minimum Bubbling Velocity, Fluidization Index and range of Particle Fluidization for Gas-Solid Fluidization in Cylindrical and Non-Cylindrical Beds, Powder Tech., 159 (2005) 150.
132. Sasic, S., Johnsson, F. and Leckner, B., Chem. Engg. Sc., 61 (2006) 5183.
133. Sathiyamoorthy, D. and Horio, M., Chemical Engineering Journal, 93 (2003) 215.
134. Satija,S., and Fan, L.S., AIChE J.,31(9) (1985) 1554.
135. Sau, D.C., Mohanty, S. and Biswal, K. C., Minimum Fluidization Velocity and Maximum Pressure Drop for Gas-solid Tapered fluidized Bed, Chemical Engineering Journal, 132 (2007) 151.
136. Saxena, S.C., Chatterjee, A. and Patel, R.C., Effect of distributors in gas – solid fluidization, Powder Tech., 22 (1979) 191.
137. Schnitzlein, M.G., and Weinstein, H., Flow Characterization in High Velocity Fluidized Beds Using Pressure Fluctuations,Chem. Eng. Sci., 43(10), (1988) 2605.

138. Simone,S., and Harrott, P., Fluidization of Fine Powder with in the Particulate and the Bubbling Region, Powder Technology, 26 (1980) 161.
139. Singh R.K. and Roy, G.K., Prediction of Bed Fluctuation Ratio for Gas-solid Fluidization in Cylindrical and Non-cylindrical Beds, Indian Journal of Chemical Technology, 13 (2006) 139.
140. Singh R.K., Studies on Certain Aspects of Gas-solid Fluidization in Non-cylindrical Conduits, Ph.D. Thesis – Sambalpur University – (April 1995).
141. Singh S.P. and Singh, A.N., Direct Prediction of Expanded Bed Height in Gas-solid Fluidization, Indian Chemical Engineer, 45 (2003) 268.
142. Singh, R.K. and Roy, G.K., Prediction of Minimum Bubbling Velocity, Fluidization Index and Range of Particulate Fluidization for Gas-solid Fluidization in Cylindrical and Non-cylindrical Beds, Powder Tech. 159 (2005) 168.
143. Singh, B. B and Mohanty, B., Journal of Institution of Engineers (India), 82 (2002) 46.
144. Squires, A.M., Wauk, M.K, and Avidan, A.A.,Fluid Beds: At Last, Challenging Two Entrenched Practices, Science, 230(1985) 1329.
145. Stromberg, L., Studsvik Report, E 4 – 79/83(1983).
146. Sutanto, W., Epstein, N. and Grace, J.R., Hydrodynamics of spout – fluid beds, Powder Technology, 77 (1985) 205.
147. Svoboda, K. and Hartman, M., Influence of Temperature on Incipient Fluidization of Limestone, Lime, Coal Ash, and Corundum, Ind. Eng. Chem. Process Des. Der., 20, No.2, (1981) 319.
148. Swain, P, Nayak, P.K. and Roy, G.K., Effect of Distributor Parameters on the Quality of Fluidization, Indian chemical Engineers, 38 (1996) 39.
149. Takeuchi, H., Hirama, T., Chiba, T., Biswas, J. and Leung L.S., A Quantitative Definition and Flow Regime Diagram for Fast Fluidization, Powder Tech., 47 (1986) 195.
150. Thiel, W.J. and Potter, O.E., Slugging in Fluidized Beds, Ind. Eng. Chem. Fund., 16 (1977) 242.

151. Tsuji Y., Kawoguahi, T. and Tanaka, T., Discrete Particle Simulation of Two Dimensional Fluidized Bed, Powder Tech., 77 (1993) 79.
152. Vakovic, D.V., Hadzismajlovic, DZ.E. Grabavic, Z.B., Garic, R.V. and Littman, H., Flow Regimes for Spout-fluid Feds, Canadian Journal of Chemical Engineering, 62 (1984) 825.
153. Verloop, J. and Heetjes, P.M., Piriodic Pressure Fluctuations in Fluidized Bed, Chem. Eng. Sci., 29 (1974) 1035.
154. Wasserman, P.D., Neural Computing: Theory and Practice, Van Nastrank Reinhold, 1st ed., New York (1989).
155. Wu,R. L.., Lim, C..J., Chaouki, J., Grace, J.R., Heat Transfer from a Circulating Fluidized Bed to Membrane Waterwall Surfaces, AIChE J., 33 (2007) 1888.
156. Yang, W.C., A Criterion for Fast Fluidization, Pmemo Transport 3 Proc., BHRA Fluid Engineering, Bed Ford E5-49 (1976).
157. Yang, W. C. and Keairns, K.L. Rate of Particle Separation in a Gas Fluidized Bed, 21 (1982) 228.
158. Yang, W.C. and Chitester, D.C., Transition between Bubbling and Turbulent Fluidization at Elevated Pressure, AIChE Symp. Ser., (1988) 10.
159. Yang, Y.R., Rong, S.X., Chen, G.T., Chen, B.C., Chem. Reaction Eng. and Technol., 6 (1990) 9.
160. Yerushalmi, J. and Cankurt, N.T., Geldart, D. and Liss, B.,Flow Regimes in Gas-Solid Contact Systems, AIChE Symp. Ser., 74 (176), 1 (1978).
161. Yerushalmi, J. and Cankurt, N.T., High-velocity Fluid Beds, Chem Tech., 8 (1978) 564.
162. Yerushalmi, J. and Cankurt, N. T., Further Studies of Regimes of Fluidization, Powder Technology, 24 (1979) 187.
163. Zenz, F. A., Visualising Gas-solid Dynamics in Catalytic Processes, Petroleum Refiner, 32(7) 1953) 123.
164. Zhang J.Y., and Tang, G., Classification and Determination of Flow Regimes in Spout-fluidized Beds, Proceedings of the 11th International Conference on Fluidization, 491, (2004).

165. Zhang, R., Chen, D. and Yang, G., Study on Pressure Drop of Fast Fluidized Bed, Fluidization ’85 Science and Technology, p. 148, M. Kwauk, D. Kunii, Z. Jiansheng, and M. Hasatani, Science Press, Beijing , China, Elsevier, Amsterdam (1985).
166. Zhao, G.B., Chen, J.Z. and Yang, Y.R., Predictive Model and Deterministic Mechanism in a Bubbling Fluidized Bed, AIChE, 47, 7 (2001) 1524.
167. Zhong, W., Chen, X. and Zhang, M., Hydrodynamic Characteristics of Spout-Fluid Bed: Pressure Drop and Minimum Spouting/Spout-Fluidizing velocity, Chemical Engineering Journal, 118 (2006) 37.

Experimental Aspects *Chapter – 2*

The experimental set-up as shown in **Fig. 2.1** and **Fig. 2.2** consists of the fallowing accessories:

2.1 Air Compressor

A multistage air compressor of capacity 1297 KPa has been used for the experimentation as shown in **Fig. 2. 3**.

2.2 Air Accumulator

It is a horizontal cylinder used for storing compressed air from the compressor as in **Fig. 2.4**. There is an inlet pipe to the accumulator and a bypass from other end of the cylinder. The exit line is a G.I. pipe taken from central part of the cylinder. The purpose of using the air accumulator is to maintain a constant pressure output. The accumulator is fitted with a pressure gauge of capacity 6kg/cm^2.

2.3 Silica Gel Column

A silica gel column is provided with in the line immediately after the air accumulator to arrest the moisture carried by air from the accumulator in **Fig. 2. 5**.

2.4 Rotameters

Calibrated rotameters are provided with to measure the flow rates of air to the column of capacities120m^3/hr for primary air supply and 20m^3/hr for secondary air supply as shown in **Fig. 2. 6**.

2.5 Air Distributor

The air distributor consists of a perforated plate followed by a conical bottom. Distributor plates having open areas of 6%, 8%, 10% and 12% of the column cross-sectional area have been used for the experimentation as shown in **Fig. 2.7** and **Fig. 2.8**. The calming section filled with glass beads, a fine mesh (to prevent the fines falling in to the conical section) and the distributor plate in that order, ensures uniform distribution of air. Equal number holes each of diameters 1mm, 1.5 mm and 2mm have been made on the distributor plate. The total number of holes in the 8% plate is more than that of the 6% plate. Effect of distributor plates on pressure drop, fluctuation and expansion ratios has been found out by observing the pressure drop in the manometer, and maximum and minimum heights occupied by the particles inside the column. Except for the comparison of four distributor plates, the distributor plate having 10% open area of cross-section has been used in all the cases for exhaustive studies.

2.6 Fluidizer

Three Perspex columns 9.9cm, 12.5cm and 15cm in internal diameters and 1m in length each, are used for the experiments. Out of the three columns, the one of 9.9cm diameter is used for an exhaustive study (as shown in **Fig. 2. 9)** and the other two columns have been used for comparison studies only. The bottom of the column is fixed to a Perspex flange as shown in **Fig. 2.10**. Two pressure tapings are provided with for observing the bed pressure drop. Provisions have also been made to collect samples through side ports at equal intervals of 4cm on diametrically opposite sides of the column for the analysis of mixing and segregation characteristics. Secondary air supplied from the side ports at heights of 4cm, 5cm, 6cm and 7cm, on diametrically opposite sides of the column and at right angles to the direction in which sample collection is made, for static bed heights of 8cm, 10cm, 12cm and 14cm respectively from the distributor plate through a pipe having fine holes directed towards the top of the column like a sparger pipe.

2.7 Manometer

Two pressure tapings,90 cm apart (one at the bottom, i.e., just above the distributor plate and the other at the top.) have been provided with in the column for measuring the bed pressure drop through differential monometer, in which carbon tetrachloride (density 1.59 kg/m^3) is used as the manometric fluid.

2.8 Supporting Structure

A steel supporting structure is provided with to keep the experimental setup vertical and erect.

2.9 Experimental Procedure

Four static bed heights, particle sizes, particle densities, and varying air flow rates have been considered for experimentation. Air has been used as the fluidizing medium. Each run has started with a particular fixed bed height. The airflow through the bed has been increased gradually. The increased airflow rates have made the bed to expand gradually after crossing the minimum fluidization velocity. The pressure drop and the expanded bed heights (upper and lower heights) against the airflow rates have been noted for each experiment. A high speed digital camera has been used for the verification of some of the experimental data. Samples have also been collected through the side ports at a fixed velocity of air to analyse the mixing characteristics in the case of rod promoter, disc promoter, primary air and simultaneous primary and secondary air supplies.

2.10 Baffles/Promoters

A rod and a disc type of promoters have been used to improve the quality of fluidization as shown in **Fig. 2.11**. Five rods each of 4 mm in diameter and 600mm in height have been taken in the case of rod type of promoter. Ten numbers of discs (each of

2mm in thickness and 60mm in diameter) with a spacing of 50mm has been taken in the case of disc promoter Fluctuation and expansion ratios have been calculated for both promoted and unprompted beds by observing the maximum and the minimum heights occupied by the particle inside the column. Different bed heights, particle sizes, flow rates and particle densities have been taken as the variables for experimentation.

2.11 Secondary Air

Air supplied from the bottom of the column, i.e. through the distributor plate is termed as primary air. Air supplied through the side ports of the column, i.e. through the sparger pipe at the middle of each static bed is termed as secondary air. In order to fluidize the entire bed material, the secondary air flow begins only after the minimum fluidization condition is reached due to the primary air for different bed heights, bed materials and particle sizes. The pressure drop, fluctuation and expansion ratios have been calculated for both primary, and simultaneous primary and secondary air supply conditions.

2.12 Segregation and Mixing

During fluidization, samples have been collected through the side ports on diametrically opposite sides at different heights of the fluidizer for promoted bed, primary air, and simultaneous primary and secondary air supply conditions. Homogeneous mixtures with respect to densities and particle sizes have been considered for experimentation. Particles of different sizes have been separated through sieves, while that of densities, through the magnetic separator. The weights have been taken in an electronic balance for the calculation of jetsam (for particles having higher densities and larger sizes) and flotsam (for particles having lower densities and smaller sizes) percentages, and then the mixing index values calculated.

Figures of the Experimental set-up and other accessories

Fig. 2.1 Experimental set-up

Fig. 2. 2 Taking observations for static bed height

Fig. 2. 3 Compressor

Fig. 2. 4 Compressor connected to the air accumulator

Fig. 2. 5 Silica gel column

Fig. 2. 6 Rotameters and manometers connected with the set-up

Fig. 2. 7 Distributor plates (6, 8 and 10% open area of cross-section of the column cross section)

Fig. 2. 8 Distributor plate (12% open area of cross-section)

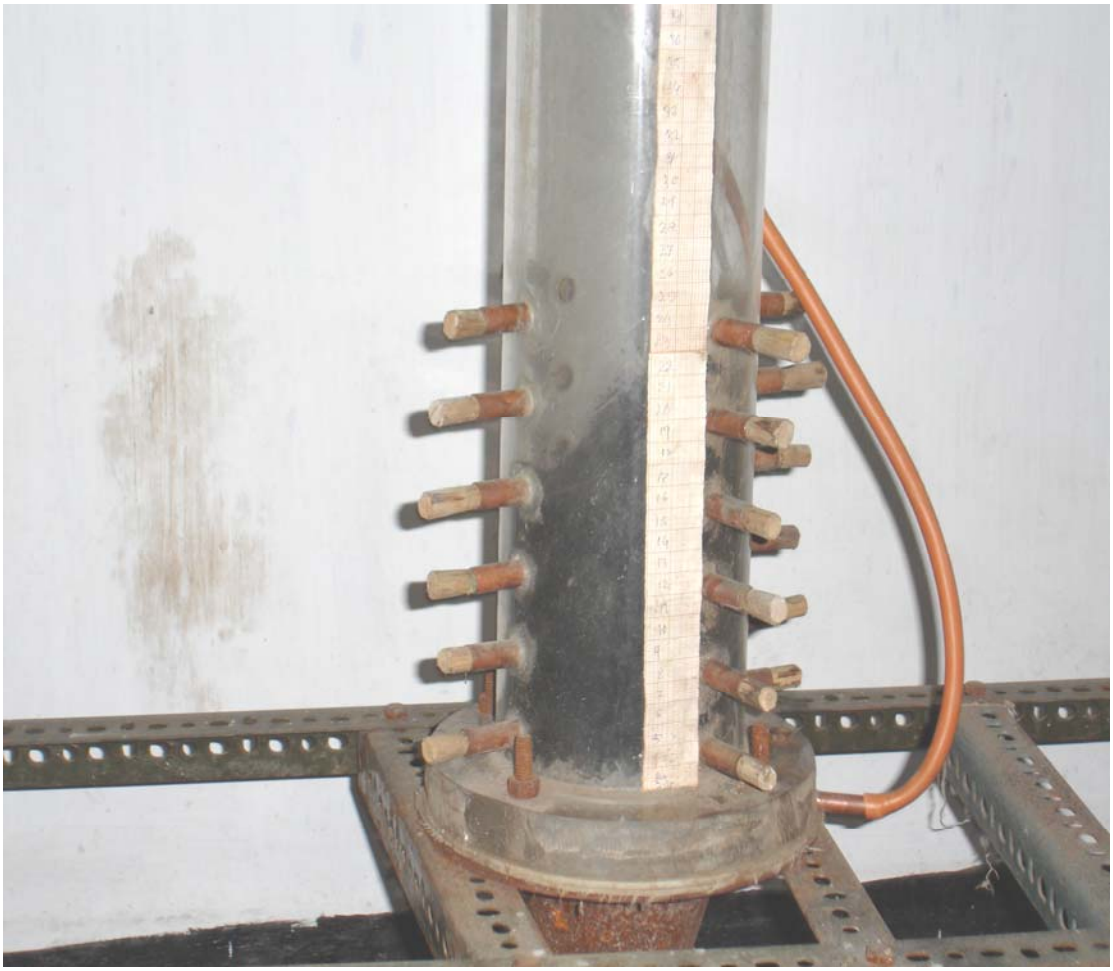

Fig. 2. 9 Fluidizer

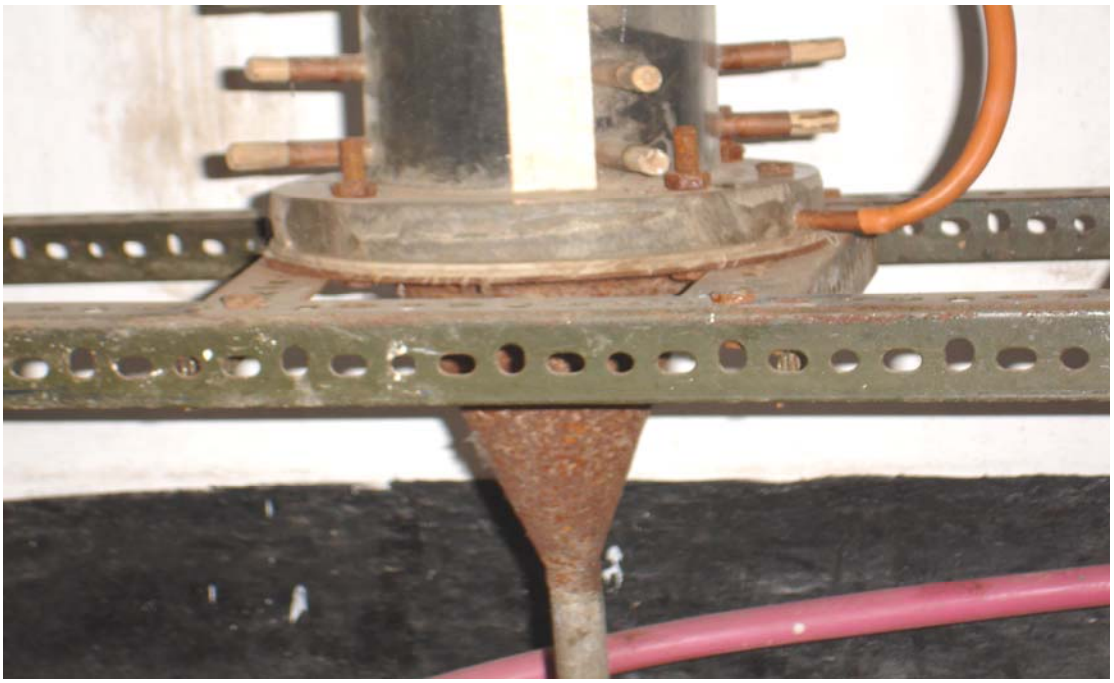

Fig. 2. 10 Perspex flange and conical section of the column

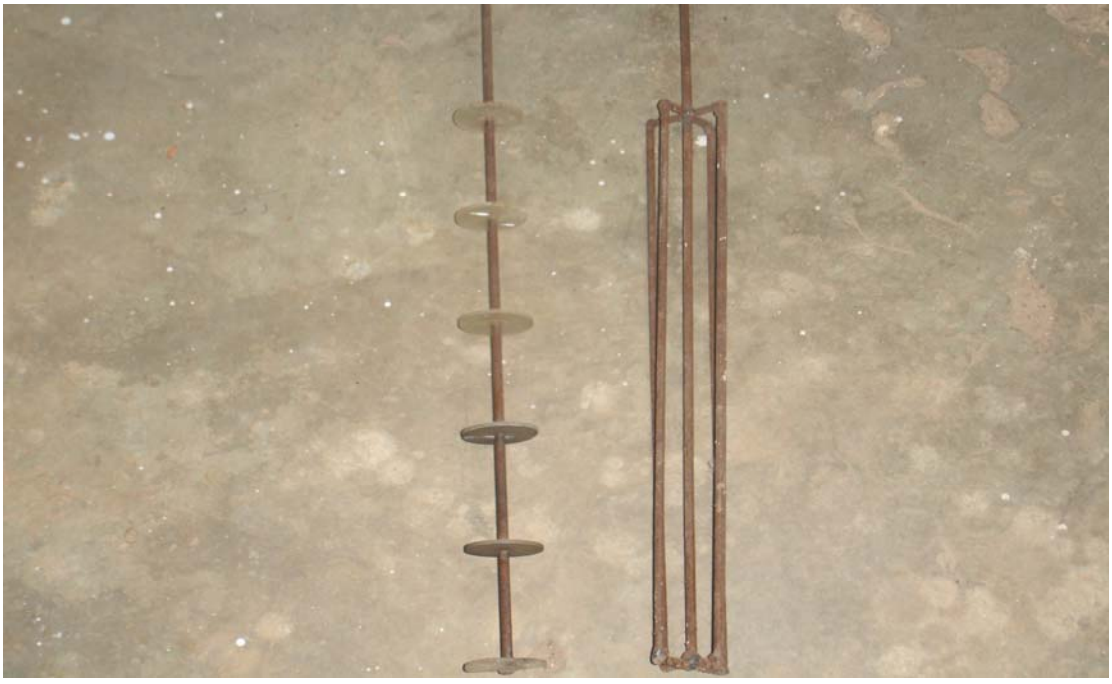

Fig. 2.11 Disc and rod types of promoters

3.1 Introduction

Fluidization is the operation by which fine solids are transformed into a fluid-like state. It has extensive industrial applications primarily due to enhancement of the rate of all transfer processes. When the flow of gas is more than the minimum fluidization velocity, the top of the fluidized bed may fluctuate considerably leading to instability in operation. Bed fluctuation and fluidization quality are interrelated. The quality of fluidization can largely be improved by introducing distributors of varying cross sectional areas of the column cross-section in a gas-solid fluidized bed. It can also be affected by using various distributor designs, which are now-a-days widely in practice in the industry, Kunii and Levenspiel (1990). Perforated plate distributors are widely used in the industry because they are cheap and easy to fabricate. Upward-curved distributor plates achieve good contacting only with more orifices near the perimeter and fewer near the centre—a disadvantage for fabrication. Ergun (1951) found that the pressure losses are caused by simultaneous kinetic and viscous energy losses and proposed the following equation:

$$\frac{\Delta P}{L} g_c = 150(1-\in)^2 \frac{\mu U_m}{\in^3 D_p^{\,2}} + 1.75 \frac{(1-\in)}{\in^3} \frac{G U_m}{D_p} \qquad \ldots (3.1)$$

$$\varepsilon = \frac{\text{volume of bed - volume of solids}}{\text{volume of bed}}$$

$$= 1 - \frac{m_s \rho_b}{m_b \rho_s}$$

Since voids are empty spaces, $m_b = m_s$

$$\varepsilon = 1 - \frac{\rho_b}{\rho_s}$$

where, ρ_b is the bulk density of the bed (= m_s/bed volume)

Out of the three methods, viz, uniformity index, fluctuation ratio and expansion ratio, the latter two have widely been used to quantify fluidization quality. The use of a suitable distributor can improve fluidization quality with a better gas-solid contact through minimization of channelling and slugging and limiting the size of bubbles. A number of investigations have stressed the use of distributors to improve fluidization quality and to increase the range of applicability of gas-solid fluidized beds. In this work, an attempt has been made to bring the effect of distributors on the dynamics of the gas-solid fluidized bed with reference to pressure drop, expansion and fluctuation ratios.

For a uniform gas flow, $u>u_{mf}$, a highly expanded gas-solid dispersion forms directly above the distributor. This is unstable, and a few millimetres above the plate, the dispersion divides into many little bubbles plus an emulsion phase. On rising upward, these bubbles grow very rapidly by coalescence. When bubbles detach from the distributor plates and its rise velocity exceeds its linear growth rates, Davidson and Schuler (1960) found the bubble volume as:

$$v_b = 1.138 \frac{v_{or}^{6/5}}{g^{3/5}}. \qquad \ldots (3.2)$$

However, Harrison and Leung (1961) found that the above equation fits well only at low gas flow rate. Nguyen and Leung (1972) found that a fraction of the gas, i.e. K= 0.53 of the orifice gas becomes a part of the bubble and the rest enters the emulsion region.

Later on Yates et al. (1984) obtained the following values in beds of Geldart AB particles

at height of 10 cm; K = 0.36
at height of 25 cm ; K = 0.79.

Wen et al. (1978) investigated the effect of operating conditions on the dead zone (places in between the orifices) and found that it shrank with increasing gas velocity,

particle size and orifice size. They also found that at high enough gas-flow rates and with large enough particle size these dead zones could be completely eliminated.

Although considerable studies have been reported on bed dynamics, viz, improvement obtained in the homogeneity of the fluidized bed, bubble phenomenon, particle motion, fluid-solid mixing, pressure drop for different types of distributors, limited information is available on the improvement of fluidization quality in terms of fluctuation and expansion ratios for such beds.

Song et al. (1997) studied the effect of gas distributor on the circulation rate of solids and gas bypassing between the draft tube and the annulus sections and found that gas bypassing strongly depends on the type of gas distributor used for annulus aeration.

Investigations state that distributors should have a moderate pressure drop (Δp_d) to achieve equal flows over the entire cross section of the bed. Zuiderweg (1967) proposed the following equation for the calculation of bed pressure drop across a distributor. However, an excessive Δp_d has its draw backs.

$$\Delta p_d = (0.2 – 0.4)\, \Delta p_b \quad \ldots (3.3)$$

Power consumption and construction cost for the blower or compressor increases with the total pressure drop, i.e.

$$\Delta p_t = \Delta p_b + \Delta p_d \quad \ldots (3.4)$$

Several papers have been published and the recommendations for relating Δp_d with Δp_b for satisfactory operations (Hiby, 1964; Siegel, 1976; Mori and Moriyama, 1978; Satiyamoorthy and Rao, 1979; Qureshi and Creasy; 1979; Sirotkin, 1979; and Shi and Fan, 1984); Hiby, 1964) recommended that for stable operations, one should have

$$\Delta p_d / \Delta p_b = 0.15; \text{ for } u_o = (1–2)\, u_{mf},$$

and $$\Delta p_d / \Delta p_b = 0.015; \text{ for } u_o > 2\, u_{mf}.$$

Siegel (1976) suggested the following criterion for stable operations;

$$\Delta p_d / \Delta p_b \geq 0.14.$$

Shi and Fan (1984) concluded that one can guarantee full fluidization if

$(\Delta p_d + \Delta p_b)_{\text{at any } u_o} \cong (\Delta p_d + \Delta p_b)_{\text{at } u_{mf,}}$

where at u_{mf}, $\Delta p_d / \Delta p_b >$ {0.14 for porous particles, 0.07 for perforated plates}.

In this work, an attempt has been made on the gas-solid contacting above the distributor plate to express the quality of fluidization through pressure drop, fluctuation and expansion ratios. Good contacting leads to fast heat transfer, mass transfer and reaction processes. The objective of the present work is to find a suitable distributor for the improvement of quality of fluidization. Mathematical models have been developed for determining pressure drop, fluctuation and expansion ratios in a fluidized bed through factorial analysis approach. Many researchers have developed different methods for the calculation of pressure fluctuations, whereas very little is available on fluctuation ratio and expansion ratio.

Four distributors of varying open areas of cross-section for air flow— 6, 8, 10 and 12 % of column cross-sectional area have been used. During fluidization, the bed pressure drop, fluctuation and expansion data have been noted. The experimental runs have been repeated with different bed heights, particle sizes and gas mass velocities for all the four types of distributors. The scope of the experiment has been presented in **Table 3.1**. The variables affecting fluctuation ratio, expansion ratio and pressure drop are static bed height, particle size, mass velocity and free area of the distributor plate. Thus, the total number of experiments required at two levels, maximum and minimum, for four variables is 16. Each experiment has been repeated 3 times and the average of the three values has been reported as the response value.

3.2 Development of Models

The fluctuation ratio (r) is defined as the ratio of the highest to the lowest bed heights of the fluidized bed in expansion, i.e., $r = h_2/h_1$. The expansion ratio (R) is

defined as the ratio of average of the highest and lowest bed heights to the static bed height for a particular gas flow rate, i.e., $R= (h_2+h_1) / 2h_s$.

In this work a mathematical model has been developed for the prediction of fluctuation ratio, expansion ratio and pressure drop. The model equations are assumed to be linear and the equations take the general form

$$Y = a_0 + a_1A + a_2B + a_3C + a_4D +\ldots\ldots\ldots..+ a_{12}ABD + a_{13}ACD +\ldots\ldots+ a_{15}ABCD \quad ... (3.5)$$

The coefficients are calculated by Yate's technique: $a_i = \sum \alpha_i y_i / N$ ... (3.6)

where A, B, C and D are factorial design symbols; a_i is the coefficient; y_i is the response; α_i is the level of variables and N is the total number of treatments.

The levels of variables are calculated as under for fluctuation and expansion ratios:

A: level of distributor = (A-0.09) / 0.03

B: Level of static bed height = (B-1.01) / 0.202

C: Level of particle size = (C-0.00925)/ 0.00375

D: Level of mass velocity = (D-1.5) / 0.36

The levels of variables are calculated for pressure drop: ... (3.7)

A: level of distributor = (A-0.09) / 0.03

B: Level of static bed height = (B-1.01) / 0.202

C: Level of particle size = (C-0.0103) / 0.0028

D: Level of mass velocity = (D-0.85) / 0.15

The level of variables is calculated as follows:

Level of distributor = (A- 0.09)/ 0.03
Average of maximum and minimum levels = (0.12 + 0.06) / 2 =0.09
(From Table 3.2)
0.09 – 0.06 = 0.03
0.09- 0.12 = - 0.03
If we put the maximum and minimum levels in place of A, then
Level = (0.06 – 0.09) / 0.03 = -1
Level = (0.12 – 0.09) / 0.03 = +1

Similarly for B, C and D all the levels have been calculated from Table 3.2.

The experimental data based on factorial design and analysis is presented in **Table 3. 2** and its nature of effects for fluctuation ratio, expansion ratio and pressure drop at minimum fluidization conditions in **Table 3.3**. The following **Eqs. (3.8, 3.9 and 3.10)** have been developed for fluctuation ratio, expansion ratio and pressure drop respectively (neglecting the smaller coefficients):

$$r = 1.094 - 0.0085A + 0.009B – 0.0045C + 0.028D – 0.006AB + 0.0077BC + 0.00725BD \quad \text{... (3.8)}$$

$$R = 1.57 + 0.0308A - 0.071B – 0.218C + 0.4536D – 0.0369AB + 0.0398AD - 0.0256BC - 0.0525BD + 0.1788CD - 0.039ABD \quad \text{... (3.9)}$$

$$\Delta P_{mf} = 2.559 + 0.3115A - 0.1146B + 0.3115C + 0.3696D + 0.1953AB + 0.1565BC – 0.1146ABC \quad \text{… (3.10)}$$

3.3 Results And Discussion

The method of experimentation is based on statistical design of experiments (Factorial Design and Analysis) in order to bring out the interaction effect of the variables, which would not be otherwise found by conventional experimentation, and to explicitly find out the effect of all the four variables quantitatively on the response. In

addition, the number of experiments required is far less as compared to the conventional experimentation.

Dolomite with four different sizes, four static bed heights, four distributor plates of 6,8,10 and 12 % open areas of cross-section of the column cross-section have been considered for the experimentation. Distributor plates having 6 and 12 % open areas of cross-section, particles of sizes 0.00055 m and 0.0013 m, bed heights of 0.08 m and 0.12m, and mass velocities at the lowest and the highest ranges have been considered for the development of the mathematical model. Particles of different sizes start to fluidize at different mass velocities called minimum fluidization mass velocities. The experiments have been carried out up to 2.5 to 3.0 times the minimum fluidization mass velocity with a continual increment of 0.085 kg/m^2s.

Initially, when air is passed upward through the bed of particles, it percolates through the void spaces between the stationary particles. With an increase in air flow rate, particles move apart and a few vibrate and move in restricted regions called expanded bed. At some higher velocity (i.e. velocity above expanded bed) all the particles in the bed are suspended by the upward flow of air. At this point, the frictional force between the particles and fluid just counter balances the weight of the particle.

The pressure drop increases with an increase in distributor cross sectional area except for that with 10% open area of cross-section, where the pressure drop is less as evident from **Figs. 3.1 and 3.2,** and remains almost constant for different static bed heights.

Further, it has been observed that the bed fluctuation decreases after the critical gas mass velocity is reached for all the particle sizes and static bed heights (**Figs.3.3, 3.4, 3.6 and 3.7**). The bed expansion is a linear function of the gas mass velocity (**Figs. 3.9, 3.10, 3.11 and 3.12**). The critical velocity is nearly two times the minimum fluidization mass velocity. It is evident from **Fig 3.10** that expansion ratio is less in case of larger size particles. Also **Figs. 3.11 and 3.12** represent that with an increase in the static bed height the expansion ratio decreases.

When a bed of particles is fluidized by an upward flow of air, the surface of the bed is forced upward to a higher level than the level prior to fluidization. The expansion beyond the point of incipient fluidization is primarily due to gas bubbles, which increase the bed volume. It is evident that the fluctuation ratio decreases with an increase in particle size as in **Fig.3.5** and decreases with static bed height as in **Figs.3.3 and 3.4**. Further, it is observed that there is a reduction in fluctuation ratio for the distributor having the largest free area of cross-section, i.e., for 12% at lower velocities, may be owing to the reduction of channelling and slugging effects, and 10% for higher velocities due to proper distribution of gas through the distributor plate, which is evident from **Figs. 3.6, 3.7 and 3.8.**

There is a gradual increase in expansion ratio for distributors having cross-sectional area ranging from 6—12% for all velocity ranges, which may be attributed to the formation of small length spouts (at the origin) in the case of small diameter orifices. On the other hand, lower expansion is observed for 10% distributor for lower velocity ranges as evident from **Fig.3.9**. Further, it is also observed that expansion ratio is large for small particle sizes as in **Fig.3.10**.

Comparison of pressure drop, fluctuation ratio and expansion ratio is presented in **Figs. 3.13, 3.14 and 3.15**. The values obtained from the developed equations have been compared with experimental data taken at conditions other than those used for development of correlations and found to agree within a standard deviation of ± 3.21 percent for fluctuation ratio , ± 9.19 percent for expansion ratio and ± 21.98 percent for pressure drop. The deviation is more in the case of pressure drop and expansion ratio due to varying particle sizes and distributor cross-sectional areas. **Tables 3.4, 3.5 and 3.6** represent comparison of values obtained by the developed model with the experimental values.

It is evident from equation 3.8 that mass velocity and the distributor area have a larger effect on fluctuation ratio as compared to that of static bed height and particle size. Equation 3.9 reveals that the mass velocity has a larger effect on expansion as compared to distributor area, particle size and static bed height. But equation 3.10 presents a

different picture, i.e., mass velocity and particle size have a larger effect on pressure drop as compared to that of the other two variables.

Further the following has been observed for pressure drop, fluctuation ratio and expansion ratio:

i) Fluctuation ratio bears a direct relation with static bed height and mass velocity, and an inverse relation with the other two variables as evident from equation 3.8.

ii) Expansion ratio varies directly with mass velocity only but inversely with the other three variables as evident from equation 3.9.

iii) Pressure drop has a direct relationship with distributor area, particle size and mass velocity whereas the static bed height has a negligible effect on it as evident from equation 3.10.

3.4 Conclusions

It is apparent that the quality of fluidization can be improved by lowering the bed height, particle size, and using a distributor of optimum cross-sectional area. But a 10% distributor plate, in particular, offers the best fluidization quality as evident from the experimental findings. The above developed equations can be successfully utilized for the prediction of fluctuation ratio, expansion ratio and pressure drop at minimum fluidization velocity. The factorial design and analysis approach is suitable in these circumstances as it can take into account the individual and the interaction effects of the variables. Further, it requires a considerably less number of experimental data for the development of model equations as compared to the other conventional methods considered by earlier workers.

Notations

Ad_o Open area of distributor, m^2
A_C Area of column, m^2
A_A Distributor annular area, m^2
h_s Static bed height, m
d_p Particle diameter, m
d_o Orifice diameter, m
D_c Column diameter, m
G_f Fluidization mass velocity, Kg / m^2s
G_{mf} Minimum fluidization mass velocity, Kg / m^2s
G_R Mass velocity ratio, $\left(\frac{G_f - G_{mf}}{G_t - G_{mf}}\right)$
G_t Terminal mass velocity, Kg / m^2s
g Acceleration of gravity, m/s^2
K Rate of coefficients of growth or shrinkage of particles, m/s
ΔP Pressure drop, N/m^2
ΔP_{mf} Pressure drop at minimum fluidization velocity, N/m^2
r Fluctuation ratio
R Expansion ratio
h_1 Minimum height occupied by the particles of the expanded bed, m
h_2 Maximum height occupied by the particles of the expanded bed, m
Re_p Particle Reynolds number, dimensionless
u Velocity of gas, m/s
u_o Superficial gas velocity, m/s
u_{mf} Superficial gas velocity at minimum fluidization condition, m/s
v_b Velocity of bubble rising through the bed, m/s
v_{or} Volumetric flow rate of gas through an orifice, m^3/s
Δp_d Pressure drop across a distributor, Pa
Δp_b Pressure drop across the bed, Pa
Δp_t Total pressure drop, Pa

Greek Letters

ρ_S Density of solid, Kg/m^3
ρ_f Density of fluid, Kg/m^3
ε Fractional void volume
μ Absolute viscosity of fluid, Pa.s

References

1. Davidson, J.F. and Schuler, B.O.G., Trans. Inst. Chem. Eng.,38 (1960) 335.

2. Ergun, S., Chem. Eng. Prog., 48, 2 (1951) 89.

3. Harrison, D. and leung, L.S., Trans. Inst. Chem.Eng.,39 (1961) 409.

4. Hiby, J.W., Chim.- Ing.- Techn., 36 (1964) 228.

5. Kunii, D. and Levenspiel, O., Fluidization Eng., Wiley New York, 2nd ed.(1990).

6. Mori, S. and Moriyama, A., Int. Chem. Eng., 18 (1978) 245.

7. Nguyen, X.T. and Leung, L.S., Chem. Eng. Sci., 27 (1972) 1748.

8. Qureshi, A.E. and Creasy, D.E., Powder Tech., 22 (1979) 113.

9. Siegel, R., AIChE J., 22 (1976) 590.

10. Soritkin, G.L., Chem. Petrol. Eng., 15 (1979) 113.

11. Sathiyamoorthy, D. and Rao, C.S., Powder Tech., 24 (1979) 215.

12. Shi, Y.F. and Fan, L.T., AIChE J., 30, (1984) 860.

13. Song, B.H., Kim, Y.T. and Kim, S.D., Chem. Engg. Jr., 68 (1997) 115.

14. Yates, J.G., Rowe, P.N. and Cheesman, D.J., AIChE J., 30 (1984) 890.

15. Zuiderweg, F.J., Proc. Int. Symp. On fluidization, A.A.H. Drinkenburg, ed., p. 739, Netherlands Univ. Press, Amsterdam (1967).

Figures

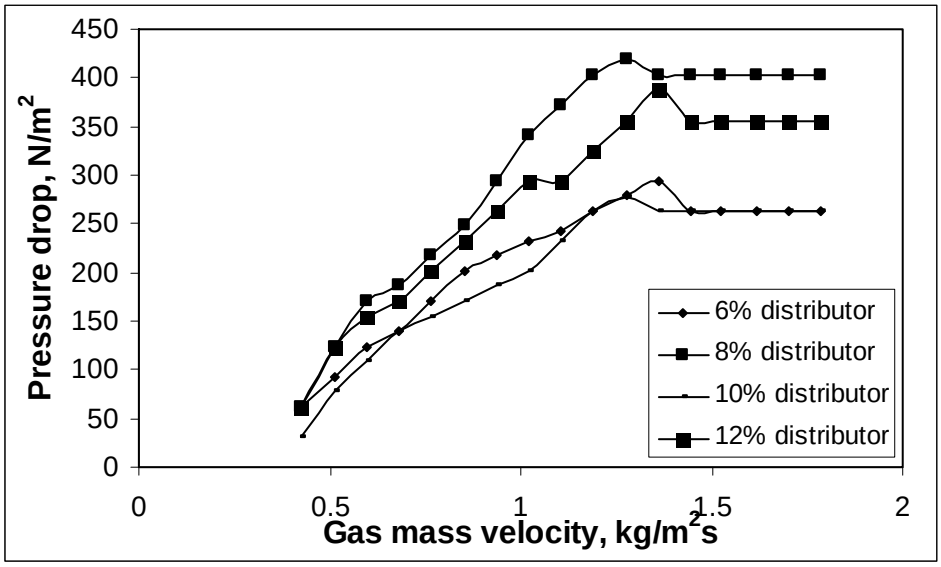

Fig 3.1 Effect of distributor plate on Pressure drop for d_p = 0.000725m and h_s = 0.08 m

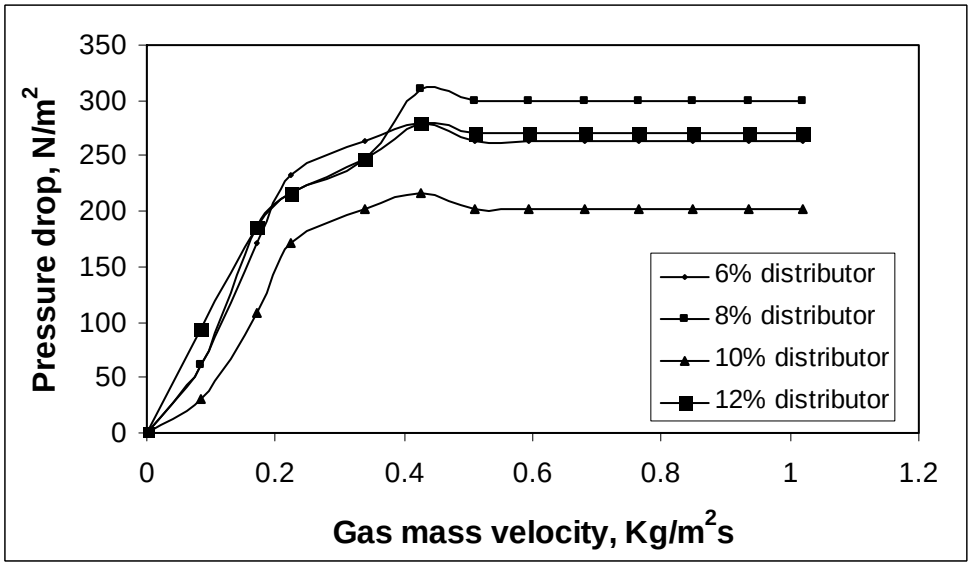

Fig 3.2 Effect of distributor plate on Pressure drop for d_p = 0.000725m and h_s = 0.08 m

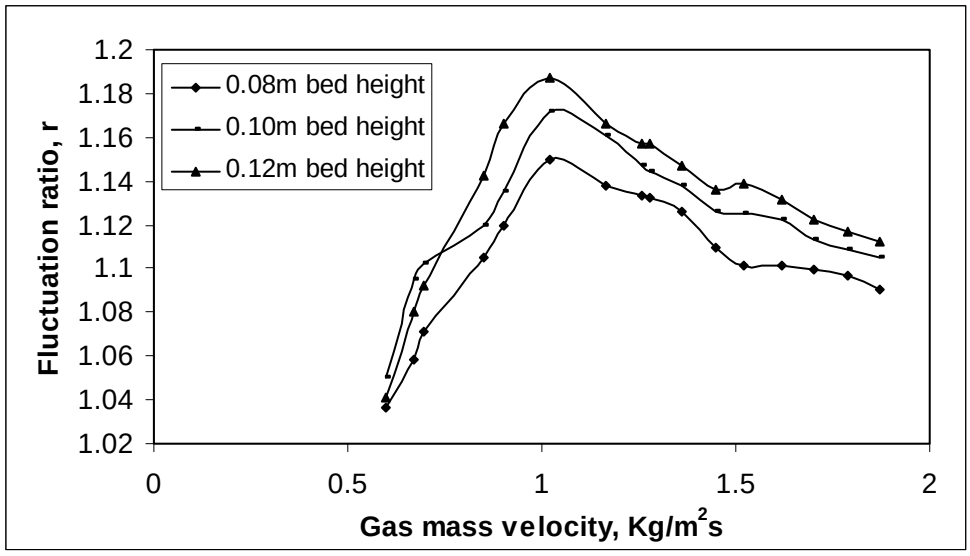

Fig 3.3 Effect of bed height on fluctuation ratio for 8% distributor plate and d_p = 0.00055m

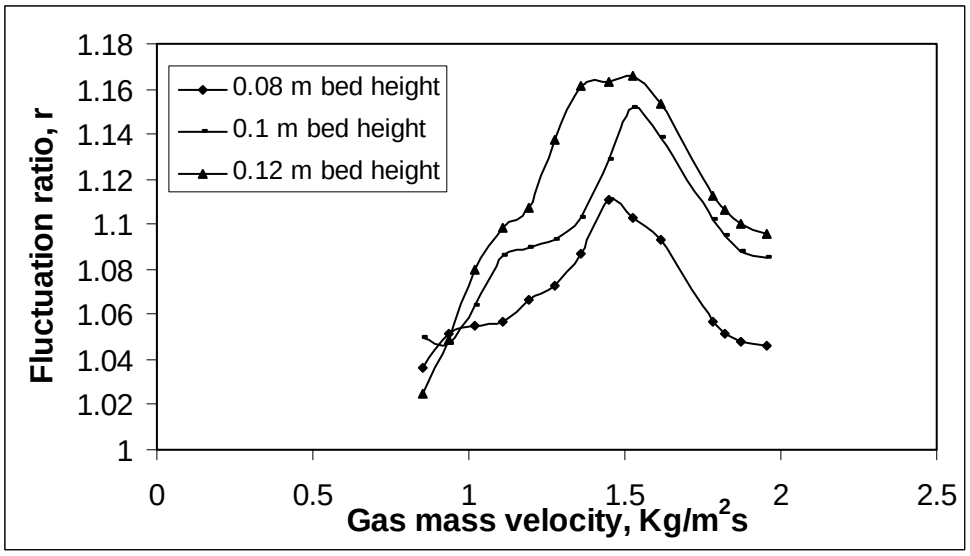

Fig 3.4 Effect of bed height on fluctuation ratio for 12% distributor plate and d_p = 0.000725m

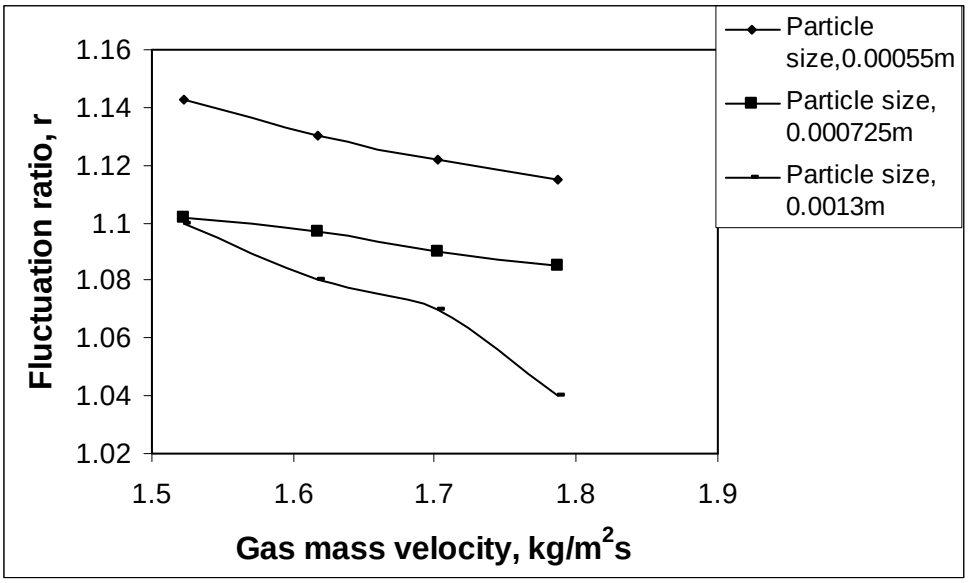

Fig 3.5 Effect of particle size on fluctuation ratio for 10% distributor plate

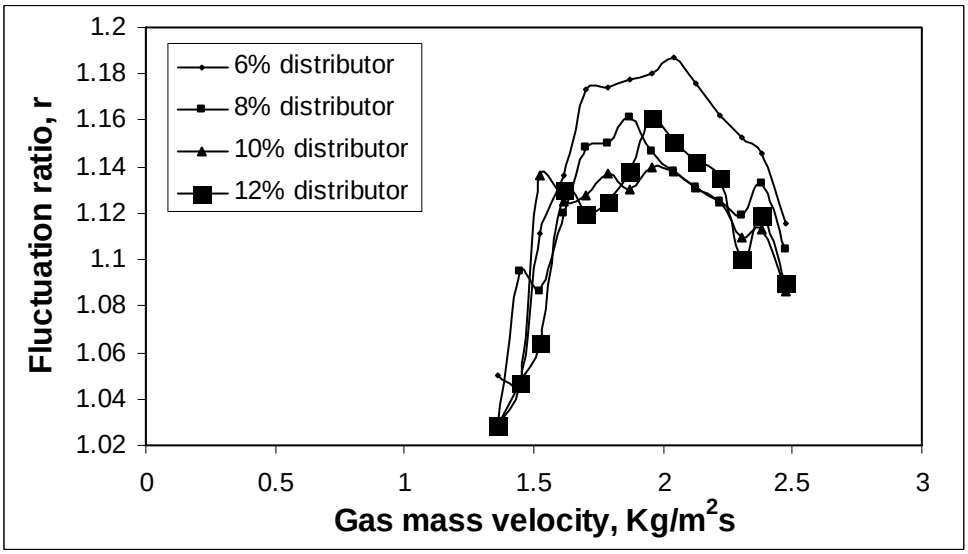

Fig. 3.6 Effect of distributor plate on fluctuation ratio for d_p = 0.013m and h_s = 0.01m

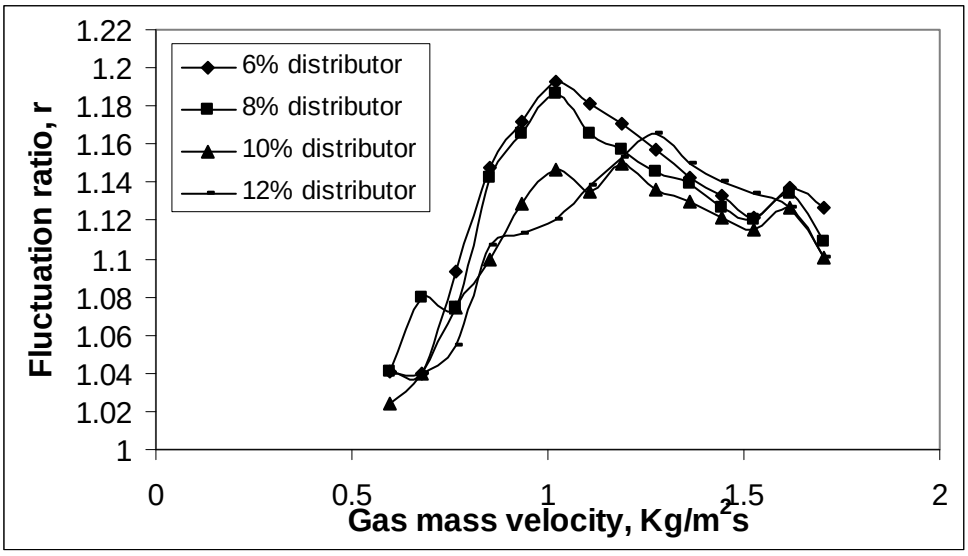

Fig. 3.7 Effect of distributor plate on fluctuation ratio for d_p = 0.00055m and h_s = 0.12m

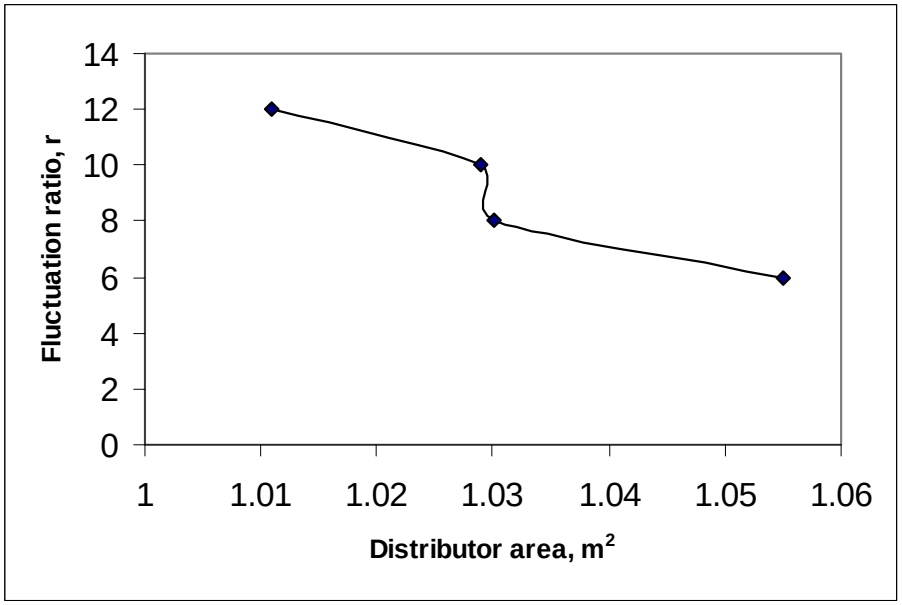

Fig. 3.8 Effect of distributor area on fluctuation ratio for d_p = 0.00055m, h_s =0.12m and mass flow rate = 0.0052 kg/s

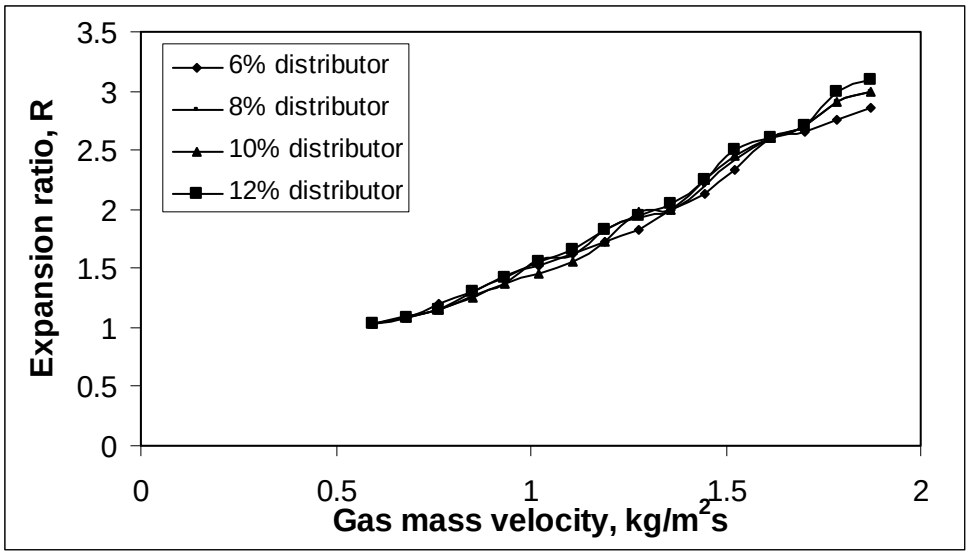

Fig. 3.9 Effect of distributor plate on expansion ratio for d_p = 0.00055m and h_s = 0.10m

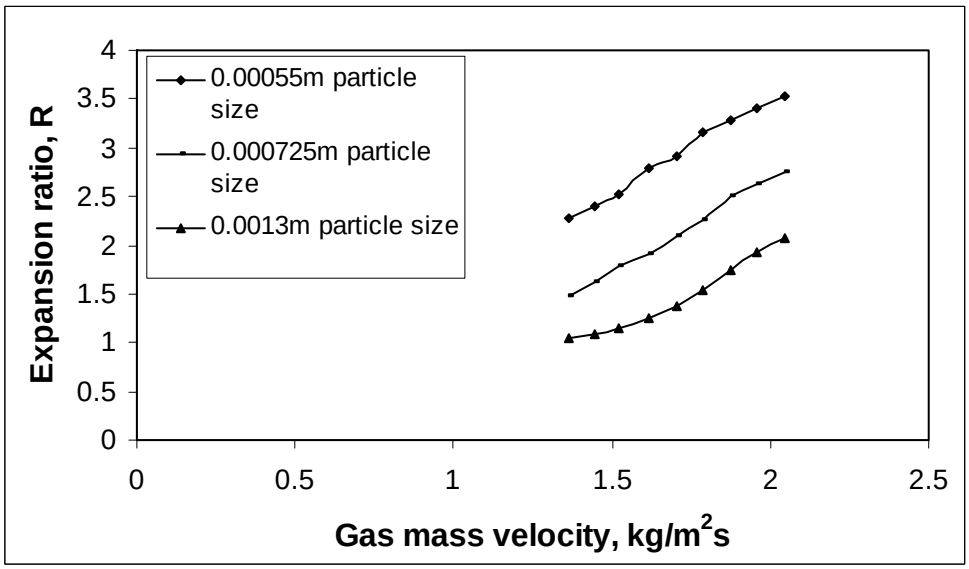

Fig. 3.10 Effect of particle size on expansion ratio for 12% distributor plate and h_s = 0.08m

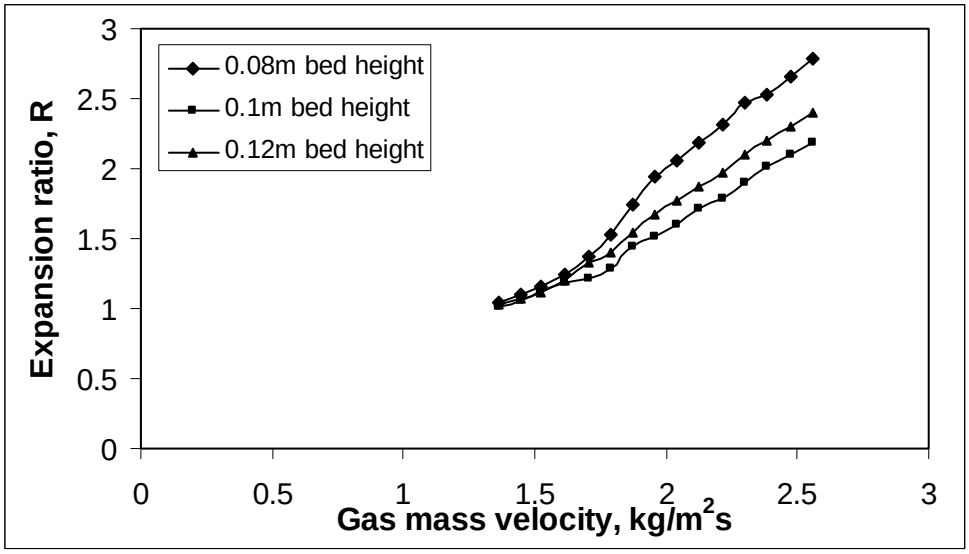

Fig. 3.11 Effect of bed height on expansion ratio for 12% distributor plate and d_p = 0.0013m

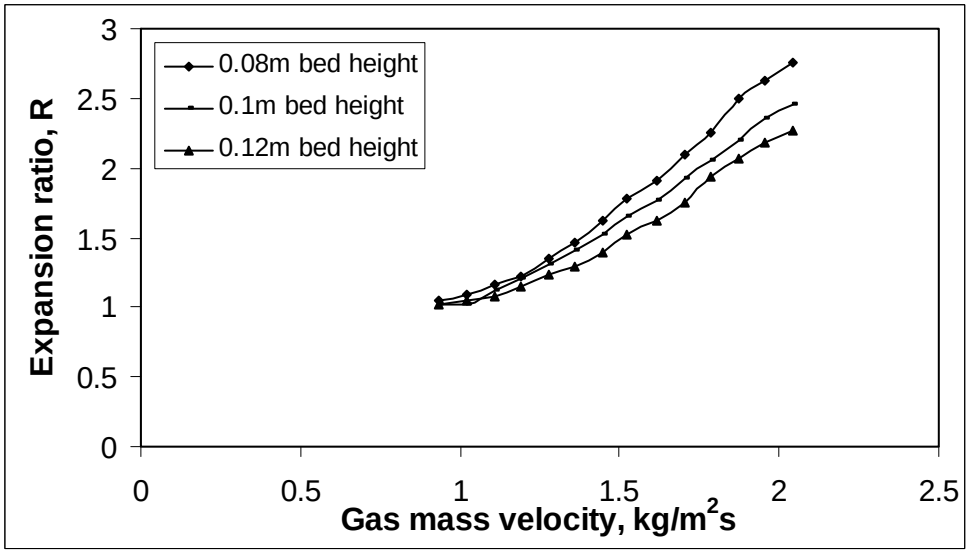

Fig. 3.12 Effect of bed height on expansion ratio for 12% distributor plate and d_p = 0.000725m

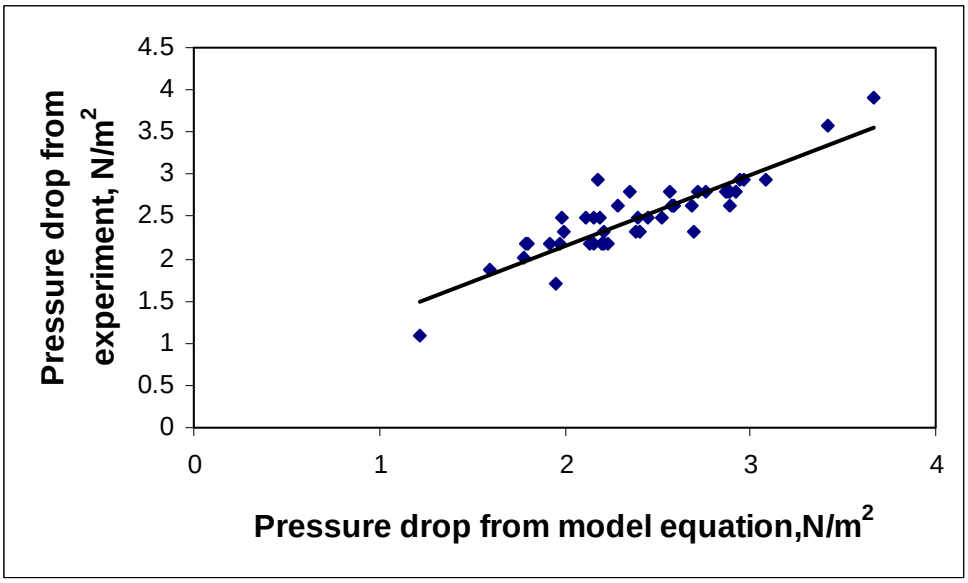

Fig.3.13 Comparison of pressure drop data

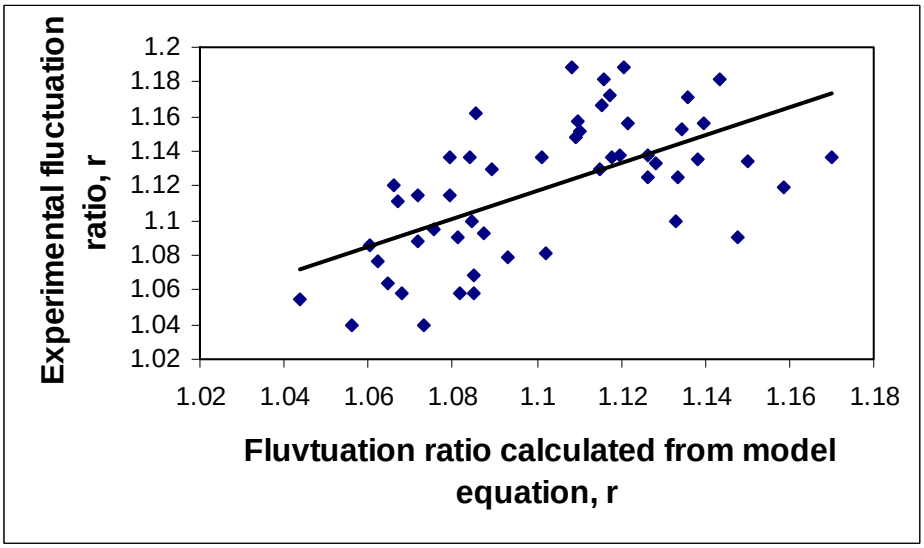

Fig. 3.14 Comparison of fluctuation ratio data

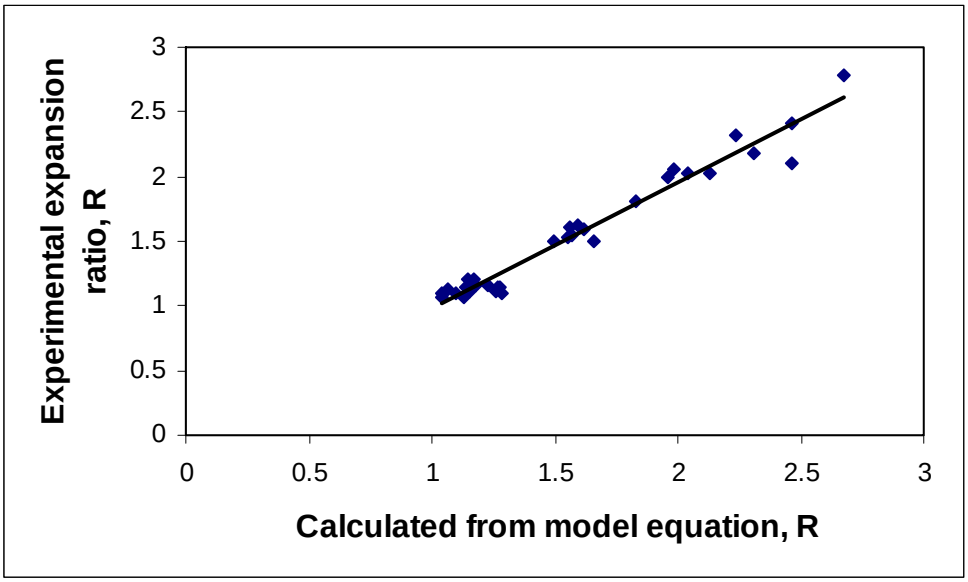

Fig. 3.15 Comparison of expansion ratio data

Table 3.1 Scope of the Experiment

Properties of the Bed Materials

Materials	**$d_{p \times 10^3}$, m**	**$\rho_{s \times 10^{-3}}$, kg/m^3**
Dolomite	0.55, 0.725, 1.3	2.817

Bed Parameter

Initial static bed height, $h_{s \times 10^2}$, m 8, 10, 12

Diameter of column, D_c, m 0.099

Density of air at 25^0c, Kg/m^3 1.18

Distributor parameters

6% open area, $A_{do} \times 10^4$, m^2 = 4.618

8% open area, $A_{do} \times 10^4$, m^2 = 6.158

10% open area, $A_{do} \times 10^4$, m^2 = 7.697

12% open area, $A_{do} \times 10^4$, m^2 = 9.237

Flow property

Range of Mass velocity

Sl. No.	**Particle size, d_p,(m)**	**Mass velocity,G_{mf}, (Kg/m^{2}s)**	**Mass velocity,G_f, (Kg/m^{2}s)**
1	0.00055	0.596	0.681 to 1.957
2	0.000725	0.851	0.935 to 1.957
3	0.00129	1.361	1.446 to 2.555

Table 3.2 Factorial Design and Analysis

Sl. No	Name of the variable	Variable general symbol	Factorial design symbol	Minimum level (-1)	Maximum level (+1)	Magnitude of variables
1	Distributor area	A_{do}/A_c	A	0.06	0.12	0.06, 0.08, 0.10,0.12
2	Static bed height	h_s/D_c	B	0.808	1.212	0.808, 1.01, 1.212
3	Particle size	d_P/D_c	C	0.0055	0.013	0.0055, 0.00725, 0.013
4	Mass velocity	G_f/G_{mf}	D	0.7, 1.14	1.0, 1.86	1.062 to 3.283

Table 3.3 Analysis of Fluctuation Ratio, Expansion Ratio and Pressure Drop Data

Sl. No.	Treatment combination	A	B	C	D	r	D	R	D	ΔP/ 100
					Experimental		Experimental		Experimental	
1	1	0.06	0.808	0.0055	1.14	1.058	1.14	1.093	0.7	2.325
2	a	0.12	0.808	0.0055	1.14	1.058	1.14	1.093	0.7	2.17
3	b	0.06	1.212	0.0055	1.14	1.04	1.14	1.062	0.7	1.085
4	c	0.12	1.212	0.0055	1.14	1.04	1.14	1.062	0.7	2.17
5	d	0.06	0.808	0.013	1.14	1.086	1.14	1.2	0.7	2.17
6	ab	0.12	0.808	0.013	1.14	1.055	1.14	1.156	0.7	2.635
7	ac	0.06	1.212	0.013	1.14	1.115	1.14	1.145	0.7	2.17
8	ad	0.12	1.212	0.013	1.14	1.076	1.14	1.125	0.7	2.79
9	bc	0.06	0. 088	0.0055	1.86	1.125	1.86	1.593	1.0	2.79
10	bd	0.12	0.808	0.0055	1.86	1.148	1.86	1.812	1.0	2.79
11	cd	0.06	1.212	0.0055	1.86	1.181	1.86	1.5	1.0	1.705
12	abc	0.12	1.212	0.0055	1.86	1.138	1.86	1.604	1.0	2.945
13	abd	0.06	0.808	0.013	1.86	1.081	1.86	2.406	1.0	2.945
14	acd	0.12	0.808	0.013	1.86	1.069	1.86	2.781	1.0	3.565
15	bcd	0.06	1.212	0.013	1.86	1.134	1.86	2.312	1.0	2.79
16	abcd	0.12	1.212	0.013	1.86	1.1	1.86	2.187	1.0	3.9

(Columns indicating A, B and C are common for all set of calculations)

Table 3.4 Comparison of Fluctuation Ratio Data

A	B	C	D	r_{cal}	r_{exp}	%Deviation
0.06	0.808	0.0055	1.14	1.0849	1.058	2.5472
0.12	0.808	0.0055	1.14	1.0679	1.058	0.9404
0.06	1.212	0.0055	1.14	1.0730	1.04	3.1778
0.12	1.212	0.0055	1.14	1.0560	1.04	1.5432
0.06	0.808	0.013	1.14	1.0605	1.086	-2.3434
0.12	0.808	0.013	1.14	1.0435	1.055	-1.0853
0.06	1.212	0.013	1.14	1.0794	1.115	-3.1883
0.12	1.212	0.013	1.14	1.0624	1.076	-1.2592
0.06	0.808	0.0055	1.86	1.1264	1.125	0.1288
0.12	0.808	0.0055	1.86	1.1094	1.148	-3.3580
0.06	1.212	0.0055	1.86	1.1435	1.181	-3.1710
0.12	1.212	0.0055	1.86	1.1265	1.138	-1.0061
0.06	0.808	0.013	1.86	1.1020	1.081	1.9472
0.12	0.808	0.013	1.86	1.0850	1.069	1.5014
0.06	1.212	0.013	1.86	1.1499	1.134	1.4065
0.12	1.212	0.013	1.86	1.1329	1.1	0.0299
0.06	0.808	0.0055	1.283	1.0931	1.079	0.0131
0.06	0.808	0.0055	1.998	1.1344	1.153	-0.0161
0.06	0.808	0.0055	1.713	1.1179	1.136	-0.0158
0.06	1.01	0.0073	1.299	1.0892	1.13	-0.0361
0.06	1.01	0.0073	1.9	1.1359	1.171	-0.0299
0.06	1.01	0.0073	1.199	1.0814	1.09	-0.0078
0.06	1.212	0.013	1.437	1.1085	1.189	-0.0676
0.06	1.212	0.013	1.188	1.0841	1.137	-0.0464
0.06	1.212	0.013	1.062	1.0718	1.088	-0.0148
0.08	0.808	0.0055	1.283	1.0875	1.093	-0.0050
0.08	0.808	0.0055	1.855	1.1204	1.189	-0.0576
0.08	0.808	0.0055	2.713	1.1699	1.137	0.02897
0.08	1.01	0.0073	1.199	1.0757	1.095	-0.0175
0.08	1.01	0.0073	1.789	1.1216	1.156	-0.0297
0.08	1.01	0.0073	2	1.1380	1.135	0.0026
0.08	1.212	0.013	1.119	1.0717	1.115	-0.0388
0.08	1.212	0.013	1.563	1.1152	1.166	-0.0435

Table 3.5 Comparison of Expansion Ratio

A	B	C	D	R_{cal}	R_{exp}	%Deviation
0.06	0.808	0.0055	1.14	1.0414	1.093	-4.7209
0.12	0.808	0.0055	1.14	1.101	1.093	0.7319
0.06	1.212	0.0055	1.14	1.1274	1.062	6.1581
0.12	1.212	0.0055	1.14	1.039	1.062	-2.1657
0.06	0.808	0.013	1.14	1.1698	1.2	-2.5166
0.12	0.808	0.013	1.14	1.2294	1.156	6.3494
0.06	1.212	0.013	1.14	1.1558	1.145	0.9432
0.12	1.212	0.013	1.14	1.0674	1.125	-5.12
0.06	0.808	0.0055	1.86	1.617	1.593	1.5065
0.12	0.808	0.0055	1.86	1.8326	1.812	1.1368
0.06	1.212	0.0055	1.86	1.495	1.5	-0.3333
0.12	1.212	0.0055	1.86	1.5626	1.604	-2.5810
0.06	0.808	0.013	1.86	2.4606	2.406	2.2693
0.12	0.808	0.013	1.86	2.6762	2.781	-3.7684
0.06	1.212	0.013	1.86	2.2386	2.312	-3.1747
0.12	1.212	0.013	1.86	2.3062	2.187	5.4503
0.1	0.808	0.0073	1.199	1.1817	1.156	2.2235
0.1	0.808	0.0073	1.599	1.6546	1.5	10.308
0.1	0.808	0.0073	2	2.1287	2.031	4.8113
0.1	1.01	0.0073	1.199	1.1548	1.115	3.5738
0.1	1.01	0.0073	1.599	1.5699	1.55	1.2894
0.1	1.01	0.0073	2	1.9861	2.05	-3.1140
0.08	1.01	0.0073	1.33	1.2818	1.1	16.534
0.08	1.212	0.0073	1.33	1.2607	1.116	12.972
0.06	0.808	0.0073	1.33	1.2694	1.143	11.059
0.06	1.01	0.0073	1.33	1.2729	1.15	10.692
0.06	1.01	0.0073	2.66	2.4611	2.1	17.192
0.06	0.808	0.013	1.125	1.1429	1.2	-4.7576
0.06	0.808	0.013	1.375	1.5911	1.625	-2.0859
0.06	0.808	0.013	1.625	2.0392	2.031	0.4085
0.06	1.01	0.013	1.125	1.1380	1.14	-0.16886
0.06	1.01	0.013	1.375	1.5501	1.525	1.649727
0.06	1.01	0.013	1.625	1.962242	2	-1.88792

Table 3.6 Comparison of Pressure Drop Data

A	B	C	D	d_{Pcal}	d_{Pexp}	%Deviation
0.06	0.808	0.0073	0.7	2.14451	2.325	-7.7628
0.12	0.808	0.0073	0.7	2.13134	2.17	-1.7814
0.06	1.121	0.0073	0.7	1.21424	1.085	11.9121
0.12	1.212	0.0073	0.7	2.20295	2.17	1.51876
0.06	0.808	0.013	0.7	2.22675	2.17	2.61553
0.12	0.808	0.013	0.7	2.68017	2.635	1.71428
0.06	1.121	0.013	0.7	2.15163	2.17	-0.8463
0.12	1.212	0.013	0.7	2.92237	2.79	4.74475
0.06	0.808	0.0073	1	2.88371	2.79	3.35893
0.12	0.808	0.0073	1	2.87054	2.79	2.88684
0.06	1.121	0.0073	1	1.95344	1.705	14.5716
0.12	1.212	0.0073	1	2.94215	2.945	-0.0965
0.06	0.808	0.013	1	2.96595	2.945	0.7116
0.12	0.808	0.013	1	3.41937	3.565	-4.0849
0.06	1.121	0.013	1	2.89083	2.79	3.6141
0.12	1.212	0.013	1	3.66157	3.9	-6.1133
0.06	0.808	0.013	0.692	2.20704	2.325	-5.0733
0.06	0.808	0.013	0.769	2.39677	2.48	-3.3559
0.06	0.808	0.013	0.846	2.58650	2.635	-1.8405
0.06	1.01	0.013	0.538	1.77910	2.015	-11.706
0.06	1.01	0.013	0.615	1.96883	2.17	-9.2702
0.06	1.01	0.013	0.692	2.15856	2.48	-12.961
0.06	1.01	0.013	0.769	2.34829	2.79	-15.831
0.06	1.212	0.013	0.615	1.92035	2.17	-11.504
0.06	1.212	0.013	0.692	2.11008	2.48	-14.916
0.06	1.212	0.013	0.765	2.28995	2.635	-13.094
0.08	0.808	0.013	0.461	1.78899	2.17	-17.557
0.08	0.808	0.013	0.384	1.59927	1.86	-14.017
0.08	1.01	0.013	0.461	1.79704	2.17	-17.186
0.08	1.01	0.013	0.538	1.98677	2.48	-19.888
0.08	1.212	0.013	0.538	1.9948	2.325	-14.201
0.08	1.212	0.013	0.769	2.5640	2.79	-8.1002

4.1 Introduction

The top oscillations beyond certain limiting value of $(G_f-G_{mf})/G_{mf}$ are due to slugging. Since slugging is affected by "aspect ratio", h_s/D_c, the fluctuation ratio is dependent on this. A special characteristic of gas-solid fluidized bed reactor is the formation of gas bubbles, which are responsible for particle circulation in the bed. For any fluidization unit, the velocity at which fluidization starts and the velocity at which slugging or enhanced rate of entrainment occurs, are the two limits of the operating range. At higher velocities, most of the gas bypasses the bed in the form of bubbles. Thus much of the gas entering the bed bypasses the solids. Therefore, the overall efficiency of the bed decreases, since a small portion of the gas finds its way up through the dense phase portion of the bed at a much lower velocity. The bubble phase is exposed entirely to a different condition than the dense phase gas because of the difference in the gas-solid contact. The increase in the size of bubbles results in poorer gas-solid contact. Hence in order to maintain good fluidization, gas bubbles should be kept as small as possible and interchange of gas should take place between the bubble phase and the dense phase. The ultimate size of the bubbles formed depends upon the size of the fluidized bed, gas velocity, relative density of the gas and the solid, column diameter, gas entry configuration and the size of the solid.

Three fluidizers 0.099 m, 0.127 m and 0.1524 m in internal diameters and 0.96 m in height each, with one of its ends fixed to the Perspex flange, have been taken. Two pressure tappings have also been provided with to measure the bed pressure drop through a differential manometer in which carbon tetrachloride is used as the manometric fluid.

For a particular run, data for bed fluctuation and expansion at varying flow rates and bed heights have been noted. Thus, the total number of experiments required at two levels, viz, maximum and minimum, for three variables is eight for responses in the case of the factorial design method. Each experiment is repeated three times and the average

of the three values are reported as the response value. Qualitative models for bed fluctuation and expansion ratios in the gas–solid fluidized bed have been developed for factorial and dimensional analysis. The scope of the experiment is presented in **Table 4.1**.

4.2 Development of Models

In this work, mathematical models have been developed for the prediction of fluctuation and expansion ratios. Static bed height, column internal diameter and mass velocity of air are the variables that affect fluctuation and expansion ratios. The model equations are assumed to be linear and the equations take the general form:

$$Y = a_0 + a_1A + a_2B + a_3C + ... + a_7ABC \quad \ldots (4.1)$$

The coefficients are calculated by the Yate's technique $a_i = \sum \alpha_i y_i / N$ ... (4.2)

where A, B and C are the factorial design symbols, a_i is the coefficient, y_i is the response, α_i is the level of variables and N is the total number of treatments.

The levels of variables are calculated as under:

Level of static bed height = (A- 0.868) / 0.344

Level of column diameter = (B- 0.00455) / 0.00095

Level of mass velocity = (C-1.94 / 0.61). … (4.3)

The experimental data based on factorial design, nature of the effects and its analysis are presented for fluctuation and expansion ratios in **Tables 4.2 and 4.3** respectively.

The following **Eqs. (4.4 and 4.5)** have been developed through factorial design and analysis approach for fluctuation and expansion ratios (neglecting smaller coefficients).

$r_1 = 1.1185 - 0.0185A + 0.0047B + 0.0535C - 0.0185AC + 0.0152BC$ ... (4.4)

$R_1 = 1.659 - 0.1726A - 0.1363B + 0.5143C - 0.1371AC + 0.1163BC$ ... (4.5)

The following **Eqs. (4.6 and 4.7)** have also been developed through dimensional analysis approach for fluctuation and expansion ratios respectively.

$$r_2 = 1.3922\left(\frac{h_s}{D_c}\right)^{-0.0705}\left(\frac{d_p}{D_c}\right)^{0.0443}\left(\frac{G_f}{G_{mf}}\right)^{0.082} \quad \text{... (4.6)}$$

$$R_2 = 0.8676\left(\frac{h_s}{D_c}\right)^{-0.166}\left(\frac{d_p}{D_c}\right)^{-0.0325}\left(\frac{G_f}{G_{mf}}\right)^{0.7168} \quad \text{... (4.7)}$$

Equations 4.6 and 4.7 have been calculated through dimensional analysis approach.

Step-1: r_2 vs (h_s/D_c) data are plotted to get the equation $r_2 = 1.152\ (h_s/D_c)^{-0.0861}$

r_2 vs (d_p/D_c) ; $r_2 = 1.5741\ (d_p/D_c)^{0.542}$

and r_2 vs (G_f/G_{mf}) ; $r_2 = 1.067\ (G_f/G_{mf})^{0.1002}$

Step-2: Again r_2 vs $(h_s/D_c)\ (d_p/D_c)\ (G_f/G_{mf})$; $r_2 = 1.3922\ X^{0.819}$,

where $X = (h_s/D_c)\ (d_p/D_c)\ (G_f/G_{mf})$

4.3 Results and Discussion

In this work, cylindrical columns of different internal diameters, viz, 0.099m, 0.127m and 0.1524 m have been considered for experimentation. The variables considered in this experimentation are: dolomite of the size 0.00055m, static bed of heights 0.08m, 0.1 m and 0.12m, and mass velocity ranging up to 3 times the minimum fluidization mass velocity. As fluidization quality depends greatly on column diameter, which can be attributed to wall effect in the case of columns having very small diameters. Fluidization quality greatly varies when scaling up of from laboratory scale to industrial scale is done. Keeping this fact in view, in this present experimentation, columns having diameters falling in the intermediate range have been considered to ensure that the findings equally suit industrial needs.

Statistical design and dimensional analysis approaches have been used in the present work. The statistical approach requires a far less number of experimental data as compared to the other conventional methods. This approach can also explicitly find out the effect of each of the variables apart from the interaction effects, quantitatively on the response.

When a bed of particles is fluidized by an upward flow of air, the surface of the bed is pushed up to a higher level. Any further expansion beyond this point can be attributed to the presence of gas bubbles that are responsible for an increase in bed volume.

It is evident from **equations 4.4 and 4.6** that the fluctuation ratio varies directly with mass velocity of air and inversely with the static bed height and internal column diameter. It is also evident from **Figs 4.1, 4.2 and 4.3** that in the lower mass velocity range, i.e. up to two and a half times the minimum fluidization mass velocity, the fluctuation ratio is less in the case of columns having larger diameters compared to that having smaller diameters, as in the latter case the bubble diameter reaches the column diameter and consequently bursts. On the other hand, for columns having larger

diameters, the bubbles do not reach column diameter in this mass velocity range and hence the fluctuation ratio is more beyond this limit. But at mass velocity more than 2.5 times the minimum fluidization mass velocity, the bubbles achieve the column the diameter first and hence burst ($r=h_2/h_1$, h_2 is less), for which fluctuation ratio is less. Here channelling effect is also prominent for larger diameter columns. It is also evident from the experiment that in the case of smaller diameter columns the fluctuation ratio first increases and then either remains constant or decreases a little in this mass velocity range. It is evident from **Figs 4.4 and 4.5** that in the lower mass velocity range, the fluctuation ratio is less for smaller static bed height, i.e. for 0.08 m.

From **Figs 4.6, 4.7 and 4.8,** it is evident that the expansion ratio decreases with an increase in column diameter but increases linearly with an increase in mass velocity. Again **Fig 4.9** reveals that expansion goes down with an increase in bed heights, i.e., less in the case of 0.12m static bed height. **Equations 4.5 and 4.7** shows that expansion ratio is a direct function of mass velocity but varies inversely with static bed height and particle size.

Tables 4.4 and 4.5 represent comparison of experimental and calculated values (factorial analysis) for fluctuation and expansion ratios. It is clearly evident from **Tables 4.6 and 4.7** that both the models can be suitably used for the prediction of fluctuation and expansion ratios, as the values obtained by the model equations gives approximately the same experimental values.

The experimental data obtained have been verified with the developed model and also with the model equation developed by Singh and Roy (2006) is presented in **Tables 4.8 and 4.9** for fluctuation ratio and it is found that the present models gives better result as compared to the earlier model. **Table 4.7** represents a comparison of expansion ratio data, calculated through factorial design and dimensional analysis approaches. It is clearly evident from **Tables 4.7, 4.8 and 4.9** that the developed equations are fit to any number of experimental data (the developed equations give approximately the same values as the experimental ones). The present model has not considered the density as one of the variable, but still gives better result as compared to the other model and hence can be suitably used for the purposes.

The standard deviations for fluctuation and expansion ratios have been found to be ± 0.0368 and ± 0.1658 for factorial analysis, and ± 0.0419 and ± 0.2104 for dimensional analysis approaches.

4.4 Conclusions

Column diameter is an important parameter, which exerts considerable effect on fluidization quality of a bed, expressed through fluctuation and expansion ratios. The following conclusions can be made about the effect of column diameters:

1. Fluctuation ratio is small for columns having larger diameters in the lower velocity range.
2. Fluctuation ratio has also a smaller value for columns having smaller diameters in the upper velocity range, i.e. when $G_f \geq 2.5\ G_{mf}$.
3. Fluctuation ratio bears an direct relation with bed height The wall effect (d_p/D_c) is prominent in columns having smaller diameters in the lower velocity range, channelling dominate in that having larger diameters in the upper velocity range.
4. Expansion ratio is in inverse proportion to column diameters and bed heights.
5. Expansion ratio is a direct function of mass velocity.
6. Factorial analysis and dimensional analysis approaches can be suitably used for the development of model equations. But factorial analysis approach is better than the dimensional analysis approach, as it expresses the individual and interaction effects. Apart from this the number of experimental data required is far less as compared to other conventional methods.

Notations

d_p	Diameter of particle, m
D_c	Diameter of column, m
G_f	Mass velocity corresponding to fluidization, kg/m^{2}s
G_{mf}	Mass velocity corresponding to minimum fluidization, kg/m^{2}s
h_S	Static bed height, m
h_1	Lower height of the expanded bed, m
h_2	Upper height of the expanded bed, m
r	Fluctuation ratio
r_1	Fluctuation ratio calculated through factorial analysis approach
r_2	Fluctuation ratio calculated through dimensional analysis approach
r_{cal}	Fluctuation ratio calculated through the developed equations
r_{exp}	Fluctuation ratio calculated from the experiment
R	Expansion ratio
R_1	Expansion ratio calculated through factorial analysis approach
R_2	Expansion ratio calculated through dimensional analysis approach
R_{cal}	Expansion ratio calculated through the developed equations
R_{exp}	Expansion ratio calculated from the experiment

Greek Symbols

ρ_f	Density of fluid, kg/m^3
ρ_s	Density of solid particle, kg/m^3

Figures

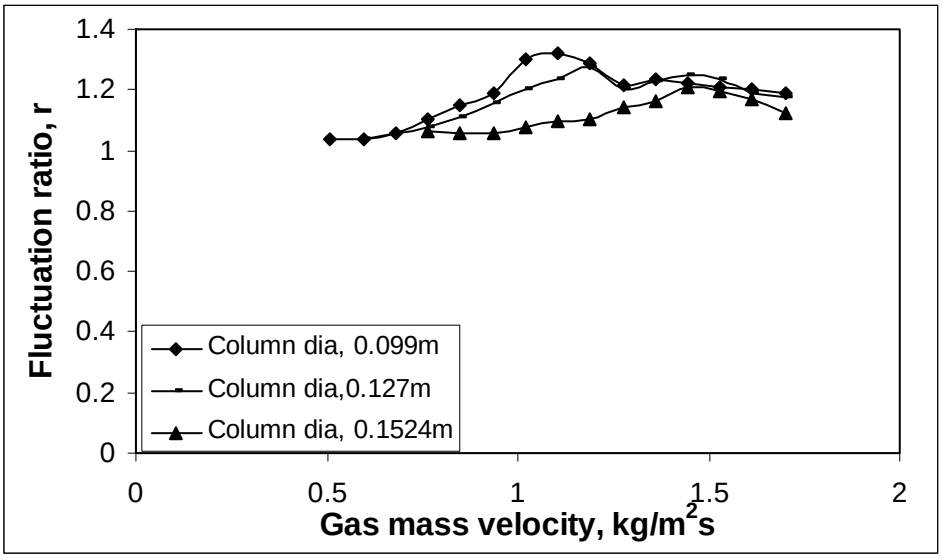

Fig. 4.1 Effect of column diameter on fluctuation ratio for d_p = 0.00055m and h_s = 0.08m

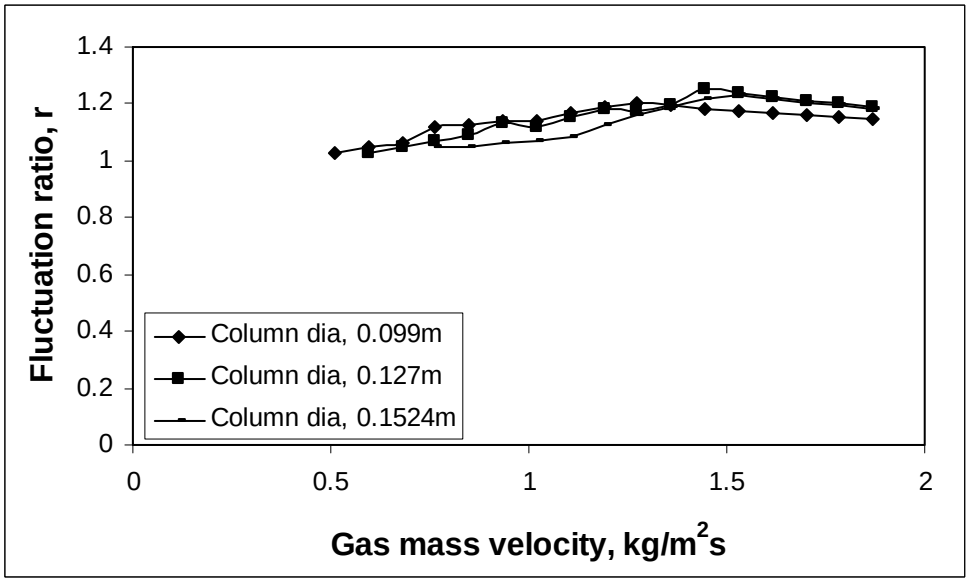

Fig. 4.2 Effect of column diameter on fluctuation ratio for d_p = 0.00055m and h_s = 0.10m

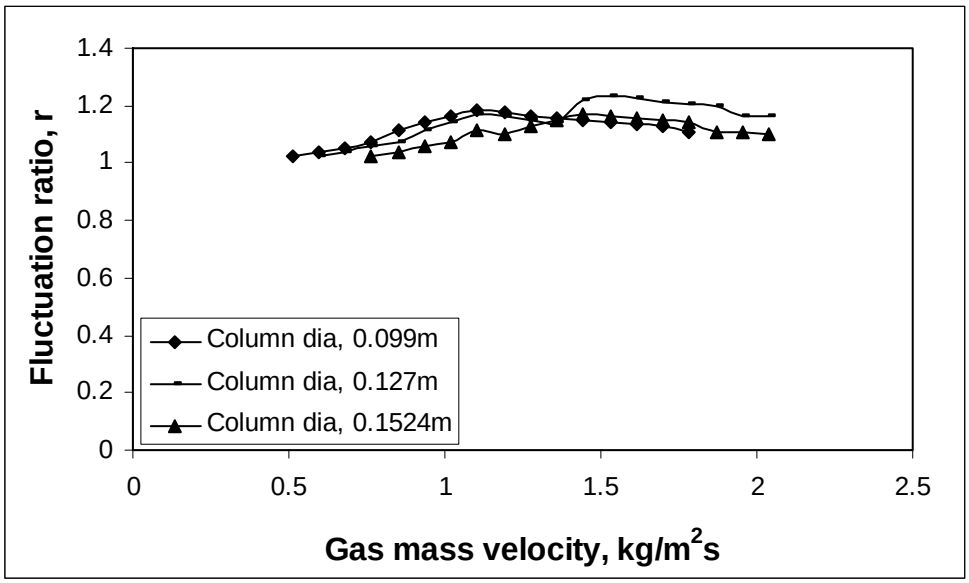

Fig. 4.3 Effect of column diameter on fluctuation ratio for d_p = 0.00055m and h_s = 0.12m

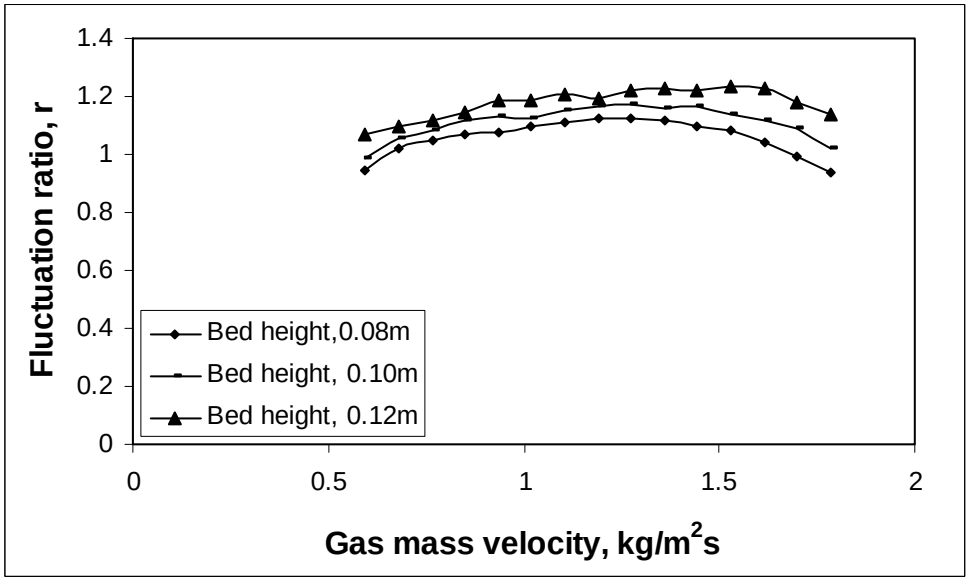

Fig. 4.4 Effect of bed height on fluctuation ratio for d_p = 0.00055m and D_c = 0.127m

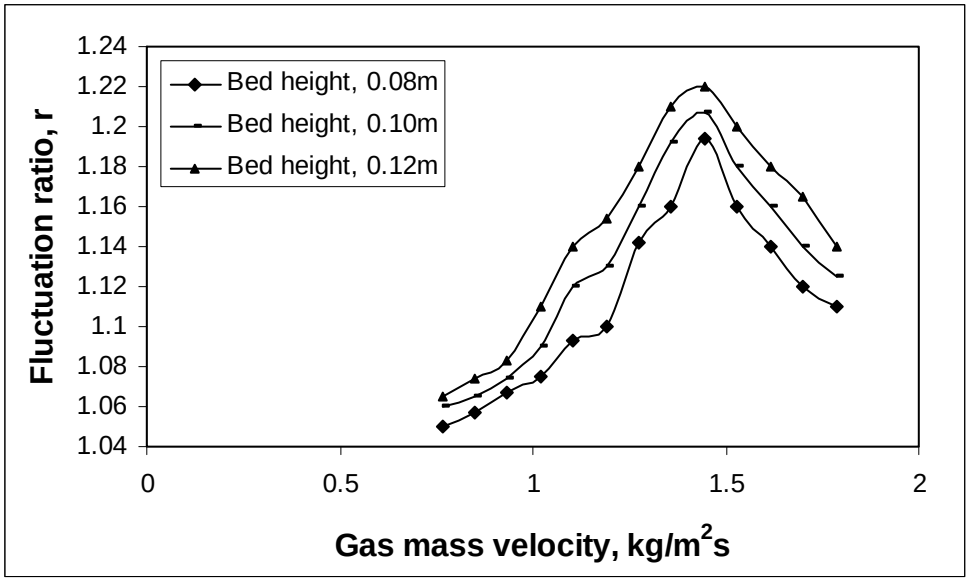

Fig. 4.5 Effect of bed height on fluctuation ratio for d_p = 0.00055m and D_c = 0.1524m

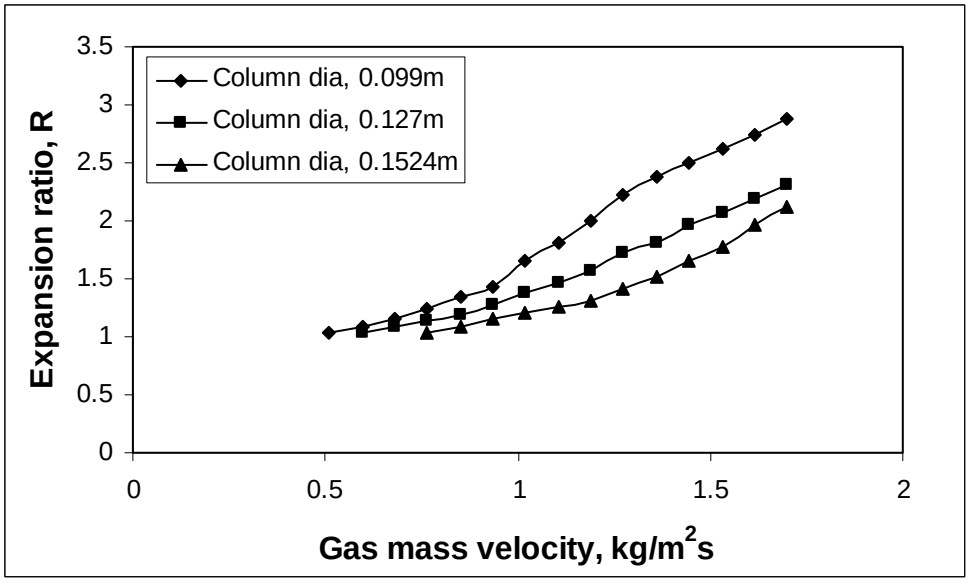

Fig. 4.6 Effect of column diameter on expansion ratio for d_p = 0.00055m and h_s = 0.08m

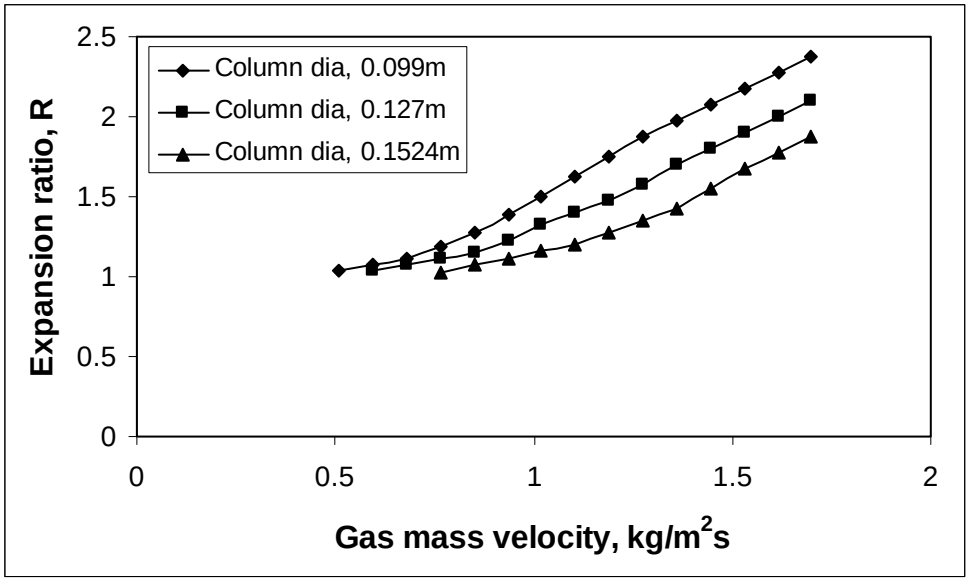

Fig. 4.7 Effect of column diameter on expansion ratio for d_p = 0.00055m and h_s = 0.10m

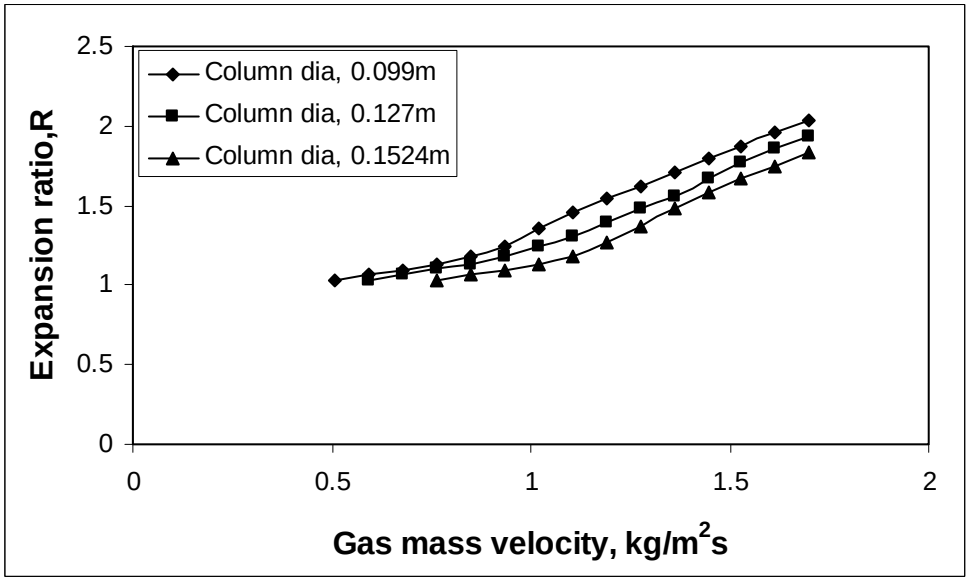

Fig. 4.8 Effect of column diameter on expansion ratio for d_p = 0.00055m and h_s = 0.12m

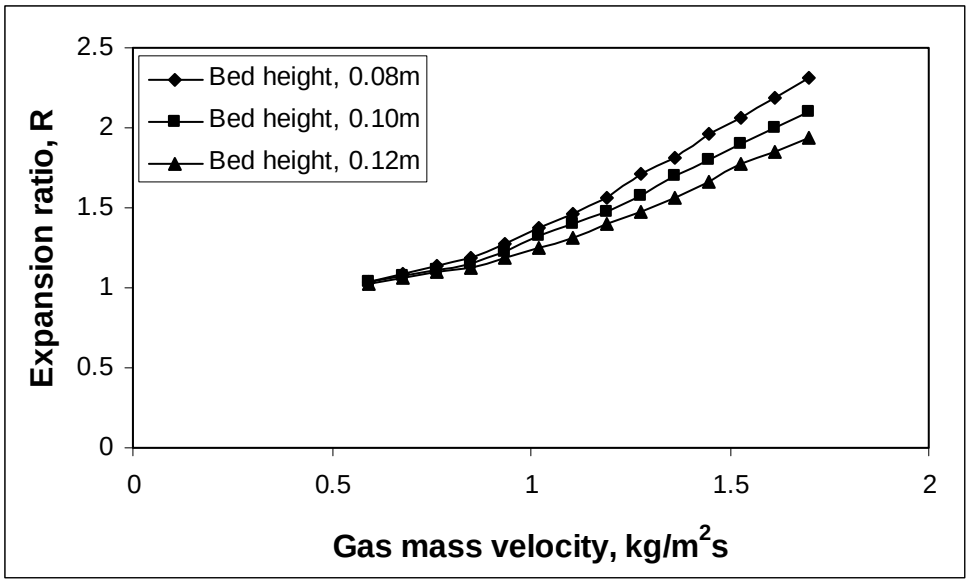

Fig. 4.9 Effect of bed height on expansion ratio for d_p = 0.00055m and D_c = 0.127m

Table 4.1 Scope of the Experiment

Properties of the Bed Materials		
Materials	**$d_{p \times 10}^{3}$, m**	**$\rho_{s \times 10}^{-3}$, kg/m^3**
Dolomite	0.55	2.817
Density of fluid, ρ_f	1.18 kg/m^3 at 25^{0}c	
Diameter of column, D_c	0.099m, 0.127m, 0.1524m	
Bed Parameter		
Initial static bed height, $h_{s \times 10}^{2}$, m	8, 10, 12	
Flow property		
Column diameter, m	G_{mf}, kg/m^{2}s	G_f, kg/m^{2}s
0.099	0.51	0.595 to 1.87
0.127	0.364	0.416 to 1.404
0.1524	0.36	0.396 to 0.9

Table 4.2 Factorial Design and Analysis

Sl. No	Name of the variable	Variable general symbol	Factorial design symbol	Minimum level (-1)	Maximum level (+1)	Magnitude of variables
1	Static bed height	h_s/D_c	A	0.524	1.212	0.808, 0.629, 0.524, 1.01, 0.787, 0.656, 1.212, 0.944, 0.7877
2	Particle size	d_P/D_c	B	0.0036	0.0055	0.0055, 0.00433, 0.0036
3	Mass velocity	G_f/G_{mf}	C	1.33	2.55	1.133 to 3.142

Table 4.3 Analysis of Fluctuation and Expansion Ratios Data, (r) and (R)

Sl. No.	Treatment Combination	A	B	C (G_f/G_{mf})	r_{exp}	c (G_f/G_{mf})	R_{exp}
1	1	0.524	0.0036	1.33	1.075	1.33	1.206
2	a	1.212	0.0036	1.33	1.076	1.33	1.125
3	b	0.524	0.0055	1.33	1.055	1.33	1.156
4	c	1.212	0.0055	1.33	1.054	1.33	1.095
5	ab	0.524	0.0036	2.55	1.2	2.55	2.75
6	ac	1.212	0.0036	2.55	1.104	2.55	2.104
7	bc	0.524	0.0055	2.55	1.218	2.55	2.218
8	abc	1.212	0.0055	2.55	1.166	2.55	1.625

(Columns indicating A and B are common.)

Table 4.4 Comparison of Fluctuation Ratio (Factorial Design Method)

A	B	C	r_{cal}	r_{exp}	% Deviation
0.524	0.0036	1.33	1.0755	1.075	0.0465
1.212	0.0036	1.33	1.0755	1.076	-0.046
0.524	0.0055	1.33	1.0545	1.055	-0.047
1.212	0.0055	1.33	1.0545	1.054	0.0474
0.524	0.0036	2.55	1.1891	1.2	-0.908
1.212	0.0036	2.55	1.1151	1.104	1.0054
0.524	0.0055	2.55	1.2289	1.218	0.894
1.212	0.0055	2.55	1.1549	1.166	-0.951
0.808	0.0055	1.33	1.1042	1.055	4.6680
0.808	0.0055	1.83	1.125	1.19	-5.452
0.808	0.0055	2.5	1.153	1.218	-5.331
1.01	0.0055	1.5	1.097	1.116	-1.669
1.01	0.0055	2	1.118	1.142	-2.08
1.01	0.0055	2.667	1.146	1.194	-4.015
1.212	0.0055	1.667	1.09	1.111	-1.858
1.212	0.0055	2.166	1.111	1.187	-6.387
1.212	0.0055	2.833	1.139	1.15	-0.955
0.629	0.0043	1.285	1.09	1.079	1.033
0.629	0.0043	1.857	1.107	1.238	-10.50
0.629	0.0043	2.714	1.134	1.187	-4.417
0.787	0.0043	1.285	1.087	1.064	2.2480
0.787	0.0043	2.142	1.114	1.172	-4.9011
0.787	0.0043	3	1.141	1.2	-4.8976
0.944	0.0043	1.428	1.09	1.076	1.3150
0.944	0.0043	2.142	1.112	1.151	-3.3584
0.944	0.0043	3.142	1.1434	1.195	-4.3156
0.524	0.0036	1.444	1.0778	1.093	-1.3853
0.524	0.0036	1.777	1.0861	1.16	-6.3670
0.524	0.0036	2.222	1.0972	1.125	-2.4699
0.656	0.0036	1.444	1.0802	1.086	-0.5306
0.656	0.0036	1.777	1.0885	1.192	-8.681
0.656	0.0036	2.555	1.1078	1.146	-3.3267
0.787	0.0036	1.444	1.0825	1.111	-2.5564

Table 4.5 Comparison of Expansion Ratio Data (Factorial Design Method)

A	B	C	R_{cal}	R_{exp}	% Deviation
0.524	0.0036	1.33	1.1292	1.206	-0.4809
1.212	0.0036	1.33	1.1602	1.125	0.3733
0.524	0.0055	1.33	1.0892	1.156	0.3633
1.212	0.0055	1.33	2.7356	1.095	-0.529
0.524	0.0036	2.55	2.1162	2.75	-0.523
1.212	0.0036	2.55	2.2304	2.104	0.5798
0.524	0.0055	2.55	1.611	2.218	0.5590
1.212	0.0055	2.55	1.2051	1.625	-0.8615
1.01	0.0055	1.5	1.4850	1.185	1.7039
1.01	0.0055	2	1.8583	1.75	-15.141
1.01	0.0055	2.667	1.2333	2.175	-14.559
1.212	0.0055	1.667	1.4467	1.187	3.9036
1.212	0.0055	2.166	1.732	1.625	-10.968
1.212	0.0055	2.833	1.127	1.958	-11.540
0.629	0.0043	1.285	1.727	1.187	-5.0208
0.629	0.0043	1.857	2.627	1.968	-12.211
0.629	0.0043	2.714	1.1157	2.562	2.5390
0.787	0.0043	1.285	1.926	1.15	-2.978
0.787	0.0043	2.142	2.738	1.9	1.4023
0.787	0.0043	3	1.224	2.3	19.064
0.944	0.0043	1.428	1.827	1.187	3.1841
0.944	0.0043	2.142	1.3436	1.667	9.6070
0.524	0.0036	1.444	1.7627	1.206	11.415
0.524	0.0036	1.777	2.322	1.512	16.584
0.524	0.0036	2.222	1.3202	2.562	-9.336
0.656	0.0036	1.444	1.710	1.2	10.018
0.656	0.0036	1.777	1.296	1.675	2.1246
0.787	0.0036	1.444	1.539	1.125	15.283
0.787	0.0036	1.667	2.383	1.583	-2.762
0.787	0.0036	2.444	1.20	2.075	14.873

Table 4.6 Comparison of Fluctuation Ratio

A	B	C	r_{cal}	r_{exp}	% Deviation	r_{cal}	r_{exp}	% Deviation
Common input data			**Dimensional analysis**			**Factorial analysis**		
0.808	0.0055	1.33	1.1489	1.055	8.9006	1.0545	1.055	-0.0473
0.808	0.0055	2.33	1.2029	1.285	-6.3846	1.294	1.285	-0.007
0.808	0.0055	3.16	1.2333	1.2	2.7827	1.270	1.2	5.833
1.01	0.0055	1.5	1.1421	1.116	2.3458	1.0715	1.116	-3.9858
1.01	0.0055	2	1.1694	1.142	2.4031	1.1215	1.142	-1.789
1.01	0.0055	3	1.2089	1.175	2.8918	1.2216	1.175	3.9722
1.212	0.0055	1.33	1.1165	1.054	5.9321	1.0545	1.054	0.0474
1.212	0.0055	2	1.1545	1.166	-0.985	1.1096	1.166	-4.8338
1.212	0.0055	2.67	1.1821	1.157	2.1770	1.1647	1.157	0.6720
0.629	0.00433	1.285	1.1537	1.079	6.9305	1.0627	1.079	-1.5017
0.629	0.00433	1.857	1.1891	1.238	-3.9460	1.1217	1.238	-9.3929
0.629	0.00433	2.714	1.2267	1.187	3.3471	1.2099	1.187	1.9368
0.629	0.00433	3.285	1.2460	1.125	10.763	1.268	1.125	12.711
0.787	0.00433	1.285	1.1356	1.064	6.7382	1.0634	1.064	-0.0542
0.787	0.00433	1.857	1.1705	1.153	1.5184	1.1143	1.153	-3.3500
0.787	0.00433	3	1.2174	1.2	1.4552	1.2161	1.2	1.3489
0.944	0.00433	1.285	1.1212	1.062	5.5766	1.0640	1.062	0.1926
0.944	0.00433	1.857	1.1555	1.172	-1.3998	1.1070	1.172	-5.5392
0.944	0.00433	3	1.2019	1.204	-0.1702	1.1930	1.204	-0.9076
0.525	0.0036	1.222	1.1542	1.055	9.4112	1.0654	1.055	0.9908
0.525	0.0036	1.666	1.1840	1.142	3.6778	1.1067	1.142	-3.0860
0.525	0.0036	2	1.2018	1.192	0.8283	1.1378	1.192	-4.5446
0.525	0.0036	2.44	1.2216	1.157	5.5862	1.1787	1.157	1.8806
0.656	0.0036	1.222	1.1363	1.064	6.7953	1.0667	1.064	0.2538
0.656	0.0036	1.667	1.1656	1.16	0.4835	1.1029	1.16	-4.9174
0.656	0.0036	2.222	1.1934	1.205	-0.9624	1.1481	1.205	-4.7155
0.787	0.0036	1.222	1.1218	1.062	5.6318	1.0679	1.062	0.5600
0.787	0.0036	1.667	1.1507	1.129	1.9258	1.0990	1.129	-2.6514
0.787	0.0036	2.222	1.1781	1.146	2.8082	1.1378	1.146	-0.7089

Table 4.7 Comparison of Expansion Ratio

R_{cal}	R_{exp}	% Deviation	R_{cal}	R_{exp}	% Deviation
Dimensional analysis			**Factorial analysis**		
1.3537	1.437	-5.7916	1.6223	1.712	-5.239
1.7018	2	-14.906	1.5355	1.675	-8.328
2.1269	2.625	-18.975	1.4487	1.625	-10.847
1.4198	1.185	19.822	1.5319	1.8	-14.893
1.7458	1.75	-0.2359	1.6205	1.775	-8.7018
2.1468	2.175	-1.2930	0.9853	1.075	-8.3429
2.1750	1.958	11.087	1.2125	1.15	5.4380
1.3365	1.187	12.601	1.4397	1.325	8.6612
1.7412	1.968	-11.519	1.6669	1.475	13.016
2.2869	2.562	-10.734	1.7934	1.7	5.494
1.2876	1.15	11.972	2.1206	1.9	11.612
1.8588	1.9	-2.1680	2.1478	2.1	2.238
2.3677	2.3	2.9460	2.3742	2.3	3.226
1.3476	1.187	13.538	2.8015	2.5	12.060
1.8034	1.667	8.1835	3.0287	2.7	12.175
2.3748	2.104	12.871	1.2051	1.185	1.7039
1.4681	1.206	21.739	1.4850	1.75	-15.141
1.7041	1.512	12.711	1.8583	2.175	-14.559
2.0009	2.562	-21.897	1.7320	1.958	-11.540
1.4143	1.2	17.8610	1.1274	1.187	-5.0208
1.6417	1.675	-1.9880	1.7276	1.968	-12.211
2.1310	2.075	2.6998	2.6270	2.562	2.5390
1.5212	1.583	-3.8993	1.1157	1.15	-2.9788
2.0025	2.075	-3.4921	1.9266	1.9	1.4023

Table 4.8 Comparison of Fluctuation Ratio

D_p/D_c	D_c/h_s	P_f/ρ_s	$(G_f-G_{mf})/G_{mf}$	r_{cal}	r_{exp}	% Deviation	r_{cal}	r_{exp}	% Deviation
Used for Equation (1.27), Other Model							**Present Dimensional Analysis Model, Eq. (4.6)**		
0.0055	1.2375	0.000539	0.333	1.1187	1.055	6.0435	1.1489	1.055	8.9006
0.0055	1.2375	0.000539	0.571	1.1493	1.285	-10.557	1.2029	1.285	-6.3846
0.0055	1.2375	0.000539	2.16	1.2283	1.2	2.36604	1.2333	1.2	2.7827
0.0055	0.99	0.000539	0.5	1.1315	1.116	1.39636	1.1421	1.116	2.3458
0.0055	0.99	0.000539	1	1.1714	1.142	2.58219	1.1694	1.142	2.4031
0.0055	0.99	0.000539	2	1.2128	1.175	3.21711	1.2089	1.175	2.8918
0.0055	0.825	0.000539	0.333	1.1007	1.054	4.43652	1.1165	1.054	5.9321
0.0055	0.825	0.000539	1	1.1629	1.166	-0.2593	1.1545	1.166	-0.9855
0.0055	0.825	0.000539	1.67	1.1931	1.157	3.12721	1.1821	1.157	2.1770
0.00433	1.587	0.000539	0.285	1.1105	1.079	2.92042	1.1537	1.079	6.9305
0.00433	1.587	0.000539	0.857	1.1733	1.238	-5.2216	1.1891	1.238	-3.946
0.00433	1.587	0.000539	1.714	1.2147	1.187	2.33650	1.2267	1.187	3.3471
0.00433	1.587	0.000539	2.285	1.2323	1.125	9.53995	1.2460	1.125	10.763
0.00433	1.27	0.000539	0.285	1.1006	1.064	3.44522	1.1356	1.064	6.7382
0.00433	1.27	0.000539	0.857	1.1629	1.153	0.86246	1.1705	1.153	1.5184
0.00433	1.27	0.000539	2	1.2132	1.2	1.10673	1.2174	1.2	1.4552
0.00433	1.058	0.000539	0.285	1.0926	1.062	2.88565	1.1212	1.062	5.5766
0.00433	1.058	0.000539	0.857	1.1544	1.172	-1.4949	1.1555	1.172	-1.3998
0.00433	1.058	0.000539	2	1.204	1.204	0.0373	1.2019	1.204	-0.1702
0.0036	1.905	0.000539	0.222	1.0966	1.055	3.9468	1.1542	1.055	9.4112
0.0036	1.905	0.000539	0.666	1.1585	1.142	1.4503	1.184	1.142	3.6778
0.0036	1.905	0.000539	1	1.1823	1.192	-0.8095	1.2018	1.192	0.8283
0.0036	1.905	0.000539	1.444	1.2042	1.157	4.08569	1.2216	1.157	5.5862
0.0036	1.524	0.000539	0.222	1.0868	1.064	2.1517	1.1363	1.064	6.7953
0.0036	1.524	0.000539	0.667	1.1483	1.16	-1.0039	1.1656	1.16	0.4835
0.0036	1.524	0.000539	1.177	1.1814	1.205	-1.9559	1.1934	1.205	-0.9624
0.0036	1.27	0.000539	0.222	1.0789	1.062	1.6004	1.1218	1.062	5.6318

(Columns indicating P_f/ρ_s is used only for equation 4.7 and other symbols are as represented in the model equations, i.e. h_s/D_c, d_p/D_c, and G_f/G_{mf})

Table 4.9 Comparison of Fluctuation Ratio

D_p/D_c	D_c/h_s	P_f/ρ_s	$(G_f-G_{mf})/G_{mf}$	r_{cal}	r_{exp}	% Deviation	r_{cal}	r_{exp}	% Deviation
Used for Equation (1.27), Other Model							**Present Factorial Analysis Model, Eq. (4.4)**		
0.0055	1.2375	0.000539	0.333	1.1187	1.055	6.0435	1.0545	1.055	-0.0473
0.0055	1.2375	0.000539	0.571	1.1493	1.285	-10.557	1.1724	1.285	-8.7616
0.0055	1.2375	0.000539	2.16	1.2283	1.2	2.3660	1.2702	1.2	5.8566
0.0055	0.99	0.000539	0.5	1.1315	1.116	1.3963	1.0715	1.116	-3.9858
0.0055	0.99	0.000539	1	1.1714	1.142	2.5821	1.1215	1.142	-1.789
0.0055	0.99	0.000539	2	1.2128	1.175	3.2171	1.2216	1.175	3.9722
0.0055	0.825	0.000539	0.333	1.1007	1.054	4.4365	1.0545	1.054	0.0474
0.0055	0.825	0.000539	1	1.1629	1.166	-0.2593	1.1096	1.166	-4.8338
0.0055	0.825	0.000539	1.67	1.1931	1.157	3.1272	1.1647	1.157	0.6720
0.00433	1.587	0.000539	0.285	1.1105	1.079	2.9204	1.0627	1.079	-1.5017
0.00433	1.587	0.000539	0.857	1.1733	1.238	-5.2216	1.1217	1.238	-9.3929
0.00433	1.587	0.000539	1.714	1.2147	1.187	2.3365	1.2099	1.187	1.9368
0.00433	1.587	0.000539	2.285	1.2323	1.125	9.5399	1.2688	1.125	12.782
0.00433	1.27	0.000539	0.285	1.1006	1.064	3.4452	1.0634	1.064	-0.0542
0.00433	1.27	0.000539	0.857	1.1629	1.153	0.8624	1.1143	1.153	-3.3500
0.00433	1.27	0.000539	2	1.2132	1.2	1.1067	1.2161	1.2	1.3489
0.00433	1.058	0.000539	0.285	1.0926	1.062	2.8856	1.0640	1.062	0.1926
0.00433	1.058	0.000539	0.857	1.1544	1.172	-1.4949	1.1070	1.172	-5.5392
0.00433	1.058	0.000539	2	1.2044	1.204	0.0373	1.1930	1.204	-0.9076
0.0036	1.905	0.000539	0.222	1.0966	1.055	3.9468	1.0654	1.055	0.9908
0.0036	1.905	0.000539	0.666	1.1585	1.142	1.4503	1.1067	1.142	-3.086
0.0036	1.905	0.000539	1	1.1823	1.192	-0.8095	1.1378	1.192	-4.544
0.0036	1.905	0.000539	1.444	1.2042	1.157	4.0856	1.1787	1.157	1.8806
0.0036	1.524	0.000539	0.222	1.0868	1.064	2.1517	1.0667	1.064	0.2538
0.0036	1.524	0.000539	0.667	1.1483	1.16	-1.0039	1.1029	1.16	-4.917
0.0036	1.524	0.000539	1.177	1.1814	1.205	-1.9559	1.1481	1.205	-4.715
0.0036	1.27	0.000539	0.222	1.0789	1.062	1.6004	1.0679	1.062	0.5600

(Columns indicating P_f/ρ_s is used only for equation 4.7 and other symbols are as represented in the model equations, i.e. h_s/D_c, d_p/D_c, and G_f/G_{mf})

Effect of Promoters on Bed Dynamics *Chapter - 5*

5.1. Introduction

Industrial products are increasingly engineered for very specific purposes. Under conditions of gas flow at more than the minimum fluidization velocity, the top of the fluidized bed may fluctuate considerably leading to instability in operation. Depending on the bed material, fine or sticky, the bed will be cohesive. It will then tend to form channels through which the gas will escape rather than being dispersed through the interstices supporting the particles. In the other extreme, if the particles are too large and heavy, the bed will not fluidize properly, but tend to be very turbulent and form a spout.

The formation of bubbles and their ultimate growth to form slugs, and the collapsing of bubbles cause erratic bed expansion with intense bed fluctuation. Out of the four methods, viz, uniformity index, pressure drop, fluctuation ratio and expansion ratio, the later two have widely been used to quantify fluidization quality. Bed fluctuation and expansion, and fluidization quality are inter-related. The extent of fluctuation and its estimation are important for specifying the height of the fluidizer. Hence consistent efforts have been made to reduce the bed fluctuation and to correlate it with dynamic parameters of the system. Several techniques such as vibration and rotation of the bed, use of different distributor plates and promoters have been used to improve the quality of fluidization. The use of promoter has been found to be more effective in controlling fluidization quality. In the present case, the effect of rod and disc promoters has been used to predict the value of fluctuation and expansion ratios.

Stewart and Davidson (1967) stated that at superficial gas velocity, which is below the bubble rise velocity, slugging should not take place and the bed should be sufficiently deep for coalescing bubbles to attain the size of a slug.

Jin et al. (1980, 1982) observed an improvement in breaking up of bubbles and circulation of solid particles in the fluidized bed with pagoda-shaped promoters. Chandra et al. (1981) compared the effect of multi-baffled fluidized bed with the fluidized bed

having concentric baffles with a spacing of 18.5mm and concluded that the fluidization in concentric baffled beds are non-uniform. Kono and Jinnai (1983) reported that the bubble sizes can be kept significantly smaller in a promoted fluidized bed than in the conventional beds and maintained almost constant regardless of the bed height. Tsuchiya and Fan (1989) reported that in gas-liquid or gas-liquid-solid contacting devices, bubble coalescence and break-up play a crucial role in determining the bubble size, rise velocity and gas-liquid interfacial area. .

The objective of the present work is to find out a suitable promoter for the development of fluidization quality. As the quality of fluidization is expressed in terms of fluctuation and expansion ratios, mathematical models for determining the same have been developed. It is also evident from the literature that the ANN and dimensional analysis approaches can be suitably applied for calculation of the same. In the present case, a software package for artificial neural network in Mat Lab has been used for back propagation algorithm. Three typical layers, viz, (i) input, (ii) hidden and (iii) output have been chosen. Four nodes in the input layer, three neurons in the hidden layer and one node in the output layer have been taken as shown in **Fig. 5.1**.

For a particular run, data for bed fluctuation and expansion at varying air flow rates, bed heights, densities and particle sizes both for the promoted and un-promoted beds has been noted. Static bed height, particle density, particle size and mass velocity of air are the variables that affect fluctuation and expansion ratios. Thus, the total number of experiments required at two levels, viz, maximum and minimum, for four variables is sixteen for responses in the case of the factorial design method. Each experiment has been repeated three times and the average of the three values have been reported as the response value. Qualitative models for bed fluctuation and expansion ratios in the gas–solid fluidized bed have been developed. The scope of the experiment is presented in **Table 5.1.**

5.2. Development of Models

In this work, a mathematical model has also been developed for the prediction of fluctuation and expansion ratios. The model equations are assumed to be linear and the equations take the general form:

$Y = a_0 + a_1A + a_2B + a_3C + a_4D + \ldots\ldots\ldots + a_{12}ABD + a_{13}ACD + \ldots\ldots + a_{15}ABC$ … (5.1)

The coefficients are calculated by the Yate's technique, $a_i = \sum \alpha_i y_i / N$ … (5.2)

where A, B, C and D are the factorial design symbols, a_i is the coefficient, y_i is the response, α_i is the level of variables and N is the total number of treatments.

The experimental data based on factorial design, nature of the effects and its analysis is presented for fluctuation and expansion ratios in **Tables 5.2, 5.3 and 5.4** respectively. The following **equations 5.3, 5.4, 5.5, 5.6, 5.7 and 5.8** have been developed for fluctuation and expansion ratios both for promoted and un-promoted beds and for both the promoters (neglecting smaller coefficients).

$r = 1.113 - 0.00525A - 0.00037B - 0.00225C + 0.0095D - 0.01AD - 0.0225BC - 0.0136CD$ … (5.3)

$r_r = 1.071 - 0.00925A - 0.00087B - 0.0005C + 0.0088D - 0.0112CD - 0.0115ABD$ ... (5.4)

$r_c = 1.079 - 0.0038A + 0.0094B - 0.0018C + .0125D + 0.0125CD$ ... (5.5)

$R = 1.4726 - .0565A - 0.0466B + 0.204C + 0.2573D - 0.0216AB + 0.0493AC - 0.0489AD - 0.0363BC - 0.023BD + 0.1459CD - 0.011ABC - 0.0245ABD + 0.0116ACD$ ... (5.6)

$R_r = 1.4273 - 0.0371A - 0.0449B + 0.1738C + 0.2151D - 0.033AB + 0.029AC - 0.041AD - 0.0521BC + 0.106CD$ ... (5.7)

$R_c = 1.452 - 0.07A - 0.054B + 0.185C + 0.2118D - 0.0234AB - 0.0489AD - 0.084BC - 0.0219BD + 0.1178CD - 0.0249ABD$ ... (5.8)

In the present communication, the ANN model using back propagation algorithm both for promoted and un-promoted beds have been developed. In both the cases, the ANN structures (Input layer × Hidden layer × Output layer) have been tested at constant epochs (cycles), learning rate, error goal and net trained parameter. Structures of the ANN model are selected for training of input and output data in each case as shown in **Table 5.5**.

The following **Eqs. (5.9, 5.10, 5.11, 5.12, 5.13 and 5.14)** for fluctuation and expansion ratios have been developed for primary as well as both primary and secondary (simultaneous) gas flow conditions respectively, for irregular particles (dimensional analysis approach) as:

$$r_d = 0.9302\left(\frac{h_s}{D_c}\right)^{0.074}\left(\frac{\rho_s}{\rho_f}\right)^{0.0713}\left(\frac{d_p}{D_c}\right)^{-0.0262}\left(\frac{G_f}{G_{mf}}\right)^{0.0557} \quad \text{... (5.9)}$$

$$r_{dr} = 0.9758\left(\frac{h_s}{D_c}\right)^{-0.0451}\left(\frac{\rho_s}{\rho_f}\right)^{0.011}\left(\frac{d_p}{D_c}\right)^{-0.02}\left(\frac{G_f}{G_{mf}}\right)^{0.0373} \quad \text{... (5.10)}$$

$$r_{dc} = 0.922\left(\frac{h_s}{D_c}\right)^{-0.0396}\left(\frac{\rho_s}{\rho_f}\right)^{0.0191}\left(\frac{d_p}{D_c}\right)^{-0.0327}\left(\frac{G_f}{G_{mf}}\right)^{0.0487} \quad \text{... (5.11)}$$

$$R_d = 0.5673\left(\frac{h_s}{D_c}\right)^{-0.0422}\left(\frac{\rho_s}{\rho_f}\right)^{0.0098}\left(\frac{d_p}{D_c}\right)^{-0.0906}\left(\frac{G_f}{G_{mf}}\right)^{1.055} \quad \text{... (5.12)}$$

$$R_{dr} = 2.0334\left(\frac{h_s}{D_c}\right)^{0.027}\left(\frac{\rho_s}{\rho_f}\right)^{0..4209}\left(\frac{d_p}{D_c}\right)^{0.2243}\left(\frac{G_f}{G_{mf}}\right)^{1.111} \quad \text{... (5.13)}$$

$$R_{dc} = 1.6255\left(\frac{h_s}{D_c}\right)^{-0.1166}\left(\frac{\rho_s}{\rho_f}\right)^{0.2142}\left(\frac{d_p}{D_c}\right)^{0.1471}\left(\frac{G_f}{G_{mf}}\right)^{1.1583} \quad \text{... (5.14)}$$

5.3. Results and Discussion

In the present work, statistical design of experiments, dimensional analysis and ANN approaches have been used for calculation of fluctuation and expansion ratios for both promoted and un-promoted beds. In the experimentation, four different bed materials, viz., dolomite, sand, refractory brick and coal have been considered. Out of which, coal and dolomites have been considered for calculation of the model equations, as these two have the lowest and highest densities respectively. Apart from this, particles of sizes 0.00055m and 0.0017m, bed heights 0.08m and 0.14m, and mass velocities in the lowest and the highest ranges have been considered for development of the mathematical model. It has been observed that all the different particles in the bed start to fluidize at different mass velocities called the minimum fluidization mass velocity. The experiments have been carried out up to 2.5 times the minimum fluidization mass velocity with a continual increment of 0.085 kg/m^{2}s.

Beyond the minimum fluidization mass velocity, the bed starts to fluidize. With further rise in mass velocity of air, the bed exhibits fluid-like behaviour and the bed volume increases due to the gas bubbles. A distributor plate having 10% open area of cross-section of the column cross-section and two different types of promoters, viz., rod and disc have been used for the experimentation as shown in **Fig. 5.2**.

Fluctuation ratio increases with an increase in bed height as evident from **Figs. 5.3 and 5.4**, up to about twice the minimum fluidization velocity and then reduces a little at higher velocities as gas bubbles break up at greater heights. It is clearly evident from **Figs. 5.6 and 5.7** that the fluctuation ratio is less for promoted beds due to an increase in blockage volume by the promoters, and the rod type promoter, in particular, has a greater effect as compared to disc type promoter because of smooth fluidization with negligible channeling and slugging. It is also evident from **Equations 5.3, 5.4 and 5.5** that mass

velocity has a larger effect on fluctuation ratio than on bed height, density and particle size for both promoted and unprompted beds. Fluctuation ratio increases with an increase in mass velocity and increases with an increase in static bed height. The predicted values of fluctuation ratio using ANN and statistical approaches have been compared with the experimental values for promoted and un-promoted beds as shown in **Figs. 5.10 and 5.11**. It has also been observed that both the ANN approach and the statistical approach holds good for all the velocity ranges. The values of expansion ratio obtained by both the approaches compare well with their experimental counterpart for the disc promoted bed as evident in **Fig. 5.12**. The statistical approach considers the entire range, i.e. (-1) to (+1) of particle sizes, bed heights, densities and mass velocities and hence gives a better approximation as compared to ANN approach. The results obtained through ANN approach also provide an authentication to the developed model and experimentation.

The expansion ratio is less in the case of the promoted bed as compared to the un-promoted one as evident from **Figs. 5.8 and 5.9**. In the lower mass velocity range, both the promoters behave identically, whereas in the higher mass velocity range, the expansion is more for the rod type of promoter as compared to the disc type of promoter due to intermittent resistance offered by the disc promoter. The expansion ratio decreases with an increase in bed height as evident from **Fig. 5.5**. It is also evident from **Equations 5.6, 5.7 and 5.8** that the mass velocity has a larger effect on the expansion ratio as compared to the static bed height, particle size and density. It has been found that the expansion ratio increases linearly with an increase in mass velocity. Hence for development of the model equations through factorial analysis approach, the intermediate values for the bed expansion have been considered in lieu of the smallest and largest ones, i.e., for (–1) and (+1) ranges, for both promoted and un-promoted bed, for if the largest value of expansion ratio is taken, then it gives a standard deviation of more than ± 30 %, which is not suitable for the purpose. Also, for development of the model equations, the values of fluctuation ratios considered are those whose corresponding mass velocity ratio values remain constant. The fluctuation ratio first increases up to about twice the minimum fluidization mass velocity ($G_f = 2G_{mf,}$), then decreases, and remains constant thereafter in some cases. The expansion ratio is a direct function of mass

velocity and particle size, whereas it bears an inverse relation to static bed height and density for both promoted and un-promoted beds, which is clearly evident from **Equations 5.6, 5.7 and 5.8**.

It is evident from **Equations 5.9 - 5.14** that both fluctuation and expansion ratios increase with an increase in mass velocity and density both for promoted and un-promoted beds. Also **Equations 5.10 and 5.11** reveal that fluctuation ratio decreases with an increase in static bed and particle size in the case of rod and disc types of promoters. Again expansion ratio increases with an increase in particle size in the case of promoted beds but decreases in the case of un-promoted beds.

Comparison of the values of fluctuation and expansion ratios between dimensional and factorial analysis approaches has been presented in **Tables 5.6, 5.7, 5.8, 5.9, 5.10 and 5.11** and it is found the latter gives better approximation to the former.

The standard deviations for fluctuation and expansion ratios have been found to be ± 0.041, ±0.0304 and ± 2.55, and ± 0.2083, ± 0.0883 and ±0.2048 for un-promoted, rod and disc types of promoters respectively for values other than those taken for development of the model equations.

5.4. Conclusions

Bed fluctuation and expansion ratios increase with an increase in mass velocity for identical operating parameters. A knowledge of fluctuation ratio in gas-solid fluidization is of importance in the design of fluidized bed reactors and combustors, specifically for calculation of bed height. The above equations can be successfully utilized for the prediction of fluctuation and expansion ratios within the specified ranges of particle sizes and densities as presented in Table-1. The numerical values of fluctuation and expansion ratios quantify fluidization quality. A lower static bed height and smaller particle size have been found to give a lower fluctuation ratio, which indirectly points to better fluidization quality.

The introduction of rod and disc types of promoters in the bed improves bubble behaviour by breaking the bubbles of larger sizes into a number of bubbles of smaller sizes, for almost the complete regime of fluidization, except in the neighbourhood of the minimum fluidization conditions, where the bed dynamics are of transitional in nature. The use of the rod type promoter in gas- solid fluidized bed has been found to be more effective in reducing bed fluctuation and increasing bed expansion in higher mass velocity ranges, which in turn helps in reducing the overall size of a fluidizer.

Factorial design, dimensional analysis and ANN approaches can be suitably used for prediction of fluctuation and expansion ratios. In terms of the suitability for calculation of fluctuation and expansion ratios, the factorial design and analysis approach is better than the ANN and dimensional analysis approaches. The factorial design and analysis, in particular, explains both individual and interaction effects among all the variables and gives better result as discussed above. The number of experimental runs required to develop the model equation from statistical design is also considerably less in comparison to conventional experimentation.

Notations

d_p	Diameter of particle, m
D_c	Diameter of column, m
G_f	Mass velocity corresponding to fluidization, kg/m^{2}s
G_{mf}	Mass velocity corresponding to minimum fluidization, kg/m^{2}s
h_S	Static bed height, m
h_1	Lower height of the expanded bed, m
h_2	Upper height of the expanded bed, m
r	Fluctuation ratio
r_c	Fluctuation ratio for disc promoted bed
r_r	Fluctuation ratio for rod promoted bed
r_d	Fluctuation ratio in the case of dimensional analysis approach
r_{dc}	Fluctuation ratio for disc promoted bed in the case of dimensional analysis approach
r_{dr}	Fluctuation ratio for rod promoted bed in the case of dimensional analysis approach
R	Expansion ratio
R_r	Expansion ratio for rod promoted bed
R_c	Expansion ratio for disc promoted bed
R_d	Expansion ratio in the case of dimensional analysis approach
R_{dr}	Expansion ratio for rod promoted bed in the case of dimensional analysis approach
R_{dc}	Expansion ratio for disc promoted bed in the case of dimensional analysis approach
Re_p	Particle Reynolds Number, dimensionless
$X_1 \ldots X_4$	Factorial design symbols

Greek Symbols

ρ_f	Density of fluid, kg/m^3
ρ_s	Density of solid particle, kg/m^3

Abbreviations

cal	Calculated from the model equations
exp	Calculated from the experimental values

References

1. Jin, Z.Y., Shen, J. and Zhang, L., *International Chemical Engineering*, 20 (1980) 191.

2. Jin, Z.Y., Zhang, L., Shen, J. and Wang, Z., *International Chemical Engineering*, 22 (1982) 269.

3. Kono and Jinnai, M., AIChE Symposium Series, 80 (1983) 169.

4. Stewart, B. and Davidson, J.F., Powder technology, 01 (1967) 61.

5. Tsuchiya, K., Miyahara,T. and Fan, L.S., International Journal of Multiphase Flow, 15 (1989) 35.

6. Mat lab version, 6.5.0.180913a release 13.

Figures

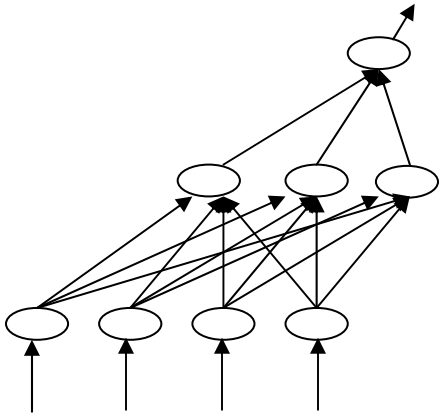

Fig. 5.1 A typical three layer Neural Network

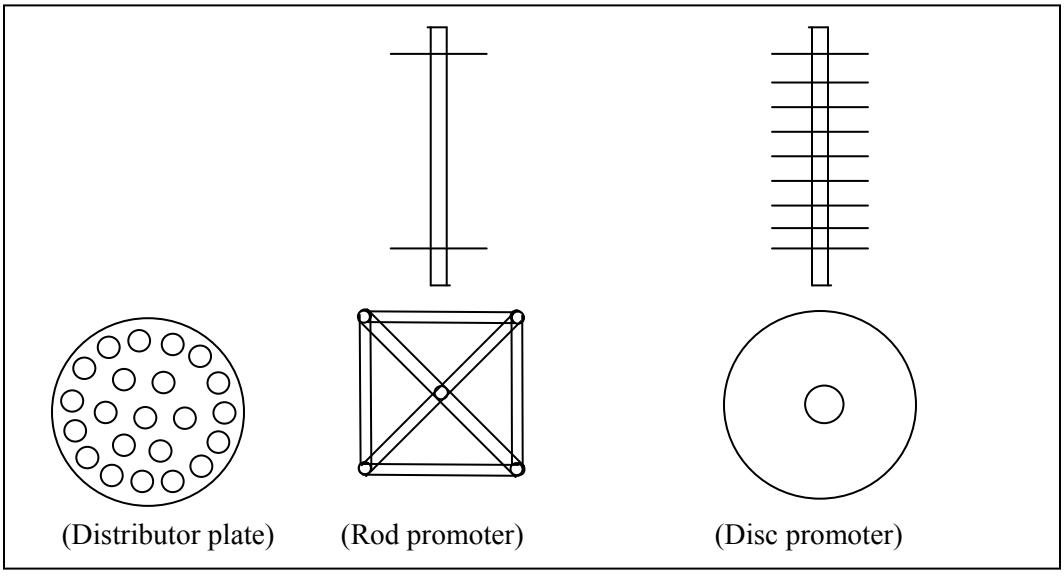

Fig. 5.2 Schematic representation of distributor plate and promoters

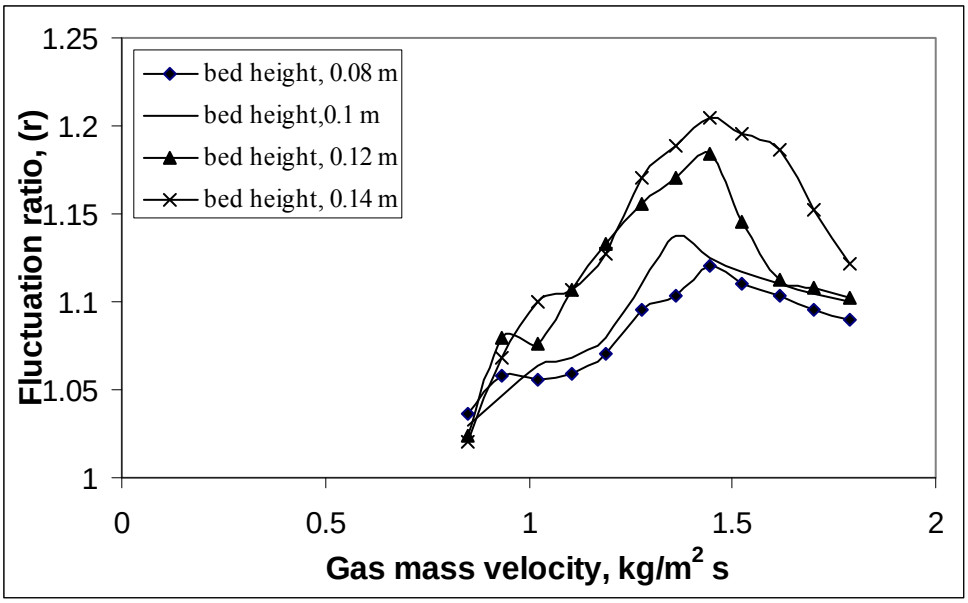

Fig. 5.3 Effect of bed height on fluctuation ratio for dolomite (particle size = 0.000725m)

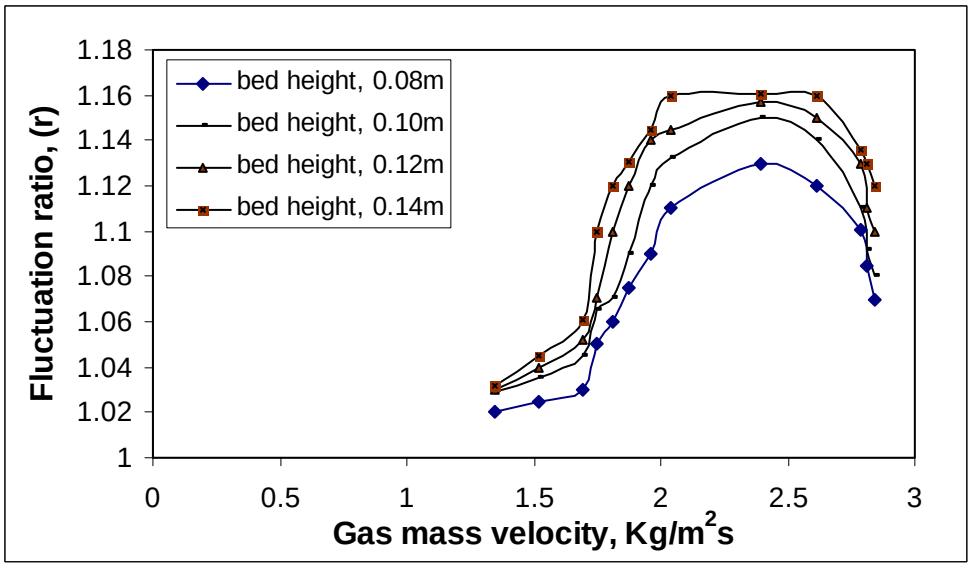

Fig. 5.4 Effect of bed height on fluctuation ratio for dolomite (particle size = 0.0013m in the case of rod promoter)

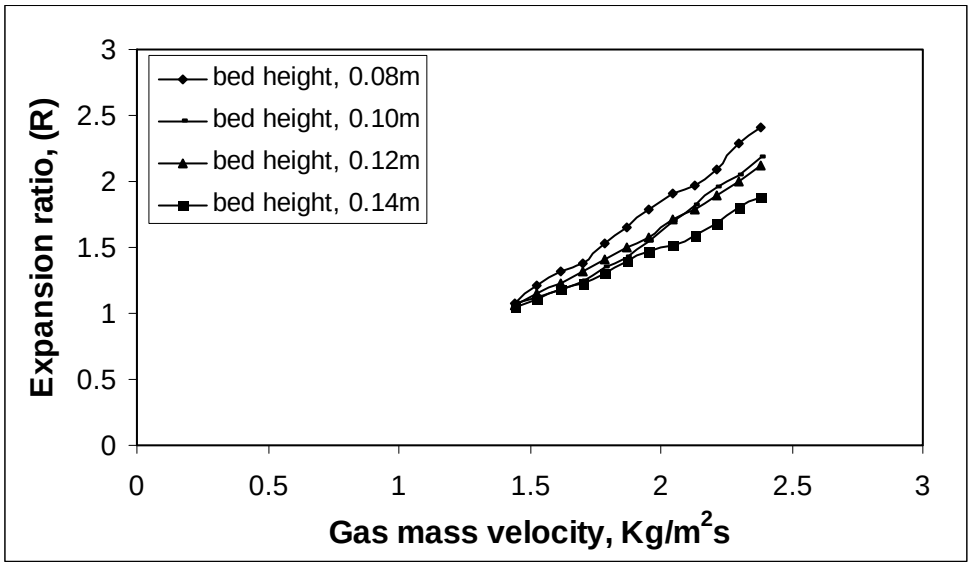

Fig. 5.5 Effect of bed height on expansion ratio for sand (particle size = 0.00055m in the case of disc promoter)

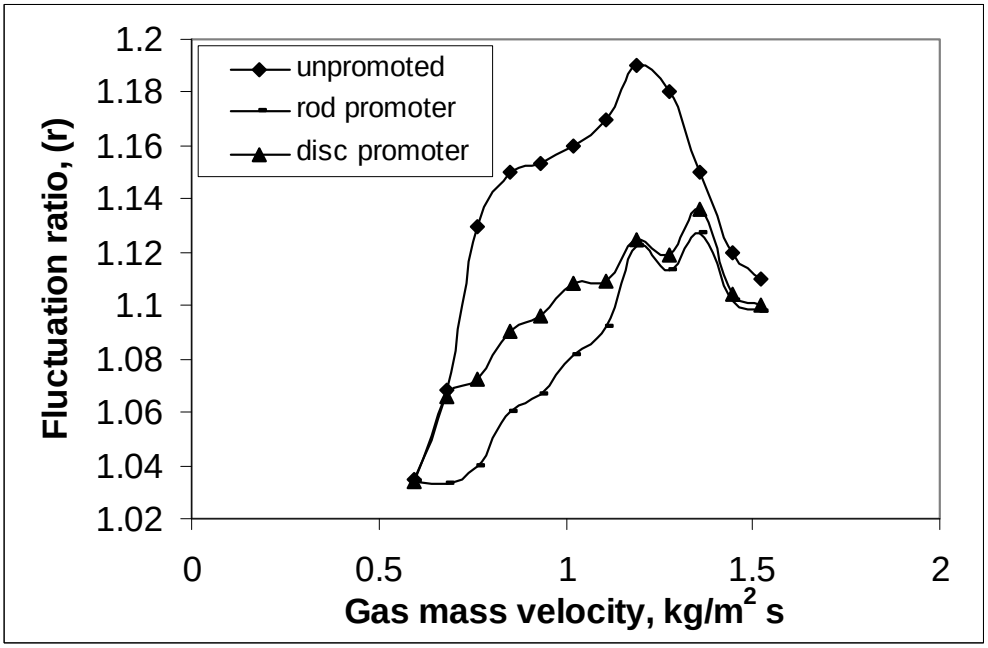

Fig. 5.6 Effect of promoters on fluctuation ratio for sand (particle size = 0.00055m and static bed height = 0.14m)

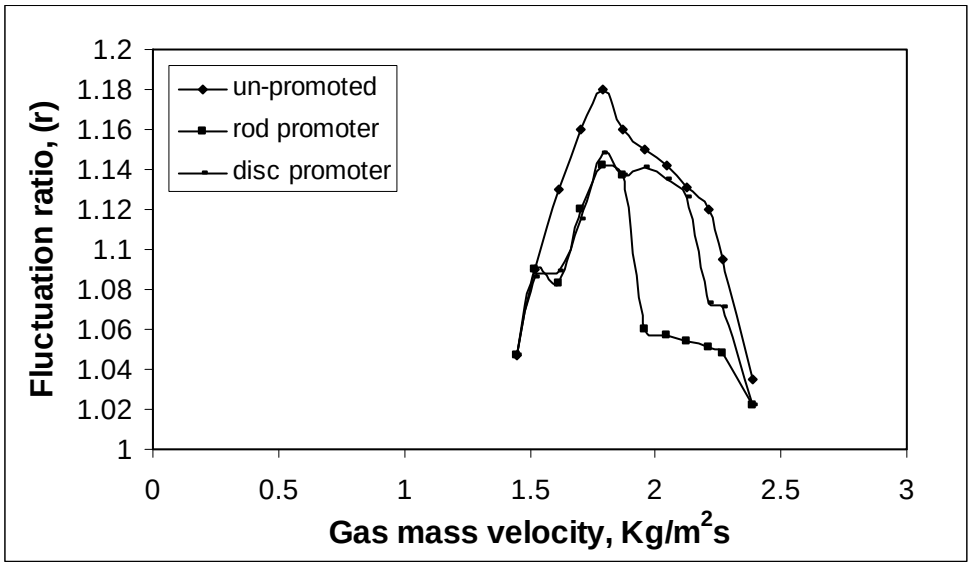

Fig. 5.7 Effect of promoters on fluctuation ratio for refractory brick (particle size = 0.0013m, static bed height = 0.10m)

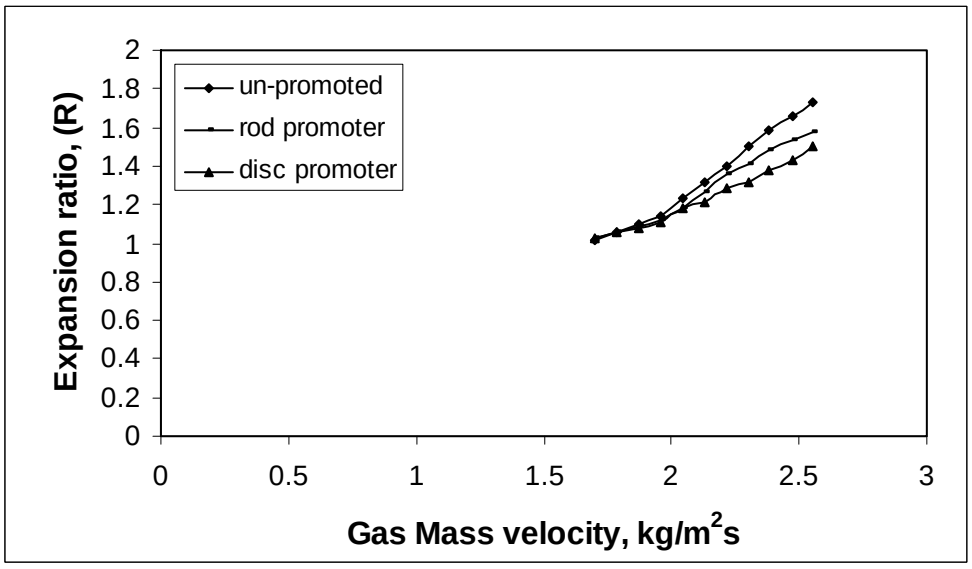

Fig. 5.8 Effect of promoters on expansion ratio for refractory brick (particle size = 0.0017m and static bed height = 0.10m)

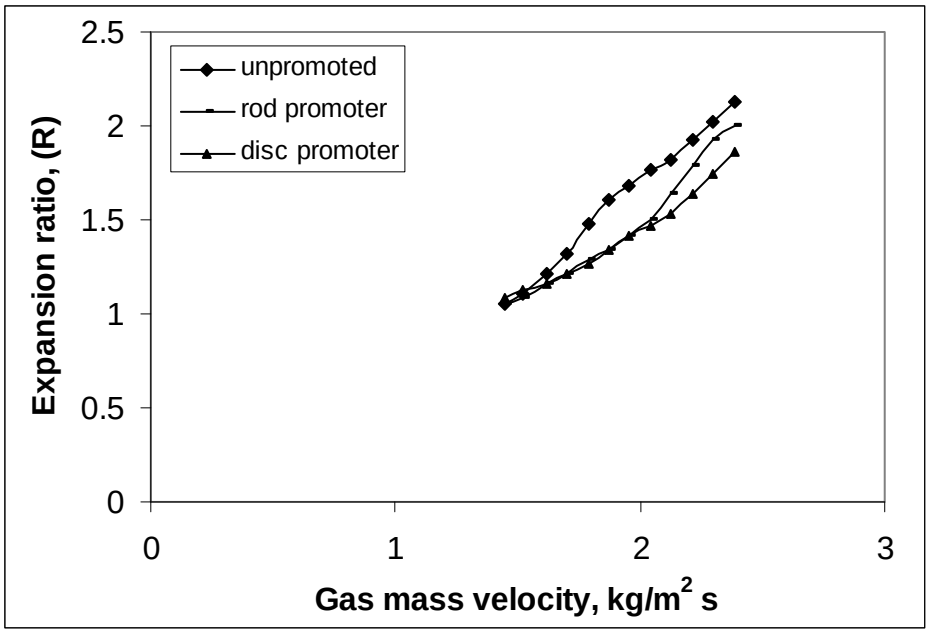

Fig. 5.9 Effect of promoters on expansion ratio for refractory brick (particle size = 0.0013m and static bed height = 0.14m)

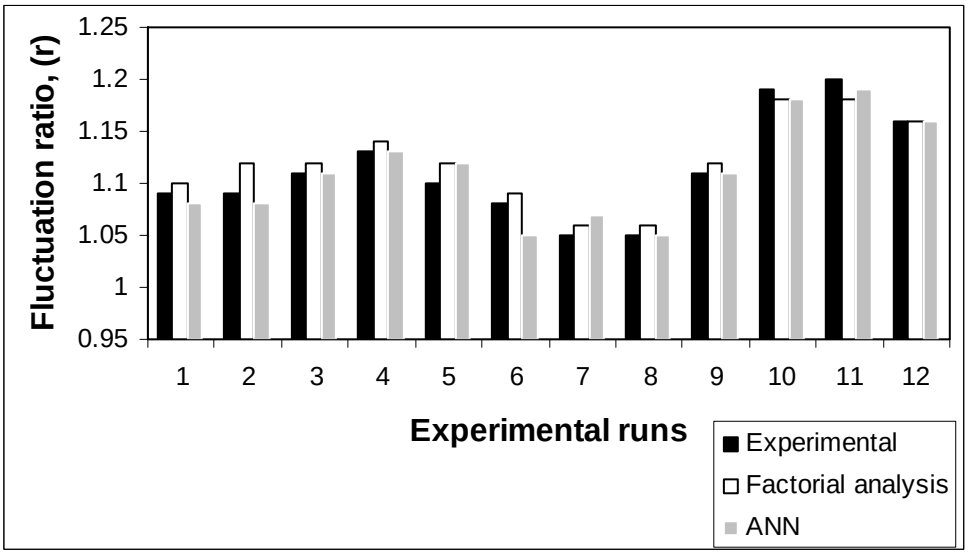

Fig. 5.10 Comparison of fluctuation ratio for un-promoted bed

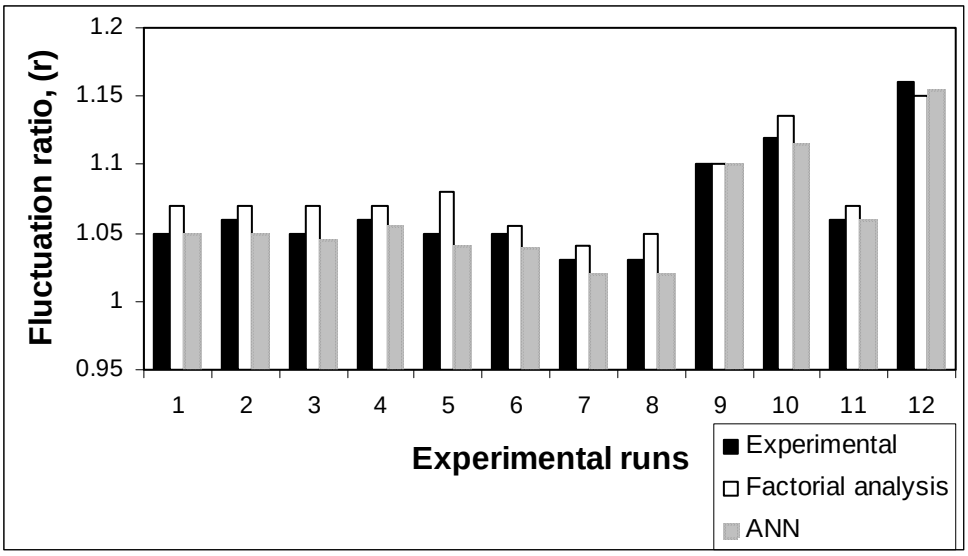

Fig. 5.11 Comparison of fluctuation ratio for rod promoter

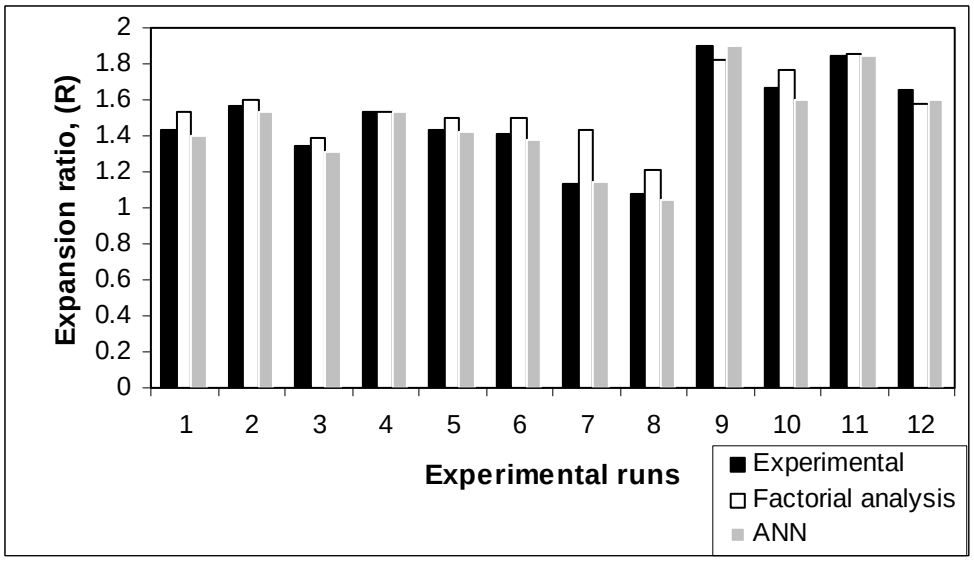

Fig. 5.12 Comparison of expansion ratio for disc promoter

Table 5.1 Scope of the Experiment

Properties of the Bed Materials						
Materials	**$d_{p \times 10^3}$, m**			**$\rho_{s \times 10^{-3}}$, kg/m^3**		
Dolomite	0.55, 0.725, 1.3, 1.7			2.817		
Sand	0.55			2.61		
Refractory brick	0.55, 0.725, 1.3, 1.7			2.5		
Coal	0.55, 0.725, 1.3, 1.7			1.6		
Density of fluid, ρ_f	1.18 kg/m^3 at 25^{0}c					
Diameter of column, D_c	0.099 m					
Bed Parameter						
Initial static bed height, $h_{s \times 10^2}$, m	8, 10, 12, 14					
Flow property						
Materials	A	B×10^{-3}	C×10^2	G_{mf},kg/m^{2}s	G_f,kg/m^{2}s (For 'r')	G_f, kg/m^{2}s (For 'R')
Coal	0.808,1.414	1.356	0.55	0.425	0.595, 1.19	0.68,1.02
Coal	0.808,1.414	1.356	1.7	1.275	1.445,1.955	1.53,1.87
Dolomite	0.808,1.414	2.387	0.55	0.68	0.85,1.53	0.935,1.36
Dolomite	0.808,1.414	2.387	1.7	1.7	1.87, 2.21	1.87, 2.38

Table 5.2 Factorial Design and Analysis

Sl. No	Name of the variable	Variable general symbol	Factorial design symbol	Minimum level (-1)	Maximum level (+1)	Magnitude of variables
1	Static bed height	h_s/D_c	A	0.808	1.414	0.808, 1.01, 1.212, 1.414
2	Density	ρ_s/ρ_f	$B\times10^{-3}$	1.356	2.372	1.356, 2.118, 2.22, 2.372
3	Particle size	d_P/D_c	C	0.0055	0.017	0.0055, .0073, 0.013, 0.017
4	Mass velocity	G_f/G_{mf} (For 'r')	D	1.2	1.6	1.1 to 2.8
		G_f/G_{mf} (For 'R')	D	1.2	1.6	1.1 to 2.4

Table 5.3 Analysis of Fluctuation Ratio Data (r)

Sl. No.	Treatment Combination	A	B	C	D (G_f/G_{mf})	r	r_r	r_c
						experimental		
1	1	0.808	1.356	0.0055	1.2	1.052	1.055	1.055
2	a	1.414	1.356	0.0055	1.2	1.075	1.033	1.033
3	b	0.808	2.387	0.0055	1.2	1.11	1.056	1.052
4	c	1.414	2.387	0.0055	1.2	1.133	1.062	1.093
5	d	0.808	1.356	0.017	1.2	1.157	1.1	1.09
6	ab	1.414	1.356	0.017	1.2	1.138	1.078	1.079
7	ac	0.808	2.387	0.017	1.2	1.075	1.052	1.075
8	ad	1.414	2.387	0.017	1.2	1.091	1.062	1.062
9	bc	0.808	1.356	0.0055	1.6	1.13	1.09	1.09
10	bd	1.414	1.356	0.0055	1.6	1.117	1.085	1.088
11	cd	0.808	2.387	0.0055	1.6	1.175	1.13	1.15
12	abc	1.414	2.387	0.0055	1.6	1.133	1.062	1.093
13	abd	0.808	1.356	0.017	1.6	1.121	1.064	1.058
14	acd	1.414	1.356	0.017	1.6	1.12	1.071	1.071
15	bcd	0.808	2.387	0.017	1.6	1.129	1.096	1.1
16	abcd	1.414	2.387	0.017	1.6	1.058	1.042	1.09

(Columns indicating A, B, C and D are common)

Table 5.4 Analysis of Expansion Ratio Data (R)

Sl. No.	Treatment Combination	A	B	C	D (G_f/G_{mf})	R	R_r	R_c
						experimental		
1	1	0.808	1.356	0.0055	1.2	1.218	1.156	1.156
2	a	1.414	1.356	0.0055	1.2	1.082	1.089	1.089
3	b	0.808	2.387	0.0055	1.2	1.187	1.156	1.25
4	c	1.414	2.387	0.0055	1.2	1.142	1.178	1.196
5	d	0.808	1.356	0.017	1.2	1.281	1.312	1.437
6	ab	1.414	1.356	0.017	1.2	1.375	1.41	1.41
7	ac	0.808	2.387	0.017	1.2	1.206	1.218	1.206
8	ad	1.414	2.387	0.017	1.2	1.232	1.178	1.178
9	bc	0.808	1.356	0.0055	1.6	1.531	1.437	1.437
10	bd	1.414	1.356	0.0055	1.6	1.285	1.303	1.267
11	cd	0.808	2.387	0.0055	1.6	1.562	1.531	1.543
12	abc	1.414	2.387	0.0055	1.6	1.142	1.178	1.196
13	abd	0.808	1.356	0.017	1.6	2.187	2	2.187
14	acd	1.414	1.356	0.017	1.6	2.196	2.071	2.071
15	bcd	0.808	2.387	0.017	1.6	2.062	1.906	1.968
16	abcd	1.414	2.387	0.017	1.6	1.875	1.714	1.642

(Columns indicating A, B, C and D are common.)

Table 5.5 Selected Structures of Neural Network Models

Net train parameter	: 500			
Percentage set learning rate	: 0.2—10			
Net train parameter learning	: 0.2—10			
Percentage set error goal	: 0.001			
Net train parameter epochs	: 50,000			
Performance	: 0.02368/1e^{-5}			
Bed Particular	Input Nodes	Hidden Nodes	Output Nodes	No of cycles
Primary air	4	3	1	50,000
Secondary air	4	3	1	50,000

Table 5.6 Comparisons of Fluctuation Ratio Data in the Case of Un-Promoted Bed

r_{cal}	r_{exp}	%Deviation	r_{cal}	r_{exp}	%Deviation
Factorial analysis			Dimensional analysis		
1.0657	1.052	1.3089	1.0833	1.052	2.9798
1.075	1.075	0.0256	1.1291	1.075	5.0374
1.109	1.11	-0.087	1.1274	1.11	1.5688
1.118	1.133	-1.274	1.1750	1.133	3.7142
1.1318	1.157	-2.1684	1.0517	1.157	-9.0936
1.1413	1.138	0.2933	1.0962	1.138	-3.6681
1.0879	1.075	1.2026	1.0945	1.075	1.8203
1.0974	1.091	0.5878	1.1408	1.091	4.5690
1.1319	1.13	0.1743	1.1008	1.13	-2.5799
1.1014	1.117	-1.390	1.1473	1.117	2.7208
1.1752	1.175	0.0195	1.1456	1.175	-2.5000
1.1447	1.133	1.0353	1.1940	1.133	5.3894
1.1441	1.121	2.0663	1.0687	1.121	-4.6587
1.1136	1.12	-0.5657	1.1139	1.12	-0.5388
1.1001	1.129	-2.5524	1.1122	1.129	-1.4836
1.0696	1.058	1.1042	1.1592	1.058	9.5724
1.1203	1.148	-2.4124	1.1643	1.148	1.4284
1.1944	1.173	1.8269	1.1952	1.173	1.8997
1.0922	1.1	-0.7064	1.0890	1.1	-0.9939
1.1196	1.151	-2.7270	1.1058	1.151	-3.9223
1.0981	1.13	-2.8174	1.1072	1.13	-2.0177
1.1159	1.12	-0.3580	1.1263	1.12	0.5680
1.1040	1.107	-0.2623	1.1222	1.107	1.3765
1.1079	1.113	-0.4542	1.1395	1.113	2.3842
1.0977	1.095	0.2482	1.1373	1.095	3.8674
1.2666	1.18	7.341	1.1859	1.12	5.8869
1.1169	1.13	-1.154	1.1734	1.13	3.8456
1.1824	1.15	2.8223	1.2118	1.15	5.3742
1.1162	1.105	1.0212	1.1260	1.105	1.9093
1.2346	1.178	4.8062	1.1541	1.133	1.8703

Table 5.7 Comparisons of Fluctuation Ratio Data in the Case of Rod Promoted Bed

$r_{r\,cal}$	$r_{r\,exp}$	%Deviation	$r_{r\,cal}$	$r_{r\,exp}$	%Deviation
Factorial analysis			Dimensional analysis		
1.0730	1.055	1.7109	1.1044	1.055	4.6851
1.0315	1.033	-0.1403	1.0769	1.033	4.2500
1.0484	1.056	-0.7149	1.1112	1.056	5.2313
1.0529	1.062	-0.8521	1.0835	1.062	2.0289
1.0942	1.1	-0.5213	1.0797	1.1	-1.8380
1.0527	1.078	-2.3408	1.0528	1.078	-2.3311
1.0696	1.052	1.6792	1.0864	1.052	3.2741
1.0741	1.062	1.1455	1.0593	1.062	-0.2479
1.0900	1.09	0.0045	1.1163	1.09	2.4168
1.0945	1.085	0.8801	1.0885	1.085	0.3245
1.1114	1.13	-1.6415	1.1232	1.13	-0.598
1.0699	1.062	0.7485	1.0952	1.062	3.1296
1.0668	1.064	0.2680	1.0914	1.064	2.5780
1.0713	1.071	0.0328	1.0642	1.071	-0.6322
1.0882	1.096	-0.7069	1.0981	1.096	0.1975
1.0467	1.042	0.4560	1.0707	1.042	2.7634
1.0559	1.086	-2.7708	1.1017	1.086	1.4541
1.1005	1.137	-3.2017	1.1126	1.137	-2.1435
1.1601	1.122	3.4027	1.1238	1.122	0.1619
1.0554	1.068	-1.1711	1.0927	1.068	2.3192
1.0858	1.138	-4.5866	1.1035	1.138	-3.0302
1.1262	1.142	-1.3817	1.1146	1.142	-2.3981
1.0559	1.056	-0.0090	1.0896	1.056	3.1877
1.0718	1.1	-2.5621	1.0959	1.1	-0.3699
1.0984	1.103	-0.4127	1.1047	1.103	0.1551
1.0646	1.037	2.6668	1.0699	1.037	3.1742
1.0662	1.125	-5.2240	1.0760	1.125	-4.3491
1.0688	1.116	-4.2236	1.0846	1.116	-2.8052
1.0637	1.05	1.3105	1.0880	1.05	3.6205
1.0737	1.12	-4.13109	1.0940	1.12	-2.321

Table 5.8 Comparisons of Fluctuation Ratio Data in the Case of Disc Promoted Bed

$r_{c\ cal}$	$r_{c\ exp}$	%Deviation	$r_{c\ cal}$	$r_{c\ exp}$	%Deviation
Factorial analysis			Dimensional analysis		
1.0752	1.055	1.9146	1.1188	1.055	6.0502
1.0676	1.033	3.3494	1.0943	1.033	5.9349
1.094	1.052	3.9923	1.1308	1.052	7.4946
1.0864	1.093	-0.6038	1.1060	1.093	1.1947
1.0468	1.09	-3.9590	1.0782	1.09	-1.0737
1.0392	1.079	-3.6842	1.0546	1.079	-2.2554
1.0656	1.075	-0.8700	1.0898	1.075	1.3837
1.058	1.062	-0.3722	1.0659	1.062	0.3755
1.075	1.09	-1.3578	1.1346	1.09	4.0931
1.067	1.088	-1.875	1.1097	1.088	1.9988
1.094	1.05	4.1904	1.1467	1.05	9.2189
1.086	1.093	-0.6038	1.1216	1.093	2.6225
1.0964	1.058	3.6309	1.0935	1.058	3.3563
1.0888	1.071	1.6634	1.0695	1.071	-0.136
1.1152	1.1	1.3832	1.1052	1.1	0.4774
1.1076	1.09	1.6161	1.0810	1.09	-0.8231
1.0914	1.086	0.5033	1.1231	1.086	3.4185
1.0914	1.136	-3.9201	1.1525	1.136	1.4548
1.0889	1.103	-1.2753	1.1150	1.103	1.0921
1.0694	1.086	-1.5242	1.0960	1.086	0.9233
1.0845	1.125	-3.5946	1.1042	1.125	-1.8430
1.1098	1.114	-0.3719	1.1158	1.114	0.1644
1.0643	1.076	-1.0798	1.0785	1.076	0.2388
1.0794	1.156	-6.6181	1.0866	1.156	-5.9967
1.1047	1.119	-1.2698	1.0980	1.119	-1.8713
1.0641	1.105	-3.7013	1.0932	1.105	-1.0607
1.0973	1.121	-2.1054	1.1101	1.121	-0.970
1.0615	1.08	-1.7067	1.0836	1.08	0.3389
1.0948	1.073	2.0377	1.1003	1.073	2.5496
1.0590	1.107	-4.3329	1.0758	1.107	-2.8125

Table 5.9 Comparisons of Expansion Ratio Data in the Case of Un-Promoted Bed

R_{cal}	R_{exp}	%Deviation	R_{cal}	R_{exp}	%Deviation
Factorial analysis			Dimensional analysis		
1.2034	1.218	-0.0119	1.1150	1.218	-8.4563
1.0843	1.082	0.0021	1.0889	1.082	0.6449
1.2229	1.187	0.0302	1.1211	1.187	-5.5493
1.1156	1.142	-0.0230	1.0949	1.142	-4.1188
1.2934	1.281	0.0097	1.0066	1.281	-21.417
1.3686	1.375	-0.0046	0.9831	1.375	-28.498
1.1690	1.206	-0.0306	1.0121	1.206	-16.072
1.2560	1.232	0.0195	0.9885	1.232	-19.760
1.5209	1.531	-0.0065	1.5103	1.531	-1.3469
1.3044	1.285	0.0151	1.4751	1.285	14.795
1.5466	1.562	-0.0098	1.5186	1.562	-2.7734
1.1455	1.142	0.0031	1.4832	1.142	29.880
2.1895	2.187	0.0011	1.3635	2.187	-37.650
2.1673	2.196	-0.0130	1.3317	2.196	-39.354
2.0712	2.062	0.0045	1.3710	2.062	-33.507
1.8644	1.875	-0.0056	1.3390	1.875	-28.582
1.2884	1.25	0.0307	1.2042	1.25	-3.6604
1.8653	2	-0.0673	1.9204	2	-3.9762
1.0612	1.312	-0.1911	0.9604	1.312	-26.792
1.5735	2.062	-0.2368	1.2280	2.062	-40.443
1.1747	1.35	-0.1297	1.0045	1.35	-25.587
1.6289	2.025	-0.1955	1.2712	2.025	-37.223
1.1060	1.229	-0.1000	0.9441	1.229	-23.174
1.4211	1.75	-0.1879	1.1548	1.75	-34.006
1.1284	1.214	-0.0704	0.938	1.214	-22.729
1.3297	1.607	-0.1725	1.0955	1.607	-31.827
1.5968	1.928	-0.1717	1.3064	1.928	-32.239
1.0563	1.143	-0.0758	0.968	1.143	-15.239
1.3840	1.418	-0.0239	1.1394	1.418	-19.644
1.9326	2.062	-0.0627	1.4279	2.062	-30.747

Table 5.10 Comparisons of Expansion Ratio Data in the Case of Rod Promoted Bed

$R_{r\ cal}$	$R_{r\ exp}$	%Deviation	$R_{r\ cal}$	$R_{r\ exp}$	%Deviation
Factorial analysis			Dimensional analysis		
1.1559	1.156	-0.0086	0.8760	1.156	-24.217
1.1179	1.089	2.6538	0.8893	1.089	-18.330
1.1819	1.156	2.2404	1.1085	1.156	-4.1075
1.1199	1.178	-4.9320	1.1253	1.178	-4.4657
1.2827	1.312	-2.2258	1.1283	1.312	-13.996
1.4668	1.41	4.0330	1.1455	1.41	-18.755
1.2096	1.218	-0.6848	1.4278	1.218	17.225
1.1555	1.178	-1.9024	1.4495	1.178	23.051
1.4561	1.437	1.32915	1.2059	1.437	-16.078
1.2541	1.303	-3.7528	1.2243	1.303	-6.0386
1.4821	1.531	-3.1939	1.5259	1.531	-0.3277
1.2561	1.178	6.6298	1.5492	1.178	31.512
2.0033	2	0.16706	1.5533	2	-22.334
2.0234	2.071	-2.2979	1.5769	2.071	-23.855
1.9302	1.906	1.26985	1.9655	1.906	3.1223
1.7121	1.714	-0.1088	1.9954	1.714	16.419
1.1919	1.2	-0.6729	1.1669	1.2	-2.7534
1.4221	1.55	-8.2508	1.5618	1.55	0.7662
1.1644	1.25	-6.846	1.1727	1.25	-6.1825
1.3433	1.604	-16.249	1.5695	1.604	-2.1456
1.0923	1.156	-5.509	1.2514	1.156	8.2527
1.3608	1.312	3.7208	1.4845	1.312	13.150
1.8102	1.906	-5.0242	1.8828	1.906	-1.2126
1.074	1.145	-6.119	1.2651	1.145	10.495
1.2923	1.416	-8.7344	1.5008	1.416	5.9941
1.6561	1.895	-12.602	1.9036	1.895	0.4545
1.0904	1.281	-14.871	1.1837	1.281	-7.5939
1.0965	1.25	-12.277	1.1908	1.25	-4.7299
1.3264	1.55	-14.420	1.4022	1.55	-9.5296
1.1025	1.166	-5.44	1.1967	1.166	2.6374

Table 5.11 Comparisons of Expansion Ratio Data in the Case of Disc Promoted Bed

$R_{c\ cal}$	$R_{c\ exp}$	%Deviation	$R_{c\ cal}$	$R_{c\ exp}$	%Deviation
Factorial analysis			Dimensional analysis		
1.144	1.156	-1.038	1.0219	1.156	-11.59
1.0988	1.089	0.8999	0.9574	1.089	-12.08
1.2436	1.25	-0.512	1.1520	1.25	-7.839
1.2044	1.196	0.7023	1.0792	1.196	-9.762
1.4443	1.437	0.5141	1.2065	1.437	-16.04
1.3991	1.41	-0.7668	1.1302	1.41	-19.83
1.2108	1.206	0.40501	1.3600	1.206	12.77
1.1716	1.178	-0.5361	1.2741	1.178	8.1592
1.4238	1.437	-0.9185	1.4261	1.437	-0.7579
1.2826	1.267	1.2312	1.3360	1.267	5.4477
1.5354	1.543	-0.4925	1.6075	1.543	4.1851
1.201	1.196	0.4180	1.5060	1.196	25.922
2.1913	2.187	0.1977	1.6836	2.187	-23.016
2.0501	2.071	-1.0079	1.5772	2.071	-23.840
1.9698	1.968	0.0926	1.8978	1.968	-3.5641
1.6354	1.648	-0.7632	1.7779	1.648	7.8867
1.2547	1.2	4.5590	1.1767	1.2	-1.9359
1.4360	1.6	-10.248	1.5946	1.6	-0.3329
1.6777	2.19	-23.389	2.1758	2.19	-0.6482
1.2293	1.27	-3.2014	1.1520	1.27	-9.2901
1.3184	1.52	-13.262	1.561	1.52	2.7058
1.4371	2.02	-28.853	2.1300	2.02	5.4474
1.1104	1.2	-7.4643	1.2132	1.2	1.1025
1.3892	1.593	-12.789	1.449	1.593	-8.9918
1.8559	2.312	-19.723	1.8574	2.312	-19.65
1.1211	1.125	-0.3382	1.1572	1.125	2.8628
1.3080	1.437	-8.9746	1.3828	1.437	-3.7707
1.6207	1.854	-12.58	1.771	1.854	-4.4385
1.1285	1.25	-9.7174	1.1744	1.25	-6.0477

6.1 Introduction

Fluidization is an established fluid–solid contacting technique, which finds extensive applications in combustion, gasification, carbonization, drying of solids, coating of objects and many other processes. With the flow of gas more than the minimum fluidization mass velocity, the top of the fluidized bed fluctuates considerably leading to instability in operation. The use of secondary air in fluidized bed offers several advantages, viz., creation of oxidation and reduction zone in the fluidized bed combustor, control over particle residence time, reduction of toxic gases like SO_X and NO_X in the flue gas, control over reaction rates, pneumatic transport etc.

Many thermal power generating units are, of late, increasingly following the concept of circulating fluidized bed and are using secondary air in the fluidizer for the improvement of quality of fluidization and combustion without understanding the real hydro-dynamics involved. Owing to the scarcity of good quality of coal and an ever-increasing demand for electricity, for the complete combustion of low grade coal, the introduction of secondary air is one of the best solutions. Several sponge iron production units have been entangled with the problem of converting carbon into carbon dioxide.

Extensive experimental work and industrial applications provide unambiguous evidence. It is precisely these fluctuations that are responsible for extremely high values of effective coefficients of heat and mass transport to determine the dynamic properties of disperse mixtures. In general, large scale fluctuations strongly depend on various external conditions, such as geometric properties of the disperse flow and quality of the gas distribution in fluidized beds. Whereas the small scale fluctuations depend merely on the local hydrodynamic situations and more inherent to macroscopically uniform states with no inner circulation and without bubbles.

Gas- solid fluidized bed, generally of aggregative nature, is marked by occurrence of bubbles of varied sizes. This results in a non-uniform bed expansion and a poor fluidization phenomenon.

Keeping in view the aforesaid inherent drawbacks, the present study aims at investigating the influence of primary as well as simultaneous primary and secondary fluidizing media on bed pressure drop, fluctuation ratio and expansion ratio.

Mohanty et al. (1993) studied the effect of temperature, velocity ratio, particle size of ore and reductant on the reduction of iron ore and concluded that for an adequately agitated fluidized bed the operating velocity should be maintained at around two times the minimum fluidization velocity. Buyevich and Kapbasov (1994) worked out a mathematical model to treat random small-scale fluctuations of particles and fluid in a macroscopically uniform disperse mixture and found that the overall phase volume fluxes and the hydraulic resistance coefficient happen to be sensitive to the fluctuations and differ from those specific to the same mixture without fluctuations.

Sanyal and Cesmebasi (1994) studied the effect of various gas-solid momentum transfer coefficient models on the bubbles formation with the use of secondary air and found that at higher gas velocity the gas seemed to choose a slender channel to pass through the bed for which there was a considerable lateral diffusion resulting in a general lifting of the bed.

Johnsson et al. (1996) studied the reduction and decomposition of N_2O in a circulating fluidized bed boiler and found that 60% of the N_2O destruction was due to thermal decomposition and in the cyclone heterogeneous destruction of N_2O was insignificant. Also it was found that more than one-half of the formation of N_2O in the combustion chamber takes place above the secondary air inlet.

Narvaez et al. (1996) studied biomass gasification with air in an atmospheric bubbling fluidized bed with secondary fluidizing medium and concluded that the raw gas

with good quality (maximum heating value and minimum tar content) can be obtained if feed is given near the bed bottom. A small secondary air injection (10% of the over) in the freeboard (the region above the average surface of the bed) improves the quality of the raw gas produced.

Corella et al. (1999) studied biomass gasification in fluidized bed both for gasification with air and with steam-O_2 mixture and found that downstream (section above the gasifier bed in the flow direction) dolomite has only a little bit higher chemical effectiveness for tar removal than that of in-bed dolomite.

Mastellone and Arena (1999) studied the effect of particle size and density on solid distribution along the riser of a circulating fluidized bed and concluded that an increase in particle density from 1800 to 2600 kg/m^3 led to a higher solid concentration at the riser bottom. The coarser particles gave flat profiles without solids flowing downwards at the walls, while smaller particles presented a relatively wider annulus, still present at the riser top.

Grace et al. (1999) studied the effect of high density (HDCFB) and low density (LDCFB) particles in a circulating fluidized bed and found that HDCFB systems offer significant advantages for reactions involving gas and particles, in particular, for low back mixing of gas and solids coupled with high solids loading and excellent – gas particle contacting.

Liu et al. (2000) investigated the polycyclic aromatic hydrocarbons in fly ash, from fluidized bed combustion and found that FBC systems have an efficient solid gas mixing process and relatively long residence time. High speed secondary air injected into the freeboard of the FBC system is an effective method for minimizing polycyclic aromatic hydrocarbon emissions.

Liu et al. (2001) studied the combustion of mercury with high-chlorine coals in a fluidized bed combustor and found that without the use of secondary air injection and after cooling the flue gas to 400 ^oC by using a convective heat exchange tube bank, the

typical concentration of gas phase mercury in FBC flue gas was 1500-3000 mg/Nm^3. Better results were obtained by using high chlorine coals and a predetermined ratio of secondary air (secondary/primary air ratio > 0.15). Only 0.5% of the total mercury input was emitted from the combustor in the elemental form.

Tardin and Goldstein (2001) studied the mechanical attrition and fragmentation of particles in a fast fluidized bed with both primary and secondary air injections and found that the particle size reduction rate to be proportional to the fluidization excess velocity and to mass inventory, as in bubbling fluidized beds.

Luis et al. (2004) studied the effect of secondary air in a bubbling fluidized bed, for the combustion of bituminous and anthracite coal, and found that due to less operational temperature the NO_X emission can be suitably controlled. The NO flue gas concentration is strongly determined by the secondary combustion zone.

Murthy et al. (2004) used statistical approach method and found that at minimum fluidization velocity the pressure drop and the power consumption decreases and increases respectively with increase in stirrer speed.Tarelho et al. (2004) studied the axial concentration profiles and NO flue gas in a pilot scale bubbling fluidized bed coal combustor and concluded that due to secondary air injection the bed temperature can be controlled significantly and hence lower NO_X emissions.

Kaynak et al. (2005) studied the combustion of peach and apricot in a bubbling fluidized bed and found that the coal has zero CO emission, but biomass fuels have very high CO emission which indicates that a secondary air addition is required for the system. SO_2 emission of the coal is around 2400-2800 mg/Nm3, whereas the biomass fuels have zero SO_2 emission. NO_x emissions are all below the limits set by the Turkish air quality control.

Cousins et al. (2006) investigated the reactivity of chars formed in fluidized bed gasifiers and found that increased in temperature, pressure and particle size had a negative impact on the char reactivity.

Mohanty et al. (2007) have developed the following fluctuation ratio correlations (6.1 and 6.2) under primary as well as both primary and secondary (simultaneous) gas flow conditions respectively, for irregular particles (dimensional analysis approach) as:

$$r_1 = 0.8869\left(\frac{h_s}{D_C}\right)^{0.0095}\left(\frac{\rho_s}{\rho_f}\right)^{0.022}\left(\frac{d_p}{D_C}\right)^{-0.0339}\left(\frac{G_f}{G_{mf}}\right)^{0.1736} \quad \ldots (6.1)$$

$$r_2 = 0.998\left(\frac{h_s}{D_C}\right)^{-0.073}\left(\frac{\rho_s}{\rho_f}\right)^{0.0064}\left(\frac{d_p}{D_C}\right)^{-0.0322}\left(\frac{G_p}{G_S}\right)^{0.0034} \quad \ldots (6.2)$$

The objective of the present work is to understand the hydrodynamics of both primary and secondary (simultaneous) air supply instead of only primary air supply and to increase its applicability in fluidized bed. As the quality of fluidization is expressed in terms of pressure drop, fluctuation ratio and expansion ratio, for which mathematical models have been developed. Plenty of literature is available for the calculation of pressure fluctuations, whereas a very little literature is available on fluctuation and expansion ratios. It is also evident from the literature that the ANN approach can be suitably applied for the calculation of the same. In the present case, a software package for artificial neural networking in MatLab has been used for back propagation algorithm for the testing of the data. A typical three layers, viz., (i) the input layer (I), (ii) the hidden layer (H), and (iii) the output layer (O) with four input nodes, three numbers of neurons in the hidden layer and one output node, have been chosen.

The schematic representation of the experimental set-up is as shown in **Fig. 6.1**. Experiments have been carried out by supplying primary air from below (through the distributor plate) and secondary air (a fraction of air supplied through the side ports of

column in the middle of each static bed) through a pipe having fine holes directed only towards the top of the column like a sparger pipe as shown in **Fig. 6.2**.
Experiments have been carried out at two different conditions, viz,

(i) Primary air supply and
(ii) Simultaneous primary and secondary air supply.

In order to fluidize the entire bed material, the secondary air flow begins some time after the minimum fluidization condition is reached with the primary air. The variables affecting pressure drop, fluctuation and expansion ratios are static bed height, particle density, particle size and mass velocity of air. The scope of the experiment is presented in **Table-6.1**. Total number of experiments required at two levels (minimum and maximum) for four variables are sixteen for responses in the case of factorial design method. Each experiment is repeated three times and the average of three values are reported as response value.

6.2 Development of Models

In this work, mathematical models have been developed for the prediction of pressure drop, fluctuation and expansion ratios. The model equations are assumed to be linear and the equations take the general form:

$$Y= a_0 + a_1A + a_2B + a_3C + a_4D +\ldots\ldots\ldots + a_{12}ABD + a_{13}ACD +\ldots\ldots + a_{15}ABCD \quad \ldots (6.3)$$

The coefficients are calculated by the Yate's technique $a_i = \sum \alpha_i y_i / N$ ... (6.4)

where A, B, C and D are the factorial design symbols, a_i is the coefficient, y_i is the response, α_i is the level of variables and N is the total number of treatments.

The experimental data based on factorial design, nature of the effects and its analysis are presented for fluctuation and expansion ratios in **Tables 6.2 and 6.3** respectively.

The levels of variables are calculated as under for primary air supply:

A: level of static bed height = (A-1.111) / 0.303

B: Level of density= (B-1.864) / 0.508

C: Level of particle size = (C-0.01125)/ 0.00575

D: Level of mass velocity = (D-1.4) / 0.2

… (6.5)

The levels of variables are calculated for simultaneous primary and secondary air supplies:

A: level of static bed height = (A-1.111) / 0.303

B: Level of density= (B-1.864) / 0.508

C: Level of particle size = (C-0.01125)/ 0.00575

D: Level of mass velocity = (D-3.735) / 2.035

… (6.6)

The following **Eqs. (6.7, 6.8, 6.9, 6.10 and 6.11)** have been developed for pressure drop at minimum fluidization, fluctuation and expansion ratios (neglecting smaller coefficients) for primary as well as primary and secondary (simultaneous) air.

$\Delta P_{mfs} = 2.441 + 0.1268A + 0.85B + 0.3543C - 0.0537D + 0.03AB + 0.2831BC - 0.0262BD - 0.03CD$ … (6.7)

$r_p = 1.113 - 0.0052A - 0.00037B - 0.0022C + 0.0095D - 0.01AD - 0.022BC - 0.0136CD$ ... (6.8)

$r_s = 1.172 + 0.0181A + 0.0065B - 0.0174C + 0.01118D + 0.0215BD + 0.0393CD$ ... (6.9)

$R_p = 1.4726 - 0.0565A - 0.0466B + 0.204C + 0.2573D - 0.0216AB + 0.0493AC - 0.0489AD - 0.0363BC - 0.023BD + 0.1459CD - 0.0245ABD$ ... (6.10)

$R_s = 1.824 - 0.1318A + 0.0118B + 0.2177C - 0.37D - 0.0312AB + 0.0635AD - 0.0137BD - 0.1226CD - 0.0982ABC + 0.0213ABD + 0.0383ABCD$ ... (6.11)

In this work an ANN model using back propagation algorithm for both primary and simultaneous primary and secondary air has been developed. In both the cases, the ANN structures (Input layer × Hidden layer × Output layer) have been tested at constant epochs (cycles), learning rate, error goal and net trained parameter. Structures of neural network model are selected for training of input output data in each case as shown in **Table 6.4**.

The following **Eqs. (6.12 and 6.13)** for expansion ratio have also been developed for primary as well as simultaneous primary and secondary gas flow conditions respectively, for irregular particles (dimensional analysis approach) as:

$$R_1 = 1.5\left(\frac{h_s}{D_c}\right)^{-0.081}\left(\frac{\rho_s}{\rho_f}\right)^{-0.0772}\left(\frac{d_p}{D_c}\right)^{0.0569}\left(\frac{G_f}{G_{mf}}\right)^{0.8615} \quad \text{… (6.12)}$$

$$R_2 = 3.662\left(\frac{h_s}{D_c}\right)^{-0.365}\left(\frac{\rho_s}{\rho_f}\right)^{0.3413}\left(\frac{d_p}{D_c}\right)^{0.1608}\left(\frac{G_f}{G_{mf}}\right)^{-0.2635} \quad \ldots (6.13)$$

6.3 Results and Discussion

The method of experimentation is based on statistical analysis of experiments (Factorial Design and Analysis) in order to bring out the interaction effects of variables. Four different bed materials, viz., dolomite, sand, refractory brick and coal have been considered for the experimentation. Out of which, coal and dolomite have been considered for the calculation of the model equations, as these two have the lowest and highest densities respectively. Apart from this, particles of sizes 0.00055m and 0.0017m, bed heights 0.08m and 0.14m, and mass velocities at the lowest and the highest ranges have been considered for the development of the mathematical model. It has been observed that all the different particles in the bed start to fluidize at different mass velocity called minimum fluidization mass velocity. The experiments have been carried out up to 2.5 times the minimum fluidization mass velocity with a continual increment of 0.085kg/m^{2}s. The flow of secondary air begins after the bed starts to fluidize due to primary air supply through the bottom of the fluidizer. It has been observed that the secondary air exerts an axial thrust on the bottom of the bed and owing to this effect, the primary air supply is maintained at more than the minimum fluidization mass velocity, i.e., G_{mf} + 0.17 for all the experiments. If this extra amount of primary air (0.17 kg/m^{2}s) is not supplied, then the lower half of the bed will not fluidize properly. For any bed material this is the minimum required extra amount of air that has to be supplied in addition to the amount of minimum fluidization mass velocity i.e., G_{mf}. It has been observed that the introduction of secondary air enhances mixing among the particles of wide ranges of sizes and densities due to greater turbulence in the bed.

It is evident from **Figs. 6.3, 6.4 and 6.5** that the pressure drop is more in the case of simultaneous primary and secondary air supplies as compared to that under only primary air supply conditions. This is due to the fact that the supply of secondary air at different locations of each static bed (30%, 50% and 70%) exerts an axial thrust at the

bottom portion of the bed. It is also observed that with an increase in the inlet height of the secondary air, the pressure drop decreases due to the fact that the thrust on the lower portion of the bed decreases. When a bed of particles is fluidized by an upward flow of air, the surface of the bed is forced upward to a higher level than the one prior to fluidization. The expansion beyond the point of incipient fluidization is primarily due to gas bubbles, which increases the bed volume. The gas bubbles are the carriers of the particles. The breaking up of bubbles takes place, only when it achieves the column diameter or due to variation in pressure fluctuations. Fluctuation ratio increases with an increase in bed height as evident from **Fig. 6.6**, up to about twice the minimum fluidization mass velocity and then reduces a little at higher mass velocities, as gas bubbles break up at greater heights (after achieving the column diameter). In lieu of taking only the primary air supply, additional secondary air has also been supplied to improve the mixing of particles by creating greater turbulence in the bed. Initially with only primary air supply, the bubbles first grow at normal rates when they detach from the distributor plate. But due to the introduction of secondary air, the column is divided into two sections i.e. the entire weight of the bed material is taken care of by both primary and secondary air. Also the secondary air exerts an axial thrust on the lower portion of the bed, for which the lower level i.e., h_1 maintains a lower value whereas the value of h_2 remains almost unchanged as evident in **Fig. 6.1A**. Hence, fluctuation ratio is more in the case of simultaneous primary and secondary air supplies. Owing to the fact that less weight of the bed material predominates the effect of early bursting of the bubbles, for which the fluctuation ratio is more in the case of secondary air supply as evident from **Figs. 6.7 and 6.8**. Also it is observed that with an increase in the inlet height of secondary air supply, the bed fluctuation increases.

In the case of simultaneous supply of primary and secondary air, the expansion ratio is less as compared to that under only primary air supply condition, which is due to a lower value of h_1 as is clear from **Fig. 6.9**.

It is also evident from **Eqs. (6.8 and 6.9)** that the mass velocity has a larger effect on fluctuation ratio than on bed height, density and particle size for primary as well as

primary (maximum)and secondary (minimum) air supplies. The fluctuation ratio increases with an increase in mass velocity but decreases with particle size and density in the case of only primary air supply as evident from **Eq. (6.8)**. Whereas in the case of simultaneous primary and secondary air supplies, the fluctuation ratio increases with an increase in static bed height, density and gas mass velocity, and decreases with an increase in particle size as evident from **Eq. (6.9)**. The predicted values of fluctuation and expansion ratios using ANN and statistical approaches have been compared with the experimental values for primary as well as primary and secondary (simultaneous) air supplies as shown in **Figs. 6.10, 6.11, 6.12 and 6.13**. It has been observed that ANN approach holds good for the entire mass velocity range (after normalizing both the input and output data i.e. values are taken within 0.1 to 0.999), which is an authentication to the developed model and experimentation. **Figs. 6.14 and 6.15** represent the comparison of experimental values of fluctuation ratio with the calculated one in the case of primary and simultaneous primary and secondary air supplies.

It is also evident from **Eqs. (6.10 and 6.12)** that in the case of only primary air supply, mass velocity and particle size are direct functions of expansion ratio but static bed height and density vary inversely with it. Whereas **Eqs. (6.11 and 6.13)** represents that in the case of simultaneous primary and secondary air supplies, expansion ratio varies inversely with mass velocity and static bed height but directly with density and particle size.

For development of the model equations through factorial design approach, the intermediate values for the bed expansion have been considered in lieu of the largest one, i.e., for (+1) range, for both primary, and simultaneous primary and secondary air supplies. If the largest value of expansion ratio is taken, then it gives a standard deviation of more ± 30, which is not suitable for the purpose. But in the case of fluctuation ratio, the smallest and largest experimental values have been considered for the development of model equations. Owing to the fact the fluctuation ratio first increases up to about twice the minimum fluidization mass velocity ($G_f = 2G_{mf,}$), then decreases and remains constant in some cases. The values of fluctuation and expansion ratios obtained by the

statistical approach compare well with their experimental counterparts as presented in **Table 6.5**. The values of fluctuation and expansion ratios have been calculated from the model equations for different input data and compared with the corresponding experimental values for primary and simultaneous primary and secondary air supplies as presented in **Tables 6.6, 6.7, 6.8 and 6.9** respectively using the statistical analysis approach only. **Tables 6.10, 6.11, 6.12 and 6.13** represent a comparison of values obtained through dimensional analysis and factorial design approaches for primary and simultaneous primary and secondary air supplies and found that the latter gives better approximation as compared to the former.

The standard deviations for fluctuation and expansion ratios have been found to be ± 0.0437 and ± 0.1386 for primary, and ± 0.0603 and ± 0.2549 for simultaneous primary and secondary air supplies respectively for values other than those taken for the development of model equations.

6.4 Conclusions

For identical operating parameters, bed fluctuation and expansion ratios increase with an increase in mass velocity. Knowledge of fluctuation ratio in gas-solid fluidization is of importance in the design of fluidized bed reactors and combustors, specifically for the calculation of bed height. The above equations can be successfully utilized for the prediction of fluctuation and expansion ratios which come under the specified ranges of densities and particle sizes. The numerical value of the fluctuation ratio quantifies the fluidization quality. A lower static bed height has been found to give a lower fluctuation ratio, which indirectly points to a better fluidization quality. The use of secondary air concept may be made in the reduction of iron ore for production of sponge iron, sulfide ore, etc as part of industrial applications. The suitability of secondary air supply in the middle portion (0.5 h_s) of each static bed height is justified, i.e., below the middle portion of the static bed height, pressure drop is more and above it the fluctuation ratio is more. Apart from this, the entrainment of particles takes place when secondary air inlet is given at 70% or above the static bed height.

Owing to greater turbulence, the bed provides a better contact between particles in the bed. The use of secondary air at different heights of the column will have a direct impact on residence time of the particle, which, in turn, may affect the rate of a chemical reaction. It may be attributed to better mixing of particles of wide ranges of sizes and densities.

Notations

ANN Artificial Neural Network
d_p Diameter of particle, m
D_c Diameter of column, m
G_f Mass velocity corresponding to fluidization, kg/m^2s
G_{mf} Mass velocity corresponding to minimum fluidization, kg/m^2s
G_p Mass velocity of the medium due to primary air = $G_{mf} + 0.17$, kg/m^2s
G_s Additional mass velocity of the fluidizing medium due to secondary air, kg/m^2s
h_S Static bed height, m
h_1 Lower height of the expanded bed, m
h_2 Upper height of the expanded bed, m
ΔP_{mfs} Pressure drop at minimum fluidization velocity in case of secondary air supply, N/m^2
r Fluctuation ratio
r_1 Fluctuation ratio calculated through dimensional analysis approach at primary air supply
r_2 Fluctuation ratio calculated through dimensional analysis approach at primary and secondary air supply
r_p Fluctuation ratio calculated through factorial analysis approach at primary air supply
r_s Fluctuation ratio calculated through factorial design at simultaneous primary and secondary air supply
r_{cal} Fluctuation ratio calculated from the developed equations
r_{exp} Fluctuation ratio obtained from the experiments
R Expansion ratio
R_p Expansion ratio calculated through factorial design at primary air supply
R_s Expansion ratio calculated through factorial design at simultaneous primary and secondary air supply
R_1 Expansion ratio calculated through dimensional analysis approach at primary air supply
R_2 Expansion ratio calculated through dimensional analysis approach at Simultaneous primary and secondary air supply
R_{cal} Expansion ratio calculated from the developed equations
R_{exp} Expansion ratio obtained from the experiments
Re_p Particle Reynolds Number, dimensionless
X_1.. X_4 Factorial design symbols

Greek Symbols

ρ_f Density of fluid, kg/m^3
ρ_s Density of solid particle, kg/m^3

References

1. Corella, J., Aznar, M.P., Gil, J. and Caballero, M.A., Energy and fuels, 13 (1999) 1122.
2. Cousins.A., Paterson, N., Dugwell, D.R. and Kandiyoti, R., Energy and Fuels, 20 (2006) 2489.
3. Grace, J. R., Issangya, A.S., Bai, D. and . Bi, H., AIChE, 45 (1999) 2108.
4. Johnsson, J.E., Amand, L.E., Johansen, K.D. and Leckner, B., Energy and Fuels, 10 (1996) 970.
5. Kumar, A. and Roy, G.K., J. Institution of Engrs. India, 85 (2004) 12.
6. Kaynak, B.,Topal, H. and Atimtay,A.T., Fuel Processing Tech., 86 (2005) 1175.
7. Liu.K., Xie, W., Zaho, Z.B., Pan, W.P. and Riley, J.T., Environ. Sci. Tech., 34 (2000) 2273.
8. Liu, K., Gao, Y., Riley, J.T., Pan,W.P., Mehta, A.K., Ho, K.K. and Smith, S.R., Energy and Fuels, 15 (2001) 1173.
9. Luis, A.C., Matos, M.A.A. and Pereira, F.J.M.A., Energy and Fuels, 18, 6 (2004) 1615.
10. Mohanty, J.N., Tripathy, H.K., Murthy, B.V.R., Ray, H.S. and Saha, R.K., National Seminar, Utilisation of Natural Resources, R.R.L.Bhubaneswar, (1993) 60.
11 Mohanty, Y. K., Biswal, K.C. and Roy, G.K., Indian Chemical Engineer, 49,2 (2007) 134.
12. Narvaez, I., Orio, A., Aznar, M.P. and Corella, J., Ind. Eng. Chem. Res., 35 (1996) 2110.
13. Sanyal, J. and Cesmebasi, E., Chem. Engg. Sc., 49, 23 (1994) 3955.
14 Tardin, P.R.Jr. and Goldstein, L., Jr., Ind. Eng. Chem. Res., 40 (2001) 4141.
15. Tarelho. A.C., Matos, M.A.A. and Pereira, F.J.M.A., Energy and Fuels,18 (2004) 1615.
16. Wasserman, P. D., Neural Computing: Theory and Practice, Van Nastrank Reinhold, 1st ed., New York (1989).
17. Mat Lab Version, 6.5.0.180913a Release 13.

Figures

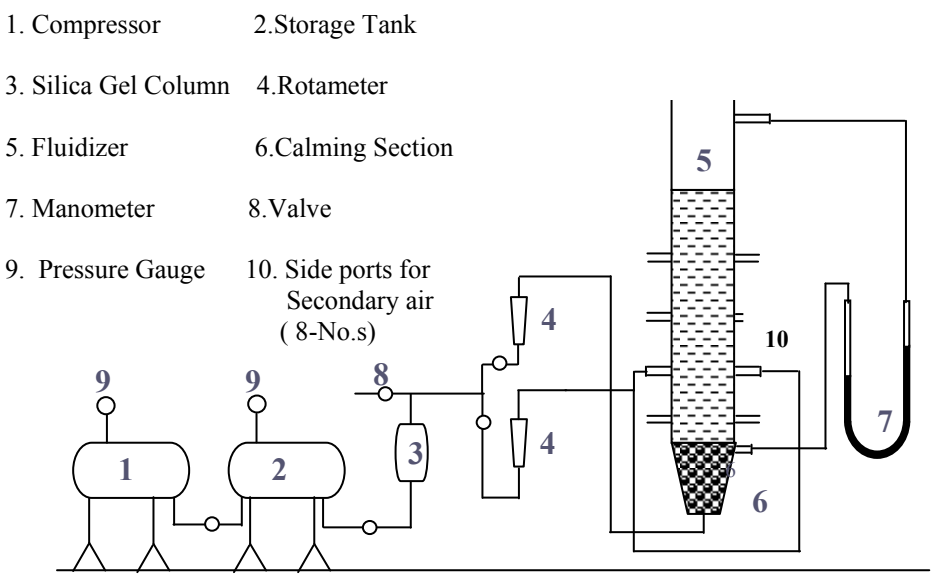

Fig. 6. 1 Schematic representation of the experimental set-up

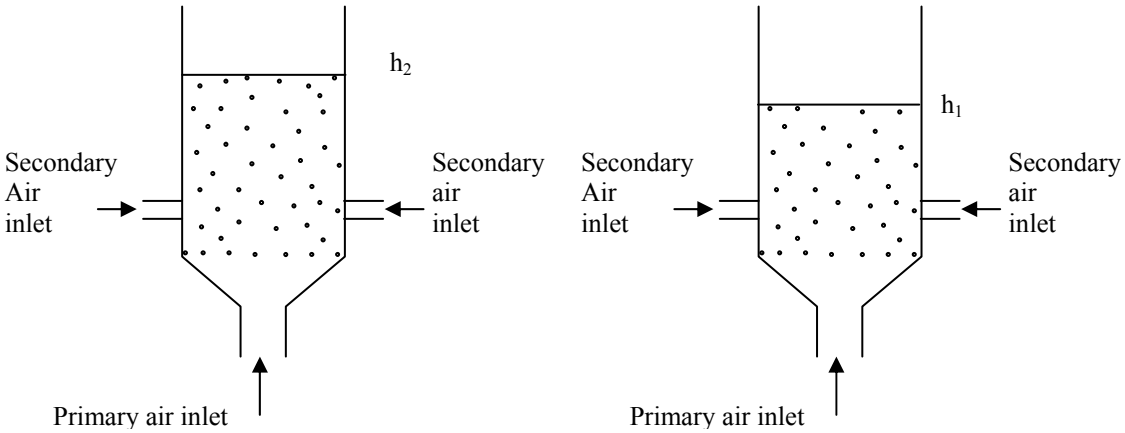

h_1; Fluctuation of the bed in the lower level.
h_2; Fluctuation of the bed at the top level.

Fig. 6. 1A Schematic representation of the bed representing lower and upper level

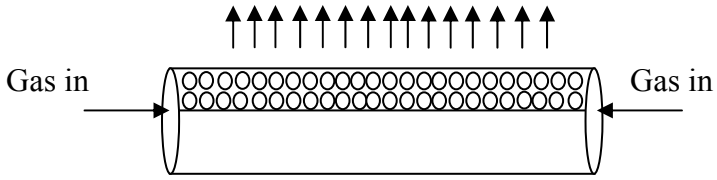

Fig. 6.2 Schematic representation of the air distributor

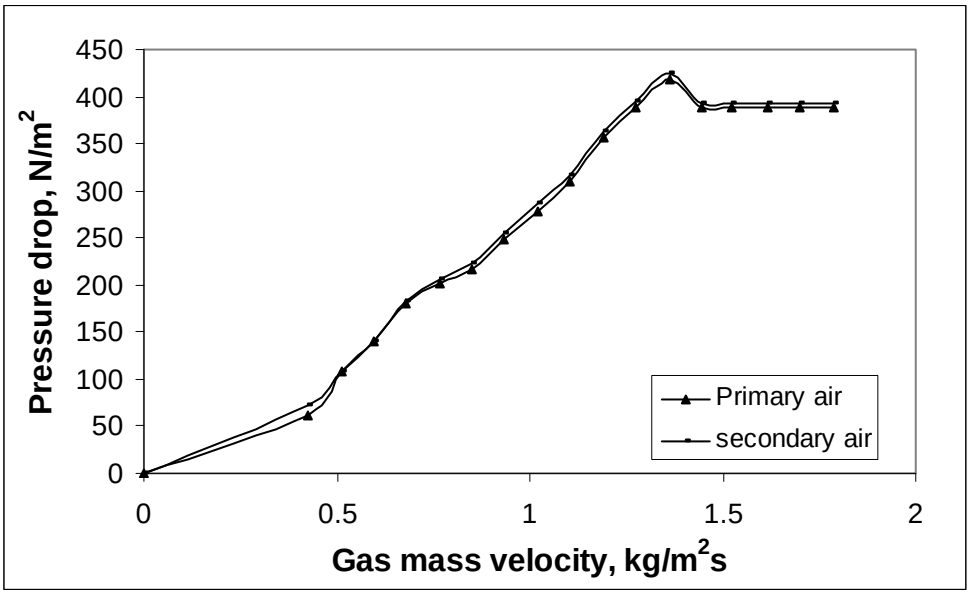

Fig. 6.3 Comparison of pressure drop

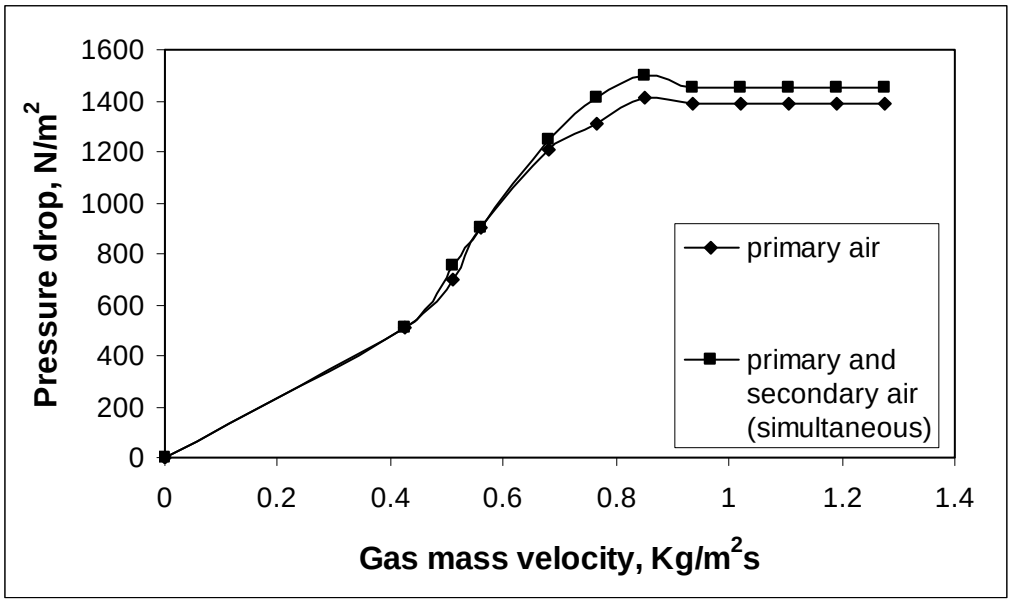

Fig. 6.4 Comparison of pressure drop for dolomite (particle size = 0.00055m and static bed height = 0.14m)

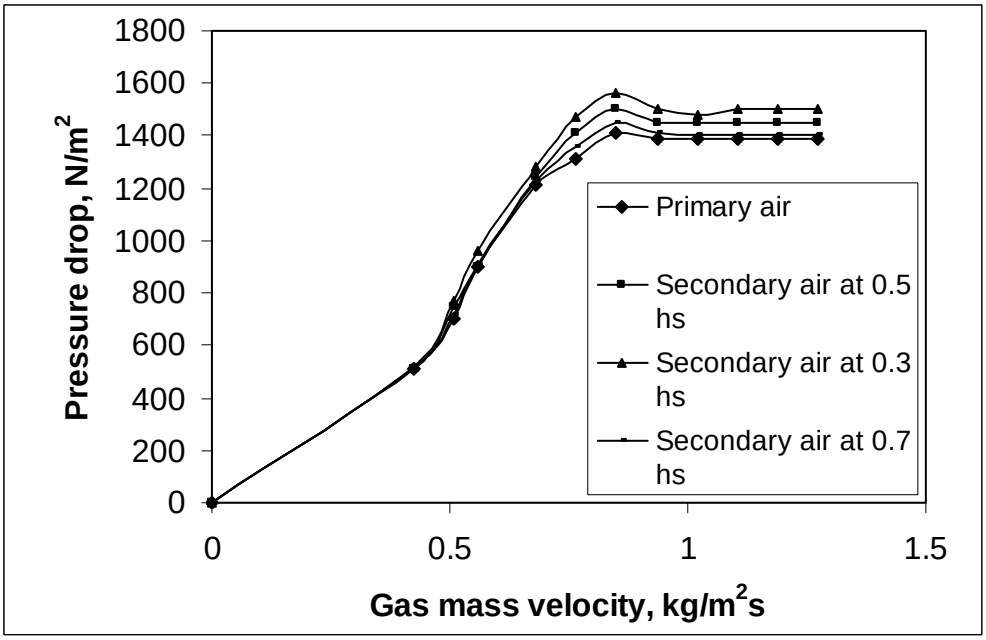

Fig. 6.5 Comparison of pressure drop for dolomite (particle size = 0.00055m and static bed height = 0.14m)

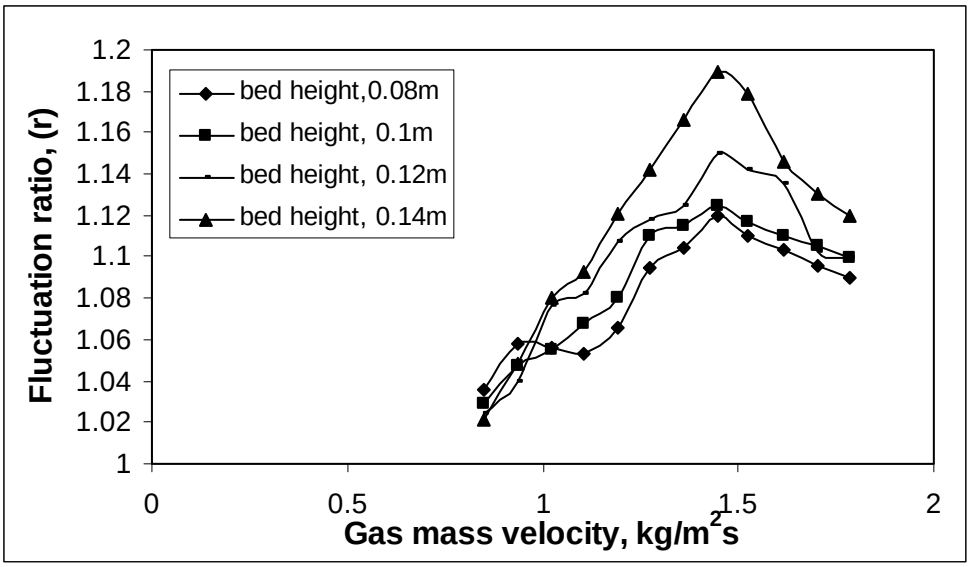

Fig. 6.6 Effect of bed height on fluctuation ratio for dolomite (particle size = 0.000725 m in the case of primary air supply)

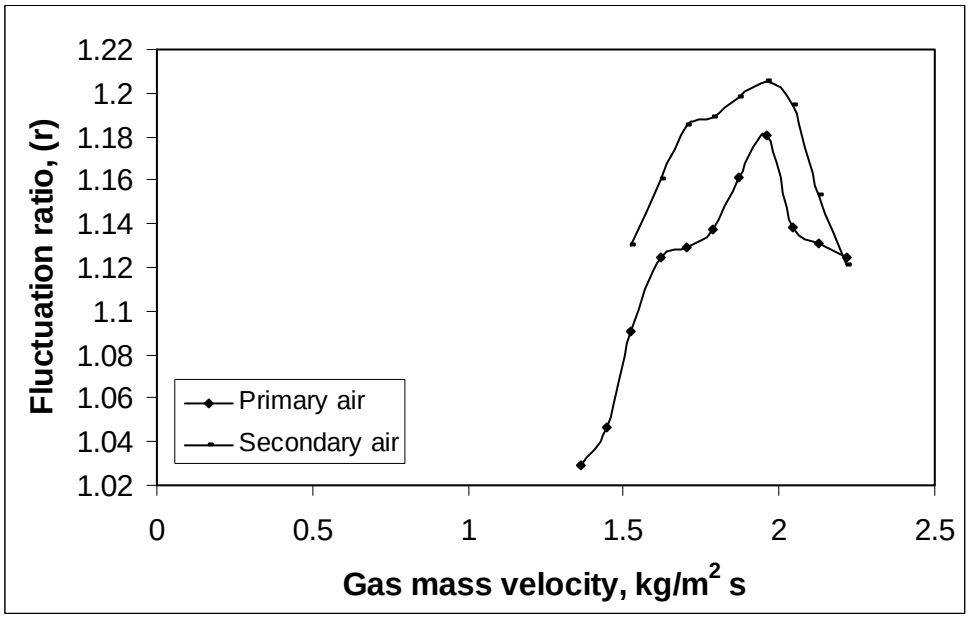

Fig. 6.7 Effect of primary, and primary and secondary (simultaneous) air on fluctuation ratio for dolomite of particle size = 0.0013 m

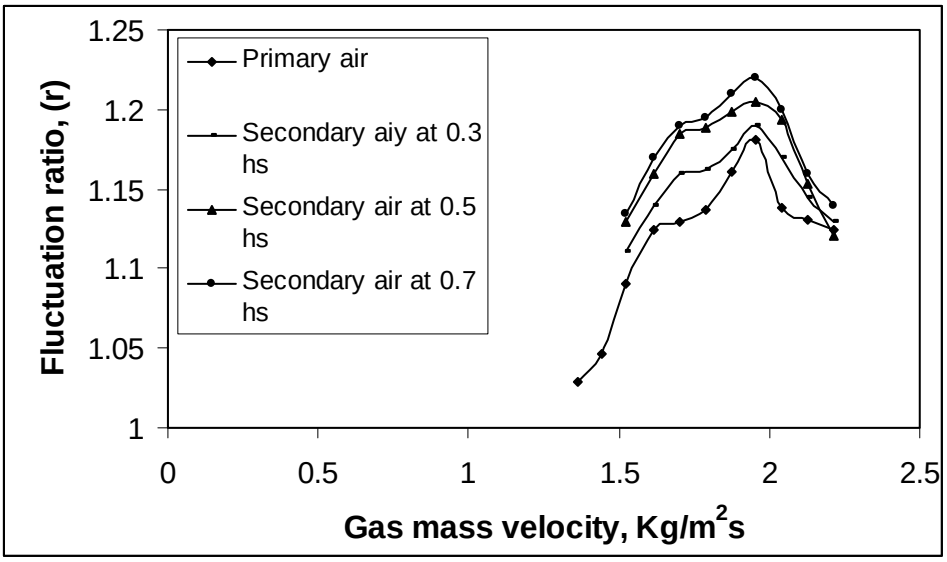

Fig. 6.8 Effect of primary, and simultaneous primary and secondary air on fluctuation ratio for dolomite of particle size = 0.0013 m

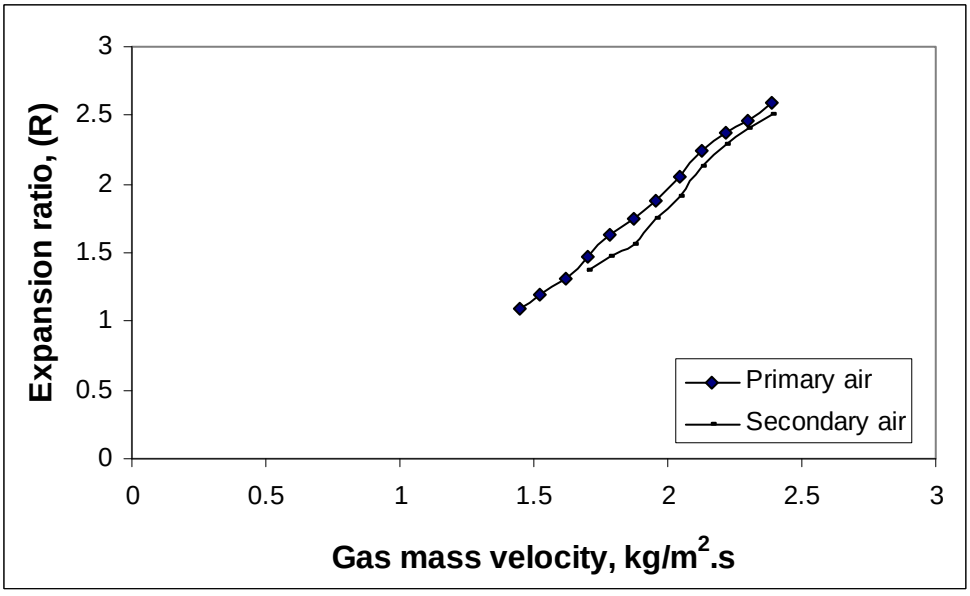

Fig. 6.9 Effect of primary, and primary and secondary air (simultaneous) on expansion ratio for refractory brick of particle size = 0.0013 m

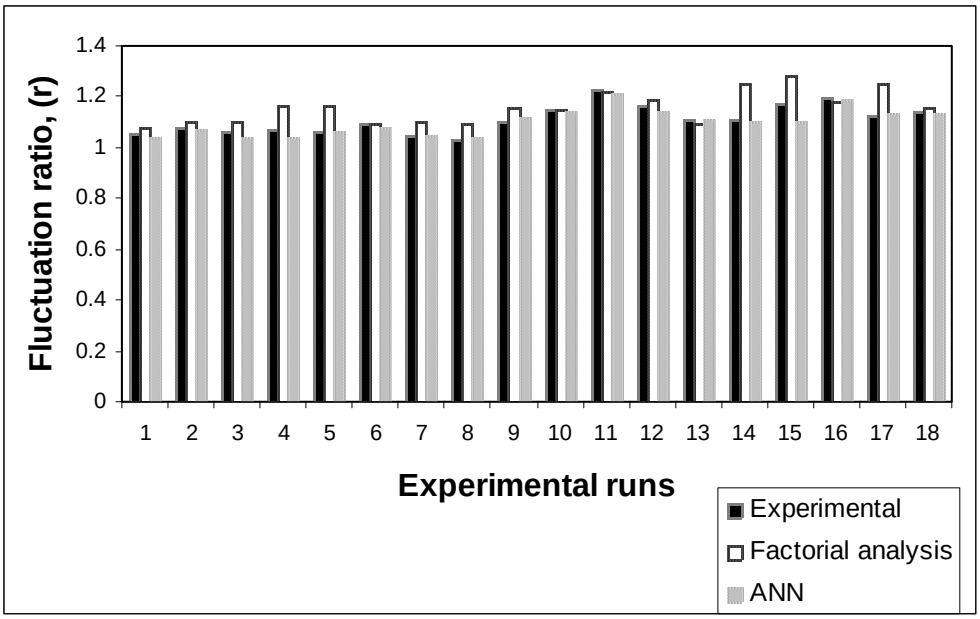

Fig. 6.10 Comparison of fluctuation ratio for primary air supply

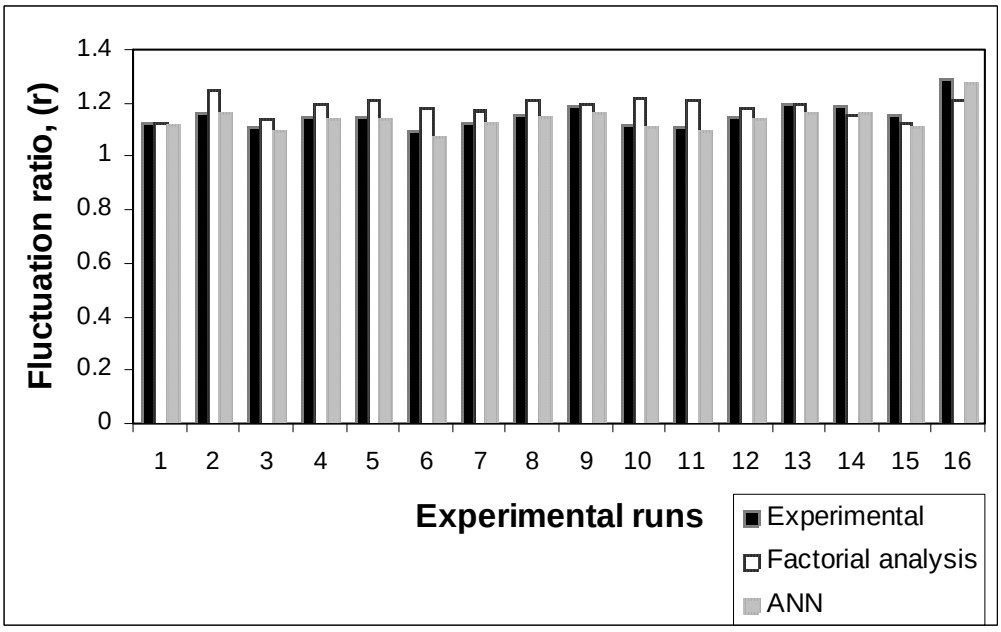

Fig. 6.11 Comparison of fluctuation ratio for secondary air supply

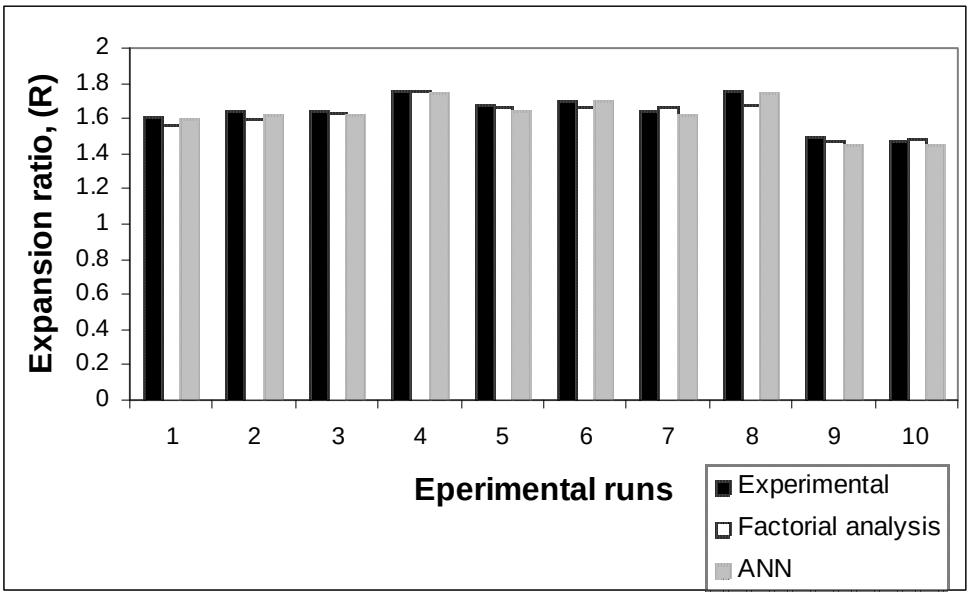

Fig. 6.12 Comparison of expansion ratio for primary air supply

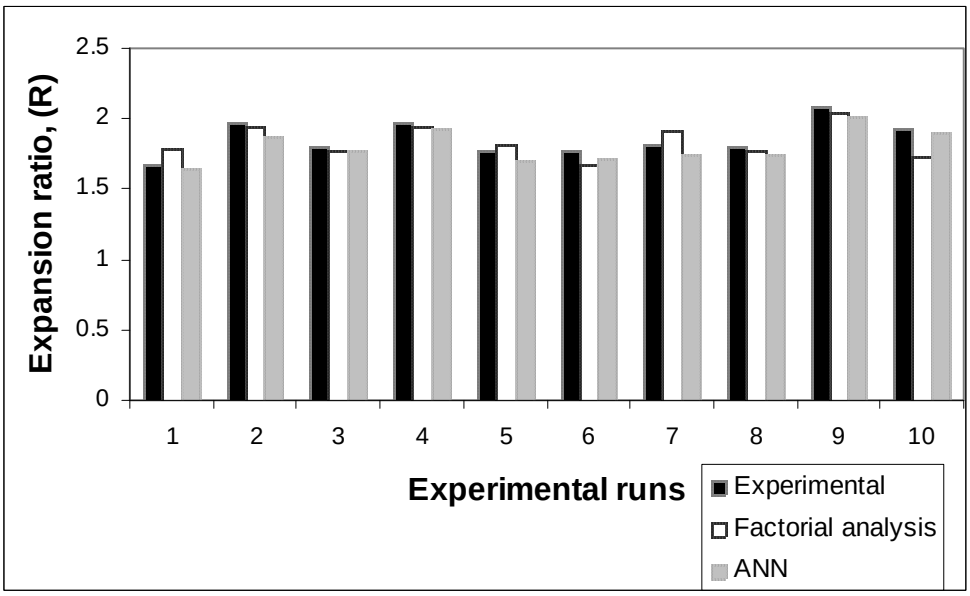

Fig. 6.13 Comparison of expansion ratio for secondary air supply

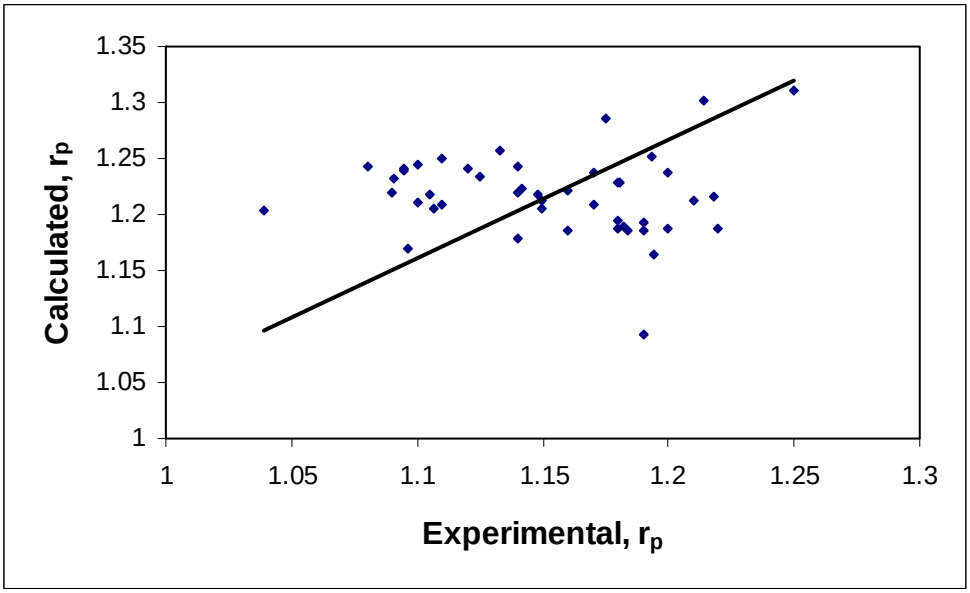

Fig. 6.14 Comparison of fluctuation ratio for primary air supply through statistical analysis approach

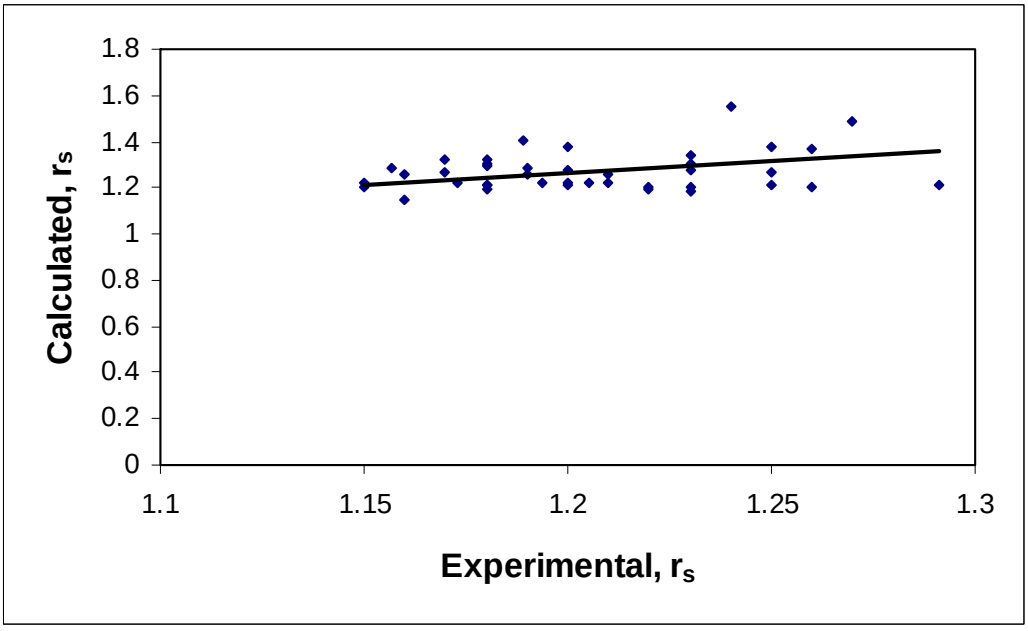

Fig. 6.15 Comparison of fluctuation ratio for secondary air supply through statistical analysis approach

Table 6.1 Scope of the Experiment

Properties of the Bed Materials							
Materials	**$d_{p\times10}{}^{3}$, m**				**$\rho_{s\times10}{}^{-3}$, kg/m^3**		
Dolomite	0.55, 0.725, 1.3, 1.7				2.817		
Sand	0.55				2.61		
Refractory brick	0.55, 0.725, 1.3, 1.7				2.5		
Coal	0.55, 0.725, 1.3, 1.7				1.6		
Density of fluid, (ρ_f)	1.18 kg/m^3 at 25^{0}c						
Diameter of column, (D_c)	0.099 m						
Bed Parameter							
Initial static bed height, $h_{s\times\ 10}{}^{2}$, m	8,	10,	12,	14			
Flow property							
Materials	A	B×10^{-3}	C×10^2	G$_{mf}$,kg/m^{2}s	G$_p$,kg/m^{2}s	G$_f$,kg/m^{2}s	G$_s$,kg/m^{2}s
Coal	0.808,1.414	1.356	0.55	0.425	0.595	0.51 to 1.275	0.085 to 0.68
Coal	0.808,1.414	1.356	1.7	1.275	1.445	1.36 to 2.125	0.085 to 0.68
dolomite	0.808,1.414	2.387	0.55	0.68	0.85	0.765 to 1.53	0.085 to 0.68
Dolomite	0.808,1.414	2.387	1.7	1.7	1.87	1.785 to 2.55	0.085 to 0.68

Table 6.2 Factorial Design Analysis

Sl. No	Name of the variable	Variable general symbol	Factorial design symbol	Minimum level (-1)	Maximum level (+1)	Magnitude of variables
1	Static bed height	h_s/D_c	A	0.808	1.414	0.808, 1.01, 1.212, 1.414
2	Density	ρ_s/ρ_f	$B\times10^{-3}$	1.356	2.372	1.356, 2.118, 2.211, 2.372
3	Particle size	d_P/D_c	C	0.0055	0.017	0.0055, .00732, 0.013, 0.017
4	Mass velocity	G_f/G_{mf} G_p/G_s	D	1.2 1.7	1.6 5.77	1.05 to 3.0 0.875 to 22.0

Table 6.3 Analysis of Fluctuation Ratio (r) and Expansion Ratio (R) Data

Treatment Combination	A	B	C	D (G_f/G_{mf})	r_p exp	D (G_p/G_s)	r_s exp	D (G_f/G_{mf})	R_p exp	D (G_p/G_s)	R_s exp
1	0.808	1.356	0.0055	1.2	1.052	1.7	1.2	1.2	1.218	1.7	2.062
a	1.414	1.356	0.0055	1.2	1.075	1.7	1.23	1.2	1.082	1.7	1.553
b	0.808	2.387	0.0055	1.2	1.11	1.7	1.2	1.2	1.187	1.7	2
c	1.414	2.387	0.0055	1.2	1.133	1.7	1.24	1.2	1.142	1.7	1.803
d	0.808	1.356	0.017	1.2	1.157	1.7	1.102	1.2	1.281	1.7	2.562
ab	1.414	1.356	0.017	1.2	1.138	1.7	1.121	1.2	1.375	1.7	2.5
ac	0.808	2.387	0.017	1.2	1.075	1.7	1.088	1.2	1.206	1.7	2.937
ad	1.414	2.387	0.017	1.2	1.091	1.7	1.105	1.2	1.262	1.7	2.142
bc	0.808	1.356	0.0055	1.6	1.13	5.77	1.13	1.6	1.531	5.77	1.468
bd	1.414	1.356	0.0055	1.6	1.117	5.77	1.17	1.6	1.285	5.77	1.225
cd	0.808	2.387	0.0055	1.6	1.175	5.77	1.14	1.6	1.562	5.77	1.406
abc	1.414	2.387	0.0055	1.6	1.133	5.77	1.205	1.6	1.142	5.77	1.339
abd	0.808	1.356	0.017	1.6	1.121	5.77	1.17	1.6	2.187	5.77	1.562
acd	1.414	1.356	0.017	1.6	1.12	5.77	1.2	1.6	2.196	5.77	1.571
bcd	0.808	2.387	0.017	1.6	1.129	5.77	1.2	1.6	2.062	5.77	1.656
abcd	1.414	2.387	0.017	1.6	1.058	5.77	1.25	1.6	1.875	5.77	1.41

(Columns indicating A, B and C are common; columns r_p, r_s, R_p and R_s are used for the development of model equations at different G_f/G_{mf} and G_p/G_s for fluctuation and expansion ratios)

Table 6.4 Selected Structures of Neural Network Models

Net train parameter : 500				
Percentage set learning rate : 0.2—10				
Net train parameter learning : 0.2—10				
Percentage set error goal : 0.001				
Net train parameter epochs : 50,000				
Performance : $0.02368/1e^{-5}$				
Bed Particular	Input Nodes	Hidden Nodes	Output Nodes	No of cycles
Primary air	4	3	1	50,000
Secondary air	4	3	1	50,000

Table 6.5 Comparison of Fluctuation Ratio and Expansion Ratio Calculated through Factorial Design Approach

Sl. No.	$r_{p\ exp}$	$r_{p\ cal}$	$r_{s\ exp}$	$r_{s\ cal}$	$R_{p\ exp}$	$R_{p\ cal}$	$R_{s\ exp}$	$R_{s\ cal}$
1	1.175	1.285	1.291	1.215	1.61	1.57	2	2.06
2	1.193	1.252	1.2	1.27	1.65	1.6	2.06	2.062
3	1.214	1.301	1.25	1.209	1.645	1.63	1.98	1.94
4	1.218	1.216	1.15	1.20	1.767	1.764	1.937	1.81
5	1.148	1.217	1.2	1.21	1.687	1.669	1.803	1.75
6	1.25	1.31	1.26	1.204	1.7	1.672	1.8	1.74
7	1.18	1.22	1.22	1.198	1.645	1.675	1.97	1.85
8	1.14	1.22	1.23	1.186	1.767	1.678	1.85	1.94
9	1.17	1.20	1.173	1.22	1.5	1.476	2.06	2.06
10	1.181	1.22	1.18	1.2	1.475	1.496	1.83	1.92
11	1.22	1.187	1.2	1.21	1.5	1.516	1.91	1.86
12	1.2	1.187	1.18	1.195	1.48	1.535	1.96	2.06
13	1.18	1.187	1.205	1.22	1.4	1.564	1.875	1.89
14	1.21	1.213	1.194	1.21	1.6	1.54	1.98	1.95
15	1.184	1.25	1.25	1.26	1.46	1.56	1.71	1.75

Table 6.6 Comparison of Fluctuation Ratio Data for Primary Air Supply (Factorial Design Approach)

A	B	C	D	$r_{p\ cal}$	$r_{p\ exp}$	% Deviation
0.808	1.356	0.0055	1.2	1.0657	1.052	1.3089
1.414	1.356	0.0055	1.2	1.0752	1.076	-0.0678
0.808	2.387	0.0055	1.2	1.1090	1.11	-0.083
1.414	2.387	0.0055	1.2	1.1185	1.133	-1.2734
0.808	1.356	0.017	1.2	1.1318	1.157	-2.1698
1.414	1.356	0.017	1.2	1.1413	1.16	-1.6038
0.808	2.387	0.017	1.2	1.0878	1.075	1.1972
1.414	2.387	0.017	1.2	1.0973	1.125	-2.4559
0.808	1.356	0.0055	1.6	1.1319	1.13	0.1743
1.414	1.356	0.0055	1.6	1.1014	1.117	-1.3903
0.808	2.387	0.0055	1.6	1.1752	1.17	0.4505
1.414	2.387	0.0055	1.6	1.1447	1.25	-8.418
0.808	1.356	0.017	1.6	1.1441	1.08	5.9411
1.414	1.356	0.017	1.6	1.1136	1.06	5.0626
0.808	2.387	0.017	1.6	1.1001	1.103	-0.259
1.414	2.387	0.017	1.6	1.0696	1.106	-3.2875
0.808	2.118	0.013	1.118	1.0924	1.1	-0.6867
0.808	2.118	0.013	1.353	1.1106	1.14	-2.572
0.808	2.118	0.013	1.532	1.1245	1.11	1.3116
1.01	2.118	0.013	1.118	1.0983	1.13	-2.8012
1.01	2.118	0.013	1.353	1.1087	1.15	-3.5877
1.01	2.118	0.013	1.532	1.1166	1.125	-0.7413
1.212	2.118	0.013	1.118	1.1042	1.107	-0.2487
1.212	2.118	0.013	1.353	1.1068	1.153	-4.0062
1.212	2.118	0.013	1.532	1.1087	1.108	0.0685
0.808	2.212	0.0055	1.283	1.1154	1.105	0.9464
0.808	2.212	0.0055	1.855	1.2101	1.148	5.4115
0.808	2.212	0.0055	2.283	1.2809	1.147	11.679
1.01	2.212	0.0055	1.283	1.1158	1.13	-1.2514
1.01	2.212	0.0055	1.855	1.1914	1.156	3.0672
1.01	2.212	0.0055	2.283	1.2480	1.15	8.5239
1.212	2.212	0.0055	1.283	1.1162	1.11	0.5638

Table 6.7 Comparison of Fluctuation Ratio Data for Simultaneous Primary and Secondary Air Supplies (Factorial Design Approach)

A	B	C	D	$r_{s\ cal}$	$r_{s\ exp}$	% Deviation
0.808	1.356	0.0055	1.7	1.1269	1.2	-6.09
1.414	1.356	0.0055	1.7	1.1629	1.23	-5.4536
0.808	2.387	0.0055	1.7	1.1149	1.2	-7.0909
1.414	2.387	0.0055	1.7	1.1509	1.24	-7.1848
0.808	1.356	0.017	1.7	1.1703	1.102	6.2016
1.414	1.356	0.017	1.7	1.2063	1.121	7.6130
0.808	2.387	0.017	1.7	1.1583	1.088	6.4642
1.414	2.387	0.017	1.7	1.1943	1.105	8.0842
0.808	1.356	0.0055	5.77	1.2028	1.13	6.4495
1.414	1.356	0.0055	5.77	1.2388	1.17	5.8871
0.808	2.387	0.0055	5.77	1.2409	1.14	8.8523
1.414	2.387	0.0055	5.77	1.2769	1.205	5.9682
0.808	1.356	0.017	5.77	1.0904	1.205	-9.5055
1.414	1.356	0.017	5.77	1.1264	1.17	-3.7215
0.808	2.387	0.017	5.77	1.1284	1.2	-5.9587
1.414	2.387	0.017	5.77	1.1644	1.2	-2.9587
0.808	2.118	0.013	9.5	1.1680	1.13	3.3664
0.808	2.118	0.013	3.16	1.1504	1.19	-3.3261
0.808	2.118	0.013	2.11	1.1475	1.05	9.2857
1.01	2.118	0.013	6.33	1.1712	1.178	-0.5746
1.01	2.118	0.013	3.16	1.1624	1.18	-1.4898
1.01	2.118	0.013	2.11	1.1595	1.1	5.4091
1.212	2.118	0.013	6.33	1.1832	1.18	0.2737
1.212	2.118	0.013	3.16	1.1744	1.18	-0.4729
1.212	2.118	0.013	2.11	1.1715	1.12	4.5982
0.808	2.212	0.0055	3	1.1544	1.153	0.1285
0.808	2.212	0.0055	1.497	1.1110	1.18	-5.8401
0.808	2.212	0.0055	1	1.0967	1.15	-4.6316
1.01	2.212	0.0055	3	1.1664	1.21	-3.5965
1.01	2.212	0.0055	1.497	1.1230	1.19	-5.623
1.01	2.212	0.0055	1	1.1087	1.16	-4.4193

Table 6.8 Comparison of Expansion Ratio Data for Primary Air Supply (Factorial Design Approach)

A	B	C	D	$R_{p\ cal}$	$R_{p\ exp}$	% Deviation
0.808	1.356	0.0055	1.2	1.204	1.218	-1.1494
1.414	1.356	0.0055	1.2	1.085	1.082	0.2772
0.808	2.387	0.0055	1.2	1.2236	1.187	3.0850
1.414	2.387	0.0055	1.2	1.1162	1.142	-2.2565
0.808	1.356	0.017	1.2	1.2940	1.281	1.0161
1.414	1.356	0.017	1.2	1.3693	1.392	-1.6287
0.808	2.387	0.017	1.2	1.1695	1.206	-3.0225
1.414	2.387	0.017	1.2	1.2564	1.214	3.4983
0.808	1.356	0.0055	1.6	1.5216	1.531	-0.6139
1.414	1.356	0.0055	1.6	1.305	1.285	1.5564
0.808	2.387	0.0055	1.6	1.5472	1.562	-0.9459
1.414	2.387	0.0055	1.6	1.1460	1.25	-8.3163
0.808	1.356	0.017	1.6	2.1901	2.281	-3.9813
1.414	1.356	0.017	1.6	2.1678	2.321	-6.5964
0.808	2.387	0.017	1.6	2.0717	1.906	8.6948
1.414	2.387	0.017	1.6	1.8648	1.767	5.5378
1.01	2.118	0.013	1.118	1.0863	1.225	-11.314
1.01	2.118	0.013	1.353	1.4497	1.725	-15.955
1.01	2.118	0.013	1.532	1.7265	2.125	-18.750
1.212	2.118	0.013	1.118	1.1084	1.229	-9.8119
1.212	2.118	0.013	1.353	1.4242	1.75	-18.613
1.212	2.118	0.013	1.532	1.6648	2.02	-17.581
0.808	2.212	0.0055	1.283	1.2872	1.25	2.97804
0.808	2.212	0.0055	1.855	1.7485	1.812	-3.5030
0.808	2.212	0.0055	2.283	2.0936	2.281	-8.2116
1.01	2.212	0.0055	1.283	1.2327	1.225	0.6330
1.01	2.212	0.0055	1.855	1.5698	1.725	-8.9920
1.01	2.212	0.0055	2.283	1.8221	2.05	-11.114
1.212	2.212	0.0055	1.283	1.1782	1.145	2.9069
1.212	2.212	0.0055	1.855	1.3912	1.645	-15.425

Table 6.9 Comparison of Expansion Ratio Data for Simultaneous Primary and Secondary Air Supplies (Factorial Design Approach)

A	B	C	D	$R_{s\ cal}$	$R_{s\ exp}$	% Deviation
0.808	1.356	0.0055	1.7	2.1015	2.062	1.9156
1.414	1.356	0.0055	1.7	1.5549	1.553	0.1223
0.808	2.387	0.0055	1.7	1.9963	2	-0.1801
1.414	2.387	0.0055	1.7	1.7621	1.803	-2.2683
0.808	1.356	0.017	1.7	2.5174	2.562	-1.7376
1.414	1.356	0.017	1.7	2.4883	2.5	-0.4646
0.808	2.387	0.017	1.7	2.9303	2.937	-0.2252
1.414	2.387	0.017	1.7	2.1775	2.142	1.6611
0.808	1.356	0.0055	5.77	1.4731	1.468	0.3474
1.414	1.356	0.0055	5.77	1.2485	1.225	1.9183
0.808	2.387	0.0055	5.77	1.3812	1.406	-1.7631
1.414	2.387	0.0055	5.77	1.3327	1.339	-0.4644
0.808	1.356	0.017	5.77	1.5547	1.562	-0.4616
1.414	1.356	0.017	5.77	1.5439	1.571	-1.7230
0.808	2.387	0.017	5.77	1.6768	1.656	1.2590
1.414	2.387	0.017	5.77	1.4142	1.41	0.3024
0.808	2.118	0.013	9.5	0.6605	1.468	-55.005
0.808	2.118	0.013	3.16	2.1920	2.125	3.1575
0.808	2.118	0.013	2.11	2.4457	2.5	-2.1699
1.01	2.118	0.013	6.33	1.3870	1.525	-9.0447
1.01	2.118	0.013	3.16	2.0707	2.025	2.2575
1.01	2.118	0.013	2.11	2.2971	2.525	-9.0233
1.212	2.118	0.013	6.33	1.3478	1.5	-10.144
1.212	2.118	0.013	3.16	1.9493	1.958	-0.4427
1.212	2.118	0.013	2.11	2.1485	2.208	-2.6916
0.808	2.212	0.0055	3	1.8170	1.75	3.8299
0.808	2.212	0.0055	1.497	2.0450	3.25	-37.075
0.808	2.212	0.0055	1	2.1204	2.625	-19.221
1.01	2.212	0.0055	3	1.7435	1.55	12.484
1.01	2.212	0.0055	1.497	1.9457	1.975	-1.4789
1.01	2.212	0.0055	1	2.0126	2.325	-13.433

Table 6.10 Comparison of Fluctuation Ratio Data in the Case of Primary Air

A	B	C	D	$r_{p\ cal}$	$r_{p\ exp}$	% Deviation	$r_{p\ cal}$	$r_{p\ exp}$	% Deviation
Common input data				Dimensional analysis			Factorial analysis		
0.808	1.356	0.0055	1.2	1.0971	1.052	4.2885	1.0657	1.052	1.3089
1.414	1.356	0.0055	1.2	1.1029	1.076	2.5059	1.0752	1.076	-0.0678
0.808	2.387	0.0055	1.2	1.1108	1.11	0.0765	1.1090	1.11	-0.0836
1.414	2.387	0.0055	1.2	1.1167	1.133	-1.4323	1.1185	1.133	-1.2734
0.808	1.356	0.017	1.2	1.0559	1.157	-8.7348	1.1318	1.157	-2.1698
1.414	1.356	0.017	1.2	1.0615	1.16	-8.4856	1.1413	1.16	-1.6038
0.808	2.387	0.017	1.2	1.0691	1.075	-0.5435	1.0878	1.075	1.1972
1.414	2.387	0.017	1.2	1.0748	1.125	-4.4572	1.0973	1.125	-2.4559
0.808	1.356	0.0055	1.6	1.1532	1.13	2.0618	1.1319	1.13	0.1743
1.414	1.356	0.0055	1.6	1.1594	1.117	3.8000	1.1014	1.117	-1.3903
0.808	2.387	0.0055	1.6	1.1677	1.17	-0.1934	1.1752	1.17	0.4505
1.414	2.387	0.0055	1.6	1.1739	1.25	-6.0831	1.1447	1.25	-8.4182
0.808	1.356	0.017	1.6	1.1100	1.08	2.7789	1.1441	1.08	5.9411
1.414	1.356	0.017	1.6	1.1159	1.06	5.2763	1.1136	1.06	5.0626
0.808	2.387	0.017	1.6	1.1239	1.103	1.8955	1.100	1.103	-0.259
1.414	2.387	0.017	1.6	1.1298	1.106	2.1608	1.069	1.106	-3.2875
0.808	2.118	0.013	1.118	1.0629	1.1	-3.3683	1.0924	1.1	-0.6867
0.808	2.118	0.013	1.353	1.0987	1.14	-3.6190	1.1106	1.14	-2.5724
0.808	2.118	0.013	1.532	1.1227	1.11	1.1441	1.1245	1.11	1.3116
1.01	2.118	0.013	1.118	1.0652	1.13	-5.7341	1.0983	1.13	-2.8012
1.01	2.118	0.013	1.353	1.1010	1.15	-4.2543	1.1087	1.15	-3.5877
1.01	2.118	0.013	1.532	1.1250	1.125	0.0073	1.1166	1.125	-0.7413
1.212	2.118	0.013	1.118	1.0670	1.107	-3.6087	1.1042	1.107	-0.2487
1.212	2.118	0.013	1.353	1.1029	1.153	-4.3379	1.1068	1.153	-4.0062
1.212	2.118	0.013	1.532	1.1270	1.108	1.7177	1.1087	1.108	0.0685
0.808	2.212	0.0055	1.283	1.1219	1.105	1.5331	1.1154	1.105	0.9464
0.808	2.212	0.0055	1.855	1.1960	1.148	4.1896	1.2101	1.148	5.4115
0.808	2.212	0.0055	2.283	1.2399	1.147	8.1073	1.2809	1.147	11.679
1.01	2.212	0.0055	1.283	1.124322	1.13	-0.5024	1.1158	1.13	-1.2514
1.01	2.212	0.0055	1.855	1.198636	1.156	3.6882	1.1914	1.156	3.0672
1.01	2.212	0.0055	2.283	1.242623	1.15	8.0541	1.2480	1.15	8.5239

Table 6.11 Comparison of Fluctuation Ratio Data in the Case of Secondary Air

A	B	C	D	$r_{p\ cal}$	$r_{p\ exp}$	% Deviation	$r_{p\ cal}$	$r_{p\ exp}$	% Deviation
Common input data				Dimensional analysis			Factorial analysis		
0.808	1.356	0.0055	1.7	1.2030	1.2	0.2532	1.1269	1.2	-6.09
1.414	1.356	0.0055	1.7	1.1548	1.23	-6.1070	1.1629	1.23	-5.4536
0.808	2.387	0.0055	1.7	1.2074	1.2	0.6167	1.1149	1.2	-7.0909
1.414	2.387	0.0055	1.7	1.1590	1.24	-6.5265	1.1509	1.24	-7.1848
0.808	1.356	0.017	1.7	1.1601	1.102	5.2731	1.1703	1.102	6.2016
1.414	1.356	0.017	1.7	1.1136	1.121	-0.6537	1.2063	1.121	7.6130
0.808	2.387	0.017	1.7	1.1643	1.088	7.0143	1.1583	1.088	6.4642
1.414	2.387	0.017	1.7	1.1177	1.105	1.1502	1.1943	1.105	8.0842
0.808	1.356	0.0055	5.77	1.2080	1.13	6.9069	1.2028	1.13	6.4495
1.414	1.356	0.0055	5.77	1.1596	1.17	-0.8810	1.2388	1.17	5.8871
0.808	2.387	0.0055	5.77	1.2124	1.14	6.3533	1.2409	1.14	8.8523
1.414	2.387	0.0055	5.77	1.1638	1.205	-3.4110	1.2769	1.205	5.9682
0.808	1.356	0.017	5.77	1.1649	1.205	-3.3244	1.0904	1.205	-9.5055
1.414	1.356	0.017	5.77	1.1183	1.17	-4.4180	1.1264	1.17	-3.7215
0.808	2.387	0.017	5.77	1.1691	1.2	-2.5696	1.1284	1.2	-5.9587
1.414	2.387	0.017	5.77	1.1223	1.2	-6.4697	1.1644	1.2	-2.9587
0.808	2.118	0.013	9.5	1.1804	1.13	4.4605	1.1680	1.13	3.3664
0.808	2.118	0.013	3.16	1.1759	1.19	-1.1769	1.1504	1.19	-3.3261
0.808	2.118	0.013	2.11	1.1743	1.05	11.845	1.1475	1.05	9.2857
1.01	2.118	0.013	6.33	1.1597	1.178	-1.5509	1.1712	1.178	-0.5746
1.01	2.118	0.013	3.16	1.1569	1.18	-1.9496	1.1624	1.18	-1.4898
1.01	2.118	0.013	2.11	1.1554	1.1	5.0369	1.1595	1.1	5.4091
1.212	2.118	0.013	6.33	1.1443	1.18	-3.0172	1.1832	1.18	0.2737
1.212	2.118	0.013	3.16	1.1416	1.18	-3.2460	1.1744	1.18	-0.4729
1.212	2.118	0.013	2.11	1.1401	1.12	1.7973	1.1715	1.12	4.5982
0.808	2.212	0.0055	3	1.2091	1.153	4.8695	1.1544	1.153	0.1285
0.808	2.212	0.0055	1.497	1.2062	1.18	2.2280	1.1110	1.18	-5.8401
0.808	2.212	0.0055	1	1.2046	1.15	4.7511	1.0967	1.15	-4.6316
1.01	2.212	0.0055	3	1.1896	1.21	-1.6852	1.1664	1.21	-3.5965
1.01	2.212	0.0055	1.497	1.1868	1.19	-0.2688	1.1230	1.19	-5.6230
1.01	2.212	0.0055	1	1.1851	1.16	2.1701	1.1087	1.16	-4.4193

Table 6.12 Comparison of Expansion Ratio Data in the Case of Primary Air

A	B	C	D	$R_{p\ cal}$	$R_{p\ exp}$	% Deviation	$R_{p\ cal}$	$R_{p\ exp}$	% Deviation
Common input data				Dimensional analysis			Factorial analysis		
0.808	2.387	0.013	1.3	1.3972	1.343	4.0375	1.3635	1.343	1.5330
1.01	2.387	0.013	1.3	1.3721	1.55	-11.471	1.3455	1.55	-13.190
1.212	2.387	0.013	1.3	1.3520	1.27	6.4631	1.3275	1.27	4.5286
1.414	2.387	0.013	1.3	1.3353	1.285	3.9147	1.3094	1.285	1.9047
1.01	2.118	0.013	1.3	1.3849	1.625	-14.774	1.3678	1.625	-15.826
1.01	1.356	0.013	1.3	1.4334	1.275	12.425	1.4308	1.275	12.225
1.01	2.387	0.013	1.3	1.3721	1.55	-11.471	1.3455	1.55	-13.190
1.01	2.387	0.0055	1.3	1.3066	1.3	0.5116	1.2442	1.3	-4.2891
1.01	2.387	0.0073	1.3	1.3278	1.21	9.7415	1.2685	1.21	4.8393
1.01	2.387	0.013	1.3	1.3721	1.55	-11.471	1.3455	1.55	-13.190
1.01	2.387	0.017	1.3	1.3933	1.35	3.2076	1.3995	1.35	3.6728
1.01	2.387	0.013	1.15	1.2346	1.15	7.3612	1.1194	1.15	-2.6586
1.01	2.387	0.013	1.425	1.4851	1.425	4.2199	1.5339	1.425	7.6484
1.01	2.387	0.013	1.679	1.7105	1.675	2.1223	1.9168	1.675	14.441
1.01	2.387	0.013	1.925	1.9243	1.925	-0.0320	2.2877	1.925	18.843
0.808	1.356	0.0055	1.2	1.2972	1.218	6.5061	1.204	1.218	-1.1494
1.414	1.356	0.0055	1.2	1.2397	1.082	14.579	1.085	1.082	0.2772
0.808	2.387	0.0055	1.2	1.2418	1.187	4.6191	1.2236	1.187	3.0850
1.414	2.387	0.0055	1.2	1.1867	1.142	3.9225	1.1162	1.142	-2.2565
0.808	1.356	0.017	1.2	1.3832	1.281	7.9837	1.2940	1.281	1.0161
1.414	1.356	0.017	1.2	1.3219	1.392	-5.0308	1.3693	1.392	-1.6287
0.808	2.387	0.017	1.2	1.3241	1.206	9.7995	1.1695	1.206	-3.0225
1.414	2.387	0.017	1.2	1.2654	1.214	4.2421	1.2564	1.214	3.4983
0.808	1.356	0.0055	1.6	1.6620	1.531	8.5628	1.5216	1.531	-0.6139
1.414	1.356	0.0055	1.6	1.5884	1.285	23.613	1.305	1.285	1.5564
0.808	2.387	0.0055	1.6	1.5910	1.562	1.8628	1.5472	1.562	-0.9459
0.808	2.387	0.017	1.6	1.6966	1.906	-10.985	2.0717	1.906	8.6948
1.414	2.387	0.017	1.6	1.6214	1.767	-8.2386	1.8648	1.767	5.5378
1.01	2.118	0.013	1.118	1.2161	1.225	-0.7204	1.0863	1.225	-11.314
1.01	2.118	0.013	1.353	1.4334	1.725	-16.902	1.4497	1.725	-15.955
1.01	2.118	0.013	1.532	1.5953	2.125	-24.923	1.7265	2.125	-18.750

Table 6.13 Comparison of Expansion Ratio Data in the Case of Secondary Air

A	B	C	D	$R_{p\ cal}$	$R_{p\ exp}$	% Deviation	$R_{p\ cal}$	$R_{p\ exp}$	% Deviation
Common input data				Dimensional analysis			Factorial analysis		
0.808	1.356	0.0055	1.7	1.6541	2.062	-19.778	1.5549	1.553	0.1223
1.414	1.356	0.0055	1.7	1.3485	1.553	-13.163	1.9963	2	-0.1801
0.808	2.387	0.0055	1.7	2.0063	2	0.3162	1.7621	1.803	-2.2683
1.414	2.387	0.0055	1.7	1.6356	1.803	-9.2813	2.5174	2.562	-1.7376
0.808	1.356	0.017	1.7	1.9832	2.562	-22.588	2.4883	2.5	-0.4646
1.414	1.356	0.017	1.7	1.6168	2.5	-35.324	2.9303	2.937	-0.2252
0.808	2.387	0.017	1.7	2.4055	2.937	-18.096	2.1775	2.142	1.6611
1.414	2.387	0.017	1.7	1.9610	2.142	-8.445	1.4731	1.468	0.3474
0.808	1.356	0.0055	5.77	1.1987	1.468	-18.340	1.2485	1.225	1.9183
1.414	1.356	0.0055	5.77	0.9772	1.225	-20.220	1.3812	1.406	-1.7631
0.808	2.387	0.0055	5.77	1.4539	1.406	3.4116	1.3327	1.339	-0.4644
1.414	2.387	0.0055	5.77	1.1853	1.339	-11.475	1.5547	1.562	-0.4616
0.808	1.356	0.017	5.77	1.4372	1.562	-7.9849	1.5439	1.571	-1.7230
1.414	1.356	0.017	5.77	1.1717	1.571	-25.414	1.6768	1.656	1.2590
0.808	2.387	0.017	5.77	1.7432	1.656	5.2689	1.4142	1.41	0.3024
1.414	2.387	0.017	5.77	1.4211	1.41	0.7935	0.6605	1.468	-55.005
0.808	2.118	0.013	9.5	1.4055	1.468	-4.2546	2.1920	2.125	3.1575
0.808	2.118	0.013	3.16	1.8784	2.125	-11.601	2.4457	2.5	-2.1699
0.808	2.118	0.013	2.11	2.0894	2.5	-16.423	1.3870	1.525	-9.0447
1.01	2.118	0.013	6.33	1.4418	1.525	-5.4499	2.0707	2.025	2.2575
1.01	2.118	0.013	3.16	1.7315	2.025	-14.491	2.297	2.525	-9.0233
1.01	2.118	0.013	2.11	1.9259	2.525	-23.723	1.3478	1.5	-10.144
1.212	2.118	0.013	6.33	1.3490	1.5	-10.062	1.9493	1.958	-0.4427
1.212	2.118	0.013	3.16	1.6200	1.958	-17.259	2.1485	2.208	-2.6916
1.212	2.118	0.013	2.11	1.8019	2.208	-18.388	1.8170	1.75	3.8299

7.1 Introduction

Particle separation phenomenon is not uncommon in industrial fluidized beds, where particles of widely different sizes or densities are handled. It has been studied that the fluidized bed reactors can be operated in different modes either to promote the particle mixing or to enhance the particle segregation. It is also not unusual to have one part of the fluidized bed reactor operated in a mixing mode while the other in a segregation mode. A typical example of this kind of reactor is the fluidized bed agglomerating combustor or gasifier developed by Westinghouse (Salvador et al, 1980). In the upper part of the reactor, where combustion or gasification occurs, a solid mixing between the combustion and gasification zones is essential.

Past studies on particle separation have concentrated primarily on the mixing aspect of the phenomenon, notably those by Rowe and Nienow (1976), using two separate layers of flotsam (low density) and jetsam (high density) as a starting mixture. A quantitative analysis was proposed for the mixing of the two segregating powders of different densities (Nienow et al, 1978). In a separate study by Burgess et al. (1977), the initial condition of the bed was found to be important. The well-mixed initial condition (as compared to the unmixed initial condition of two separate layers of flotsam and jetsam) led to less segregation at all gas flow rates. Heertjes et al. (1967) suggested that the wake material scattered into the freeboard by the bursting of the bubbles contribute significantly to the horizontal movement of solids.

Nienow et al. (1972) studied the role of particle size, density and air flow rate on the segregation or de-mixing behaviour in a gas-solid fluidized bed, and concluded that a fairly wide particle size difference can be tolerated, while small density difference leads to ready settling of denser particles.

A qualitative model for particle mixing in a gas-solid fluidized bed has been developed by Gibilaro and Rowe (1974) based on four physical mechanisms, viz, overall particle circulation, interchange between the wake and bulk phases, axial dispersion and segregation. Rowe et al. (1965) presumes that solid mixing will occur by inter-particle diffusion or eddy diffusion as in true fluids. Some solids are seen flowing up and others flowing down the bed due to the bubble rise. This up-low and down-flow of solids with an interchange between streams is the basis for various counter-flow models. Solid exchange between the bubble wake and the emulsion phase is one of the fundamental rate processes that largely affect the direct mixing in fluidized beds (Chiba et al, 1977; Kunii and Levenspiel, 1969).

Chen et al. (1975) presented a limited amount of data on the rate of separation in a char-dolomite system with an unmixed starting mixture. Kondukov and Sosna (1965) and Gelperin et al. (1967) suggested a phase equilibrium diagram for a segregating mixture. Using the analogy between a fluidized bed and a liquid, they suggested that a segregating mixture in a fluidized bed resembled a liquid-solid system. Yang and Keairns (1982) studied the rate of particle separation in a fluidized bed 7.0 cm in diameter, using crushed acrylic plastic particles as flotsam and dolomite particles as jetsam, and concluded that for mixtures of different jetsam concentrations, the rate and degree of particle separation were different but generally completed in less than 15 sec. in all cases.

Nicholson and Smith (1966) studied the axial mixing of particles differing in density in a fluidized bed and proposed a first order rate equation to describe the progress of mixing in short mixing time. Fan and Chang (1979) studied the fluidization and solid mixing characteristics of very large particles, where bubble or slug induced drift and gross solid circulation appeared to be the predominant solid mixing mechanism. Kroger et al. (1980) studied particle mixing in a centrifugal fluidized bed, and found that bubbles are the primary mechanism causing radial mixing for Geldart-B and Geldart-D particles.

Miyauchi (1981) studied the vertical mixing of solids in vigorously fluidized beds (u_o>10 cm/s) of fine Geldart -A solids and found that the mixing data could reasonably be represented by the dispersion model.

$$D_{sv} = 12\, u_o^{1/2}\, d_t^{0.9} \qquad \text{... (7.1)}$$

Avidan and Yerushalmi (1985) found that the dispersion model better represented the mixing during turbulent fluidization, where the bed looked close to homogeneous, but fitted the data poorly when the bed was in the bubbling regime.

Quin et al. (1999) studied particle mixing in rotating fluidized beds and concluded that for particles of the same material, the two layers of particles do not mix until bubbles appear. This result was similar to that of Menon and Durian (1997), who concluded that bubbles are responsible for the bulk motion of particles in a conventional fluidized bed. After the critical minimum fluidization velocity, particles inside the bed start to move radially, and mixing occurs rapidly. Bubbles are a strong source of particle motion, and the bed becomes totally fluid-like. It was also found by Quin et al. (1999) that the minimum bubbling velocity is dependent on the size and density of the particles. For Geldart-B particles, the minimum bubbling velocity is equal to the minimum fluidization velocity, whereas for Geldart-A particles, the minimum bubbling velocity is larger than the minimum fluidization velocity. Mixing occurs due to the difference in densities and fluidization properties of the two layers.

Fan et al. (1979) reviewed the major developments in solids mixing since 1976 (170 articles), in three categories: characterization of states of solids mixtures, rates and mechanism of solids mixing processes and design and scale-up of mixers or blenders. Mixtures can be classified in to two major groups, one only involves free- flowing particles and the other contains cohesive or interactive constituent(s). The mixing indexes can only depict the macroscopic behaviour of a solids mixture. Three major mechanisms, diffusion, convection and diffusion-convection have been proposed for solids mixing.

Fan et al. (1990) proposed a mathematical equation for a size variant, equal-density system of particles for mixing Index (I_M):

$$I_M = k \times \left(\frac{\overline{dp}}{d_F} \right)^k \times \left(\frac{U}{U - U_F} \right)^n \quad \ldots (7.2)$$

Hoffmann (2000) concluded that it is possible to manipulate the working of fluidized beds to some extent by introducing internals into the bed. The particle segregation can be enhanced by reducing axial mixing. Vibration can be brought into the heart of the bed by applying the vibration to internals spanning the bed vessel. Powders which are not fluidizable in a conventional bed can be fluidized in this way.

Dahl and Hrenya (2005) studied discrete particle simulation of gas-solid fluidized bed through Gaussian and Lognormal distribution and found that the average particle diameter decreases as the height within the bed increases, the level of segregation increases with an increase in the width of the particle size distribution and segregation is attenuated as bubbling becomes more vigorous.

Cooper and Coronella (2005) studied fluidization of dissimilar material, i.e., coke and rutile in a fluidized bed and found that particle mixing and segregation phenomena are dominated by bubble activity.

Sahoo and Roy (2005) studied the mixing characteristics of homogeneous binary mixture of regular particles (Geldart BD type) in a cylindrical gas-solid fluidized bed and developed a mathematical model for calculation of mixing index (I_M):

$$I_M = 0.3725 \times \left(\frac{\overline{dp}}{d_F} \right)^{0.3679} \times \left(\frac{h_B}{D_c} \right)^{-0.4864} \times \left(\frac{H_s}{D_c} \right)^{0.8258} \times \left(\frac{U}{U - U_F} \right)^{0.3084} \quad \ldots (7.3)$$

Patil et al. (2007) studied the influence of internal baffles on mixing characteristics and found that the bed without baffles showed distinctive segregation nature. Internal baffles were effective in altering the fluidization of biomass-sand

mixtures. Of the baffles tested, the annular plate showed the best performance as compared to coil and half-circle plate baffles.

Bosma and Hoffmann (2007) studied the segregation tendency of different particles which varies in size or density. They found that sieve-like baffles in the bed can greatly increase the tendency of powders to segregate.

Majumdar et al. (2007) investigated the mixing and segregation behaviour of granular flow in a sectorial container. The effect of different operating parameter such as frequency of oscillations, amplitude of oscillation, volume fraction and the size ratio of particle were studied and concluded that the mixing and segregation of particle takes place in a particular range of frequency zone.

In this present work, knowing the percentage of jetsam at different heights of the bed, the experimental values for the mixing index (I_M) at different heights have been calculated with the help of the following expression (Naimer et al, 1982):

$$I_M = \frac{X^*}{\overline{X}_{bed}} \quad \ldots (7.4)$$

Literature survey has it to say that attempts have been made to improve mixing of different particles of varying sizes and densities and under different experimental conditions such as various types of promoters, distributor plates, etc. But the concept of using secondary air to enhance mixing has not yet been reported.

The objective of the present work is to find a technique for augmenting mixing characteristic expressed through a mixing index, for which mathematical correlations through four system parameters under different experimental conditions, viz., only primary air, simultaneous primary and secondary air, disc promoter and rod promoter have been developed. The scope of the experiment is presented in **Table 1**. In the present case, a software package for artificial neural network in Mat Lab [16] has been used for back propagation algorithm. Three typical layers, viz., (i) input, (ii) hidden and (iii) output have been chosen. Four nodes in the input layer, three neurons in the hidden layer and one node in the output layer have been taken.

In order to express the mixing index, a mathematical model has also been developed. Both horizontal and vertical dispersions of the particles along with the counter flow of solids and their circulation have been considered for development of the model.

7.2 Development of Models

In this present work, the mixing index (I_M) at different heights has been calculated using equation (7.4), $I_M = \frac{X^*}{\overline{X}_{bed}}$

The mixing index (I_M) varies with static bed heights, particle sizes, densities and gas mass velocities (Sahoo and Roy, 2005). The effect of all these four variables has been calculated with primary air supply, rod promoted bed, disc promoted bed and simultaneous primary and secondary air supply.

A mathematical model has also been developed for prediction of mixing index. The model equations are assumed to be linear and take the general form:

$$Y=a_0+a_1A+a_2B+a_3C+a_4D+\ldots\ldots\ldots+a_{12}ABD+a_{13}ACD+\ldots\ldots+a_{15}ABCD \quad \ldots (7.5)$$

The coefficients are calculated by the Yate's technique $a_i = \sum \alpha_i y_i / N$ ... (7.6)

where A, B, C and D are the factorial design symbols, a_i is the coefficient, y_i is the response, α_i is the level of variables and N is the total number of treatments. The experimental data based on factorial design, nature of the effects and its analysis are presented for mixing index in **Tables 7.2 and 7.3** for primary air, disc promoter, rod promoter and simultaneous primary and secondary air supplies respectively.

The levels of variables are calculated as:

A: level of static bed height = (A-1.95) / 1.55

B: Level of density= (B-2.938) / 0.396

C: Level of particle size =(C-0.0064)/ 0.0009

D: Level of mass velocity = (D-2.7) / 0.6

… (7.7)

The following **Equations 7.8, 7. 9, 7.10 and 7.11** have been developed for mixing index for different experimental conditions (neglecting smaller coefficients).

For disc promoted bed:

I_{MD} = 0.9358 + 0.1222 A -0.00165 B -0.00465 C + 0.00152 D- 0.0211 AB + 0.0157 AC - 0.01 AD ... (7.8)

For rod promoted bed:

I_{MR} = 0.9272 + 0.1462 A -0.0021 B +0.0079 C -0.0037 D -0.027 AB + 0.019 AC -0.01 AD ... (7.9)

For primary air (un-promoted):

I_{MP} = 0.9284 + 0.1739 A -0.004 B +0.0022 C -0.012 D -0.0338 AB + 0.0163 AC -0.016 AD …(7.10)

For simultaneous primary and secondary air (un-promoted):

I_{MS} = 0.9477 + 0.0751 A -0.00241 B -0.0108 C + 0.0036 D-0.0099 AB + 0.0249 AC … (7.11)

In this present work, the ANN model using back propagation algorithm for promoted and un-promoted beds have been developed. In both the cases, the ANN structures (Input layer × Hidden layer × Output layer) have been tested at constant epochs (cycles), learning rate, error goal and net trained parameter. Structures of the ANN model are selected for training of input and output data in each case as shown in **Table 7.4**.

7.3 Results and Discussion

Experiments have been carried out by taking four different bed materials, viz, iron, coal, dolomite and laterite. Iron has been considered as the base material due to its separability through a magnetic separator. A 50:50 mixture (by weight) has been taken for experimentation. The mixture is initially well mixed and then charged into the column, and then fluidized at varying air flow rates. The variables taken are different static bed heights, particle sizes, particle densities and gas mass velocities. Two different promoters, i.e. rod and disc types have been used to promote mixing. Experiments have also been carried out with primary and simultaneous primary and secondary air supplies.

The flow of secondary air begins after the bed starts to fluidize due to primary air supply through the bottom of the fluidizer. It has been observed that the secondary air exerts an axial thrust on the bottom of the bed and owing to this effect, the primary air supply is maintained at more than the minimum fluidization mass velocity, i.e., G_{mf} + 0.17 for all the experiments. If this extra amount of primary air (0.17 kg/m^{2}s) is not supplied, then the lower half of the bed will not fluidize properly, i.e. the bed will behave like a fixed bed. For any bed material this is the minimum required extra amount of air that has to be supplied in addition to the amount of minimum fluidization mass velocity i.e., G_{mf}. It has been observed that the introduction of secondary air enhances mixing among the particles of wide ranges of sizes and densities due to greater turbulence in the bed.

During fluidization, the samples have been drawn from the side ports made on either side of the column (maintaining same velocity ratios, i.e. G_f/G_{mf} and G_p/G_s as

indicated in **Table 7.3**) and have been analysed on the basis of the assumption of uniform concentration for a particular layer of particles across the cross-section of the column at any height. Then the samples have been separated through a magnetic separator and then the weights of the flotsam and jetsam particles taken in an electronic digital balance.

Iron (larger density) has been considered as the jetsam particle while other materials, viz., dolomite, coal and lateriate as flotsam. Dolomite (larger size) has been considered as the jetsam particle and small size dolomite as flotsam (particles are homogenous with respect to their densities). The mixtures taken in each batch of experimentation are either homogeneous with respect to their sizes or densities.

It is clearly evident from the above **Eqs. (7.8, 7.9, 7.10 and 7.11)** that the effect of the variable, i.e. static bed height to the height at which samples are drawn ($h_s/h_B = A$) is prominent as compared to the densities, particle sizes and gas mass velocities. During experimentation, the segregation tendency is clearly observed in lower mass velocity ranges ($G_f < 2G_{mf}$). The jetsam concentration decreases with an increase in the height of the column.

The calculated values of the mixing index through the statistical approach (factorial design) have been compared with the experimental values and presented in **Table 7.5**. It has been found form **Eqs. (7.8, 7.9, 7.10 and 7.11)** that the mixing index is a direct function of bed heights and an inverse function of densities in all the four cases. But Mixing index is an inverse function of particle sizes and direct function of gas mass velocities for disc promoted bed and simultaneous primary and secondary air supply, whereas it is evident that in the case of only primary air supply and rod promoter, it is a direct function of particle sizes and an inverse function of gas mass velocities.

It has been observed that simultaneous primary and secondary air supply gives good mixing index values (jetsam and flotsam concentration of 0.5, i.e. $I_M = 1.0$ represents perfect mixing) owing to greater circulation and turbulence in the bed as compared to the other three conditions as evident form **Figs. 7.1, 7.2, 7.3 and 7.4**. It has

also been found that the rod promoter is superior to disc promoter as the latter provides intermittent resistance (provided with the disc) for which bubbles are not able to carry the jetsam particles to greater heights, and hence more segregation tendency develops. In the case of rod promoter, the resistance is offered both radially and axially but transport of some wake particles might occur through the gap between the column and rods, thereby causing better mixing of particles. The resistance offered by disc promoter predominates that by the rod promoter. It is also evident from **Figs. 7.5, 7.6 7.7 and 7.8** that the particles with more homogeneity (laterite and iron) with respect to density gives better mixing as compared to less homogenous particles i.e. coal and iron. The value of mixing index 1.0 indicates perfect mixing; deviation on either side represents the development of segregation tendencies. It is evident from **Figs. 7.9 and 7.10** that with an increase in mass velocity, better mixing is obtained. The values of mixing index have been calculated from the model equations for different input data and compared with the corresponding experimental values for primary air, rod promoter, disc promoter and simultaneous primary and secondary air supplies as in **Tables 7.6, 7.7, 7.8 and 7.9** respectively.

The same input data have been tested with earlier models, i.e., Sahoo and Roy (2005) and found that the present model (**Eq. 7.10**) gives better results as compared to that by Sahoo and Roy as evident in **Fig. 7.11**.

Experiments have also been carried out for particles with a wide range of sizes (same density). It is evident from **Fig. 7.12** that better mixing is obtained in the case of simultaneous primary and secondary air supply conditions due to greater turbulence and circulation in the bed. Better mixing is also obtained at higher mass velocities due to the greater turbulence in the bed as evident in **Fig. 7.13**.

The predicted values mixing index using ANN and statistical approaches have been compared with the experimental values for promoted and un-promoted beds as shown in **Table 7.10**. It has also been observed that the ANN approach holds good for all the velocity ranges, which is an authentication to the present model and experimentation.

The standard deviations for mixing index have been found to be ± 0.0347, ± 0.0564, ± 0.066 and ± 0.048 for disc-type promoter, rod-type promoter, primary air, and simultaneous primary and secondary air supplies respectively.

7.4. Conclusions

The developed models can be widely used for analysing the mixing and segregation characteristics of the homogenous binary mixtures of particles with respect to densities and sizes over a good range of the operating parameters. The developed models accurately predict the concentration of jetsam (and hence the mixing index). Mixing index decreases with an increase in the height of the column measured from the distributor plate, which is in good agreement with the experimental data. Of the two types of promoters, disc and rod, the latter type has been found to be superior to the former. However, during simultaneous primary and secondary air supplies, the best mixing is obtained. Furthermore, it has been observed that the mixing performance under four different conditions is in the increasing order as follows: primary air supply (un-promoted), disc type, rod type and simultaneous primary and secondary air supply. In the higher mass velocity range of air, better mixing is obtained, whereas better segregation is obtained in the lower mass velocity range ($G_f < 2\ G_{mf}$). Hence, simultaneous primary and secondary air supply may be considered as the best method (instead of using bed internals) to augment mixing among particles of varying densities and sizes. Both statistical analysis and ANN approaches can be suitably used for prediction mixing index.

Notations

C_j	Concentration of jetsam particles at any height in the bed (Amount of jetsam particle in the sample drawn at a height in kg / Amount of that in the original mixture in kg)
d_F	Diameter of flotsam particle, m
d_t	Bed or tube diameter, m
d_p	Particle size of the mixture, m
d_{pavg}	Average particle size of the mixture, m
$\bar{d}_p$	Average particle size of the mixture, m
d_F	Diameter of flotsam particle, m
D_c	Diameter of column, m
D_{sv}	Vertical dispersion coefficient, m^2/s
G_f	Mass velocity corresponding to fluidization, kg/m^2s
G_{mf}	Mass velocity corresponding to minimum fluidization, kg/m^2s
G_p	Mass velocity of the medium due to primary air = G_{mf} + 0.17, kg/m^2s
G_s	Additional mass velocity of the fluidizing medium due to secondary air, kg/m^2s
h_B	Height of particles layer in the bed from the distributor, m
h_s	Initial static bed height, m
I_M	Mixing index, dimensionless
I_{MD}	Mixing index in case of disc promoter
I_{MR}	Mixing index in case of rod promoter
I_{MP}	Mixing index in case of primary air supply
I_{MS}	Mixing index in case of simultaneous primary and secondary air supply
J	Weight of jetsam particles taken in the bed, kg
K	Coefficient of correlation
U	Superficial velocity of the fluidizing medium, m/s
U_c	Transition velocity from bubbling to turbulent fluidization, m/s
U_F	Minimum fluidization velocity of the flotsam particles, m/s
u_o	Operating velocity, m/s
W	Weight of the total bed material, kg
X^*	Percentage of jetsam particles in any layer
$\bar{X}_{bed}$	Percentage of jetsam particles in the bed
k, n	Exponent of the variables

Greek symbols

ρ_f	Density of fluid, kg/m^3
ρ_s	Density of solid particle, kg/m^3
ρ_{Mavg}	Average density of solid particle, kg/m^3

Abbreviations

ANN	Artificial Neural Network
cal	Values calculated from the developed model
exp	Experimental values

References

1. Avidan, A., Ph.D., Dissertation, City college of New York, 1980; Avidan, A. and Yerashalmi, J., AIChE J., 31(1985) 835.

2. Burgess, J.M., Fane, A.G. and Fell, C.J.D., Pac. Chem. Eng. Cong. 2 (1977) 1405.

3. Chen, J.L.P., Keairns, D.L. and Can., J., Chem. Eng., 53 (1975) 395.

4. Chiba, T. and Kabayashi, H., J., Chem. Eng. of Japan, 10 (1977) 205.

5. Cooper, S. and Coronella, C.J., AIChE Meeting in San Francisco, 3b Panel, 2003,151, 1-3, (2005) 27.

6. Dahl, S.R. and Hrenya, C.M., Chemical Engineering Science, 60, 23 (2005) 6658.

7. Fan, L.T. and Chang, Y., The Canadian .J. of Chem. Eng.,(1979) Feb 57.

8. Fan, L.T., Chen, Y., and Lai, F.S., Powder Tech., 61 (1990) 255.

9. Gelperin, N.I., Einstein, V.G., Nosov, G.A., Mamoshkina, V.V.and Rebrova, S.K, Teor. Osn, Khim, Tekhnol. 01 (1967) 383.

10. Gibilaro, L.G. and Rowe, P.N., Chem. Eng. Sci., 29 (1974) 1403.

11. Heertjes, P.M., Nie, L.H. de and Verloop, J., in proc., Int. Symp. On Fludization, A.A.J. Drinkenburg, ed., P.47b, Netherlands unv. Press, Amsterdam, 1967.

12. Hoffmann, A.C., NPT Process Tech, 7, (2000) 20.

13. Kondukov, N.B.and Sosna, M.H., Khim. Prom., 6 (1965) 402.

14. Kunii, D. and Levenspiel, O., Fluidization Eng., Wiley New York, 1969.

15. 14. Kroger, D.G., Levy, E.Kg., Abdelnaurg, J.C. and Chen, Fluidization, Grace, J.R. and Matsen, J.M., ed., Plenum Press, New York,(1980) 453.

16. Mat Lab Version, 6.5.0.18093a Release 13.

17. Miyauchi, T., Adv. Chem. Eng., 11, (1981)275.

18. 18. Menon, N. and Durian, D.J., Phys. Rev. Lett, 79 (1997) 3407.

19. Mazumdar, A., Horio, M., Robi, P.S, and Swarnkar, R. and Malik, M., Journal of Chemical Engg. of Japan, 40 (2007) 652.

20. Necholson, W.J. and Smith, J.C., Chem. Eng. progress, 66 (1966) 83.

21. Nienow, A.W., Rowe, P.N. and Agbim, A.J., PACHEC conference, Kyoto, Japan, 1972, Oct 10.

22. Nienow, A.W., Rowe, P.N.and Cheing, L.Y.L. , Powder Tech., 20 (1978) 89.

23. Naimer, N., Chiba, T. and Nienow, A.W., Chem., Eng., Sci, 37 (1982)1047.

24. Quin, G.H., Baggi, I., Pfeffer, R., Shaw, H. and Stevens, J.G., Particle Tech. and Fluidization, 45 (1999) 1401.

25. 24. Patil, K., Huhnke, R. and Bellmer, D., CIGR Ejournal. Manuscript EE 06 016. Vol. IX. April, (2007).

26. Rowe, P.N., Partridge, B.A., Cheney, A.G., Henwood, G.A. and Lyali, A., Trans. Inst. Chem. Eng., 43 (1965) T271.

27. Rowe, P.N., Nienow, A.W., Powder Tech., 15 (1976)141.

28. Salvador, L.A., Cherish, P. and Chelen, E.J., paper presented at the 88th AICHE National meeting, Philadelphia, PA, june 8-12 (1980).

29. Sahoo, A. and Roy, G.K., Powder Tech., 159 (2005) 150.

30. Yang, W.C and Keairns, D.L., Ind. Eng. Chem. Fundam., 21 (1982) 228.

31. Bosma, J.C. and Hoffmann, A.C., Web.ift.uib.no/mps/papershtml/wcpt4_216.pdf, (2007).

Figures

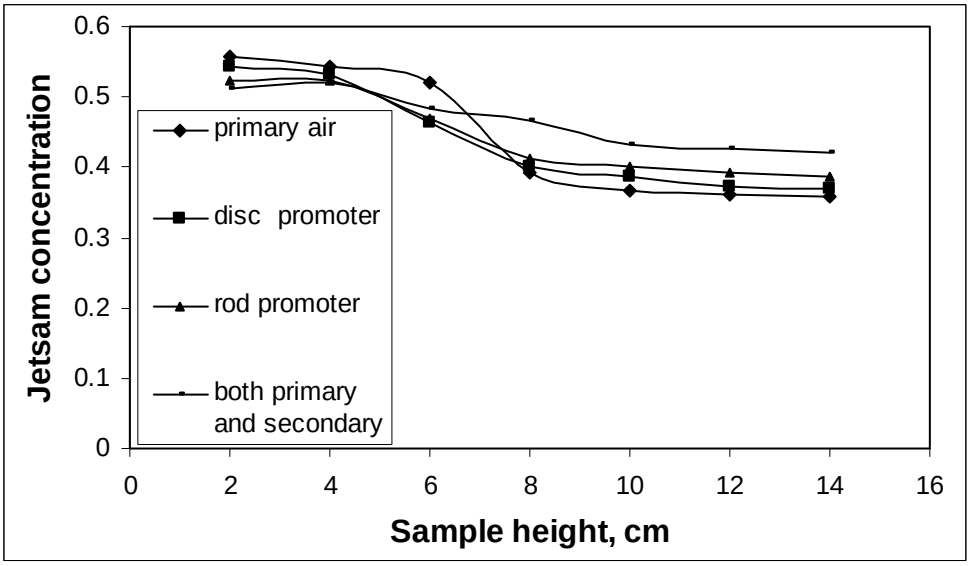

Fig 7.1 Effect of experimental conditions on jetsam concentration at different sample heights for laterite and iron particles at h_s = 0.08m and G_f=1.275 kg/m^{2}s

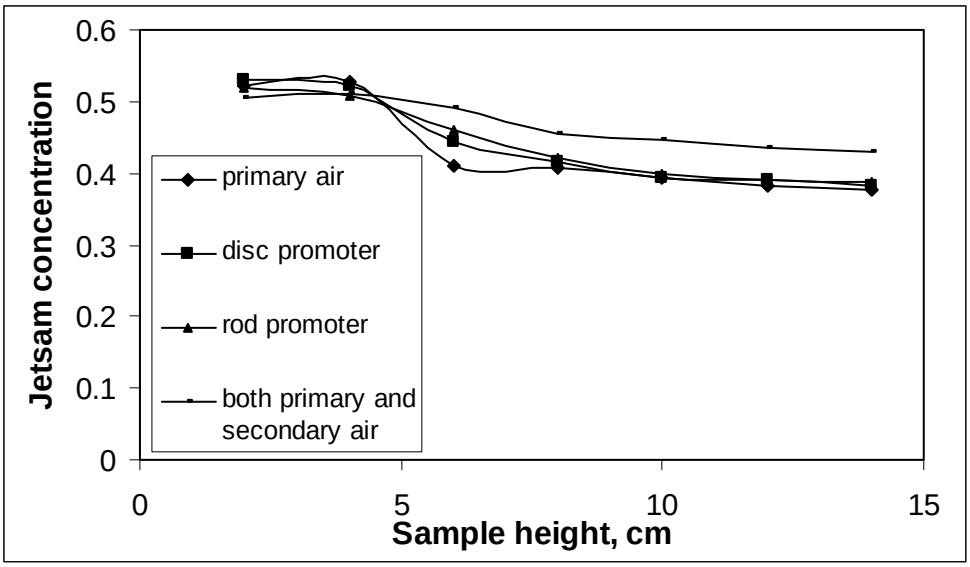

Fig 7.2 Effect of experimental conditions on jetsam concentration at different sample heights for laterite and iron particles at h_s = 0.14m and G_f = 2.55 kg/m^{2}s

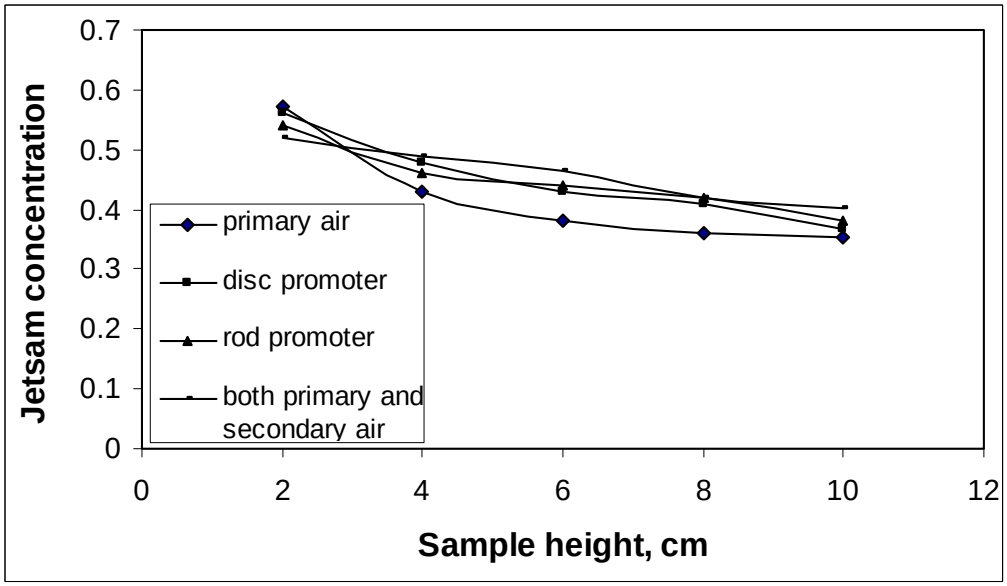

Fig 7.3 Effect of experimental conditions on jetsam concentration at different sample heights for coal and iron particles at h_s = 0.08m and G_f = 1.275 kg/m^{2}s

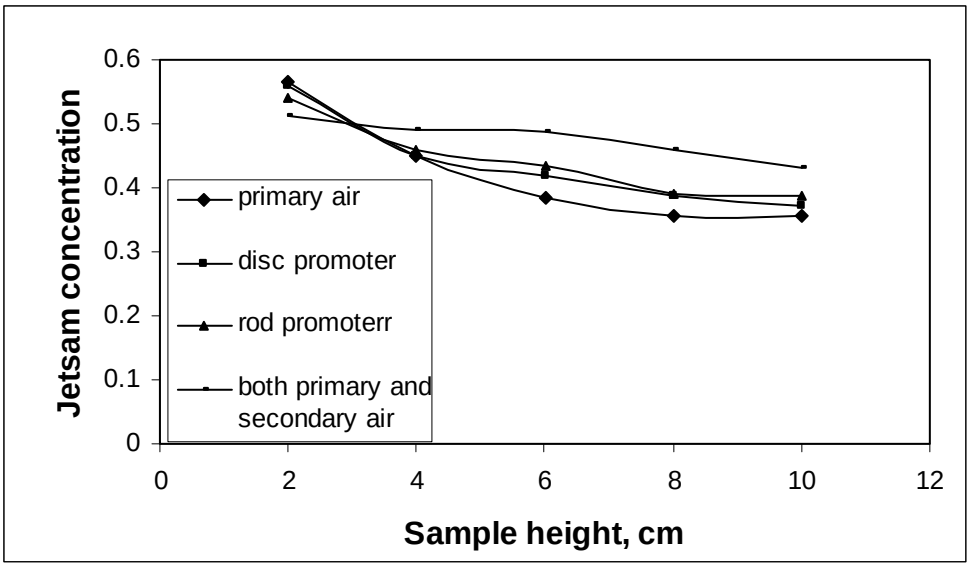

Fig 7.4 Effect of experimental conditions on jetsam concentration at different sample heights for coal and iron particles at h_s = 0.14m and G_f = 2.55 kg/m^{2}s

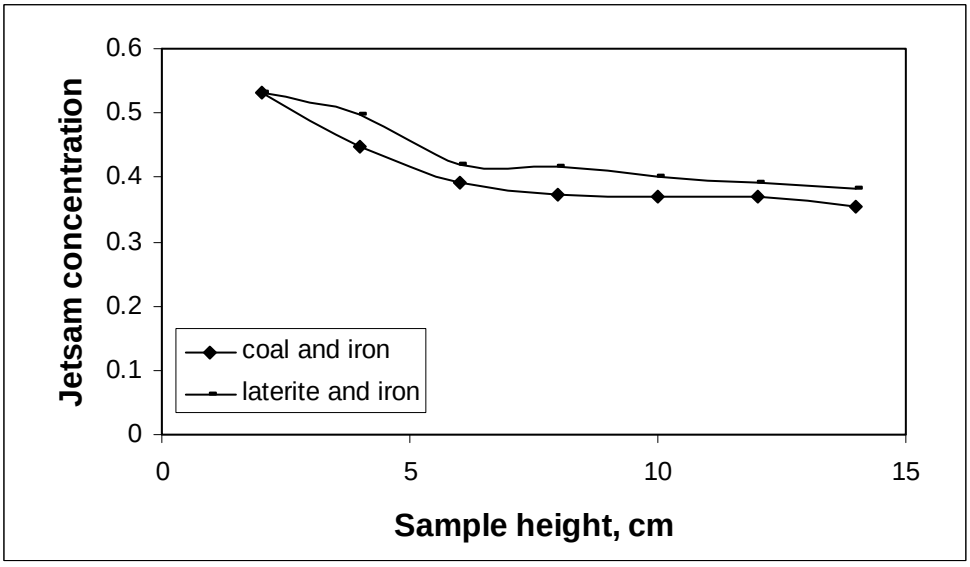

Fig 7.5 Effect of particle density on jetsam concentration at different sample heights for h_s = 0.14m and G_f=2.55 kg/m^{2}s in the case of disc promoter

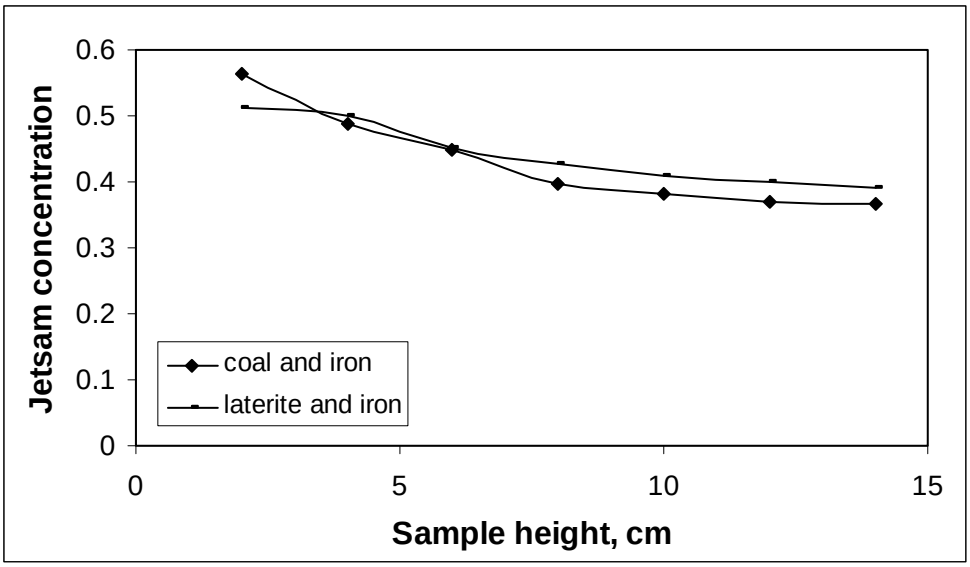

Fig 7.6 Effect of particle density on jetsam concentration at different sample heights for h_s = 0.14m and G_f=2.55 kg/m^{2}s in the case of rod promoter

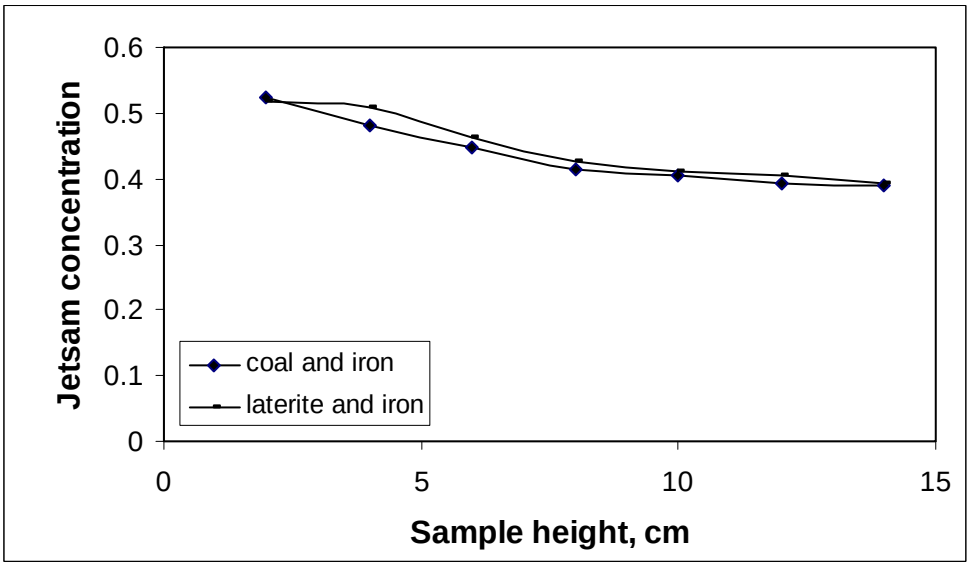

Fig 7.7 Effect of particle density on jetsam concentration at different sample heights for h_s = 0.14m and G_f=2.55 kg/m^{2}s in the case of primary air supply

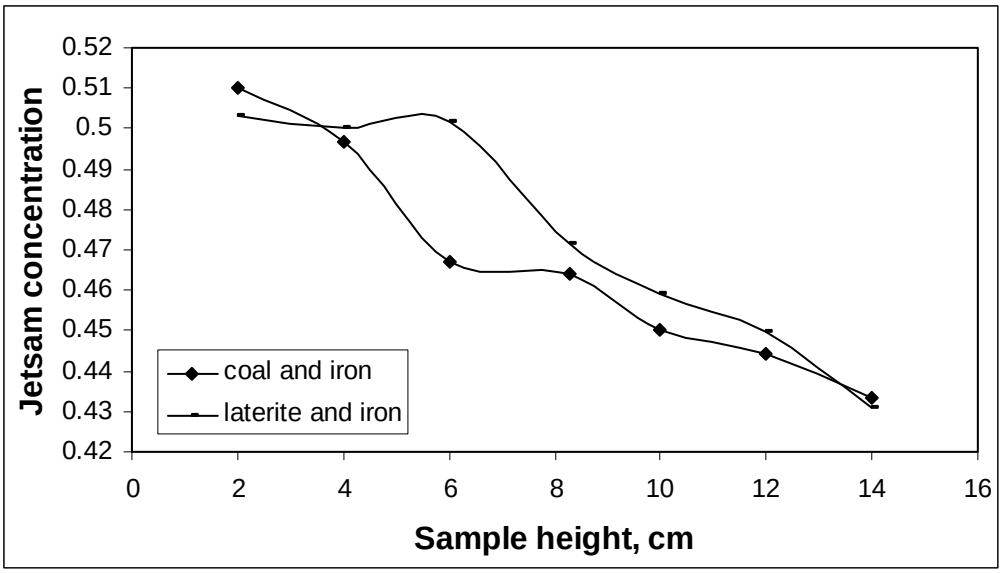

Fig 7.8 Effect of particle density on jetsam concentration at different sample heights for h_s = 0.14m and G_f=2.55 kg/m^{2}s in the case of simultaneous primary and secondary air supply

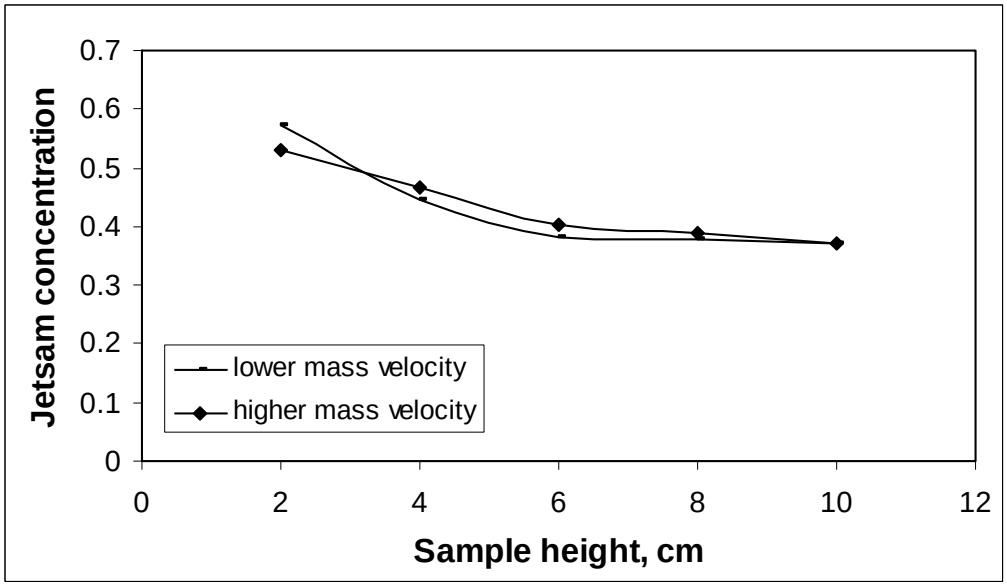

Fig 7.9 Effect of mass velocity on jetsam concentration for coal and iron particles at h_s = 0.08m and particle size of 0.00055m in the case of disc promoter

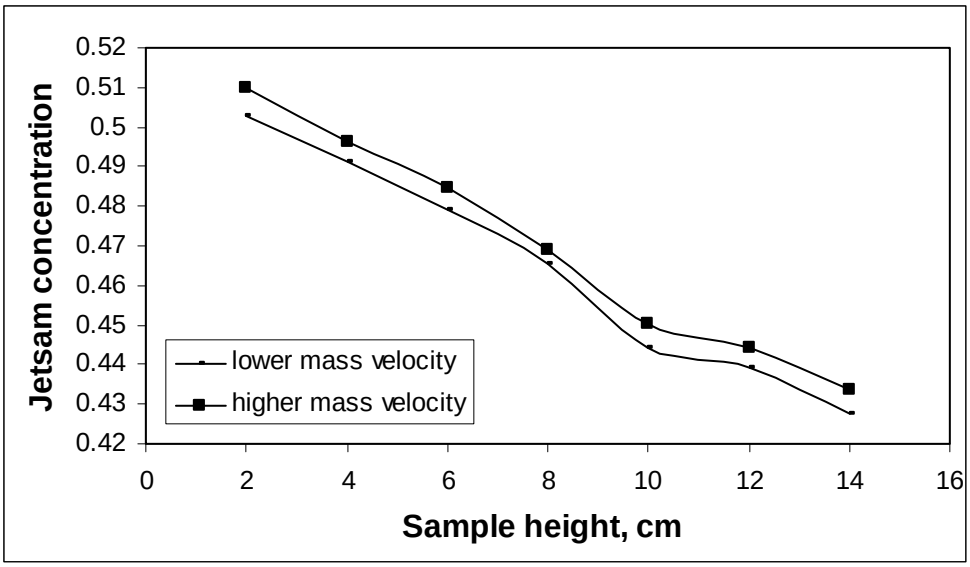

Fig 7.10 Effect of mass velocity on jetsam concentration for coal and iron particles at h_s = 0.08m and particle size of 0.00055m in the case of simultaneous primary and secondary air supply

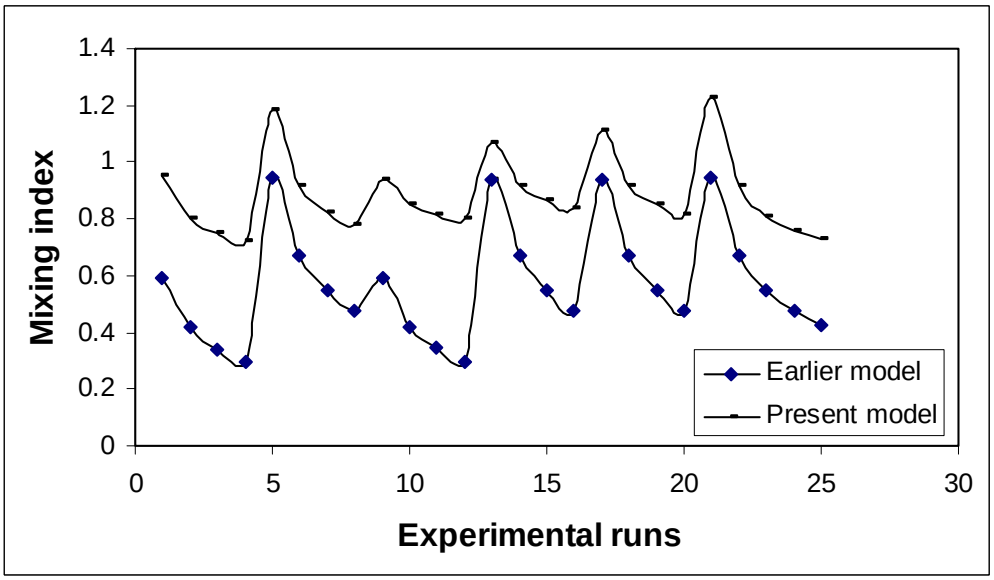

Fig. 7.11 Comparison of mixing index calculated from the same input data in the case of primary air supply

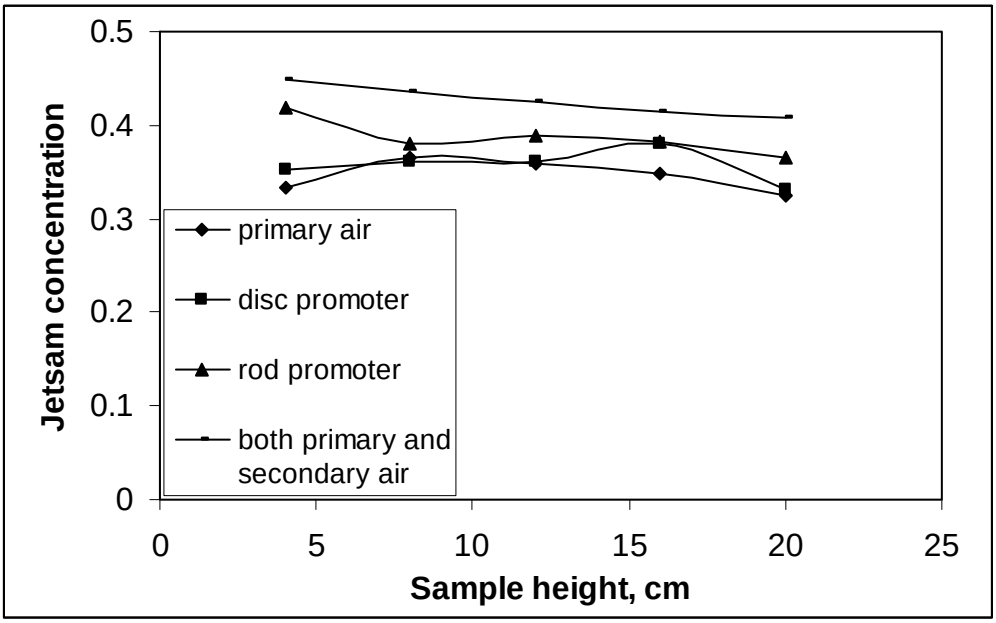

Fig. 7.12 Effect of experimental conditions on jetsam concentration at different sample heights for dolomites of different sizes; 0.00055m and 0.0013m at h_s = 0.10m and G_f=1.445 kg/m^{2}s

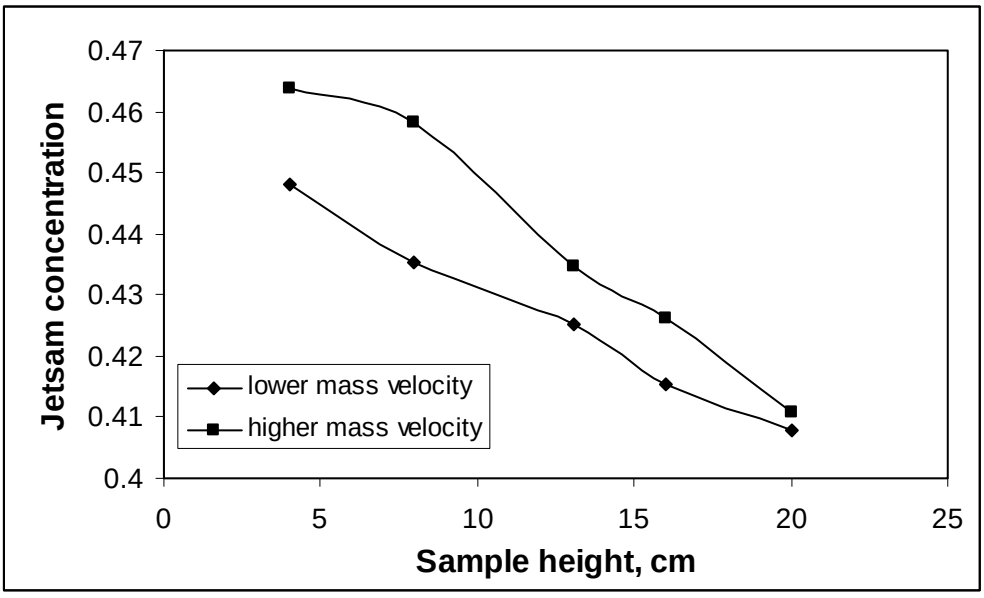

Fig. 7.13 Effect of mass velocity on jetsam concentration at different sample heights for dolomites of different sizes; 0.00055m and 0.0013m at h_s = 0.08m in the case of simultaneous primary and secondary air supply

Table 7.1 Scope of the Experiment

Properties of the Bed Materials				
Materials	**$d_{p \times 10^3}$, m**		**$\rho_{s \times 10^{-3}}$, kg/m^3**	
Dolomite	0.55, 0.725, 1.3		2.817	
Laterite	0.55, 0.725, 1.3		3.47	
Iron	0.55, 0.725, 1.3		4.4	
Coal	0.55, 0.725, 1.3		1.6	
Density of fluid, ρ_f	1.18 kg/m^3 at 25^{0}c			
Diameter of column, D_c	0.099 m			
Bed Parameter				
Initial static bed height, $h_{s \times 10^2}$, m	8, 10, 12, 14			
Heights at which samples collected, h_B x 10^2, m	4, 8, 12, 16, 20			
Flow property				
Materials	h_S x 10 ^{2}	Average Particle size, m	G_{mf},kg/m^{2}s	G_f,kg/m^{2}s
Coal+ iron	8	0.00055	0.595	1.275 to 2.55
Coal+ iron	14	0.00055	0.765	1.275 to 2.55
Coal+ iron	8	0.000725	0.68	1.275 to 2.55
Coal+ iron	14	0.000725	0.85	1.275 to 2.55
Laterite + iron	8	0.00055	0.85	1.275 to 2.55
Laterite l+ iron	14	0.00055	1.02	1.275 to 2.55
Laterite + iron	8	0.000725	0.935	1.275 to 2.55
Laterite+ iron	14	0.000725	1.105	1.275 to 2.55
Dolomite+ Iron	8	0.00055	0.765	1.275 to 2.55
Dolomite+ Iron	14	0.00055	0.935	1.275 to 2.55

Table 7.2 Factorial Design Analysis

Sl. No	Name of the variable	Variable general symbol	Factorial design symbol	Minimum level (-1)	Maximum level (+1)	Magnitude of variables
1	Static bed height	h_s/h_B	A	0.4	3.5	2.0, 1.0 , 0.67, 0.5, 0.4,2.5, 1.25, 0.83, 0.625, 3.0, 1.5, 0.75, 0.6,3.5, 1.75, 1.16, 0.875, 0.7
2	Density	ρ_{Mavg}/ρ_f	B $x10^{-3}$	2.542	3.334	2.542, 2.923, 3.334
3	Particle size	d_{Pavg}/D_c	C	0.0055	0.0073	0.0055, 0.0073, 0.013
4	Mass velocity	G_f/G_{mf} G_p/G_s	D	2.1 2.1	3.3 3.3	2.1 to 4.28 0.9 to 15.0

Table 7.3 Analysis of Mixing Index Data

Treat-ment Combi-nation	A	B x 10^{-3}	C	D (G_f/G_{mf})	I_{MP}	I_{MR}	I_{MD}	D (G_p/G_s)	I_{MS}
				Experimental				Experimental	
1	0.4	2.542	0.0055	2.1	0.7404	0.764	0.802	2.1	0.9042
a	3.5	2.542	0.0055	2.1	1.1722	1.1032	1.083	2.1	1.0054
b	0.4	3.334	0.0055	2.1	0.7934	0.803	0.8426	2.1	0.9334
c	3.5	3.334	0.0055	2.1	1.042	1.0062	1.0226	2.1	1.0004
d	0.4	2.542	0.0073	2.1	0.705	0.735	0.7602	2.1	0.801
ab	3.5	2.542	0.0073	2.1	1.1942	1.1522	1.1156	2.1	1.063
ac	0.4	3.334	0.0073	2.1	0.763	0.7958	0.8032	2.1	0.821
ad	3.5	3.334	0.0073	2.1	1.1134	1.0878	1.0456	2.1	1.021
bc	0.4	2.542	0.0055	3.3	0.7402	0.7812	0.8402	3.3	0.8926
bd	3.5	2.542	0.0055	3.3	1.0604	1.053	1.0492	3.3	1.02
cd	0.4	3.334	0.0055	3.3	0.8002	0.8214	0.852	3.3	0.9034
abc	3.5	3.334	0.0055	3.3	1.0602	1.0218	1.0326	3.3	1.006
abd	0.4	2.542	0.0073	3.3	0.713	0.743	0.775	3.3	0.8624
acd	3.5	2.542	0.0073	3.3	1.1346	1.1028	1.075	3.3	1.053
bcd	0.4	3.334	0.0073	3.3	0.7804	0.8038	0.8356	3.3	0.863
abcd	3.5	3.334	0.0073	3.3	1.042	1.061	1.0396	3.3	1.0112

(Columns indicating A, B and C are common.)

Table 7.4 Selected Structures of Neural Network Models

Net train parameter : 500				
Percentage Set Learning Rate : 1.0				
Net train parameter learning : 1.0				
Percentage set error goal : 0.001				
Net train parameter epochs : 20,000				
Performance : 0.02367/1e^{-5}				
Bed Particular	Input Nodes	Hidden Nodes	Output Nodes	No of cycles
Primary air	4	3	1	20,000
Secondary air	4	3	1	20,000
Rod promoter	4	3	1	20,000
Disc promoter	4	3	1	20,000

Table 7.5 Comparison of (Factorial Design Data with Experimental Data) Mixing Index Data

I_{MPcal}	I_{MPexp}	I_{MDcal}	I_{MDexp}	I_{MRcal}	I_{MRexp}	I_{MScal}	I_{MSexp}
0.73472	0.7404	0.8022	0.802	0.761	0.764	0.8965	0.9042
1.14952	1.1722	1.0788	1.083	1.089	1.1032	1.0165	1.005
0.79432	0.7934	0.8412	0.8426	0.811	0.803	0.9097	0.9334
1.07392	1.042	1.0334	1.0226	1.031	1.0062	0.9937	1.004
0.70668	0.705	0.763	0.7602	0.7388	0.7352	0.8285	0.801
1.18668	1.1942	1.0996	1.1156	1.1428	1.1522	1.0445	1.063
0.76628	0.763	0.802	0.8032	0.7888	0.7958	0.8417	0.821
1.11108	1.1134	1.0542	1.0456	1.0848	1.0878	1.0217	1.021
0.74272	0.7402	0.8252	0.8402	0.7736	0.7812	0.9037	0.8926
1.09352	1.0604	1.0618	1.0492	1.0616	1.053	1.0237	1.02
0.80232	0.8002	0.8642	0.852	0.8236	0.8214	0.9169	0.9034
1.01792	1.0602	1.0164	1.0326	1.0036	1.0218	1.0009	1.006
0.71468	0.713	0.786	0.775	0.7514	0.743	0.8357	0.8624
1.13068	1.1346	1.0826	1.075	1.1154	1.1028	1.0517	1.053
0.77428	0.7804	0.825	0.8356	0.8014	0.8038	0.8489	0.863
1.05508	1.0824	1.0372	1.0396	1.0574	1.061	1.0289	1.0112
0.800406	0.8626	0.872577	0.9474	0.836448	0.9878	0.877855	0.9806
0.773425	0.7638	0.863682	0.8632	0.797468	0.963	0.857997	0.973
0.845146	0.995	0.892718	0.8536	0.83994	0.9778	0.886855	0.997
0.832445	0.8826	0.876274	0.8218	0.805556	0.9522	0.866997	0.9786
0.909458	0.9934	0.788658	0.882	0.836998	0.9036	0.863599	0.9342
0.860304	0.8406	0.769788	0.8402	0.826579	0.8642	0.880147	0.9672
0.81859	1.0226	0.819151	0.8704	0.865867	0.9008	0.870523	0.9816

Table 7.6 Comparison of Mixing Index Data in the Case of Primary Air Supply

A	B	C	D	I_{MPcal}	I_{MPexp}	%Deviation
0.4	2.542	0.0055	2.1	0.7347	0.7404	-0.7671
3.5	2.542	0.0055	2.1	1.1495	1.1722	-1.9348
0.4	3.334	0.0055	2.1	0.7943	0.7934	0.1159
3.5	3.334	0.0055	2.1	1.0739	1.042	3.0633
0.4	2.542	0.0073	2.1	0.7066	0.705	0.2382
3.5	2.542	0.0073	2.1	1.1866	1.1942	-0.6297
0.4	3.334	0.0073	2.1	0.7662	0.763	0.4298
3.5	3.334	0.0073	2.1	1.1110	1.1134	-0.2083
0.4	2.542	0.0055	3.3	0.7427	0.7402	0.3404
3.5	2.542	0.0055	3.3	1.0935	1.0604	3.1233
0.4	3.334	0.0055	3.3	0.8023	0.8002	0.26493
3.5	3.334	0.0055	3.3	1.0179	1.0602	-3.9879
0.4	2.542	0.0073	3.3	0.7146	0.713	0.2356
3.5	2.542	0.0073	3.3	1.1306	1.1346	-0.3455
0.4	3.334	0.0073	3.3	0.7742	0.7804	-0.7842
3.5	3.334	0.0073	3.3	1.0550	1.0824	-2.5240
1	2.542	0.0073	1.875	0.8004	0.8626	-7.2100
0.83	2.542	0.0073	1.875	0.7734	0.7638	1.2601
1	3.334	0.0055	3	0.8451	0.995	-15.060
0.83	3.334	0.0055	3	0.8324	0.8826	-5.6826
1.75	3.334	0.0055	2.5	0.9094	0.9934	-8.4500
1.16	3.334	0.0055	2.5	0.8603	0.8406	2.3439
1.16	2.542	0.0073	3	0.8185	1.0226	-19.950
0.875	2.542	0.0073	3	0.7788	0.895	-12.975

Table 7.7 Comparison of Mixing Index Data in the Case of Rod Promoter

A	B	C	D	I_{MRcal}	I_{MRexp}	%Deviation
0.4	2.542	0.0055	2.1	0.761	0.764	-0.3926
3.5	2.542	0.0055	2.1	1.089	1.1032	-1.2871
0.4	3.334	0.0055	2.1	0.811	0.803	0.9962
3.5	3.334	0.0055	2.1	1.031	1.0062	2.4647
0.4	2.542	0.0073	2.1	0.7388	0.7352	0.4896
3.5	2.542	0.0073	2.1	1.1428	1.1522	-0.8158
0.4	3.334	0.0073	2.1	0.7888	0.7958	-0.8796
3.5	3.334	0.0073	2.1	1.0848	1.0878	-0.2757
0.4	2.542	0.0055	3.3	0.7736	0.7812	-0.9728
3.5	2.542	0.0055	3.3	1.0616	1.053	0.8167
0.4	3.334	0.0055	3.3	0.8236	0.8214	0.2678
3.5	3.334	0.0055	3.3	1.0036	1.0218	-1.7811
0.4	2.542	0.0073	3.3	0.7514	0.743	1.1305
3.5	2.542	0.0073	3.3	1.1154	1.1028	1.1425
0.4	3.334	0.0073	3.3	0.8014	0.8038	-0.2985
3.5	3.334	0.0073	3.3	1.0574	1.061	-0.3393
1.16	2.542	0.0073	1.5	0.8364	0.9878	-15.322
0.875	2.542	0.0073	1.5	0.7974	0.963	-17.189
1.16	2.542	0.0073	3	0.8399	0.9778	-14.099
0.875	2.542	0.0073	3	0.8055	0.9522	-15.400
0.67	3.334	0.0055	3	0.8369	0.9036	-7.3707
0.5	3.334	0.0055	3	0.8265	0.8642	-4.3532
1.16	3.334	0.0055	2.5	0.8658	0.9008	-3.878

Table 7.8 Comparison of Mixing Index Data in the Case of Disc Promoter

A	B	C	D	I_{MDcal}	I_{MDexp}	%Deviation
0.4	2.542	0.0055	2.1	0.8022	0.802	0.0249
3.5	2.542	0.0055	2.1	1.0788	1.083	-0.3878
0.4	3.334	0.0055	2.1	0.8412	0.8426	-0.1661
3.5	3.334	0.0055	2.1	1.0334	1.0226	1.0561
0.4	2.542	0.0073	2.1	0.763	0.7602	0.3683
3.5	2.542	0.0073	2.1	1.0996	1.1156	-1.4342
0.4	3.334	0.0073	2.1	0.802	0.8032	-0.1494
3.5	3.334	0.0073	2.1	1.0542	1.0456	0.8224
0.4	2.542	0.0055	3.3	0.8252	0.8402	-1.7852
3.5	2.542	0.0055	3.3	1.0618	1.0492	1.2009
0.4	3.334	0.0055	3.3	0.8642	0.852	1.4319
3.5	3.334	0.0055	3.3	1.0164	1.0326	-1.5688
0.4	2.542	0.0073	3.3	0.786	0.775	1.4193
3.5	2.542	0.0073	3.3	1.0826	1.075	0.7069
0.4	3.334	0.0073	3.3	0.825	0.8356	-1.2685
3.5	3.334	0.0073	3.3	1.0372	1.0396	-0.2308
0.67	3.334	0.0055	3	0.8725	0.9474	-7.8977
0.5	3.334	0.0055	3	0.8636	0.8632	0.0558
1.16	3.334	0.0055	2.5	0.8927	0.8536	4.5826
0.875	3.334	0.0055	2.5	0.8762	0.8218	6.6285
0.67	2.542	0.0073	1.875	0.7886	0.882	-10.583
0.5	2.542	0.0073	1.875	0.7697	0.8402	-8.3804
0.67	2.542	0.0073	3.75	0.8191	0.8704	-5.8879

Table 7.9 Comparison of Mixing Index Data in the Case of Simultaneous Primary and Secondary air Supply

A	B	C	D	I_{MScal}	I_{MSexp}	%Deviation
0.4	2.542	0.0055	2.1	0.8965	0.9042	-0.8515
3.5	2.542	0.0055	2.1	1.0165	1.005	1.1442
0.4	3.334	0.0055	2.1	0.9097	0.9334	-2.5391
3.5	3.334	0.0055	2.1	0.9937	1.004	-1.0259
0.4	2.542	0.0073	2.1	0.8285	0.801	3.4332
3.5	2.542	0.0073	2.1	1.0445	1.063	-1.7403
0.4	3.334	0.0073	2.1	0.8417	0.821	2.5213
3.5	3.334	0.0073	2.1	1.0217	1.021	0.0685
0.4	2.542	0.0055	3.3	0.9037	0.8926	1.2435
3.5	2.542	0.0055	3.3	1.0237	1.02	0.3627
0.4	3.334	0.0055	3.3	0.9169	0.9034	1.4943
3.5	3.334	0.0055	3.3	1.0009	1.006	-0.5069
0.4	2.542	0.0073	3.3	0.8357	0.8624	-3.0960
3.5	2.542	0.0073	3.3	1.0517	1.053	-0.1234
0.4	3.334	0.0073	3.3	0.8489	0.863	-1.6338
3.5	3.334	0.0073	3.3	1.0289	1.0112	1.7503
1.16	2.542	0.0073	1.5	0.8778	0.9806	-10.477
0.875	2.542	0.0073	1.5	0.8579	0.973	-11.819
1.16	2.542	0.0073	3	0.8868	0.997	-11.047
0.875	2.542	0.0073	3	0.8669	0.9786	-11.404
0.875	3.334	0.0073	1.153	0.8635	0.9342	-7.5574
1.16	3.334	0.0073	1.153	0.8801	0.9672	-9.0005
0.875	3.334	0.0073	2.307	0.8705	0.9816	-11.315

Table 7.10 Comparison of (Output of ANN Approach with Experimental Data) Mixing Index Data

$I_{MP\ ANN}$	$I_{MP\ EXP}$	$I_{MD\ ANN}$	$I_{MD\ EXP}$	$I_{MR\ ANN}$	$I_{MR\ EXP}$	$I_{MS\ ANN}$	$I_{MS\ EXP}$
0.81427	0.802	0.73050	0.7404	0.76010	0.764	0.88507	0.9042
1.0411	1.083	1.14057	1.1722	1.07408	1.1032	1.01279	1.005
0.8259	0.8426	0.73528	0.7934	0.77346	0.803	0.88291	0.9334
1.0408	1.0226	1.12432	1.042	1.07110	1.0062	1.01413	1.004
0.78975	0.7602	0.74126	0.705	0.77015	0.7352	0.89857	0.801
1.04233	1.1156	1.14548	1.1942	1.07518	1.1522	1.01382	1.063
0.8292	0.8032	0.75799	0.763	0.80238	0.7958	0.90413	0.821
1.0418	1.0456	1.12958	1.1134	1.07242	1.0878	1.01455	1.021
0.81049	0.8402	0.74867	0.7402	0.77081	0.7812	0.8652	0.8926
1.03477	1.0492	1.09265	1.0604	1.06050	1.053	1.0116	1.02
0.8658	0.852	0.79851	0.8002	0.82998	0.8214	0.87910	0.9034
1.0366	1.0326	1.08930	1.0602	1.06017	1.0218	1.0104	1.006
0.7906	0.775	0.78500	0.713	0.80017	0.743	0.88858	0.8624
1.0357	1.075	1.09408	1.1346	1.06083	1.1028	1.01300	1.053
0.88273	0.8356	0.86221	0.7804	0.88364	0.8038	0.91093	0.863
1.03729	1.0396	1.09026	1.0824	1.06050	1.061	1.01218	1.0112

Conclusions and Scope of Future Work *Chapter 8*

8.1. Conclusions

1. It is apparent that the quality of fluidization can be improved by lowering the bed height, particle size, and using a distributor of optimum cross-sectional area. But a 10% distributor plate, in particular, offers the best fluidization quality as evident from the experimental findings
2. Fluctuation ratio is small for columns having larger diameters in the lower velocity range, i.e., when $G_f \leq 2\ G_{mf}$.
3. Fluctuation ratio has also a small value for columns having smaller diameters in the upper velocity range, i.e., when $G_f \geq 2\ G_{mf}$.
4. Fluctuation ratio bears an direct relation with bed height.
5. in the lower velocity range.
6. Fluctuation ratio varies directly with bed height in the higher velocity range.
7. Expansion ratio is in indirect proportion with column diameters and bed heights.
8. Expansion ratio is a direct function of mass velocity in all the ranges of mass velocities.
9. The introduction of rod and disc types of promoters in the bed improves the bubble behaviour by breaking the bubbles of larger sizes into a number of bubbles of smaller sizes, for almost the complete regime of fluidization, except in the neighbourhood of the minimum fluidization conditions, where the bed dynamics are of transitional in nature. The use of the rod type promoter in gas-solid fluidized bed has been found to be more effective in reducing the bed fluctuation and increasing bed expansion in higher mass velocity ranges, which in turn helps in reducing the overall size of a fluidizer.
10. The use of secondary air at different heights of the column will have a direct impact on residence time of the particle, which, in turn, may affect the rate of a chemical reaction. It may be attributed to better mixing of particles of wide

ranges of sizes and densities. Owing to greater turbulence, the bed provides a better contact between particles in the bed.

11. The pressure drop is more in the case of simultaneous primary and secondary air supplies as compared to only primary air supply because secondary air exerts an axial thrust on the lower half of the bed.
12. In the case of combined primary and secondary air supplies, the fluctuation ratio steadily increases up to twice the minimum fluidization mass velocity and then reduces and becomes equal to only primary air supply. As primary air takes care mainly of the lower half of the bed and secondary air that of the upper half of the bed (fifty percent of the bed material), the fluctuation ratio is a little more under secondary air supply conditions. Due to secondary air supply, the lower portion of the bed will remain low (value of h_1 will be low as compared to only primary air supply) and there is no significant change in the upper values. But at higher gas mass velocities, the fluctuation ratio for primary as well as simultaneous primary and secondary air supplies become almost equal as bubbles grow faster and hence break immediately. Due to moderate pressure drop and less fluctuation, the supply of secondary air in the middle of each static bed height is justified.
13. The developed models accurately predict the concentration of jetsam (and hence the mixing index), which decreases with the height of the particle layer in the bed measured from the distributor. Of the two types of promoters, disc and rod, the latter type has been found to be superior to the former. However, during simultaneous primary and secondary air supplies, the best mixing is obtained. Furthermore, it has been observed that the mixing performance of the four different parameters is in the increasing order as follows: primary, disc type, rod type and primary and secondary (simultaneous). In the higher mass velocity range of air, better mixing is obtained, whereas better segregation is obtained in the lower mass velocity range.
14. In terms of the superiority for calculation of pressure drop, fluctuation and expansion ratios, factorial design and analysis approach is better than the ANN and dimensional analysis approaches. The factorial design and analysis, in

particular, explains both individual and interaction effects among all the variables. The number of experimental runs required to develop the model equations through statistical design is also considerably less in comparison to conventional experimentation.

8.2. Future Work

The following areas may be studied in future:

- Effect of distributor areas on various column diameters;
- Effect of combined promoter and simultaneous primary and secondary air on fluctuation and expansion ratios;
- Effect of combined promoter and simultaneous primary and secondary air on mixing;
- Use of tertiary mixture with different compositions instead of binary ones;
- Study of effect of regular particles on pressure drop, fluctuation ratio, expansion ratio and mixing.

Appendix

Table 1.3

Material = Dolomite

Particle size = 0.00055m

Static bed height = 0.08m

Distributor type = 6%

G,kg/m^{2}s	**Δp,N/m^2**	**h_1,cm**	**h_2,cm**	**r**	**R**
0	0	-	-	-	-
0.425	77.5	-	-	-	-
0.51	201.5	-	-	-	-
0.595	232.5	8.5	8.2	1.036	1.043
0.68	207.5	9.0	8.5	1.058	1.093
0.765	217.5	9.5	8.8	1.079	1.143
0.85	217.5	10.5	9.5	1.105	1.25
0.935	217.5	11.5	10.0	1.15	1.343
1.02	217.5	12.5	11.0	1.136	1.468
1.105	217.5	13.5	12.0	1.125	1.593
1.19	217.5	15.0	13.0	1.153	1.75
1.275	217.5	16.0	14.0	1.143	1.875
1.36	217.5	17.5	15.0	1.166	2.031
1.445	217.5	18.5	16.5	1.121	2.187
1.53	217.5	21.0	19.0	1.105	2.5
1.615	217.5	23.0	20.5	1.121	2.718
1.7	217.5	24.5	22.0	1.115	2.906
1.785	217.5	25.5	23	1.108	3.031
1.87	217.5	26.5	24	1.104	3.156
1.955	217.5	27.5	25	1.1	3.281

Table 2.3

Material = Dolomite Particle size = 0.00055m

Static bed height = 0.01m Distributor type = 6%

G,kg/m^{2}s	**Δp,N/m^2**	**h_1,cm**	**h_2,cm**	**r**	**R**
0	0	-	-	-	-
0.425	77.5	-	-	-	-
0.51	139.5	-	-	-	-
0.595	139.5	10.5	10.2	1.029	1.035
0.68	139.5	11.0	10.5	1.047	1.075
0.765	139.5	12.5	11.5	1.086	1.2
0.85	139.5	14.0	12.5	1.12	1.325
0.935	139.5	15.5	13.2	1.148	1.435
1.02	139.5	16.5	14.0	1.178	1.525
1.105	139.5	17.5	15.0	1.166	1.625
1.19	139.5	18.5	16.0	1.156	1.725
1.275	139.5	19.5	17.0	1.147	1.825
1.36	139.5	21.5	18.5	1.162	2.0
1.445	139.5	22.5	20.0	1.125	2.125
1.53	139.5	24.5	22	1.113	2.325
1.615	139.5	26.5	23.5	1.127	2.5
1.7	139.5	28.0	25	1.120	2.65
1.785	139.5	29.0	26	1.115	2.75
1.87	139.5	30.0	27	1.111	2.85

Table 3.3

Material = Dolomite Particle size = 0.00055m

Static bed height = 12cm Distributor type = 6%

G,kg/m^{2}s	**Δp,N/m^2**	**h_1,cm**	**h_2,cm**	**r**	**R**
0	0	-	-	-	-
0.425	77.5	-	-	-	-
0.51	124.5	-	-	-	-
0.595	139.5	12.5	12.0	1.041	1.020
0.68	139.5	13	12.5	1.04	1.060
0.765	139.5	14	12.8	1.093	1.116
0.85	139.5	15.5	13.5	1.148	1.208
0.935	139.5	17	14.5	1.172	1.312
1.02	139.5	18.5	15.5	1.193	1.416
1.105	139.5	19.5	16.5	1.181	1.5
1.19	139.5	20.5	17.5	1.171	1.583
1.275	139.5	22	19	1.157	1.708
1.36	139.5	24	21	1.143	1.875
1.445	139.5	25.5	22.5	1.133	2.0
1.53	139.5	27.5	24.5	1.122	2.116
1.615	139.5	29.0	25.5	1.137	2.270
1.7	139.5	31.0	27.5	1.127	2.437
1.785	139.5	32.0	28.5	1.122	2.520
1.87	139.5	33.0	29.5	1.118	2.604
1.955	139.5	34	30.5	1.114	2.687

Table 1.4

Material = Dolomite Particle size = 0.00055m

Static bed height = 0.08m Column diameter = 0.099m

G, kg/m^{2}s	**h_1, cm**	**h_2, cm**	**r**	**R**
0.51	8.5	8.2	1.036	1.043
0.595	8.8	8.5	1.035	1.081
0.68	9.5	9	1.055	1.156
0.765	10.5	9.5	1.105	1.25
0.85	11.5	10	1.15	1.343
0.935	12.5	10.5	1.190	1.437
1.02	15	11.5	1.304	1.656
1.105	16.5	12.5	1.32	1.812
1.19	18	14	1.285	2.0
1.275	19.5	16	1.218	2.218
1.36	21	17	1.235	2.375
1.445	22	18	1.222	2.5
1.53	23	19	1.210	2.625
1.615	24	20	1.2	2.75
1.7	25	21	1.190	2.875
1.785	26	22	1.181	3.0
1.87	27	23	1.174	3.125

Table 2.4
Material = Dolomite Particle size = 0.00055m
Static bed height = 0.10m Column diameter = 0.099m

G	h_1	h_2	r	R
0.51	-	-	-	-
0.595	-	-	-	-
0.68	10.5	10.2	1.029	1.035
0.765	11	10.5	1.047	1.075
0.85	11.5	10.8	1.064	1.115
0.935	12.5	11.2	1.116	1.185
1.02	13.5	12	1.125	1.275
1.105	14.8	13	1.138	1.39
1.19	16	14	1.142	1.5
1.275	17.5	15	1.166	1.625
1.36	19	16	1.187	1.75
1.445	20.5	17	1.205	1.875
1.53	21.5	18	1.194	1.975
1.615	22.5	19	1.184	2.075
1.7	23.5	20	1.175	2.175
1.785	24.5	21	1.166	2.275
1.87	25.5	22	1.159	2.375

Table 3.4

Material = Dolomite Particle size= 0.00055m

Static bed height = 0.12m Column diameter = 0.099m

G	h_1	h_2	r	R
0.51	-	-	-	-
0.595	-	-	-	-
0.68	12.5	12.2	1.024	1.029
0.765	13	12.5	1.04	1.062
0.85	13.5	12.8	1.054	1.095
0.935	14	13	1.076	1.125
1.02	15	13.5	1.111	1.187
1.105	16	14	1.142	1.25
1.19	17.5	15	1.166	1.354
1.275	19	16	1.187	1.458
1.36	20	17	1.176	1.541
1.445	21	18	1.166	1.625
1.53	22	19	1.157	1.708
1.615	23	20	1.15	1.791
1.7	24	21	1.142	1.875
1.785	25	22	1.136	1.958
1.87	26	23	1.130	2.041

Table 1.5
Material = Dolomite **Particle size = 0.00055m**
Static bed height = 8 cm **Un-promoted**

G, kg/m^{2}s	h_1, cm	h_2, cm	r	R
0	-	-	-	-
0.425	-	-	-	-
0.511	-	-	-	-
0.596	-	-	-	-
0.681	8.5	8.2	1.036	1.043
0.765	9	8.5	1.058	1.093
0.851	10	9.0	1.11	1.187
0.935	11	9.5	1.157	1.281
1.021	12	10.5	1.142	1.406
1.106	13.5	11.5	1.175	1.562
1.191	14.5	12.5	1.16	1.687
1.276	16.5	14.0	1.718	1.906
1.361	18.5	15.5	1.193	2.125
1.446	20.0	16.5	1.212	2.281
1.523	21.5	17.5	1.228	2.437
1.617	23.5	19.5	1.205	1.687
1.702	25	21.5	1.162	2.906

Table 2.5
Material = Dolomite **Particle size = 0.00055m**
Static bed height = 8 cm **Rod promoted**

G, kg/m^2s	h_1, cm	h_2, cm	r	R
0	-	-	-	-
0.425	-	-	-	-
0.511	-	-	-	-
0.596	-	-	-	-
0.681	8.3	8.1	1.024	1.025
0.765	9	8.5	1.058	1.093
0.851	9.5	9	1.056	1.156
0.935	10.5	9.5	1.05	1.25
1.021	11.5	10.5	1.095	1.375
1.106	13	11.5	1.13	1.531
1.191	14.3	12.5	1.144	1.675
1.276	15	13	1.153	1.75
1.361	15.5	13.5	1.148	1.812
1.446	17.5	14.5	1.206	2.0
1.523	19	16	1.187	2.187
1.617	20	17.5	1.142	2.343
1.702	21.5	19.5	1.102	2.562

Table 3.5
Material = Dolomite **Particle size = 0.00055m**
Static bed height = 8 cm **Disc promoted**

G, kg/m^2s	h_1, cm	h_2, cm	r	R
0	-	-	-	-
0.425	-	-	-	-
0.511	-	-	-	-
0.596	-	-	-	-
0.681	8.5	8.2	1.036	1.043
0.765	9.5	9	1.056	1.153
0.851	10.5	9.5	1.052	1.25
0.935	11.5	10	1.15	1.343
1.021	12	10.5	1.142	1.406
1.106	13.2	11.5	1.15	1.543
1.191	14.5	12.5	1.16	1.687
1.276	15.5	13.5	1.148	1.812
1.361	16.5	14	1.178	1.906
1.446	17.5	14.5	1.206	2.
1.523	19	16	1.187	2.187
1.617	20.5	17.5	1.171	2.375
1.702	21.5	19	1.131	2.531

Table 4.5
Material = Dolomite **Particle size = 0.00055m**
Static bed height = 10 cm **Un-promoted**

G, kg/m^2s	h_1, cm	h_2, cm	r	R
0	-	-	-	-
0.425	-	-	-	-
0.511	-	-	-	-
0.596	-	-	-	-
0.681	10.5	10.2	1.029	1.035
0.765	11	10.5	1.047	1.075
0.851	12.5	11	1.136	1.175
0.935	14	12	1.167	1.3
1.021	15.5	13	1.92	1.425
1.106	17	14	1.214	1.55
1.191	18.5	15.5	1.193	1.7
1.276	21.5	18	1.194	1.975
1.361	22.5	19.5	1.153	2.1
1.446	24	21	1.143	2.25
1.523	26	23	1.13	2.45
1.617	27	24	1.125	2.55
1.702	28	25	1.12	2.65

Table 1.6 h_s **= 8 cm**
Material = Dolomite **Particle size = 0.00055m**

Primary Air					Secondary Air				
G_P	h_1	h_2	r_1	R_1	G_s	H_1	H_2	r_2	R_2
0.681	8.5	8.3	1.02	1.05	-	-	-	-	-
0.765	9	8.5	1.058	1.093	-	-	-	-	-
0.851	10	9	1.11	1.187	0.085	10	9	1.11	1.187
0.935	11	9.5	1.15	1.281	0.17	12	10.5	1.14	1.406
1.021	12	10.5	1.14	1.406	0.255	13.5	11.5	1.17	1.562
1.106	13.5	11.5	1.17	1.562	0.34	15	12.5	1.2	1.718
1.191	15	12.5	1.2	1.718	0.425	16.5	13.5	1.22	1.875
1.276	16.5	14.0	1.178	1.906	0.511	17.5	14.5	1.2	2.0
1.361	17	15	1.13	2.0	0.596	18.3	16	1.14	2.143
1.446	18	16	1.125	2.125	0.681	22	18.5	1.189	2.531
1.523	21.5	17.5	1.228	2.243	0.765	23	20.5	1.121	2.718

Table 2.6 h_s **=10 cm**
Material = Dolomite **Particle size = 0.00055m**

Primary Air					Secondary Air				
G_P	h_1	h_2	r_1	R_1	G_s	H_1	H_2	r_2	R_2
0.681	10.5	10.2	1.029	1.035	-	-	-	-	-
0.765	11	11.5	1.046	1.125	-	-	-	-	-
0.851	12.5	11	1.136	1.175	0.085	13.5	11.5	1.17	1.25
0.935	14	12	1.16	1.3	0.17	14.5	12	1.2	1.325
1.021	15.5	13	1.19	1.425	0.255	16	13	1.23	1.45
1.106	17	14	1.214	1.55	0.34	17.5	14	1.25	1.575
1.191	18.5	15.5	1.193	1.7	0.425	19.5	16	1.21	1.775
1.276	21.5	18	1.194	1.975	0.511	23	19	1.21	2.1
1.361	22.5	19.5	1.153	2.1	0.596	25	21	1.19	2.3
1.446	24	21	1.14	2.25	0.861	26.5	23	1.15	2.475
1.523	26	23	1.13	2.45	0.765	28.5	25	1.14	2.675

Table 3.6 **h_s =12 cm**
Material = Dolomite **Particle size = 0.00055m**

Primary Air					Secondary Air				
G_P	h_1	h_2	r_1	R_1	G_s	H_1	H_2	r_2	R_2
0.681	12.5	12.2	1.024	1.029	-	-	-	-	-
0.765	13.5	12.5	1.08	1.083	-	-	-	-	-
0.851	15.5	13.5	1.148	1.208	0.085	17	14.5	1.17	1.312
0.935	17	14.5	1.17	1.312	0.17	18.5	15	1.23	1.395
1.021	19.5	16	1.218	1.479	0.255	20	16	1.25	1.5
1.106	21	17	1.235	1.583	0.34	21.5	17	1.26	1.604
1.191	23	19	1.210	1.75	0.425	23.5	19	1.23	1.770
1.276	25	21	1.190	1.916	0.511	25.5	21	1.21	1.937
1.361	27	23	1.173	2.083	0.596	27.5	23	1.19	2.104
1.446	28.5	24.5	1.163	2.208	0.681	30	25.5	1.17	2.312
1.523	30	26	1.15	2.333	0.765	32.5	28.5	1.14	2.541

Table 4.6 **h_s =14 cm**
Material = Dolomite **Particle size = 0.00055m**

Primary Air					Secondary Air				
G_P	h_1	h_2	r_1	R_1	G_s	H_1	H_2	r_2	R_2
0.681	14.5	14	1.035	1.017	-	-	-	-	-
0.765	15.5	14.5	1.068	1.017	-	-	-	-	-
0.851	17	15	1.133	1.142	0.085	18.5	16	1.156	1.232
0.935	19	16	1.18	1.25	0.17	20.5	17	1.205	1.339
1.021	20.5	17	1.20	1.339	0.225	22.5	18	1.25	1.446
1.106	22.5	18	1.25	1.446	0.34	24.5	19	1.28	1.553
1.191	24.5	20	1.22	1.589	0.425	26	20.5	1.26	1.660
1.276	26.5	22	1.20	1.732	0.511	28	22.5	1.24	1.803
1.361	28.5	24	1.187	1.875	0.596	30	25	1.2	1.964
1.446	29.5	25	1.18	1.946	0.681	33	27.8	1.187	2.171
1.523	31.5	27	1.166	2.089	0.765	35	30.5	1.147	2.339

Table 1.7
Iron: Coal = 50:50 **Primary air**
G_{mf} = 0.595 kg/m^{2}s, G_f = 1.275 kg/m^{2}s **h_s= 0.08 m**

Sl.No	Height at which samples drawn, m	Weight of Jetsam sample, gm	Weight of Flotsam sample, gm	Weight fraction of Jetsam particle	Mixing Index, I_{MD}
1	0.04	21.235	15.915	0.5716	1.1432
2	0.08	18.269	22.674	0.4462	0.8924
3	0.12	17.012	27.463	0.3825	0.765
4	0.16	12.76	21.077	0.3771	0.7542
5	0.20	9.265	15.762	0.3702	0.7404

Table 2.7
Iron: Coal = 50:50 **Disc Promoter**
G_{mf} = 0.595 kg/m^{2}s, G_f = 1.275 kg/m^{2}s **h_s= 0.08 m**

Sl.No	Height at which samples drawn, m	Weight of Jetsam sample, gm	Weight of Flotsam sample, gm	Weight fraction of Jetsam particle	Mixing Index, I_{MR}
1	0.04	19.245	15.726	0.5503	1.1006
2	0.08	22.04	23.79	0.4809	0.9618
3	0.12	14.465	19.885	0.4211	0.8422
4	0.16	11.709	17.425	0.4019	0.8038
5	0.20	9.671	15.645	0.382	0.764

Table 3.7
Iron: Coal = 50:50 **Rod Promoter**
G_{mf} = 0.595 kg/m^{2}s, G_f = 1.275 kg/m^{2}s **h_s= 0.08 m**

Sl.No	Height at which samples drawn, m	Weight of Jetsam sample, gm	Weight of Flotsam sample, gm	Weight fraction of Jetsam particle	Mixing Index, I_{MP}
1	0.04	16.269	13.511	0.5463	1.0926
2	0.08	24.43	28.667	0.4601	0.9202
3	0.12	16.249	20.339	0.4441	0.8882
4	0.16	10.263	14.178	0.4199	0.8398
5	0.20	9.632	14.387	0.4010	0.802

Table 4.7
Iron: Coal = 50:50 **Simultaneous Primary and Secondary air**
G_{mf} = 0.595 kg/m^{2}s, G_f = 1.275 kg/m^{2}s **h_s= 0.08 m**

Sl.No	Height at which samples drawn, m	Weight of Jetsam sample, gm	Weight of Flotsam sample, gm	Weight fraction of Jetsam particle	Mixing Index, I_{MS}
1	0.04	19.82	19.027	0.5102	1.0204
2	0.08	20.569	20.884	0.4962	0.9924
3	0.12	17.298	18.206	0.4872	0.9744
4	0.16	11.568	13.013	0.4706	0.9412
5	0.20	10.02	12.143	0.4521	0.9042

Table 5.7
Iron: Coal = 50:50 **Primary air**
G_{mf} = 0.765 kg/m^{2}s, G_f = 1.275 kg/m^{2}s **h_s= 0.14 m**

Sl.No	Height at which samples drawn, m	Weight of Jetsam sample, gm	Weight of Flotsam sample, gm	Weight fraction of Jetsam particle	Mixing Index, I_{MD}
1	0.04	18.691	13.199	0.5861	1.1722
2	0.08	14.927	15.742	0.4867	0.9734
3	0.12	11.72	18.525	0.3875	0.775
4	0.16	16.673	29.576	0.3605	0.721
5	0.20	10.242	18.207	0.3601	0.7202
6	0.24	9.037	16.629	0.3521	0.7042
7	0.28	8.356	16.184	0.3405	0.6804

Table 6.7
Iron: Coal = 50:50 **Disc Promoter**
G_{mf} 0.765 kg/m^{2}s, G_f = 1.275 kg/m^{2}s **h_s= 0.14 m**

Sl.No	Height at which samples drawn, m	Weight of Jetsam sample, gm	Weight of Flotsam sample, gm	Weight fraction of Jetsam particle	Mixing Index, I_{MR}
1	0.04	18.7	15.201	0.5516	1.1032
2	0.08	23.067	28.641	0.5216	1.0432
3	0.12	13.269	19.086	0.4101	0.8202
4	0.16	14.155	22.139	0.39	0.78
5	0.20	12.46	20.183	0.3897	0.7634
6	0.24	9.65	16.021	0.3759	0.7518
7	0.28	8.953	15.895	0.3603	0.7206

Table 7.7
Iron: Coal = 50:50 **Rod Promoter**
G_{mf} = 0.765 kg/m^{2}s, G_f = 1.275 kg/m^{2}s **h_s= 0.14 m**

Sl.No	Height at which samples drawn, m	Weight of Jetsam sample, gm	Weight of Flotsam sample, gm	Weight fraction of Jetsam particle	Mixing Index, I_{MP}
1	0.04	24.268	20.548	0.5415	1.083
2	0.08	17.055	20.861	0.4498	0.8996
3	0.12	18.765	25.181	0.427	0.854
4	0.16	10.709	16.016	0.4007	0.8014
5	0.20	9.097	13.846	0.3965	0.793
6	0.24	11.673	18.227	0.3904	0.7808
7	0.28	8.758	13.925	0.3861	0.7722

Table 8.7
Iron: Coal = 50:50 **Simultaneous Primary and Secondary air**
G_{mf} = 0.765 kg/m^{2}s, G_f = 1.275 kg/m^{2}s **h_s= 0.14 m**

Sl.No	Height at which samples drawn, m	Weight of Jetsam sample, gm	Weight of Flotsam sample, gm	Weight fraction of Jetsam particle	Mixing Index, I_{MS}
1	0.04	16.275	16.1	0.5027	1.0054
2	0.08	20.296	21.04	0.491	0.982
3	0.12	16.897	18.363	0.4792	0.9584
4	0.16	19.05	21.877	0.4657	0.9314
5	0.20	12.679	15.858	0.4443	0.8886

Notations

h_1 Minimum height possesses by the particles of the bed at primary air supply, cm

h_2 Maximum height possesses by the particles of the bed at primary air supply, cm

H_1 Minimum height possesses by the particles of the bed at secondary air supply, cm

H_2 Maximum height possesses by the particles of the bed at secondary air supply, cm

Artificial Neural Network: (Programming)

```
clear; close all;
%Define a 2-2-1 MLP with sigmoidal Neurons at the Hidden.
%and output layers; train using gradient descent backpror
net=newff([0 1; 0 1; 0 1;0 1],[4,3,1], {'logsig', logsig', 'logsig'}, 'traingd');
%Show training progress every 10 epochs
Net.trainParam.Show=100;
%Set learning rate to 0.1
net.trainParam.lr=0.1
%Set error goal to 0.01
Net.trainparam.goal=1e-5;
%Set maximum epochs to 1000
net.trainParam.epochs=4000;
num_pat=16;
input_list=[ __;
                    ;
                    ;
                     ;
                    ];
figure;
output_list= [__ ]
aa=input_list;

%-----Define training input and taiget data vectors
net=train(net, aa, output_list);

%--------------TESTING(Test the network)
for i=1: num_pat
x=input_list(1:4,i);
op(i)=sim(net, x);
```

```
end
op
%-------------------------------------
x1=input('enter your input data');
%for i=1:num_pat
x=x1;
op=sim(net,x)
end
%---------------------------
```